



University of  
**Nottingham**  
UK | CHINA | MALAYSIA

Studies on the host-pathogen  
interactions for *Rhizoctonia*  
*solani* AG2-1 causing damping-  
off disease of *Brassica napus*  
(Oilseed Rape)

Isabelle Louise Sims

Thesis submitted to the University of Nottingham for the  
degree of Doctor of Philosophy

November 2022

Division of Plant and Crop Sciences, School of Biosciences,  
University of Nottingham, Sutton Bonington, LE12 5RD, UK

## Acknowledgements

I would like to thank my supervisors Professor Rumiana Ray, Professor Michael Holdsworth and Dr Guillermina Mendiondo for their support throughout my PhD and for supervising my DTP rotation projects. I would like to thank all past and present members of the Ray, Holdsworth and Mendiondo groups for their day-to-day support and friendship. I would like to thank Dr Kamal Swarup for her work as Laboratory Manager in South Laboratory, and for being there to help with any questions. I would like to thank the SB Glasshouses team for their support in running experiments in the phytotron and glasshouses. Finally, I would like to thank the BBSRC and University of Nottingham for funding this PhD.

Special thanks go to my family and friends, whose support and belief in me has been invaluable throughout these few years, I couldn't have done it without you.

This thesis is dedicated to those at the University of Bath who inspired my love of plant sciences, and particularly plant pathology, thank you.

# Table of Contents

Acknowledgements .....	2
Table of Contents .....	3
List of Abbreviations .....	5
List of Figures .....	7
List of Tables .....	25
List of Supplementary Information .....	27
Abstract .....	33
Chapter 1: <i>Rhizoctonia solani</i> AG2-1 – <i>Brassica napus</i> host-pathogen interactions and control .....	35
1.1 Introduction.....	35
1.2 Oilseed rape diseases .....	38
1.3 <i>Rhizoctonia solani</i> isolate pathogenicity, disease symptoms and significance .....	39
1.4 Host-pathogen interactions for <i>Rhizoctonia solani</i> .....	45
1.5 Disease management .....	59
1.6 PhD aims and objectives.....	74
Chapter 2: Molecular characterisation of defence of <i>Brassica napus</i> (Oilseed rape) to <i>Rhizoctonia solani</i> AG2-1 confirmed by functional analysis in <i>Arabidopsis thaliana</i> .....	76
2.1 Abstract .....	76
2.2 Introduction.....	77
2.3 Methods .....	80
2.4 Results .....	90
2.5 Discussion.....	108

Chapter 3: Examining the role of auxins and <i>Rhizoctonia solani</i> AG2-1	118
3.1 Abstract .....	118
3.2 Introduction.....	119
3.3 Methods .....	124
3.4 Results .....	135
3.5 Discussion .....	156
Chapter 4: Identification and characterisation of candidate genes for resistance to <i>Rhizoctonia solani</i> AG2-1 in <i>Brassica napus</i> (Oilseed Rape)	165
4.1 Abstract .....	165
4.2 Introduction.....	166
4.3 Methods .....	172
4.4 Results .....	184
4.5 Discussion .....	224
General discussion .....	231
Bibliography.....	235
Supplementary Information .....	263
Professional Internships for PhD Student (PIPS) reflection.....	326
Note to examiners.....	326
PIPS Reflective Statement.....	326
COVID Impact Statement .....	329

## List of Abbreviations

2,4-D	2,4-Dichlorophenoxyacetic acid
ABA	Abscisic Acid
AG	Anastomosis Group
BNR	Binucleate <i>Rhizoctonia</i>
BR	Brassinosteroids
Cv.	Cultivar
CWDE	Cell-Wall Degrading Enzymes
DMSO	Dimethyl Sulfoxide
dpi	days post-inoculation
EMS	Ethyl Methane Sulfonate
ET	Ethylene
GEMs	Gene Expression Markers
GLPs	Germin-Like Proteins
GM	Genetically Modified
GO	Gene Ontology
GWAS	Genome-Wide Association Study
hpi	hours post-inoculation
IAA	Indole-3-Acetic Acid
ICS pathway	Isochorismate Synthase pathway
ISR	Induced Systemic Resistance
JA	Jasmonic Acid
LC-MS/MS	Liquid Chromatography Mass Spectrometry
LECA	Light Expanded Clay Aggregate
MAPK	Mitogen-Activated Protein Kinase
MeOH	Methanol
NAA	1-Naphthalene Acetic Acid
NBS-LRR	Nucleotide-Binding Site – Leucine Rich Repeats
NPA	1-Naphthylphthalamic Acid
NTA	N-Terminal Acetylation
OA	Oxalic Acid
OSR	Oilseed Rape
PAA	Phenyl Acetic Acid
PAL pathway	Phenylalanine Ammonia-Lyase pathway
PDA	Potato Dextrose Agar

PDB	Potato Dextrose Broth
R genes	Resistance genes
RLK	Receptor-Like Kinase
ROS	Reactive Oxygen Species
rpm	Revolutions Per Minute
RT-qPCR	Reverse Transcription quantitative real-time Polymerase Chain Reaction
S genes	Susceptibility genes
SA	Salicylic Acid
SAR	Systemic Acquired Resistance
SNPs	Single Nucleotide Polymorphisms
TIBA	2,3,5-Triiodobenzoic Acid
TILLING	Targeting Induced Local Lesions In Genomes
VOCs	Volatile Organic Compounds

## List of Figures

Figure 1-1: Growth of *Rhizoctonia solani* AG2-1 in culture. A) Image of *R. solani* AG2-1 growing on PDA medium showing its colourless to yellow to brown colouration and the production of dark brown sclerotia. B) Microscope image of *R. solani* AG2-1 showing hyphal branching at right-angles with slight constriction at the branching point and a cross wall near the junction. 100µm scale bar shown. .... 36

Figure 1-2: The triangle of U and *Brassica* crop products. The triangle of U shows the genetic and evolutionary relationships between common *Brassica* spp.. Images of commonly available products are shown and chromosome number and genomes indicated below species names. (Adapted from U, 1935). .... 37

Figure 1-3: *Rhizoctonia solani* AG2-1 symptoms on Oilseed Rape (OSR). A) Post-germination damping-off causing death of a highly susceptible OSR seedling, B) hypocotyl and root rot of an OSR seedling, which can lead to post-emergence damping-off, C) necrotic lesion on a young OSR plant, D) wirestem of a young OSR plant. .... 42

Figure 1-4: Life cycle of *Rhizoctonia solani*. A) In the absence of a susceptible host, fungal mycelium survives on seeds, plant debris, or as mycelium and sclerotia in the soil. B) Young hyphae grow and mature into mycelium with characteristic right-angled branching and constriction near nodes. C) Mycelium grows across the plant surface before forming

an infection cushion. D) Invasion of the host causes necrosis and symptoms such as seed rot, damping off, wire stem and cankers. (Adapted from Agrios, 2005) ..... 46

Figure 1-5: Flow chart summarising the infection process of *R. solani*. Adapted from (Keijer, 1996). ..... 47

Figure 1-6: Confocal microscopy images showing *Rhizoctonia solani* AG2-1 infection on *Brassica napus*. A) Germination of *R. solani* AG2-1 sclerotia on roots of *B. napus*; B) hyphal growth over root tissues; and C) development of an infection cushion. Plants were grown on water agar plates and *R. solani* sclerotia was placed close to the root tissue. Samples were taken 48hours after the addition of sclerotia, and were stained using Alexa Fluor Wheat Germ Agglutinin 488, and Propidium Iodide. The roots of *B. napus* are shown in blue and the sclerotia and hyphae of *R. solani* are shown in red/pink. The sclerotia in (A) is indicated with a white arrow, and the infection cushion in (C) with a yellow arrow. White scale bars are shown in the top right corner of the images and represent 250µm..... 49

Figure 2-1: Photograph showing the experimental setup used for growing *Brassica napus* seedlings under *Rhizoctonia solani* AG2-1 inoculation in LECA particles..... 82

Figure 2-2: *Brassica napus* symptom scores under *Rhizoctonia solani* AG2-1 inoculation. Plants were scored from 0-4; 0: symptomless, 1: 25% symptoms, 2: 50% symptoms, 3: 75% symptoms, 4: death. .... 83



Figure 2-3: Photograph showing the experimental setup used for growing *Arabidopsis thaliana* plants under *Rhizoctonia solani* AG2-1 inoculation in compost. .... 88

Figure 2-4: *Brassica napus* symptom scores and percentage reductions in root length at seven days post inoculation with *Rhizoctonia solani* AG2-1. A) Average symptom scores for five commercially available *B. napus* varieties. Dark grey bars show average hypocotyl symptom scores and light grey bars show average root symptom scores. Non-inoculated data not shown as no individuals showed symptoms. B) Percentage reduction in root length measured using ImageJ and SmartRoot plugin. The total length included lateral roots. Tukey test was used to provide letters. .... 92

Figure 2-5: Confocal microscopy images showing *Rhizoctonia solani* AG2-1 sclerotia infection on different *Brassica napus* varieties up to two days post-inoculation. Alexa Fluor Wheat Germ Agglutinin 488 and Propidium Iodide staining of *B. napus* showed differences in the development of infection structures in Anastasia, Skye, and Campus. Scale bars shown in the bottom right of each image represent 250µm. Yellow arrowheads indicate infection cushions. Red shows staining with Alexa Fluor Wheat Germ Agglutinin 488. Blue shows staining with Propidium Iodide. The images shown were chosen as representatives from a larger sample of infected roots for each variety. .... 94

Figure 2-6: Proposed diagram of interactions between hormonal defence pathways..... 96

Figure 2-7: Differential gene expression of auxin genes in *Brassica napus* varieties following inoculation with *Rhizoctonia solani* AG2-1 at 8, 24 and 48 hours post inoculation. Significant differences between the varieties (t-test,  $p < 0.05$ ) are indicated by a bracket and \*. ..... 97

Figure 2-8: Differential gene expression of jasmonate and abscisic acid genes in *Brassica napus* varieties following inoculation with *Rhizoctonia solani* AG2-1 at 8, 24 and 48 hours post inoculation. Significant differences between the varieties (t-test,  $p < 0.05$ ) are indicated by a bracket and \* ..... 99

Figure 2-9: Differential gene expression of ethylene genes in *Brassica napus* varieties following inoculation with *Rhizoctonia solani* AG2-1 at 8, 24 and 48 hours post inoculation. Significant differences between the varieties (t-test,  $p < 0.05$ ) are indicated by a bracket and \*. ..... 101

Figure 2-10: Differential gene expression of salicylic acid and reactive oxygen species genes in *Brassica napus* varieties following inoculation with *Rhizoctonia solani* AG2-1 at 8, 24 and 48 hours post inoculation. Significant differences between the varieties (t-test,  $p < 0.05$ ) are indicated by a bracket and \*. ..... 103

Figure 2-11: Total plant leaf areas of *Arabidopsis thaliana* mutant plants at 11 days post inoculation with *Rhizoctonia solani* AG2-1. Significant

differences between the inoculated and non-inoculated plants (t-test,  $p < 0.05$ ) are indicated by a bar and \*. ..... 105

Figure 2-12: Response of *Arabidopsis thaliana* IAA2<sub>pro</sub>:GUS lines to *Rhizoctonia solani* AG2-1 at one and three days post-inoculation. Light microscopy images showing GUS staining in Ws IAA2<sub>pro</sub>:GUS plants. At the time of sampling, *R. solani* growth had not reached the root of plants. Scale bar represents 100 $\mu$ m. .... 106

Figure 2-13: Confocal microscopy images of *Arabidopsis thaliana* Jas9:VENUS seedlings showing JA response to *Rhizoctonia solani* AG2-1 inoculation. Images are ordered left to right reflecting their location within the taproot relative to the root tip, i.e. Most right is the root tip, and most left is furthest from the root tip. Fluorescence from the Jas9:VENUS biosensor is shown in green. Scale bar represents 100 $\mu$ m. .... 107

Figure 3-1: Schematic diagrams showing the plate layouts and angle of root growth measurements. A) Plate layout used to test the effects of the presence and location of *Rhizoctonia solani* AG2-1 on *Arabidopsis thaliana* auxin mutants. Plants were grown in the locations marked 1-4 with one genotype used per plate. A sterile or *R. solani* inoculated plug was added at location A, B or C after the plants had grown for 7 days. Distances are shown between each plug-plant combination. B) Plate layout used for inoculation with *R. solani* and auxins. Media was supplemented with auxins or the same volume of DMSO, and *R. solani*

inoculated or sterile plugs were added. C) Examples of root growth angle measurements. The angle was measured at the root tip, with 180° representing gravitropic growth..... 128

Figure 3-2: Photographs showing the experimental setup of A) testing the effects of the presence and location of *Rhizoctonia solani* AG2-1 on the root architecture of *Arabidopsis thaliana* auxin mutants, B) testing the effects of 2,4-D, PAA and NAA with *Rhizoctonia solani* AG2-1 inoculation on the root architecture of *Arabidopsis thaliana* auxin mutants..... 129

Figure 3-3: A) Bar chart of the total plant leaf areas of *Arabidopsis thaliana* mutant plants at 17 days post inoculation with *Rhizoctonia solani* AG2-1. Standard error bars are shown. \* indicates a significant difference between the non-inoculated and inoculated plants (p=0.05). B) Representative images of the same experiment. A 1cm scale bar is shown for the plant images..... 137

Figure 3-4: Line graphs showing the effect of the presence of *Rhizoctonia solani* AG2-1 on the root length of *Arabidopsis thaliana* auxin mutants. Analysis of variance was carried out for each genotype separately. Standard error bars are shown. Inoculation had a significant effect on the root length of WT plants (p<0.001). Both inoculation (p<0.001) and distance (p=0.004) and the interaction between them (p=0.003) were significant for *aux1*. For *axr1*, the interaction between distance and inoculation was almost significant (p=0.051). Full analysis

is shown in Supplementary Information 6-8. Growth was consistently inhibited, regardless of distance for WT plants, while the *aux1* mutant was only inhibited in growth close to the pathogen. Neither inoculation nor distance affected *axr1* growth. .... 139

Figure 3-5: Line graphs showing the effect of the presence of *Rhizoctonia solani* AG2-1 on the number of lateral roots of *Arabidopsis thaliana* auxin mutants. Analysis of variance was carried out for each genotype. Standard error bars are shown. The effect of inoculation ( $p < 0.001$ ) and the interaction between inoculation and distance ( $p = 0.003$ ) were significant for WT plants. Inoculation also had a significant effect on *aux1* ( $p < 0.001$ ) and *axr1* ( $p = 0.023$ ) lateral root numbers. Full analysis is shown in Supplementary Information 9-11. For both WT and *aux1* plants, the number of lateral roots was reduced close to the pathogen, while *axr1* plants grew few lateral roots under either inoculated or non-inoculated conditions. .... 140

Figure 3-6: Line graphs showing the effect of the presence of *Rhizoctonia solani* AG2-1 on the angle of root growth of *Arabidopsis thaliana* auxin mutants. Analysis of variance was carried out for each genotype separately. The absolute proportion of 180° was calculated, which is the angle of growth when the plant is growing towards the bottom of the plate. Standard error bars are shown. There were no significant effects of inoculation or distance for WT or *axr1* plants. For *aux1* plants, there was a significant interaction between inoculation and distance ( $p = 0.027$ ). Full analysis is shown in Supplementary Information

12-14. Although the effects of inoculation and distance were not significant for WT and *axr1* plants, an increase in the straightness of WT and *axr1* roots was observed up to 6.5cm, while *aux1* roots were more gravitropic at 1.5cm and 3.5cm from the pathogen. .... 141

Figure 3-7: Line graphs showing the effect of 2,4-D, PAA and NAA auxin concentrations on the root length of *Arabidopsis thaliana* auxin mutants. Analysis of variance was carried out for each auxin separately. The standard errors of differences of means are shown. Analysis of the root length was calculated using proportions of the 0M auxin concentration control. Values on the graph that are greater than 1 represent an increase in root growth compared to the 0M control. The effect of genotype was significant for all auxins (2,4-D  $p=0.012$ , PAA  $p=0.01$ , NAA  $p=0.016$ ). The effect of NAA concentration was also significant ( $p=0.005$ ). Full analysis is shown in Supplementary Information 15-17. .... 144

Figure 3-8: Line graphs showing the effect of 2,4-D, PAA and NAA auxin concentrations on the number of lateral roots of *Arabidopsis thaliana* auxin mutants. Analysis of variance was carried out for each auxin separately. The standard errors of differences of means are shown. The effect of genotype was significant for all auxins (2,4-D  $p<.001$ , PAA  $p<.001$ , NAA  $p<.001$ ). The effect of auxin concentration was also significant for all auxins (2,4-D  $p=0.033$ , PAA  $p<.001$ , NAA  $p<.001$ ). There was an interaction between PAA concentration and

genotype ( $p=0.01$ ) and NAA concentration and genotype ( $p<.001$ ). Full analysis is shown in Supplementary Information 18-20..... 145

Figure 3-9: Line graphs showing the effect of 2,4-D, PAA and NAA auxin concentrations on the angle of root growth of *Arabidopsis thaliana* auxin mutants. Analysis of variance was carried out for each auxin separately. The standard errors of differences of means are shown. The angle of root growth was calculated using the absolute proportion of  $180^\circ$  (the angle at which plants are growing gravitropically). Values on the graph that are closer to 0 indicate that the root growth angle was growing gravitropically. The effect of genotype was significant for all auxins (2,4-D  $p<.001$ , PAA  $p<.001$ , NAA  $p<.001$ ). Full analysis is shown in Supplementary Information 21-23..... 146

Figure 3-10: Bar charts showing the effect of high 2,4-D, PAA and NAA auxin concentrations with and without the presence of *Rhizoctonia solani* AG2-1 on the root length of *Arabidopsis thaliana* auxin mutants. Analysis of variance was carried out for each auxin separately. A) There was a significant effect of 2,4-D ( $p<.001$ ), genotype ( $p<.001$ ) and an interaction between them ( $p=0.003$ ). B) There was a significant effect of PAA ( $p<.001$ ), inoculation ( $p=0.034$ ) and an interaction between PAA, genotype and inoculation ( $p=0.03$ ). C) There was a significant effect of genotype ( $p<.001$ ). Full analysis is shown in Supplementary Information 24-26. .... 148

Figure 3-11: Bar charts showing the effect of high 2,4-D, PAA and NAA auxin concentrations with and without the presence of *Rhizoctonia solani* AG2-1 on the number of lateral roots of *Arabidopsis thaliana* auxin mutants. Analysis of variance was carried out for each auxin separately. A) There was a significant effect of 2,4-D ( $p=0.016$ ), genotype ( $p=0.001$ ) and an interaction between them ( $p<.001$ ). B) There was a significant effect of PAA ( $p=0.023$ ), genotype ( $p=0.001$ ) and an interaction between them ( $p=0.006$ ). C) There was a significant effect of NAA ( $p<.001$ ), genotype ( $p<.001$ ) and an interaction between them ( $p<.001$ ). Full analysis is shown in Supplementary Information 27-29. .... 149

Figure 3-12: Bar charts showing the effect of high 2,4-D, PAA and NAA auxin concentrations with and without the presence of *Rhizoctonia solani* AG2-1 angle of root growth of *Arabidopsis thaliana* auxin mutants. Analysis of variance was carried out for each auxin separately. The angle of root growth was calculated using the absolute proportion of 180° (the angle at which plants are growing gravitropically). Values on the graph that are closer to 0 indicate that the root growth angle was growing gravitropically. There was a significant effect of genotype for all auxins (2,4-D  $p<.001$ , PAA  $p<.001$ , NAA  $p<.001$ ). There was also a significant effect of NAA ( $p=0.004$ ) and an interaction between NAA and genotype ( $p<.001$ ). Full analysis is shown in Supplementary Information 30-32. .... 150



Figure 3-13: Effect of exogenous PAA concentrations on the growth of *Rhizoctonia solani* AG2-1 in liquid media. The growth of *R. solani* was calculated as a proportion of the 0mM control and nonlinear regression analysis used to plot a critical exponential standard curve. The F pr. value was <.001. Full analysis is shown in Supplementary Information 33. Values above 1 represent growth stimulated by PAA..... 152

Figure 3-14: LC-MS/MS peak area ratios obtained from testing A) IAA and B) PAA standards..... 154

Figure 3-15: Measured concentrations of A) IAA and B) PAA from *Rhizoctonia solani* AG2-1 isolate cultures. *R. solani* isolates were grown in Vogel's media for three weeks, then the mycelium separated from the broth. Liquid-liquid extractions were carried out on the broth samples, and they were prepared for LC-MS/MS analysis. Full analysis is shown in Supplementary Information 34-5..... 155

Figure 4-1: AgriGO gene ontology: biological processes analysis for the hypocotyl disease index data. Singular Enrichment Analysis was used with the TAIR9 background, hypergeometric statistical test method and Yekutieli multi-test adjustment method. The gene list used was filtered to only contain genes with a log<sub>10</sub>P greater than 3. Significant terms are shown by coloured boxes, where the degree of colour saturation is positively correlated with the term's enrichment level. Dotted, dashed and solid lines show zero, one and two enriched terms at both ends of the line..... 186

Figure 4-2: AgriGO gene ontology: biological processes analysis for the root disease index data. Singular Enrichment Analysis was used with the TAIR9 background, hypergeometric statistical test method and Yekutieli multi-test adjustment method. The gene list used was filtered to only contain genes with a log10P greater than 3. Significant terms are shown by coloured boxes, where the degree of colour saturation is positively correlated with the term's enrichment level. Dotted, dashed and solid lines show zero, one and two enriched terms at both ends of the line..... 187

Figure 4-3: AgriGO gene ontology: cellular component analysis for the hypocotyl disease index data. Singular Enrichment Analysis was used with the TAIR9 background, hypergeometric statistical test method and Yekutieli multi-test adjustment method. The gene list used was filtered to only contain genes with a log10P greater than 3. Significant terms are shown by coloured boxes, where the degree of colour saturation is positively correlated with the term's enrichment level. Dotted, dashed and solid lines show zero, one and two enriched terms at both ends of the line. Green lines represent negative regulation. .... 188

Figure 4-4: AgriGO gene ontology: cellular component analysis for the root disease index data. Singular Enrichment Analysis was used with the TAIR9 background, hypergeometric statistical test method and Yekutieli multi-test adjustment method. The gene list used was filtered to only contain genes with a log10P greater than 3. Significant terms are shown by coloured boxes, where the degree of colour saturation is

positively correlated with the term's enrichment level. Dotted, dashed and solid lines show zero, one and two enriched terms at both ends of the line. Green lines represent negative regulation. .... 189

Figure 4-5: AgriGO gene ontology: molecular function analysis for the hypocotyl disease index data. Singular Enrichment Analysis was used with the TAIR9 background, hypergeometric statistical test method and Yekutieli multi-test adjustment method. The gene list used was filtered to only contain genes with a log<sub>10</sub>P greater than 3. Significant terms are shown by coloured boxes, where the degree of colour saturation is positively correlated with the term's enrichment level. Dotted, dashed and solid lines show zero, one and two enriched terms at both ends of the line..... 190

Figure 4-6: AgriGO gene ontology: molecular function analysis for the root disease index data. Singular Enrichment Analysis was used with the TAIR9 background, hypergeometric statistical test method and Yekutieli multi-test adjustment method. The gene list used was filtered to only contain genes with a log<sub>10</sub>P greater than 3. Significant terms are shown by coloured boxes, where the degree of colour saturation is positively correlated with the term's enrichment level. Dotted, dashed and solid lines show zero, one and two enriched terms at both ends of the line..... 191

Figure 4-7: Panther overrepresentation test showing the GO categories which were overrepresented in the hypocotyl disease index GEMs with

log<sub>10</sub>p > 3. Fisher's exact test with false discovery rate (FDR) multiple test correction was used. The expected number of genes based on the *Arabidopsis thaliana* reference gene list is plotted (Reference) for comparison with the number of genes found in the GEMS (DIH GEMs). Only the top 20 categories are shown here. .... 193

Figure 4-8: Panther overrepresentation test showing the GO categories which were overrepresented in the root disease index GEMs with log<sub>10</sub>p > 3. Fisher's exact test with false discovery rate (FDR) multiple test correction was used. The expected number of genes based on the *Arabidopsis thaliana* reference gene list is plotted (Reference) for comparison with the number of genes found in the GEMS (DIR GEMs). .... 194

Figure 4-9: STRING network showing significant GEMs with a role in defence. The required score was medium confidence (0.400) and FDR stringency was medium (5 percent). *Arabidopsis thaliana* gene identifiers were used. Line thickness shows the strength of data support for each interaction. The full list of genes is given in Supplementary Information 36. .... 196

Figure 4-10: *Arabidopsis thaliana* plant leaf areas at 16 days post *Rhizoctonia solani* AG2-1 inoculation. Genotypes with a significant difference (t-test, p<0.05) between the inoculated and non-inoculated plants are indicated by a bar and \*. Representative photographs of the inoculated plants are shown in Figure 4-11. .... 201

Figure 4-11: Representative photographs of inoculated *Arabidopsis thaliana* plant leaf areas at 16 days post *Rhizoctonia solani* AG2-1 inoculation. Scale bar is shown in white in the bottom right corner of each image and represents 1 cm. .... 202

Figure 4-12: Full STRING networks showing the functional partners of *Arabidopsis thaliana* A) CIPK4 and B) NAA15. The minimum required interaction score was high confidence (0.7) with a size cut-off of no more than 10 interactors. Line thickness shows the strength of data support for each interaction. NB. NAA15 is shown as EMB2753 in this diagram. .... 205

Figure 4-13: Graphs showing the log<sub>2</sub> fold change of differential gene expression of *Arabidopsis thaliana* wild-type, *cipk4* and *naa15* plants following inoculation with *Rhizoctonia solani* AG2-1 at 8, 24 and 48 hours post inoculation and network of genes relating to systemic acquired resistance (SAR). *naa15* mutants and wild-type plants show increased expression under inoculation of many genes involved in SAR, while reduced expression was seen in *cipk4* plants. Brackets and a \* show significant differences between the genotypes at each time point. .... 207

Figure 4-14: Graphs showing the log<sub>2</sub> fold change of differential gene expression of *Arabidopsis thaliana* wild-type, *cipk4* and *naa15* plants following inoculation with *Rhizoctonia solani* AG2-1 at 8, 24 and 48 hours post inoculation and network of genes relating to induced

systemic resistance (ISR). *naa15* mutants show the greatest increase in expression under inoculation, while *cipk4* often showed a reduction in expression and the responses for the wild-type plants were more variable. Brackets and a \* show significant differences between the genotypes at each time point..... 208

Figure 4-15: Protein alignment for CIPK4 genes in *Arabidopsis thaliana* and *Brassica rapa*. Protein sequences were obtained from TAIR (Huala *et al.*, 2001) and Ensembl (Howe *et al.*, 2021) and the Multiple Sequence Alignment tool used in Clustal Omega (<https://www.ebi.ac.uk/Tools/msa/clustalo/>). Mutations for TILLING lines were chosen as indicated. .... 213

Figure 4-16: Protein alignment for NAA15 genes in *Arabidopsis thaliana* and *Brassica rapa*. Protein sequences were obtained from TAIR (Huala *et al.*, 2001) and Ensembl (Howe *et al.*, 2021) and the Multiple Sequence Alignment tool used in Clustal Omega (<https://www.ebi.ac.uk/Tools/msa/clustalo/>). Mutations for TILLING lines were chosen as indicated. .... 216

Figure 4-17: Bra036868 gene map showing the mutation locations and key features for the TILLING lines. Information shown was gathered from SMART (Letunic and Bork, 2017) and NCBI conserved domains (Marchler-Bauer and Bryant, 2004) tools. Gene maps were created using SnapGene software. .... 219

Figure 4-18: Bra036869 gene map showing the mutation locations and key features for the TILLING lines. Information shown was gathered from SMART (Letunic and Bork, 2017) and NCBI conserved domains (Marchler-Bauer and Bryant, 2004) tools. Gene maps were created using SnapGene software. .... 219

Figure 4-19: Bra036870 gene map showing the mutation locations and key features for the TILLING lines. Information shown was gathered from SMART (Letunic and Bork, 2017) and NCBI conserved domains (Marchler-Bauer and Bryant, 2004) tools. Gene maps were created using SnapGene software. .... 220

Figure 4-20: Bra003565 gene map showing the mutation locations and key features for the TILLING lines. Information shown was gathered from SMART (Letunic and Bork, 2017) and NCBI conserved domains (Marchler-Bauer and Bryant, 2004) tools. Gene maps were created using SnapGene software. .... 221

Figure 4-21: Bra008474 gene map showing the mutation locations and key features for the TILLING lines. Information shown was gathered from SMART (Letunic and Bork, 2017) and NCBI conserved domains (Marchler-Bauer and Bryant, 2004) tools. Gene maps were created using SnapGene software. .... 222

Figure 4-22: Bra035184 gene map showing the mutation locations and key features for the TILLING lines. Information shown was gathered from SMART (Letunic and Bork, 2017) and NCBI conserved domains

(Marchler-Bauer and Bryant, 2004) tools. Gene maps were created using SnapGene software. .... 223

Figure 4-23: Inoculation of *Brassica rapa* TILLING lines with *Rhizoctonia solani* AG2-1. Plants were pre-germinated then inoculated in LECA particles to enable them to be removed cleanly for photographing the root symptoms. Photographs of inoculated plants at 7dpi. Scale bar indicates 1cm..... 224

Figure 4-24: Defence signalling hub centred on BAK1 (Figure 4C: Bürger and Chory, 2019). BAK1 integrates signals from BR, JA, ABA and peptide immune signalling pathways. Encircled arrows represent protein-protein interactions. .... 227



## List of Tables

Table 1-1: Host pathogenicity of anastomosis groups of <i>Rhizoctonia solani</i> associated with disease of Oilseed Rape.....	43
Table 2-1: Primers used for RT-qPCR analysis. All primers were designed using NCBI Primer-BLAST, except the PAL4 primers which were taken from (Zheng, Koopmann and von Tiedemann, 2019). .....	85
Table 3-1: University of Nottingham <i>Rhizoctonia solani</i> AG2-1 isolates. Isolates were grown on PDA plates at room temperature. ....	125
Table 4-1: Chromosome locations of the top SNPs and GEMS for disease responses identified with a $-\log_{10}P > 6.7$ significance threshold (Ray <i>et al.</i> , 2020).....	174
Table 4-2: Identification details for <i>Arabidopsis thaliana</i> mutants used in <i>Rhizoctonia solani</i> AG2-1 inoculation assay.....	175
Table 4-3: Primers used for RT-qPCR analysis. All primers were designed using NCBI Primer-BLAST, except the primers indicated by a * which were taken from Sharon <i>et al.</i> (2011).....	178
Table 4-4: <i>Brassica rapa</i> TILLING lines primers and PCR details. ....	182
Table 4-5: Gene information for genes selected from GWAS. Genes were matched to their <i>Arabidopsis thaliana</i> homolog and gene names, GO biological processes and additional descriptions were taken from	

TAIR (Huala *et al.*, 2001). Pr (>F) and log10P values for these genes  
are shown in Supplementary Information 37. .... 198

Table 4-6: Information about the selected *Brassica rapa* TILLING lines.  
..... 217

## List of Supplementary Information

Supplementary Information 1: Preparation of Vogel's media.....	263
Supplementary Information 2: Chromatogram showing peaks for d5-IAA (top) and IAA (bottom). These were extracted from samples with known concentrations of 500nM for IAA and 5000nM for d5-IAA. ....	266
Supplementary Information 3: Chromatogram showing peaks for d5-IAA (top) and IAA (bottom). These were extracted from samples with known concentrations of 10nM for IAA and 5000nM for d5-IAA. ....	267
Supplementary Information 4: Chromatogram showing peaks for d7-PAA (top) and PAA dimer (bottom). These were extracted from samples with known concentrations of 5000nM for PAA and 5000nM for d7-PAA. ....	268
Supplementary Information 5: Chromatogram showing peaks for d7-PAA (top) and PAA dimer (bottom). These were extracted from samples with known concentrations of 100nM for PAA and 5000nM for d7-PAA. ....	269
Supplementary Information 6: Analysis of the effects of <i>Rhizoctonia solani</i> AG2-1 on the root length of <i>Arabidopsis thaliana</i> Col-0 (wild type) plants.....	270

Supplementary Information 7: Analysis of the effects of <i>Rhizoctonia solani</i> AG2-1 on the root length of <i>Arabidopsis thaliana aux1</i> plants.	271
Supplementary Information 8: Analysis of the effects of <i>Rhizoctonia solani</i> AG2-1 on the root length of <i>Arabidopsis thaliana axr1</i> plants.	272
Supplementary Information 9: Analysis of the effects of <i>Rhizoctonia solani</i> AG2-1 on the number of lateral roots of <i>Arabidopsis thaliana</i> Col-0 (wild type) plants.	273
Supplementary Information 10: Analysis of the effects of <i>Rhizoctonia solani</i> AG2-1 on the number of lateral roots of <i>Arabidopsis thaliana aux1</i> plants.	275
Supplementary Information 11: Analysis of the effects of <i>Rhizoctonia solani</i> AG2-1 on the number of lateral roots of <i>Arabidopsis thaliana axr1</i> plants.	276
Supplementary Information 12: Analysis of the effects of <i>Rhizoctonia solani</i> AG2-1 on the absolute proportion of 180° of <i>Arabidopsis thaliana</i> Col-0 (wild type) plants.	277
Supplementary Information 13: Analysis of the effects of <i>Rhizoctonia solani</i> AG2-1 on the absolute proportion of 180° of <i>Arabidopsis thaliana aux1</i> plants.	279

Supplementary Information 14: Analysis of the effects of <i>Rhizoctonia solani</i> AG2-1 on the absolute proportion of 180° of <i>Arabidopsis thaliana</i> <i>axr1</i> plants. ....	280
Supplementary Information 15: Analysis of the effects of 2,4-D concentration on the root length proportion of <i>Arabidopsis thaliana</i> auxin mutant plants. ....	281
Supplementary Information 16: Analysis of the effects of PAA concentration on the root length proportion of <i>Arabidopsis thaliana</i> auxin mutant plants. ....	282
Supplementary Information 17: Analysis of the effects of NAA concentration on the root length proportion of <i>Arabidopsis thaliana</i> auxin mutant plants. ....	284
Supplementary Information 18: Analysis of the effects of 2,4-D concentration on the number of lateral roots of <i>Arabidopsis thaliana</i> auxin mutant plants. ....	285
Supplementary Information 19: Analysis of the effects of PAA concentration on the number of lateral roots of <i>Arabidopsis thaliana</i> auxin mutant plants. ....	286
Supplementary Information 20: Analysis of the effects of NAA concentration on the number of lateral roots of <i>Arabidopsis thaliana</i> auxin mutant plants. ....	287

Supplementary Information 21: Analysis of the effects of 2,4-D concentration on the angle of root growth as an absolute proportion of 180° of <i>Arabidopsis thaliana</i> auxin mutant plants.....	288
Supplementary Information 22: Analysis of the effects of PAA concentration on the angle of root growth as an absolute proportion of 180° of <i>Arabidopsis thaliana</i> auxin mutant plants.....	289
Supplementary Information 23: Analysis of the effects of NAA concentration on the angle of root growth as an absolute proportion of 180° of <i>Arabidopsis thaliana</i> auxin mutant plants.....	291
Supplementary Information 24: Analysis of the effects of 2,4-D and <i>Rhizoctonia solani</i> AG2-1 inoculation on the root growth of <i>Arabidopsis thaliana</i> auxin mutant plants.....	292
Supplementary Information 25: Analysis of the effects of PAA and <i>Rhizoctonia solani</i> AG2-1 inoculation on the root growth of <i>Arabidopsis thaliana</i> auxin mutant plants.....	294
Supplementary Information 26: Analysis of the effects of NAA and <i>Rhizoctonia solani</i> AG2-1 inoculation on the root growth of <i>Arabidopsis thaliana</i> auxin mutant plants.....	295
Supplementary Information 27: Analysis of the effects of 2,4-D and <i>Rhizoctonia solani</i> AG2-1 inoculation on the number of lateral roots of <i>Arabidopsis thaliana</i> auxin mutant plants. ....	297

Supplementary Information 28: Analysis of the effects of PAA and <i>Rhizoctonia solani</i> AG2-1 inoculation on the number of lateral roots of <i>Arabidopsis thaliana</i> auxin mutant plants. ....	298
Supplementary Information 29: Analysis of the effects of NAA and <i>Rhizoctonia solani</i> AG2-1 inoculation on the number of lateral roots of <i>Arabidopsis thaliana</i> auxin mutant plants. ....	300
Supplementary Information 30: Analysis of the effects of 2,4-D and <i>Rhizoctonia solani</i> AG2-1 inoculation on the angle of root growth as an absolute proportion of 180° of <i>Arabidopsis thaliana</i> auxin mutant plants. ....	302
Supplementary Information 31: Analysis of the effects of PAA and <i>Rhizoctonia solani</i> AG2-1 inoculation on the angle of root growth as an absolute proportion of 180° of <i>Arabidopsis thaliana</i> auxin mutant plants. ....	304
Supplementary Information 32: Analysis of the effects of NAA and <i>Rhizoctonia solani</i> AG2-1 inoculation on the angle of root growth as an absolute proportion of 180° of <i>Arabidopsis thaliana</i> auxin mutant plants. ....	305
Supplementary Information 33: Nonlinear regression analysis using a critical exponential standard curve to measure the effect of exogenous PAA concentrations on <i>Rhizoctonia solani</i> AG2-1 growth in liquid media ....	307

Supplementary Information 34: Analysis of variance for the concentrations of IAA identified by LC-MS/MS analysis from broth cultures of <i>Rhizoctonia solani</i> AG2-1.....	308
Supplementary Information 35: Analysis of variance for the concentrations of PAA identified by LC-MS/MS analysis from broth cultures of <i>Rhizoctonia solani</i> AG2-1.....	309
Supplementary Information 36: Promising candidate genes identified through GEMs analysis. Additional information from TAIR (Huala <i>et al.</i> , 2001) is shown along with the highest log <sub>10</sub> P value for the GEMs associated with these genes. ....	311
Supplementary Information 37: Pr (>F) and log <sub>10</sub> P values for the genes selected from GWAS analysis. Pr (>F) values are given for both the hypocotyl and root disease indices (DIH%, DIR%) and log <sub>10</sub> P values. These are given for all GEMs across the <i>Brassica napus</i> genomes and differentiated by the chromosome on which they were found. GEMs with a Pr (>F) value greater than 0.05 are not shown. ....	323



## Abstract

*Rhizoctonia solani* is a necrotrophic soil-borne plant pathogen species complex, of which anastomosis group (AG) 2-1 causes devastating disease on oilseed rape (OSR, *Brassica napus*). It is frequently isolated from arable crop fields where it affects establishment and yield via pre- and post-emergence damping off, hypocotyl and root rot. Genetic resistance to *R. solani* AG2-1 has not been observed and long-lived sclerotia, plus a broad host range allow the pathogen to survive in the soil for many years. Here, the interactions between *Rhizoctonia solani* AG2-1, its crop host OSR and the model organism *Arabidopsis thaliana* were explored. Variation in responses to *R. solani* were observed between commercial OSR varieties and gene expression data showed that susceptibility was associated with auxin and abscisic acid signalling, and the MYC2 branch of jasmonate signalling, while reactive oxygen species, ethylene signalling and the ERF/PDF branch of jasmonate signalling were associated with increased tolerance. This was supported by inoculation of *A. thaliana* defence mutants and microscopy using Jas9:VENUS and IAA2<sub>pro</sub>:GUS lines. Further investigations into the role of auxins in *R. solani* AG2-1 – *A. thaliana* interactions showed that *R. solani* was able to differentially affect the root architecture of WT and *aux1* transport mutants. Experiments showing the effects of 2,4-D, PAA and NAA demonstrated that PAA was able to restore gravitropism in *aux1*. *R. solani* produced both IAA and PAA when grown in broth culture and growth stimulation was

observed when *R. solani* was grown in broth with low concentrations of exogenous PAA. Analysis of gene expression markers (GEMS) from a previous genome wide association study (GWAS) provided further evidence for the involvement of auxins, jasmonates and ethylene in the defence responses of OSR to *R. solani* AG2-1. Corresponding *A. thaliana* candidate gene mutants were inoculated with *R. solani* AG2-1 under experimental conditions to identify potential susceptibility genes. Two of these were taken further and *B. rapa* TILLING line resources were developed. This thesis increases understanding of the defence pathways involved in resistance and susceptibility to *R. solani* AG2-1, examines the influence that *R. solani* has on the root architecture of auxin mutants, and provides candidate gene TILLING line resources for future work.

# Chapter 1: *Rhizoctonia solani* AG2-1 – *Brassica napus* host-pathogen interactions and control

## 1.1 Introduction

*Rhizoctonia solani* J.G. Kühn is an ubiquitous, necrotrophic, soil-borne plant pathogen that causes damping off and root rot diseases on a broad range of crops (Ogoshi, 1996; Lamichhane *et al.*, 2017). It is distributed globally and identifiable microscopically by right-angled hyphal branching with characteristic constrictions at the point of branching, septate hyphae and sclerotia of uniform texture (Sneh, Burpee and Ogoshi, 1991) (Figure 1-1). *Rhizoctonia* is found within the Cantharellales order, in the Basidiomycota division of fungi (The Royal Botanic Gardens Kew, Landare Research-NZ and Chinese Academy of Science, 2022). The *R. solani* species complex comprises thirteen anastomosis groups (AGs) based on hyphal anastomosis reactions and rDNA-ITS sequencing (Carling, Kuninaga and Brainard, 2002). Isolates of *R. solani* show considerable variation, between and within AG, in pathogenicity and virulence to host-crop species and are further classified in AG sub-divisions (Melzer *et al.*, 2016). AG2-1 is the most aggressive group of isolates to *Brassica napus* and increasing the frequency of *B. napus* in arable rotations appears to select for AG2-1 in English soils (Brown *et al.*, 2020).

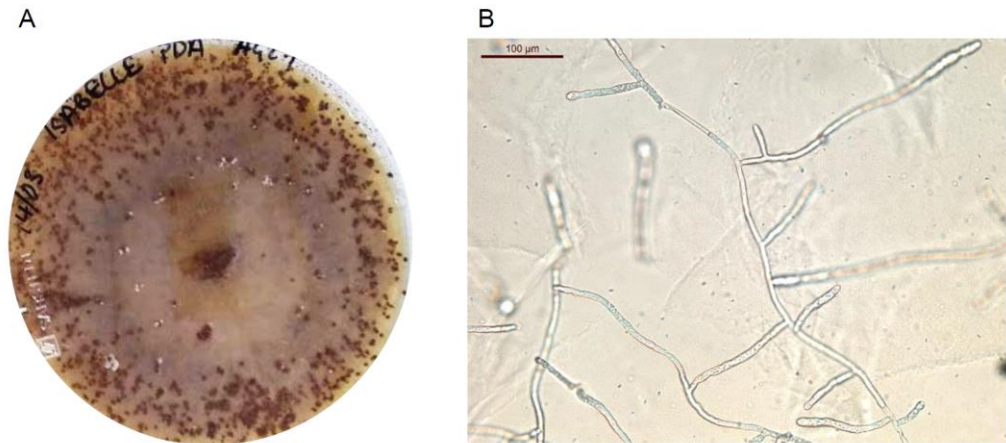


**Figure 1-1: Growth of *Rhizoctonia solani* AG2-1 in culture. A) Image of *R. solani* AG2-1 growing on PDA medium showing its colourless to yellow to brown colouration and the production of dark brown sclerotia. B) Microscope image of *R. solani* AG2-1 showing hyphal branching at right-angles with slight constriction at the branching point and a cross wall near the junction. 100µm scale bar shown.**

*Brassica napus* L., commonly known as Oilseed Rape (OSR), (n=19, genomes A and C) is the tetraploid hybrid of *B. rapa* (n=10, A genome) and *B. oleracea* (n=9, C genome). The triangle of U theory, which explains the evolution and relationships between common *Brassica* crops, demonstrates the hybridisation of *B. rapa*, *B. oleracea* and *B. nigra* in each combination to give *B. napus*, *B. juncea* and *B. carinata* (Figure 1-2) (U, 1935). This has since been validated by DNA studies (Koh *et al.*, 2017). These three species and their hybrids include crops of great economic importance such as oilseed rape, cauliflower, broccoli, cabbages, and turnips. Over 24 million tonnes of rapeseed were produced worldwide in 2019, with Canada and China being the largest producers (Food and Agriculture Organisation of the United Nations, 2022), for the production of rapeseed oil, animal feed and biofuel (biodiesel) amongst other uses. In England, 323 000 hectares of

OSR were planted in 2022 (Department for Environment Food and Rural Affairs, 2022). Estimated potential yield in the UK exceeds 6.5t/ha (Berry *et al.*, 2018), however in 2022 an average of 3.7t/ha was achieved in England (Department for Environment Food and Rural Affairs, 2022). This shortfall has not been attributed to a single factor, although there is evidence that increased cropping frequency may limit yield, potentially linked to an increased presence of soil borne diseases (Berry *et al.*, 2018). Many pests and diseases affect *B. napus*, including a range of fungal pathogens, such as *Leptosphaeria maculans*, *Leptosphaeria biglobosa*, *Pyrenopeziza brassicae*, *Sclerotinia sclerotiorum*, *Verticillium longisporum*, *Plasmodiophora brassicae*, *Alternaria* spp., *Botrytis cinerea*, *Erysiphe cruciferarum*, and *Rhizoctonia solani* (Berry *et al.*, 2018).

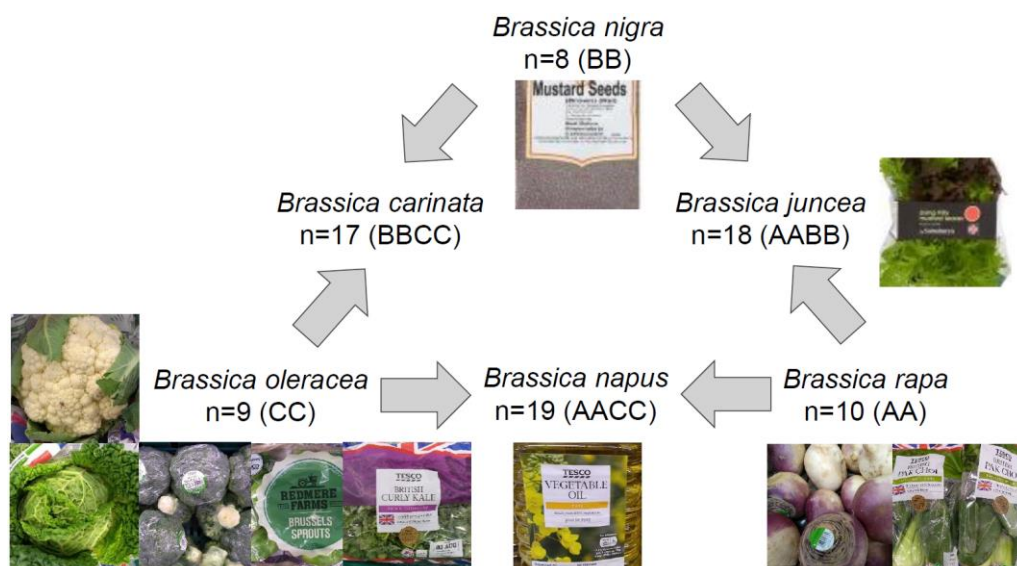


**Figure 1-2: The triangle of U and *Brassica* crop products. The triangle of U shows the genetic and evolutionary relationships between common *Brassica* spp.. Images of commonly available products are shown and chromosome number and genomes indicated below species names.**

**(Adapted from U, 1935).**

## 1.2 Oilseed rape diseases

*Leptosphaeria maculans* and *Leptosphaeria biglobosa* are the causal pathogens of Phoma leaf spot and Phoma stem canker (also known as blackleg). Airborne ascospores infect the leaves of young, susceptible plants, where *L. maculans* typically causes tawny-coloured spots with dark pycnidia, while *L. biglobosa* usually causes darker spots with fewer (if any) pycnidia (Fitt *et al.*, 2006). The pathogen then grows through the leaf petiole to the stem where canker symptoms form around the leaf scars at the stem-base. *L. maculans* typically causes relatively severe stem-base cankers while *L. biglobosa* tends to develop less damaging lesions on the upper stem (Fitt *et al.*, 2006). Lesions can develop and girdle the stem, which restricts water and nutrient transport, causing premature ripening and lodging. Flowers, buds and pods can also be affected, with pods showing brown lesions with pycnidia and a black margin. UK losses are estimated at €56 million per season (Fitt *et al.*, 2006)

*Pyrenopeziza brassicae* causes light leaf spot, with symptoms including light green circular lesions on leaf surfaces, with small, white spore masses (Dewage *et al.*, 2018). The lesions later become more discrete with pink-tinged centres. Affected leaves can curl, distort, become brittle and crack. Black flecking can be seen in resistant varieties. On stems and lateral branches, elongated fawn lesions, surrounded by black speckling form, which can develop horizontal cracks. Pods can be

affected, turning brown and shattering. Yield losses can reach £160 million per year in England (Dewage *et al.*, 2018).

*Sclerotinia sclerotiorum* causes Sclerotinia stem rot. Ascospores infect senescing petal tissue, which stick to leaves, where the pathogen can then infect and move to the stems, forming large white-grey lesions. Sclerotia are formed within the stems, disrupting water and nutrient transport, and allowing the pathogen to persist in soil after the crop has been harvested (Derbyshire and Denton-Giles, 2016). Verticillium stem stripe is caused by *Verticillium longisporum* and is characterised by dark unilateral stripes on the stems of otherwise healthy-looking plants, and the presence of microsclerotia in the stem cortex. Microsclerotia survive in the soil, and then infect the roots of the next crop, growing asymptotically within the plant until crop ripening, when stem stripe symptoms appear (Depotter *et al.*, 2016). Clubroot is caused by the protist *Plasmodiophora brassicae*. *P. brassicae* infection leads to the development of root tumours, which disrupts water and nutrient uptake, leading to wilting and stunting. In severe cases, total yield loss can occur (Struck, Rüsck and Strehlow, 2022).

### 1.3 *Rhizoctonia solani* isolate pathogenicity, disease symptoms and significance

The heterogeneity of *R. solani* isolates has long been categorised by AG classification based upon anastomosis reactions, morphology, virulence, host range and biochemistry (Carling, Kuninaga and

Brainard, 2002). Traditional classification uses hyphal fusion reactions, or anastomosis, of unknown isolates with “tester” strains. Observations of the three types of hyphal fusion (perfect, imperfect and contact) inform whether the isolate is the same AG as the tester strain or not (Sneh, Burpee and Ogoshi, 1991). Sequence similarity of the rDNA-internal transcribed spacer (ITS) regions has also been used alongside more traditional hyphal anastomosis reactions and virulence testing methods (Carling, Kuninaga and Brainard, 2002). As a multinucleate heterokaryon, genome sequencing for *R. solani* has been challenging, but draft genome sequences have now been published for AG1-1A (Zheng *et al.*, 2013; Nadarajah *et al.*, 2017), AG1-1B (Wibberg *et al.*, 2013), AG2-2IIIB (Wibberg *et al.*, 2016), AG3 (Cubeta *et al.*, 2014), AG4 (Zhang *et al.*, 2021) and AG8 (Hane *et al.*, 2014). A comparison of the first genomes published for AG1-1A, AG3 and AG8 found the sequences to be syntenic and co-linear (Hane *et al.*, 2014). Further investigations compared sequences for AG1-1A, AG1-1B, AG2-2IIIB, AG3 and AG8 and found only 52 predicted shared secreted proteins, with each isolate’s sequence having 199 to 473 predicted unique secreted proteins (Wibberg *et al.*, 2016). This suggests a high degree of variation in the behaviour of different AGs and reflects the diversity of *R. solani* seen in the field. These genomes are crucial to understanding pathogenicity and virulence genes in *R. solani* and how different AGs infect different crops. Isolates of AG2-1 from OSR have not yet been sequenced but will provide a key resource in developing understanding of this pathogen.



Disease symptoms caused by *R. solani* on OSR include pre- and post-emergence damping off, crown rot and root rot (Melzer *et al.*, 2016). Pre-germination damping off causes seeds to rot and die and is associated with losses in seedling emergence that decrease logarithmically with increasing inoculum density (Zhou *et al.*, 2014). Post-emergence damping off leads to seedlings dying soon after germination (Figure 1-3A). Root rot presents as dark brown lesions, which can lead to the severing of roots at the site of the lesion (Figure 1-3B) (Khangura, Barbetti and Sweetingham, 1999). Root rot can be difficult to assess on plants grown in the field, because the roots often break when the plant is removed from the ground. High resolution X-ray micro Computed Tomography (X-ray  $\mu$ CT) showed significant reductions in OSR root system volume and surface area under *R. solani* AG2-1 inoculation (Sturrock *et al.*, 2015). Hypocotyl rot manifests as dark brown water-soaked lesions on the hypocotyls (Figure 1-3C). Infected plants may also show “wire stem” symptoms where the stem tissue near the soil thins until it is unable to support the plant (Figure 1-3D). Post-germination losses are caused by a reduction in establishment and root rot in mature plants. Finally, *R. solani* causes delayed flowering of OSR, leading to uneven seed maturation and yield losses (Ray *et al.*, 2020; Jayaweera and Ray, 2022).

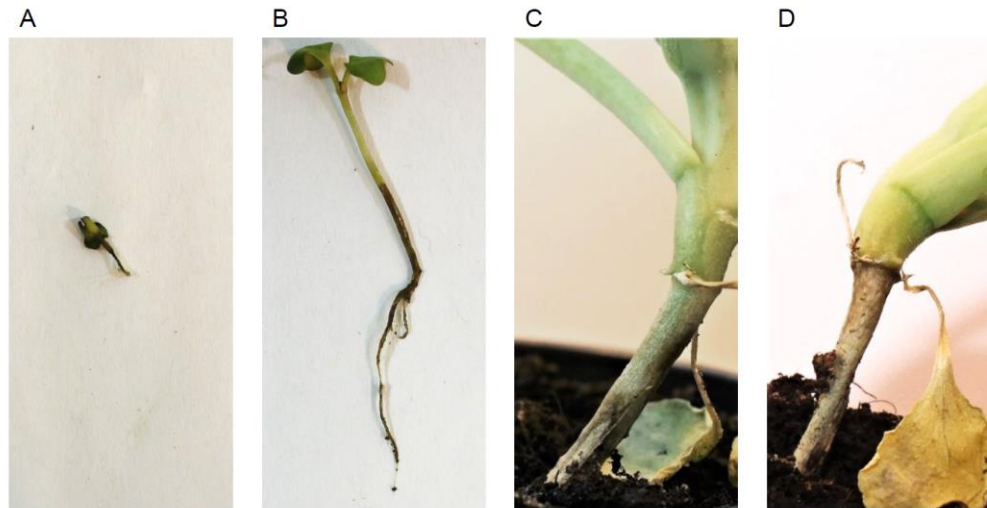


**Figure 1-3: *Rhizoctonia solani* AG2-1 symptoms on Oilseed Rape (OSR). A) Post-germination damping-off causing death of a highly susceptible OSR seedling, B) hypocotyl and root rot of an OSR seedling, which can lead to post-emergence damping-off, C) necrotic lesion on a young OSR plant, D) wirestem of a young OSR plant.**

Multiple AGs of *R. solani* cause disease in OSR (Table 1-1 **Error! Reference source not found.**) but AG2-1 contains the most aggressive isolates to *B. napus* seedlings (Khangura, Barbetti and Sweetingham, 1999; Tewoldemedhin *et al.*, 2006; Babiker *et al.*, 2013; Melzer *et al.*, 2016). AG2-1 isolates are most commonly identified in OSR plants infected with *R. solani* (Kataria and Verma, 1992; Khangura, Barbetti and Sweetingham, 1999; Broders *et al.*, 2014; Melzer *et al.*, 2016). In contrast to AG2-1 causing predominantly seedling disease, AG4 is associated with severe disease in mature plants and does not affect emergence and establishment to the same extent as AG2-1. Thus, the number of seedlings surviving AG4 inoculation has been shown to be significantly higher compared to AG2-1, but AG4 caused more severe symptoms in the survivors (Teo *et al.*, 1988). AG8 is also pathogenic to *B. napus* seedlings and capable of

initiating severe root and hypocotyl rot (Khangura, Barbetti and Sweetingham, 1999). AG10 isolates have been associated with mild hypocotyl rot in *Brassica* spp. under favourable conditions (MacNish *et al.*, 1995).

**Table 1-1: Host pathogenicity of anastomosis groups of *Rhizoctonia solani* associated with disease of Oilseed Rape.**

<u>Anastomosis group</u>	<u>Isolate origin</u>	<u>Pathogenicity</u>	<u>References</u>
2-1	Western Australia, South Africa, Canada, England	√√	(Khangura, Barbetti and Sweetingham, 1999; Tewoldemedhin <i>et al.</i> , 2006; Melzer <i>et al.</i> , 2016; Brown <i>et al.</i> , 2020)
2-2	South Africa, Canada	√√	(Tewoldemedhin <i>et al.</i> , 2006; Melzer <i>et al.</i> , 2016)
3	South Africa	√	(Tewoldemedhin <i>et al.</i> , 2006)
4	South Africa, Canada	√√	(Tewoldemedhin <i>et al.</i> , 2006; Melzer <i>et al.</i> , 2016)
8	Western Australia	√√	(Khangura, Barbetti and Sweetingham, 1999)
10	Western Australia	√	(MacNish <i>et al.</i> , 1995; Khangura, Barbetti and Sweetingham, 1999)
11	South Africa, Canada	√ to √√	(Tewoldemedhin <i>et al.</i> , 2006; Melzer <i>et al.</i> , 2016)

√√ pathogenic, √ weakly pathogenic, X non-pathogenic; ranges are given where papers have reported different results.

A study investigating the prevalence of *R. solani* in Canada found that most fields were infested by root rot to some extent in the Peace River region of Alberta, with up to 100% of OSR and canola plants infected with *R. solani* AG2-1 and in places a nearly complete loss of plant stands (Kataria and Verma, 1992). Root rot was estimated to cause a yield loss of 30% in 1983 and 1984 in the Peace River region of

Canada, with 59% of soil isolates identified as AG2-1 (Kataria and Verma, 1992). Studies in Finland observed variable necrotic lesions at stem bases in 4.5% of assessed *B. rapa* and *B. napus* (combined) plants in 1984-1989, compared to 17.3% in 2007-2009, while root rot increased from 0.5% to 22.0% in the same time period (Hannukkala *et al.*, 2016). The worst affected fields had 76.1% of plants affected by stem lesions and 94.7% of plants with blackened roots (Hannukkala *et al.*, 2016). Although *R. solani* AG2-1 was isolated from almost all fields in this study, it co-occurred with *Fusarium avenaceum*, *F. sambucinum*, *F. graminearum*, *F. tricinctum*, *F. oxysporum* and *Thielaviopsis basicola* in >60% of fields so it cannot be concluded that these symptoms were solely due to *R. solani* infection (Hannukkala *et al.*, 2016). Brown girdling root rot caused by *R. solani* (AG not specified) has been assessed as having a significant impact on single plant yield loss in *B. rapa*, causing a 17% reduction on plants with girdling and sinking lesions, and a 65% reduction on plants with decayed taproots (Klein-Gebbinck and Woods, 2002). More recently, *R. solani* AG2-1 was detected in 63% of English wheat fields tested (the predominant *Rhizoctonia* spp. identified) (Brown *et al.*, 2020) and *R. solani* AG2-1 inoculation in a field environment was been shown to reduce OSR establishment by 61% and yield by 41% (Jayaweera and Ray, 2022).

## 1.4 Host-pathogen interactions for *Rhizoctonia solani*

### 1.4.1 Survival, lifecycle and infection process

The disease life cycle of *R. solani* is shown in Figure 1-4 **Error!** **Reference source not found.** and a flow chart summarising the infection process is shown in Figure 1-5. *R. solani* fungal mycelium survives on seeds, plant debris, or as mycelium and sclerotia in the soil. Although sclerotia are often described as long-lived, work by Ritchie *et al.* showed that only 20% of *R. solani* AG3PT sclerotia were viable after 18 months buried in field plots (2013). It is likely that the long-term survival of *R. solani* in soil is also linked to saprophytic growth, and the infection of alternative hosts, such as weed species. This survival ensures that when a susceptible host is introduced to the field, the pathogen is already present, lying dormant in the soil or on seeds and plant debris (Yulianti, Sivasithamparam and Turner, 2006). The ability of *R. solani* AG2-1 to survive as a facultative saprophyte was demonstrated by a study investigating *Brassicaceae* green manures and showing that the addition of green manures to the soil provided a nutrient base for the pathogen leading to increased survival and disease severity in subsequent crops (Yulianti, Sivasithamparam and Turner, 2006).

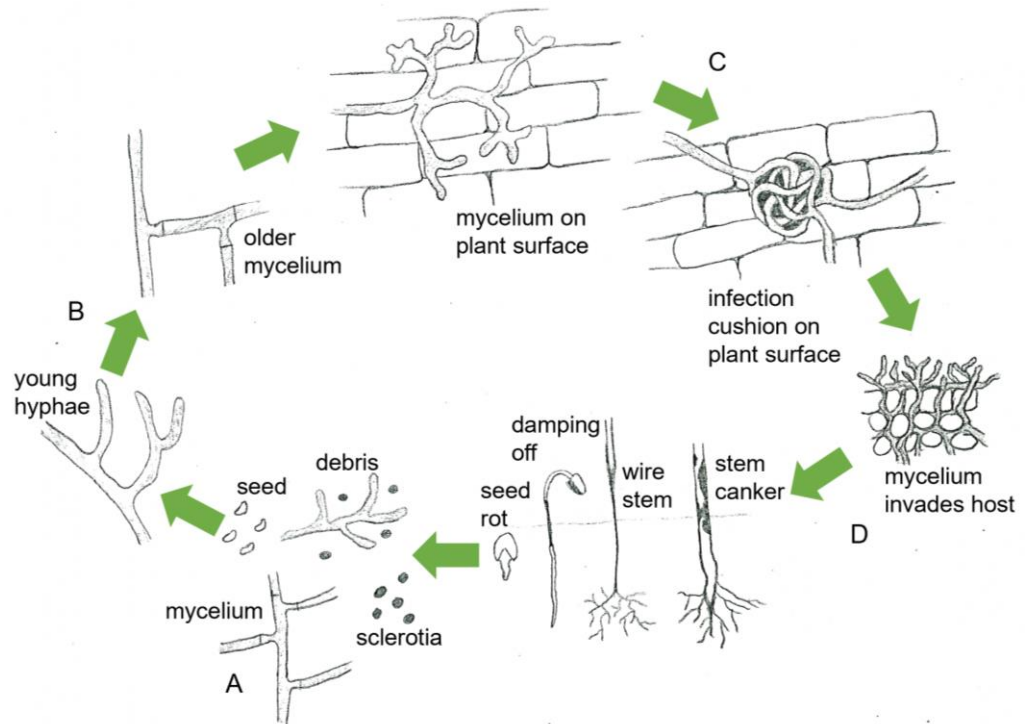


**Figure 1-4: Life cycle of *Rhizoctonia solani*. A) In the absence of a susceptible host, fungal mycelium survives on seeds, plant debris, or as mycelium and sclerotia in the soil. B) Young hyphae grow and mature into mycelium with characteristic right-angled branching and constriction near nodes. C) Mycelium grows across the plant surface before forming an infection cushion. D) Invasion of the host causes necrosis and symptoms such as seed rot, damping off, wire stem and cankers. (Adapted from Agrios, 2005)**

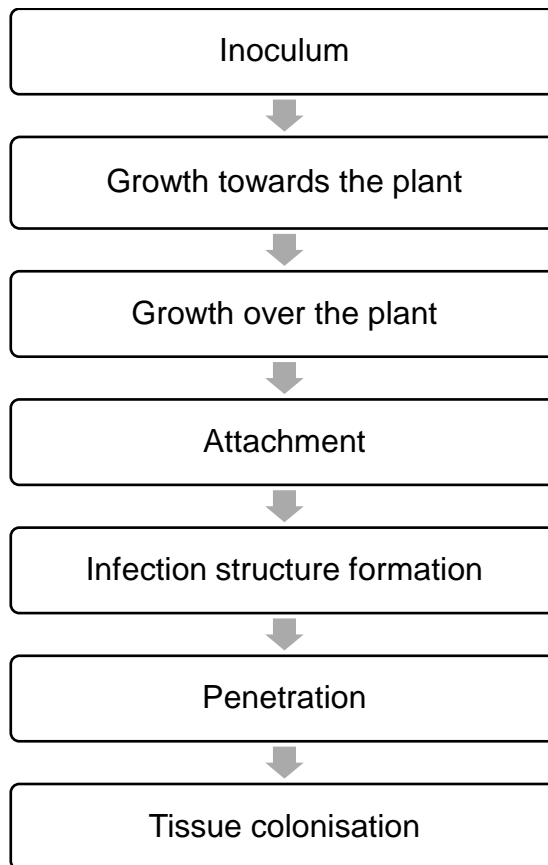


**Figure 1-5: Flow chart summarising the infection process of *R. solani*. Adapted from (Keijer, 1996).**

Sclerotia germination is moisture and temperature dependent and produces mycelial threads which grow towards the plant host.

Microscopic observations of *R. solani* AG2-1 growing on OSR show young hyphae originating from sclerotia growing rapidly across plant root tissues (Figure 1-6A). Characteristic right-angled branching is seen, with many hyphae growing parallel to the longitudinal axis of the hypocotyl or root (Figure 1-6B) (Kataria and Verma, 1992; Verma, 1996). Mucilage-like material has been observed attaching the fungal hyphae to the plant epidermis (Matsuura, 1986).

Following hyphal growth over the hypocotyl and root, specialised infection structures are formed, known as infection cushions (Figure 1-6C). These compact, dome-shaped cushions are created by coiled, overlapping hyphae, which develop numerous penetration pegs on the underside of the infection cushion (Kataria and Verma, 1992). Infection cushions have been observed on both susceptible (OSR) and resistant (mustard) hosts, although they are observed more frequently and sooner after inoculation on the susceptible hosts (Verma, 1996). Penetration pegs develop from the flattened cells of the infection cushion base that are in contact with the epidermis. Multiple invasions occur at each infection cushion site (Matsuura, 1986; Armentrout, 1987). Penetration pegs can use mechanical pressure, enzymatic destruction of host material or both to penetrate cells.

The hymenia of the teleomorph (sexual reproductive stage) of *R. solani*, *Thanatephorus cucumeris* (A.B. Frank) Donk, have been observed on sugar beet, where they preceded foliar blight symptoms (Windels, Kuznia and Call, 1997). The hymenial layer appeared as a white to grey, superficial, dusty growth on petioles. The anamorphs of these isolates were identified as *R. solani* AG3 and AG5 (Windels, Kuznia and Call, 1997).



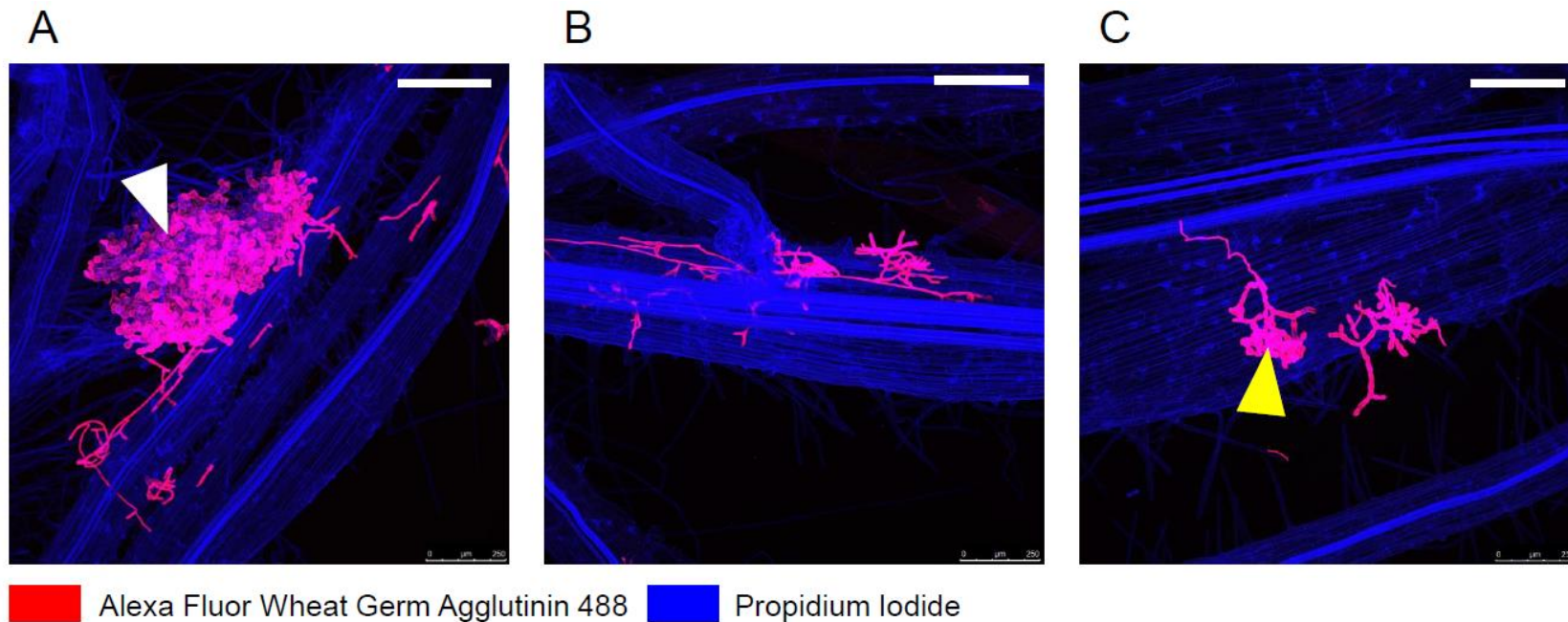


**Figure 1-6: Confocal microscopy images showing *Rhizoctonia solani* AG2-1 infection on *Brassica napus*. A) Germination of *R. solani* AG2-1 sclerotia on roots of *B. napus*; B) hyphal growth over root tissues; and C) development of an infection cushion. Plants were grown on water agar plates and *R. solani* sclerotia was placed close to the root tissue. Samples were taken 48hours after the addition of sclerotia, and were stained using Alexa Fluor Wheat Germ Agglutinin 488, and Propidium Iodide. The roots of *B. napus* are shown in blue and the sclerotia and hyphae of *R. solani* are shown in red/pink. The sclerotia in (A) is indicated with a white arrow, and the infection cushion in (C) with a yellow arrow. White scale bars are shown in the top right corner of the images and represent 250 $\mu$ m.**

The release of phytotoxins and cell wall-degrading enzymes (CWDEs) is linked to the development of disease symptoms prior to hyphal colonisation (Ajayi-Oyetunde and Bradley, 2018). CWDEs can be needed both for hyphal penetration and the release of nutrients from host tissues. *R. solani* AG1-1A is known to produce the CWDEs polygalacturonase, polymethyl-galacturonase, cellulase and  $\beta$ -glucosidase (Xue *et al.*, 2018). Polygalacturonase and polymethyl-galacturonase break down pectate and pectin by hydrolysis respectively. Proteomics analysis of *R. solani* AG8 infection on wheat roots identified novel small cysteine rich proteins, CWDEs and proteins with redox related functions (Anderson *et al.*, 2016). Volatile organic compounds (VOCs) released by *R. solani* promoted the growth and development of *A. thaliana*, however, priming with fungal VOCs did not impact disease severity when the plant was later inoculated (Cordovez *et al.*, 2017). Studying these initial stages of host-pathogen interactions can be challenging because the compounds are released at a biologically significant (low) concentration in a targeted manner, which can be difficult to replicate experimentally.

#### 1.4.2 Hormonal and cellular responses

The interplay between phytohormones and cellular responses during *R. solani* infection is currently unclear. Phytohormones are central to the control of growth, development, and responses to the environment. They include salicylic acid (SA), jasmonic acid (JA), ethylene (ET), abscisic acid (ABA), auxins, cytokinins, gibberellins, and

brassinosteroids (BR) (Denancé *et al.*, 2013). These act within complex networks, and the balance between the control of growth and the activation of defence responses allows the plant to limit defence-associated fitness costs (Denancé *et al.*, 2013). Hormone signalling pathways have been traditionally divided into Systemic Acquired Resistance (SAR) and Induced Systemic Resistance (ISR). SAR is typically induced in response to biotrophic pathogens that require live host tissue, is positively regulated by SA and its derivatives and is associated with PR proteins (Sharon, Freeman and Sneh, 2011; Denancé *et al.*, 2013). ISR is usually triggered by rhizobacteria, necrotrophic fungi and insects and depends on JA, its derivatives and ET (Sharon, Freeman and Sneh, 2011; Denancé *et al.*, 2013). There are however exceptions where JA/ET is essential to a biotrophic response and when SA is essential to a necrotrophic pathogen response (Denancé *et al.*, 2013). Necrotrophic resistance in *A. thaliana* has been shown to be impaired in *ein2-5*, *coi1-1* and *sid2-1* mutants, which are defective in ET, JA and SA signalling respectively (Llorente *et al.*, 2008) suggesting that multiple hormone pathways are required for resistance to necrotrophs.

In *A. thaliana*, SA is synthesised via two pathways, using either the isochorismate (IC) or phenylalanine ammonia-lyase (PAL) pathways (Dempsey *et al.*, 2011). The IC pathway is predominant and localised to the chloroplast (Dempsey *et al.*, 2011). It requires salicylic acid induction deficient 2 (SID2, also known as ICS1), which is activated upon pathogen infection and recognition (Denancé *et al.*, 2013). NPR1

(non-expressor of PR genes 1) is a SA receptor that forms a complex in the cytosol, and when activated, dissociates and the monomers translocate to the nucleus where they activate the transcription of genes such as pathogenesis-related (PR) genes, through their interaction with TGA transcription factors (Denancé *et al.*, 2013; Backer, Naidoo and van den Berg, 2019). Previously, transgenic rice lines were generated with NPR1 expression in green tissues, which activated defence-related PR genes and showed increased resistance to *R. solani* AG1-1A (Molla *et al.*, 2016).

SA and JA have a complex relationship and have long been thought to act antagonistically. WRKY33 acts at the interface between the two hormones as it is a positive regulator for JA-related genes but a repressor of the SA pathway (Denancé *et al.*, 2013). In *wrky33* mutants, many key SA genes show enhanced expression and SA is accumulated, increasing the plants susceptibility to necrotrophic fungi (Denancé *et al.*, 2013).

ET has been shown to regulate resistance to necrotrophic fungi such as *B. cinerea*, *Plectosphaerella cucumerina*, *Fusarium oxysporum* f. sp. *conglutinans* and *F. oxysporum* f. sp. *lycopersici*, via the *A. thaliana* transcription factor ethylene response factor 1 (ERF1) (Berrocal-Lobo and Molina, 2004). Work on *F. oxysporum* indicated that the SA, JA and ET signalling pathways are all required for effective resistance in *A. thaliana*, indicating a complex defence response (Berrocal-Lobo and Molina, 2004). The ability of phytohormones to act positively or

negatively together appears to depend upon the pathogen involved in triggering the defence response (Berrocal-Lobo, Molina and Solano, 2002). ERF1 is known to act downstream of ET and JA defence responses (Berrocal-Lobo and Molina, 2004).

ABA is an isoprenoid compound involved in the regulation of development and abiotic stress responses that is also involved in biotic stress responses (Denancé *et al.*, 2013). ABA-mediated signalling pathways have been shown to increase resistance to the soil-borne pathogens *Ralstonia solanacearum* and *Pythium irregulare* (Llorente *et al.*, 2008). *A. thaliana* ABA-deficient mutants (such as *aba2*) and ABA-signalling mutants (such as *abi1*) were found to negatively regulate necrotrophic pathogen resistance as the mutants were more resistant than wild-type plants (Llorente *et al.*, 2008). *R. solani* has been observed producing ABA (Dörffling *et al.*, 1984) though it is not known how it may act as a virulence factor. ABA may repress or interact negatively with SA, JA and ET, affecting the control of pathogen resistance (Denancé *et al.*, 2013).

Auxins such as indole-3-acetic acid (IAA) and phenylacetic acid (PAA) are known to regulate many aspects of plant development as well as having both direct and indirect effects on resistance responses (Denancé *et al.*, 2013). *A. thaliana* auxin signalling mutants *axr1*, *axr2*, and *axr6* show an increased susceptibility to necrotrophic fungi including *P. cucumerina* and *B. cinerea* (Llorente *et al.*, 2008), however *axr1*, *axr2* and *axr3* mutants showed increased resistance to *F.*

*oxysporum* (Denancé *et al.*, 2013). This may reflect differences in the pathogen's lifestyle. It has been seen in *A. thaliana* that SA treatment can stabilise auxin/IAA proteins, which leads to the down-regulation of auxin-related genes and reflects the hypothesis that auxin signalling is part of the SA-mediated resistance (Denancé *et al.*, 2013). PAA shows more activity stimulating the induction of lateral roots compared to IAA (Cook, 2019), which may make it more relevant in responses to soil-borne pathogens. It has been shown to be elevated in roots inoculated with arbuscular mycorrhizal forming fungi (Cook, 2019).

Phytoalexins are inducible, low molecular weight antimicrobial metabolites such as flavonoids, terpenoids and indoles, which are synthesised in response to a pathogen attack (Zhou, Tootle and Glazebrook, 1999). Camalexin is produced in *A. thaliana* and PAD3 is required for its biosynthesis (Zhou, Tootle and Glazebrook, 1999). The phytoalexins isalexin, brassicanate A, rutalexin, brassinin, 1-methoxybrassinin, spirobrassinin, brassicanal A and brassilexin have been isolated from *B. napus* ssp. *rapifera* (rutabaga), and brassicanal A and brassicanate A were both able to inhibit the growth of *R. solani* AG2-1 (Pedras, Montaut and Suchy, 2004). Cyclobrassinin and cyclobrassinin sulfoxide were also identified in *B. napus* and have been studied in relation to *L. maculans* (Pedras, Zheng and Sarma-Mamillapalle, 2007). Many necrotrophs have shown an ability to detoxify or sequester plant defence compounds such as phytoalexins (Westrick, Smith and Kabbage, 2021), including the ability of *R. solani* AG2-1 to detoxify camalexin (Pedras and Liu, 2004).

Colonisation of *A. thaliana* by hypovirulent binucleate isolates of *Rhizoctonia* (Ru18-1, Ru89-1 [AG-B(o)], Rh521, and Ru56-8 (AG-A)) resulted in increased expression of the genes PR5, PDF1.2, lipoxygenase (LOX)2, LOX1, coronatine induced-3 (CORI3) and phytoalexin-deficient 3 (PAD3), suggesting the involvement of the Systemic Acquired Resistance (SAR), Induced Systemic Resistance (ISR) and phytoalexin production pathways (Sharon, Freeman and Sneh, 2011). However, another study tested *Arabidopsis* ecotypes and mutants (including those defective in auxin, camalexin, salicylic acid, abscisic acid, ethylene and jasmonic acid) with *R. solani* AG8, and found no variation in responses (Foley *et al.*, 2013). The purinoceptor P2K1 (also known as DORN1), which recognises extracellular ATP released by wounding or necrosis (a Damage-Associated Molecular Pattern or DAMP), has been linked to *R. solani* AG2-1 and AG8 resistance in *A. thaliana* (Kumar *et al.*, 2020). Plants with overexpression of P2K1 showed stronger growth and increased expression of PR1, PDF1.2 and jasmonate zim domain 5 (JAZ5) following AG8 inoculation, while its mutant *dorn1-3* showed a significant growth reduction and a reduced expression of the same genes (Kumar *et al.*, 2020). This indicated the involvement of both the salicylate and jasmonate defence signalling pathways in resistance, and the potential for DAMP-mediated defence (Kumar *et al.*, 2020). The diversity of *R. solani* AGs with virulence to different hosts suggests that defence pathways vary for host – *R. solani* AG compatible interactions.

### 1.4.3 *Rhizoctonia solani* causes acidic and oxidative stress

Phenyl acetic acid (PAA) is a natural auxin, which has an overlapping regulatory role with the more well-studied auxin, indole-3-acetic acid (IAA) (Sugawara *et al.*, 2015). PAA and its derivatives have previously been shown to be produced by *R. solani* AG3 and AG4 and investigated as virulence factors in host-pathogen interactions (Iacobellis and DeVay, 1987; Bartz *et al.*, 2012). Necrosis was induced in up to 85% of the root system of tomato seedlings when grown in medium containing PAA or its derivatives and the injection of PAA into tomato seedling stems led to the development of cankers (Bartz *et al.*, 2012). A correlation was also observed between PAA production in isolates of *R. solani* and the mortality of infected seedlings (Bartz *et al.*, 2012). It remains unknown if all *R. solani* AGs produce PAA and thus may be able to manipulate host growth and development or initiate more severe disease.

Oxalic acid (OA) is widely produced and secreted by soil-borne fungi, and can play a role in pathogenesis (Dutton and Evans, 1996). The accumulation of OA acidifies host tissues, sequestering calcium to form calcium oxalate crystals, and weakening the host cell walls, which promotes degradation by polygalacturonase (Dutton and Evans, 1996). Low quantities of OA have been reported during the growth of *R. solani* AG2-1 in culture, and calcium oxalate crystals have formed on infected OSR tissues (Yang, Tewari and Verma, 1993). Crystals were more



abundant in severely infected tissues, and increased in number as the infection progressed (Yang, Tewari and Verma, 1993).

Reactive oxygen species (ROS) are also involved in mediating a defence response to pathogens. ROS include singlet O<sub>2</sub>, hydroxyperoxyl radical (HO<sub>2</sub>·), superoxide anion (O<sub>2</sub><sup>·-</sup>), hydroxyl radical (OH·), hydrogen peroxide (H<sub>2</sub>O<sub>2</sub>) and superoxide radical (O<sub>2</sub><sup>-</sup>) (Wang *et al.*, 2016). NADPH oxidases (NOX) generate ROS through the catalysis of superoxides and can produce ROS in response to pathogens (Sagi and Fluhr, 2006; Foley *et al.*, 2013), including promoting the establishment of SAR (Wang *et al.*, 2016). Expression of respiratory burst oxidase homolog (RBOH) genes that code for NOX is tissue specific with RBOHA-G and I occurring in the roots of *A. thaliana* (Sagi and Fluhr, 2006). Extracellular ROS can be involved in the oxidative cross-linking of cell wall components during defence but can also have depolymerisation properties that result in cell loosening preceding cell wall expansion (Sagi and Fluhr, 2006). Intracellularly, ROS concentration is key; at a low concentration ROS can act as signalling molecules during stress responses, and at a high concentration can lead to the induction of programmed cell death (PCD), including during the hypersensitive response (Wang *et al.*, 2016).

RBOHC is induced in response to *B. cinerea* and RBOHD is induced in response to chitin (Sagi and Fluhr, 2006). It is known that *rboh*d and *rboh*f mutants generate less H<sub>2</sub>O<sub>2</sub> and are more susceptible to pathogens (Wang *et al.*, 2016) and indeed the *A. thaliana* double

mutant *rbohF rbohD* shows an almost complete loss of resistance to *R. solani* AG8 (Foley *et al.*, 2013). Germin-like proteins (GLPs) have sequence similarity to characterised germin enzymes, which reduce the toxic effects of OA and produce hydrogen peroxide (H<sub>2</sub>O<sub>2</sub>) (Foley *et al.*, 2016). The sugar beet germin-like protein 1 (*BvGLP1*) gene has been shown to confer partial resistance to *R. solani* AG2-1 when transferred to *Arabidopsis thaliana* (Knecht *et al.*, 2010). Elevated H<sub>2</sub>O<sub>2</sub> and a reduction in fungal hyphae were observed in *A. thaliana* with *BvGLP1*, as well as the activation of pathogenesis related proteins PR1, PR4 and plant defensin PDF1.2 (Knecht *et al.*, 2010). A study investigating the responses of *R. solani* AG8 during infection of wheat, showed the induction of the *R. solani* OAH (oxaloacetate acetylhydrolase) gene, which is homologous to genes involved in the production of OA (Foley *et al.*, 2016). At the same time point, two GLP genes were strongly induced in the infected wheat plants (Foley *et al.*, 2016). *OAH1* has previously been characterised in *Sclerotinia sclerotiorum*, and was required for OA accumulation (Liang *et al.*, 2015). *ss-oah1* mutants were defective in appressorium development and produced limited lesions in wound inoculated pathogenicity testing (Liang *et al.*, 2015). H<sub>2</sub>O<sub>2</sub> accumulation and callose deposition were indicated at the infection front of hosts infected with *ss-oah1* suggesting elevated host defences (Liang *et al.*, 2015). Proteomics analysis identified an over-representation of oxidoreductase and antioxidant activity in *R. solani* AG8 culture filtrate samples, which could be linked to limiting the effects

of plant-based ROS on the fungus, or to manipulate ROS levels in the plant for pathogenesis (Anderson *et al.*, 2016).

A simple mechanism of infection is not expected in *R. solani* and there are likely to be complex, dynamic host-pathogen interactions that support or resist disease development. Although *R. solani* as a complex possesses broad host range, adaptation of pathogenicity strategies for specific hosts appears to be associated with individual AGs.

## 1.5 Disease management

Current management strategies rely on cultural methods and fungicides to provide effective disease reduction (Kataria and Verma, 1992; Babiker *et al.*, 2013) though there is potential to incorporate biological controls. *R. solani* is also affected by soil properties such as texture and nutrition, knowledge of which can offer a role in soil and disease management planning.

### 1.5.1 Soil, temperature, moisture and nutrition effects

Studies using *R. solani* AG2-1 and AG4 have shown that mycelial spread was affected by soil bulk-density, the size of aggregates and of air-filled pore spaces (Otten *et al.*, 2001, 2004; Sturrock *et al.*, 2015). Furthermore, *R. solani* soil colonisation in the absence of a host is substantially influenced by soil type and texture. Growth of AG4 and AG8 was shown to be limited in clay soils when compared to sandy soils (Gill, Sivasithamparam and Smettem, 2000; Harries *et al.*, 2020).

Studies using wheat also showed greater disease severity in sandy soils compared to loamy sand and sandy clay soils (Gill, Sivasithamparam and Smettem, 2000). AG8 was more aggressive to wheat roots in sandy soils compared to silty loam soils (Mahoney *et al.*, 2016). Increased soil compaction limited pathogen growth and resulted in smaller, denser AG4 colonies (Otten *et al.*, 2001). However, the lowest AG2-1 disease severity was observed in soils with high porosity around the seedling, which had a beneficial effect on shoot and root growth of the host (Gill, Sivasithamparam and Smettem, 2000; Sturrock *et al.*, 2015).

Ambient temperature influences the growth of the host and the severity of disease caused by *R. solani*, and this varies between AG. For example, lower temperatures favour AG2-1 seedling disease because the emergence of *Brassica* seedlings is also slower in cooler temperatures (Kataria and Verma, 1992). Indeed, AG2-1 has been shown to be most virulent to *B. napus* at cooler temperatures (7-12°C night-day air temperature), causing greater pre-emergence damping-off than AG4 at a range of inoculum densities (0 to 22 800 viable propagules per litre of soil-free growth medium) (Teo *et al.*, 1988). In contrast, AG4 was favoured by warmer temperatures (26-35°C), causing greater pre-emergence damping-off than AG2-1 at all inoculum densities (Teo *et al.*, 1988). Similarly to AG2-1, *R. solani* AG8 has been shown to cause root rot at low temperatures (6-19°C) with the most severe disease at 10°C on winter wheat (Smiley and Uddin, 1993; Gill, Sivasithamparam and Smettem, 2000).

Research on the effect of soil moisture on *R. solani* infection is inconsistent. It has been observed previously that high rainfall and high soil moisture (equivalent to 500-700mm of water) compared to medium or low soil moisture (equivalent to 130-300mm of water) were more favourable for *R. solani* development (Teo *et al.*, 1988; Kataria and Verma, 1992), while other studies have shown that low soil moisture favours *R. solani* infection (Ploetz and Mitchell, 1985). Hwang *et al.* (2014) showed that four times more inoculum was required to reduce canola emergence by 53% under dry conditions (no significant (>10mm) rainfall events during three weeks following sowing) compared to moist conditions (two significant rainfall events).

The application of fertilisers and nutrients has been shown to benefit plant vigour at the seedling stage leading to positive effects on disease control. Furthermore, the addition of nutrients such as nitrogen, phosphorus and sulphur affected the quality of the rhizosphere microbial community and its structure, and could influence the suppressiveness of a soil (Donn *et al.*, 2014). Liquid chromatography-mass spectrometry (LC-MS) and proton nuclear magnetic resonance spectroscopy (<sup>1</sup>H NMR) used to study the biochemical profiles of suppressive and non-suppressive soil types, revealed more abundant sugar molecules in *R. solani* AG8 suppressive soils and more abundant lipids and terpenes in non-suppressive soils (Hayden *et al.*, 2019). Root rot severity caused by AG2-1 was greater in fields deficient in nitrogen, phosphorus, potassium or with high content of copper (Kataria and Verma, 1992). Hannukkala *et al.* (2016) showed that maintaining soil

pH above 6.6 through the application of 150kg/ha of nitrogen/phosphorus and potassium fertilisation reduced *R. solani* infection in *Brassica* spp. under no soil tillage. Similarly, increasing the quantity and bioavailability of carbon in topsoil, with phosphorus fertilization, aided in the suppression of disease by *R. solani* AG8 on wheat in calcareous topsoils (Davey *et al.*, 2021). Phosphorus deficiency was shown to limit plant growth as well as microbial populations, which reduced the potential for *R. solani* AG8 suppression (Davey *et al.*, 2021).

#### 1.5.2 Cultural control and cropping practices

Soil tillage, fertilisation and sowing practices have been shown to impact *R. solani* inoculum presence and density in soil. Conservation tillage, direct sowing or no-till are practices used to reduce erosion and improve soil structure by planting directly into the previous crop residues without traditional ploughing (Paulitz, 2006). Herbicide sprays are often used to kill weeds and crop volunteers before sowing the next seeds. The presence of crop residues within the top layer of soils and soil surface enables the short-term survival of the pathogen and conservation tillage allows for undisturbed mycelial spread. *R. solani* can survive on both living and dying crop residues, resulting in increased inoculum during this “green bridge” before sowing (Mahoney *et al.*, 2016). *R. solani* AG8 bare patch disease of wheat and barley became more severe following the widespread adoption of no-till practices in Australia in the 1970s (Paulitz, 2006; Schlatter *et al.*, 2017).

Paulitz *et al.* (2006) also observed lower yields, more symptoms on the root, and higher *R. solani* levels in the third and fourth years after converting plots to no-till after long-term conventional tillage. The removal of straw or burning of residues is ineffective for reducing soil inoculum as *R. solani* survives in root tissues and burning does not heat the soil to lethal temperatures at depth (Paulitz, Schroeder and Schillinger, 2010). Where direct sowing is used, allowing a time gap of at least 3 weeks between herbicide sprays and sowing has been shown to reduce the damage caused by *Rhizoctonia* by allowing substrate depletion or microbial breakdown of crop residues (Paulitz, 2006).

Teo *et al.* (1988) tested canola sowing dates in fields inoculated with *R. solani* AG2-1 and AG4 and showed that sowing in warmer periods reduced the impact of AG2-1 whilst cooler conditions reduced the impact of AG4 (Teo *et al.*, 1988). Hwang *et al.* (2014) also tested sowing dates in fields inoculated with *R. solani* AG2-1, and found that early sowing resulted in greater emergence at three weeks old and greater seed yield compared to later sowing of canola, however, this wasn't consistent when inoculum pressure was high. Therefore, while sowing date may have some impact on emergence, it cannot be a substitute for other management methods, especially in fields with high levels of pathogenic *R. solani*. Sowing depth can alter soil temperature, moisture, and the duration of time that the seedling is exposed to soil microorganisms before emergence. Khangura *et al.* (1999) found that increasing sowing depth from 1cm to 3cm delayed seedling emergence and increased disease severity. At 1cm sowing depth, in soil inoculated

with isolates of AG2-1 or AG8, canola seedling emergence varied between 69—88%, while at 3cm sowing depth, it varied from 34—52% (Khangura, Barbetti and Sweetingham, 1999). However, Hwang *et al.* (2014) found little or no consistent effect of sowing depth on emergence and yield. Increasing the sowing rate from 40 seeds/m<sup>2</sup> to 80 seeds/m<sup>2</sup> has the potential to compensate for establishment losses due to *R. solani* AG2-1, although this was inconsistent between growing seasons (Jayaweera and Ray, 2022).

Crop rotations are often first deployed for the control of soil-borne pathogens. However, this may not be effective in reducing *R. solani* AG2-1 inoculum due to its diverse host range in rotations, including OSR, wheat, peas and potatoes and the ability of the pathogen to survive as a saprophyte or the formation of long-lived resting structures, such as sclerotia, in soil (Hannukkala *et al.*, 2016; Lamichhane *et al.*, 2017).

### 1.5.3 Biological control

To establish colonisation, pathogens must compete with other rhizosphere microorganisms. This has led to the identification of disease suppressive soils, where pathogen growth is restricted by soil microbiomes. The study of a suppressive soil using *R. solani* AG2-2 III-B and sugar beet led to the hypothesis that *R. solani* causes acidic and oxidative stress on rhizo-bacterial families and the plant during hyphal growth (Chapelle *et al.*, 2016). The resultant stress on rhizobacteria in



the suppressive soil may then negatively affect the fungus, lead to a plant defence response, and/or send recruitment signals to other microorganisms (Chapelle *et al.*, 2016).

During an 8-year experiment looking at the effects of tillage and rotations on AG8 bare patch disease on wheat and barley, a reduction in total bare patch area was observed in no-till wheat-barley rotations in years 6, 7 and 8 of the study, which was hypothesised as linked to a suppressive microbial effect (Schillinger and Paulitz, 2006). *Rhizoctonia* bare patch disease decreased until it essentially disappeared in several Australian fields over ten years of continuous no-till wheat cropping (Schlatter *et al.*, 2017). These soils were investigated, and suppression was associated with the synergistic interaction between three groups of bacteria (*Pantoea agglomerans*, *Exiguobacterium acetylicum* and *Microbacteria*) (Barnett, Roget and Ryder, 2006). Donn *et al.* (2014) found that *R. solani* AG8 disease suppression could not be transferred from a suppressive soil to a conducive soil with a different soil type. In the United States, bacterial communities were sampled from inside and outside of *Rhizoctonia* bare patches to reveal higher frequencies of *Acidobacteria* and *Gemmatimonas* in the rhizosphere of healthy plants outside the patches, *Dyella* and *Acidobacteria* in recovered patches, and *Chitinophaga*, *Pedobacter*, *Oxalobacteriaceae* and *Chysoeobacterium* in the rhizosphere of diseased plants inside the patches (Yin *et al.*, 2013). Three isolates of *Chysoeobacterium* inhibited *R. solani* AG8 *in vitro*, and reduced disease in inoculated natural soil under greenhouse conditions (Yin *et al.*, 2013). It is unknown at this

stage whether the suppression seen in *R. solani* AG8 could be repeated with other AGs, but further research into the mechanisms of suppressive soil will inform cropping practices and may lead to the identification of novel biocontrol agents.

Aggeli *et al.* (2020) used lettuce to demonstrate the plant protective ability of *Arthrobacter* sp. strain FP15 and *Blastobotrys* sp. strain FP12 against *R. solani* AG2-1. Bacteria can be applied effectively as biocontrol agent-coated seeds, and have been tested using *Streptomyces* sp. coated on wheat seeds and grown in soil with high levels of *R. solani* AG8 (Araujo *et al.*, 2019). Increased plant growth, reduced root disease and an increased number of wheat heads were observed for pots inoculated with *Streptomyces* sp., while also affecting the endosphere and rhizosphere microbiomes, leading to changes in the relative quantities of different bacteria and fungi (Araujo *et al.*, 2019). *Streptomyces griseoviridis* strain K61 (Mycostop, Verdera) is marketed for use in the USA and EU to control fungal diseases including *R. solani* in vegetables and ornamentals. *Bacillus subtilis* var. *amyloliquefaciens* strain FZB24 is also commercially available as the biofungicide Taegro and led to disease reduction caused by *R. solani* on lettuce (Gnanamanickam *et al.*, 2008), although is currently only marketed for protected crops and grapevines. RhizoVital 42 liquid (*B. amyloliquefaciens* FZB42) has been shown to selectively compensate for the impact of *R. solani* AG1-IB pathogen attack on the indigenous plant-associated microbiome of lettuce plants (Erlacher *et al.*, 2014). FZB42 can colonise the rhizosphere and significantly reduce disease

severity in lettuce (Chowdhury *et al.*, 2013). This has been linked to its capacity to produce antimicrobial metabolites such as bacillomycin D and fengycin (Chowdhury *et al.*, 2013). The strong root colonisation capability and biofilm formation of *B. amyloliquefaciens* SQR9 has been investigated as a plant-growth promoting rhizobacteria species (Qiu *et al.*, 2014). Proteins involved in biocontrol, detoxification and biofilm formation were identified using comparative proteomics analysis (Qiu *et al.*, 2014). *B. amyloliquefaciens* SQR9 has also been shown to increase the salt stress tolerance of maize plants (Chen *et al.*, 2016). A strain of the bacterium *Pseudomonas fluorescens* increased seedling survival and produced inhibitory antibiotics to *R. solani* (AG not specified) in OSR (Dahiya and Woods, 1987). *Pseudomonas* sp. strain DSMZ 13134 (Proradix, Sourcon Padena) is a preventative bacterial fungicide authorised for use in the UK and the EU to control *R. solani* on potatoes.

Binucleate *Rhizoctonia* (BNR) isolates have the potential to be used in control management strategies against pathogenic *R. solani*, although none have yet been commercialised. Non-pathogenic BNR reduced damping-off and root rot disease caused by AG2-1 and AG4 on OSR (Gugel, Verma and Kaminski, 1986). Hypovirulent BNR increased plant protection against AG4 infection by inducing SAR and ISR (Sharon, Freeman and Sneh, 2011). Disease incidence and severity were reduced when soybean plants were pre-inoculated with BNR before infection with *R. solani* AG4 (Poromarto, Nelson and Freeman, 1998). Further investigation suggested that this was due to induced resistance

in the soybean plants, as there was no evidence of antagonism between the BNR and pathogenic *R. solani* hyphae (Poromarto, Nelson and Freeman, 1998). However, other studies have noted BNR causing significant reductions in *Brassica* seedling survival (Babiker *et al.*, 2013), suggesting that some BNR isolates may be pathogenic to *Brassica* spp..

Several mycoparasitic fungi act antagonistically towards *R. solani*. For example, *Trichoderma* spp. are widely used as biocontrol and *Trichoderma harzianum* hyphae have been observed coiling around, and penetrating *R. solani* AG4 hyphae, leading to extensive damage, including cell-wall alteration, plasma membrane retraction and cytoplasm aggregation (Benhamou and Chet, 1993). Light microscopy and transmission electron microscopy showed that *R. solani* (AG not specified) growth inhibition occurs soon after contact with *T. harzianum*, and although *T. harzianum* strains differ in their coiling behaviour, this was not correlated with their production of chitinases, N-acetyl-b-D-glucosaminidase and b-1,3-glucanases (Almeida *et al.*, 2007). *T. harzianum* strain T-22 is marketed as Triatum-P (Koppert Biological Systems) for use against *Rhizoctonia* spp. in protected edibles and ornamental crops in the UK. Comparative transcriptomics identified different responses in *Trichoderma* spp. during interactions with *R. solani* (AG not specified) (Atanasova *et al.*, 2013). *T. atroviride* showed an upregulation of genes involved in producing secondary metabolites, GH16  $\beta$ -glucanases, and proteases, while *T. virens* mainly expressed genes involved in gliotoxin biosynthesis, and *T. reesei* showed

increased expression of cellulase and hemicellulase genes, suggesting that different *Trichoderma* spp. employ a range of strategies against *R. solani* (Atanasova *et al.*, 2013). *T. virens* seed treatments have been shown to aid suppression of *R. solani* seedling disease (AG not specified) on cotton (*Gossypium hirsutum*) by stimulating defence responses (Howell *et al.*, 2000). Terpenoid synthesis increased in the roots of *T. virens*-treated plants, which correlated with biocontrol efficacy when compared to other *Trichoderma* spp. (Howell *et al.*, 2000). *T. virens* strain GL-21 (previously known as *Gliocladium virens*) is marketed in the USA as the microbial fungicide SoilGard and is targeted for controlling *R. solani* on indoor and outdoor food crops and ornamentals (Eyal *et al.*, 1997). Although there are promising results from the interactions between *Trichoderma* spp. and *R. solani*, these have been primarily obtained in a controlled or protected environment, and studies have not been identified testing the efficacy of *Trichoderma* spp. as a biocontrol for *R. solani* infection in field crops.

The basidiomycete *Laetisaria arvalis* has been shown to prevent damping-off in cotton, sugar beet, lettuce and radish when added to *R. solani* AG4 infested soil in glasshouse trials (Lewis and Papavizas, 1992). *Laetisaria arvalis* has also been shown to reduce *R. solani* AG4 soil inoculum density (Lewis and Papavizas, 1992). Field studies using mycoparasitic fungi as biocontrol for *R. solani* on OSR are needed to understand whether they can be a viable treatment for arable crops.

Fungivorous nematodes have been identified as potential control agents against *R. solani*. Although their efficacy on OSR is not yet known, there is evidence to suggest they can improve disease control in vegetable crops. The addition of *Aphelenchoides* spp. to soil inoculated with *R. solani* AG2-1 increased the percentage of healthy cauliflower (*Brassica oleracea*) seedlings from 45% to 85%, and the addition of *Aphelenchus avenae* suppressed damping-off, with 65% healthy cauliflower seedlings with nematodes, compared to almost 100% dead plants without nematodes (Lagerlof *et al.*, 2011). These fungivorous nematodes can penetrate fungal cells and ingest the cell contents, which reduces the inoculum levels in compost (Lagerlof *et al.*, 2011). Fungivorous nematode applications are not currently used in agriculture, mostly due to the high costs associated with commercial applications (Zhang *et al.*, 2020). Care also needs to be taken as many fungivorous nematodes will feed on beneficial fungi such as *Trichoderma* spp. (Zhang *et al.*, 2020).

#### 1.5.4 Fungicidal control

Application of chemical fungicides is one of the most consistent and reliable methods in managing *R. solani* disease. Fungicide seed treatments protect the young seedlings against damping off and are used as a preventative measure to increase emergence and establishment in infested soils. Most seed treatments include active ingredients that are effective against multiple soil-borne pathogens, including *R. solani*. Many seed treatment mixtures have included both

fungicides and insecticides as this can have an additive effect (Kataria and Verma, 1992) due to the reduction in stress caused by insect feeding. Sedaxane was developed by Syngenta for launch in 2011 and belongs to the succinate dehydrogenase inhibitor (SDHI) class of fungicides (Zeun, Scalliet and Oostendorp, 2013). A European study of soil isolates including AG2-1, found *R. solani* had a low baseline sensitivity to sedaxane (average EC<sub>50</sub> of 0.028ppm for all samples tested, EC<sub>50</sub>: effective concentration that reduced mycelial growth by 50%), with no differences in sensitivity between the isolate's country of origin (Goll *et al.*, 2014). The efficacy of two seed treatment combinations: difenconazole, fludioxonil, metalaxyl-M and thiamethoxam; and iprodione, metalaxyl and thiram was high, and resulted in greater canola seedling survival in soil inoculated with AG2-1, AG2-2 and AG4 (Lamprecht *et al.*, 2011). Hwang *et al.* (2014) demonstrated that seed treatments consisting of thiamethoxam, difenconazole, metalaxyl and fludioxonil or clothianidin, carboxin, trifloxystrobin and metalaxyl, increased seedling emergence and seed yield in canola grown in fields inoculated with *R. solani* AG2-1. In a comparison of soybean seed treatments (carbathiin plus thiram; carbathiin, thiram and metalaxyl; metalaxyl alone; metalaxyl plus HEC5725; fludioxonil plus metalaxyl-M; fludioxonil alone; metalaxyl plus trifloxystrobin; and *Bacillus pumilus* GB34) in fields inoculated with *R. solani* AG4, all seed treatments increased emergence when compared to the inoculated control, with the carbathiin, thiram and metalaxyl mix, and carbathiin plus thiram mix being the most effective (Xue *et al.*,

2007). The same two mixes also gave the greatest yield increase compared to the inoculated control (Xue *et al.*, 2007). *In vitro* testing of *R. solani* isolates from soybean (AG2-2, AG3, AG4, AG7, AG11) found all isolates to be extremely sensitive ( $EC_{50} < 1 \mu\text{g/ml}$ ) to penflufen and sedaxane, and ranged from extremely sensitive to moderately sensitive ( $1 \leq EC_{50} \leq 10 \mu\text{g/ml}$ ) to ipconazole and prothioconazole (Ajayi-Oyetunde, Butts-Wilmsmeyer and Bradley, 2017). Recently, Jayaweera and Ray (2022) have shown that the use of seed treatment containing sedaxane, fludioxonil and metalaxyl-M was able to reduce *R. solani* AG2-1 DNA in soil, and led to increases in OSR establishment (94%) and yield (64%).

However, many of the fungicides discussed have recently been prohibited for use in key OSR growing regions. Thiamethoxam has been banned in the EU due to its properties as a neonicotinoid insecticide. Thiram-based seed treatments were banned in the UK and EU in 2018 (Commission Implementing Regulation (EU) 2018/1500, 2018), and metalaxyl-M was affected by new restrictions in 2020, and is now only available for use indoors (Commission Implementing Regulation (EU) 2020/617, 2020). The EU did not renew their approval for iprodione products in 2017 (Commission Implementing Regulation (EU) 2017/2091, 2017). Difenoconazole (Plover, Syngenta) is currently available as a fungicide for OSR and brassicas and is also used in the management of light leaf spot and phoma diseases on OSR. Fludioxonil is only available for use on other crops as a seed treatment, both alone



(Maxim, Syngenta) and mixed with other fungicides such as sedaxane (Vibrance Duo, Syngenta).

#### 1.5.5 Genetic resistance

To date, resistant varieties of OSR to *R. solani* AG2-1 have not been identified, though some variation has been shown in the degree of susceptibility observed. Experiments testing isolates of AG2-1, AG8 and AG10 to *Brassica* crops (including *B. napus* and *B. rapa*) showed that AG2-1 isolates were the most aggressive and none of the *Brassica* genotypes tested showed any resistance to AG2-1 (Babiker *et al.*, 2013). More recently, high-throughput screening methods have been developed for AG2-1 disease in OSR (Drizou *et al.*, 2017), which enabled the quantification of differences between susceptible varieties. This has been used to show that variation exists between susceptible varieties, and has been used to identify genetic markers using genome wide association studies (GWAS) (Ray *et al.*, 2020). This was the first case of GWAS being used to investigate *R. solani* AG2-1 resistance in OSR, but previous studies have taken place for other *R. solani* interactions. Major and minor *R. solani* AG2-2 resistance genes were identified in the common bean (*Phaseolus vulgaris*) using GWAS (Oladzad *et al.*, 2019). GWAS have also been used on OSR to identify loci associated with resistance to other pathogens, such as *Leptosphaeria maculans* (Fikere *et al.*, 2020; Raman *et al.*, 2020), *Sclerotinia sclerotiorum* (Wei *et al.*, 2016) and *Plasmodiophora brassicae* (Hejna *et al.*, 2019). Associative transcriptomics methods

were developed using OSR as its tetraploid nature increases the complexity of marker identification. This used measured trait variation and transcriptome sequencing to identify and analyse markers based on gene sequence variation and transcript abundance variation (Harper *et al.*, 2012; Havlickova *et al.*, 2018). These methods will enable the identification of markers associated with *R. solani* AG2-1 resistance in OSR.

## 1.6 PhD aims and objectives

The aim of this PhD has been to elucidate the biological interactions between *Rhizoctonia solani* AG2-1 and its host, focusing on *Brassica napus* and *Arabidopsis thaliana*. This has been divided into several key objectives. One of the key objectives is to investigate the defence responses of commercial *B. napus* varieties to *R. solani*, and to study differences in the degree of susceptibility and if these are reflected in the relative expression of defence genes under inoculation. PAA has previously been shown to be produced by *R. solani* AGs, so one of the key objectives of this thesis is to investigate the role of auxins in susceptibility of OSR to *R. solani*. Another objective is to investigate the role of jasmonates and ethylene in resistance responses. Another key objective is to investigate the role of auxin in *R. solani* interactions and compare the responses of *A. thaliana* auxin mutants to *R. solani* with that of the auxins 2,4-D, PAA and NAA. The production of auxins such as IAA and PAA by *R. solani* will also be examined. A final objective has been to identify potential *B. rapa* TILLING line candidates,

extending the work on a recently completed GWAS. Data on gene expression markers from the GWAS will also be analysed.

## Chapter 2: Molecular characterisation of defence of *Brassica napus* (Oilseed rape) to *Rhizoctonia solani* AG2-1 confirmed by functional analysis in *Arabidopsis thaliana*

### 2.1 Abstract

*Rhizoctonia solani* is a necrotrophic, soil-borne fungal pathogen associated with significant establishment losses in *Brassica napus* (Oilseed Rape; OSR). The Anastomosis Group (AG) 2-1 of *R. solani* is most virulent to OSR, causing damping-off, root and hypocotyl rot, and seedling death. Resistance to *R. solani* AG2-1 in OSR has not been identified, and the regulation of OSR defence to its adapted pathogen, AG2-1, has not been investigated. In this work, confocal microscopy was used to visualise the progress of infection by sclerotia of AG2-1 on *B. napus* varieties with contrasting disease phenotypes. Their defence response was defined using gene expression studies and functional analysis with *Arabidopsis thaliana* mutants. These results showed existing variation in susceptibility to AG2-1 and root growth between OSR varieties, and differential expression of genes of hormonal and defence pathways related to auxin, ethylene, jasmonic acid, abscisic acid, salicylic acid, and reactive oxygen species regulation. Auxin, abscisic acid signalling, and the MYC2 branch of jasmonate signalling increased susceptibility to AG2-1, whilst induced systemic resistance was enhanced by NAPDH RBOHD, ethylene signalling and the

ERF/PDF branch of jasmonate signalling. These results pave the way for future research, which will lead to the development of *Brassica* crops that are more resistant to *R. solani* AG2-1 and reduce dependence on chemical control options.

## 2.2 Introduction

*Brassica napus* L., known as oilseed rape (OSR), is a valuable crop species, primarily grown for use as rapeseed oil, animal feed or biofuel. *Rhizoctonia solani* J.G. Kühn is a soil-borne, fungal species complex divided into thirteen reproductively isolated Anastomosis Groups (AGs) (Carling, Kuninaga and Brainard, 2002), of which, AG2-1 is most virulent to *B. napus*. *R. solani* survives in the soil as sclerotia (resting bodies of compacted mycelia), which in the presence of a susceptible host, rapidly germinate to produce infectious hyphae. These hyphae colonise host tissues, and form infection cushions with hyphal pegs underneath to penetrate the host (Kataria and Verma, 1992). On pre-germinated seedlings, symptoms of the developing damping off disease appear as hypocotyl/root rot and necrotic lesions, although the pathogen is also known to inhibit seed germination pre-emergence. Artificial inoculation of OSR with *R. solani* AG2-1 has shown a reduction in establishment by 60% and a yield reduction of 40% (Ray *et al.*, 2020). Control is usually attempted through chemical and cultural methods, although there are currently no approved chemical seed treatments, and genetic resistance has not yet been identified.

Most of the information on the modulation of defence against *R. solani*, causing damping off, has been provided by functional studies with the model plant, *Arabidopsis thaliana* (L.) Heynh., challenged with AG8, or hypovirulent isolates of *R. solani* (Sharon, Freeman and Sneh, 2011; Foley *et al.*, 2013; Kumar *et al.*, 2020; Kidd *et al.*, 2021). Defence against *R. solani* AG8 has been shown to involve jasmonic acid (JA) and ethylene (ET) pathways since mutations in JA (*coi1*), ET (*ein2*, *ers1* or *ers2*) and *pen2* reduced plant survival under AG8 inoculation (Kidd *et al.*, 2021). The NADPH oxidases (NOXs) double mutant *rbohD rbohF* was also highly susceptible to *R. solani* AG8 (Foley *et al.*, 2013; Kumar *et al.*, 2020). In contrast to JA and ET responses to AG8, auxin (Bartz *et al.*, 2012) and ABA (Cordovez *et al.*, 2017) mediated signalling pathways have been identified as potentially increasing host susceptibility to various other AGs of *R. solani*. Transcriptomics experiments showed that exposure to volatile organic compounds released by *R. solani* AG2-2 IIIB induced upregulation of ABA and auxin signalling genes in *A. thaliana*, while ET and JA signalling pathways were down-regulated (Cordovez *et al.*, 2017). Furthermore, isolates of AG1 IA, AG3 and AG4 have been shown to produce the auxin, phenyl acetic acid (PAA) and its derivatives (Mandava *et al.*, 1980; Iacobellis and DeVay, 1987; Lakshman *et al.*, 2006; Bartz *et al.*, 2012). PAA is a natural auxin with an overlapping regulatory role with indole-3-acetic acid (IAA) (Sugawara *et al.*, 2015) and in the host interaction with *R. solani*, PAA production has been associated with increased disease severity on susceptible hosts (Bartz *et al.*, 2012). It is currently unknown

if *R. solani* AG2-1 isolates produce PAA or other auxins and what role these auxins play in the disease biology of OSR. Studies using hypovirulent binucleate *Rhizoctonia* (Ru18-1, Ru89-1 [AG-B(o)], Rh521, and Ru56-8 (AG-A)) have provided information on the early defence response to AG4 (HG-1), as increased expression of genes PR5, PDF1.2, LOX2, LOX1, COR13 involved in induced systemic resistance and PAD3 of the phytoalexin production pathway was observed (Sharon, Freeman and Sneh, 2011). Whilst previous studies with *A. thaliana* challenged by AG8 or hypovirulent *R. solani* have contributed to understanding of non-host defence regulation, further molecular studies are needed to define the host-specific interactions in defence of OSR to AG2-1.

Here new insights are provided on OSR infection and the defence response to AG2-1 using inoculation experiments with three contrasting OSR varieties and further functional studies with *A. thaliana* mutants for key genes involved in hormonal regulation. This work aimed to first quantify and characterise variation in the tolerance of small range of commercial varieties of *B. napus* to *R. solani* AG2-1. This was investigated by quantifying disease symptoms and root growth, as well as imaging the initial stages of the infection process with AG2-1 sclerotia. Varieties with contrasting resistance responses were used for molecular characterisation to identify differences in their defence pathways. It was hypothesised that host susceptibility would be associated with increased expression of genes linked to SA and auxin responses, whilst enhanced defence to AG2-1, like to AG8, with

increased expression of genes of the JA and ET pathways. RT-qPCR was used to investigate changes in gene expression and gene functionality was confirmed using *A. thaliana* mutant lines under inoculation with AG2-1.

## 2.3 Methods

### 2.3.1 Fungal inoculum

*R. solani* AG2-1 (isolate #1934 from the University of Nottingham isolate collection) was used for inoculum production. AG2-1 was cultured on potato dextrose agar plates (PDA; Sigma-Aldrich, UK) at room temperature (18°C). Inoculation was carried out using 6 mm diameter AG2-1 cultured agar plugs from plates that were grown for 6-10 days before the production of sclerotia. For microscopy experiments using sclerotia, plates were prepared in the same manner and kept at room temperature for 4 weeks.

### 2.3.2 Plant material

Oilseed rape seeds (varieties Anastasia (LG seeds), Campus (KSW), SY Saveo (Syngenta), SY Sensia (Syngenta) and Skye (Elsom seeds)) were obtained from Dr Dasuni Jayaweera, University of Nottingham. *A. thaliana* seeds were obtained from NASC, UK, Dr Ranjan Swarup and Dr Vicente Conde, University of Nottingham.



### 2.3.3 *Rhizoctonia solani* AG2-1 inoculation using light expanded clay aggregate particles

Light expanded clay aggregate (LECA) particles were used for AG2-1 inoculation in *B. napus* as roots of young seedlings were kept clean and intact for further analysis. A randomized block design was used with 2 factors resulting in 10 treatment combinations in 4 replications. The factors were the commercially available OSR varieties and pathogen inoculation. 40 pots (9 cm in diameter) were filled one third with LECA particles (size 4-10mm; Saint-Gobain Weber Limited, UK) and five either AG2-1 colonised (inoculated) or clean (non-inoculated) plugs before filling with the remaining two thirds of LECA particles. Seeds were pre-germinated on filter paper in petri dishes with 5ml sterile distilled water for three days in the dark at room temperature (18°C). Three pre-germinated seedlings were added to each LECA pot. The pots were supplemented with 25% Hoagland's (Sigma-Aldrich, UK) in 0.5 L of purified water in equal amounts once only at the start of the experiment. No further watering occurred. Clear plastic covers with the ventilation holes closed were kept over the trays for the duration of the experiment to maintain high humidity. An example photograph of the experimental setup is shown in Figure 2-1.



**Figure 2-1: Photograph showing the experimental setup used for growing *Brassica napus* seedlings under *Rhizoctonia solani* AG2-1 inoculation in LECA particles.**

#### 2.3.4 Disease assessment

The symptoms of *Rhizoctonia* infection include damping-off, root rot and stem rot. The hypocotyl and roots show necrotic lesions which become water soaked, soft and incapable of supporting the plant. Disease assessment was conducted using a scoring scale of 0-4 for both hypocotyl and root; with 0 = symptomless, 1 = 25% symptoms, 2 = 50% symptoms, 3 = 75% of symptoms, and 4 = plant death, modified from Drizou *et al.* (2017). Photographic examples for each score are shown in Figure 2-2. Root length was measured using photographs and the SmartRoot plugin for ImageJ (Lobet, Pagès and Draye, 2011; Schneider, Rasband and Eliceiri, 2012). This experiment was repeated with consistent results.

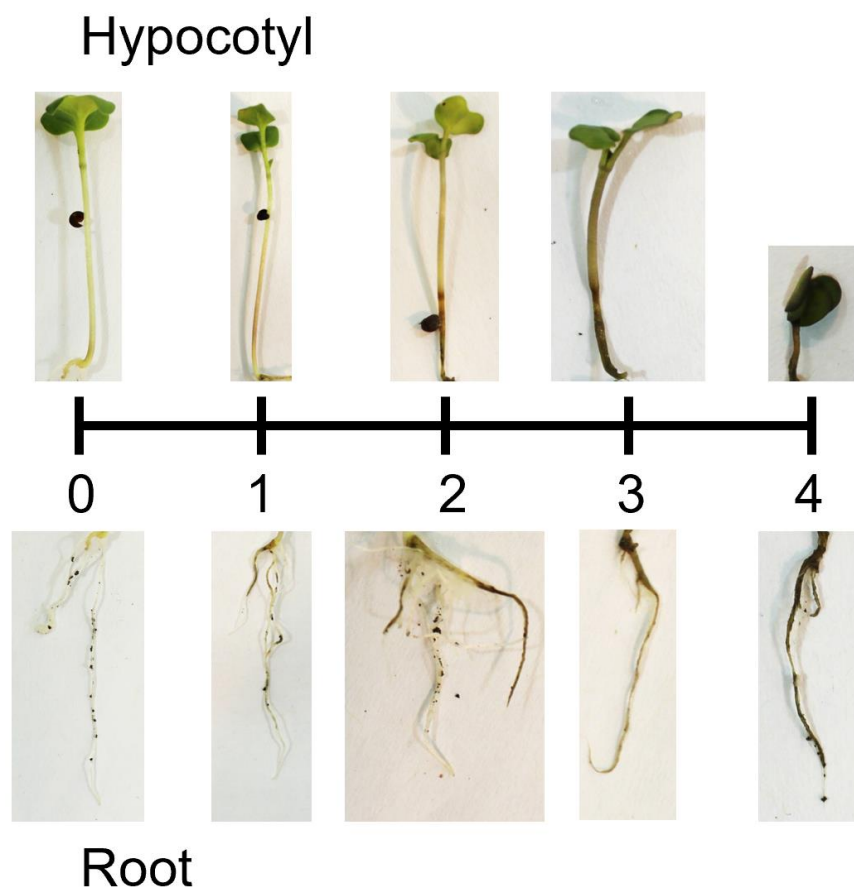


**Figure 2-2: *Brassica napus* symptom scores under *Rhizoctonia solani* AG2-1 inoculation. Plants were scored from 0-4; 0: symptomless, 1: 25% symptoms, 2: 50% symptoms, 3: 75% symptoms, 4: death.**

### 2.3.5 Gene expression analysis

Whole plant samples of *B. napus* were collected at 8, 24 and 48 hours after inoculation (hpi) for RNA extraction using RNeasy Plant kit (Qiagen) with TRIzol reagent (Invitrogen) as described in Ajjigboye *et al.* (2021). First strand cDNA was synthesized using iScript cDNA Synthesis Kit (Bio-Rad). Quantitative reverse transcription PCR (RT-qPCR) with Sybr Green (Bio-Rad) was conducted using CFX96 Touch Real-Time PCR Detection System (BioRad) consisting of 95°C for 1 minute, followed by 40 cycles with 15 seconds at both 95°C and 60°C.

The primers used are listed in Table 2-1. Relative quantification was calculated using the  $2^{-\Delta\Delta C_T}$  method (Livak and Schmittgen, 2001). Actin was used as the reference gene and the non-inoculated samples were used as the control. Arithmetic means and standard errors were calculated with three biological (each with three technical) replicates per sample.

**Table 2-1: Primers used for RT-qPCR analysis. All primers were designed using NCBI Primer-BLAST, except the PAL4 primers which were taken from (Zheng, Koopmann and von Tiedemann, 2019).**

<u>Gene</u>	<u>Gene name</u>	<u>Forward primer</u>	<u>Reverse primer</u>
AAO3	Abscisic Aldehyde Oxidase 3	TTCCAGCGTGGACTGATGAC	CACTCACATACGGCAATGCG
ABI4	ABA Insensitive 4	GGCCGTTGTTGATCCGGTTA	TTGACCGACCTTTAGGGTTCC
AUX1	Auxin Resistant 1	GCTGCCATCTTCTGGGTTCA	GGGTCCTTTAGTTCTCACTTGC
AXR1	Auxin Resistant 1	TGGCTTGAAGCACAGAGAAGA	CGGCTGAATCGTCCTGAACA
EIN2	Ethylene Insensitive 2	CCAATGGGTTGAAGAAGGACC	GAGGTTTCGACTCTTCGGCT
ERF1	Ethylene Responsive Factor 1	TGTTCAAGTCACCGTTCTCCG	CGGAACGTTTTGCTGTGTGG
IAA7	Indole-3-Acetic Acid 7	TGTTCAACCATATGACGGGTTCT	TCCACACCTCACTGGTAACAT
ICS1	Isochorismate Synthase 1	AGCAACCCAACCTCAGAGTG	ACACACTGATTCTCTATTACCCCA
JAR1	Jasmonate Resistant 1	GGGGAAACAGAGGAGAGACC	CAACGTCACCAAGCCGGTAT
MYC2	MYC2, Jasmonate Insensitive 1	GATTGGAGTACCCGAGCAGG	CCGGATTCGGGTTTTTCGATG
NPR1	Nonexpresser of PR genes 1	CCCGTGATGGTGTTACAGAGTT	GTGCATGAACGTTGCCAAAC
PAD3	Phytoalexin Deficient 3	TTGGGGATTGCCTGAGAAGG	ACAGCTACCTAAGAATAATACACCC
PAL4	Phenylalanine Ammonia-Lyase 4	GGCACGGACAGTTATGGAGT	GCCGACTTAGGTAGCGTGAG
PDF1.2	Plant Defensin 1.2	CATCACCTTCTCTTCGCTGC	ATGTCCCCTTGACCTCTCGC
RBOHC	Respiratory Burst Oxidase Homolog C	ACTCCGACGCCGAAAGCAG	TTCCGACCCGGGGGATTTG
RBOHD	Respiratory Burst Oxidase Homolog D	GACGAGGGAATTCAGGAACC	TTCGTTGTCCGAGTTGGTGT
TIR1	Transport Inhibitor Response 1	TCAACCATGAGGGTTTGCCA	GGGCGATGATGAACAGGATTG

### 2.3.6 Seed sterilisation

*B. napus* and *A. thaliana* seeds were surface sterilised for 8 minutes using a sterilisation solution containing 70% sodium hypochlorite (Parazone, Jeyes Limited, UK) and 0.2% Tween-20 and then washed three times with sterile distilled water.

### 2.3.7 Plant growth conditions

For the trays of LECA particles, a controlled environment chamber set at a constant 20°C temperature with a 12h photoperiod was used. For growth on agar plates, a controlled environment room with 16h light at 21°C, 8h dark at 15°C was used. For compost trays, a controlled environment chamber at a constant 22°C temperature with a 16h photoperiod was used.

### 2.3.8 Wheat Germ Agglutinin (WGA)-Alexa Fluor/ Propidium Iodide staining and microscopy

This method is based upon that of Redkar *et al.* (2018). *B. napus* seeds were surface sterilised, plated on 10% (w/v) water agar, cold stratified and grown for 25 days. *R. solani* sclerotia were added next to (as close as touching) to the roots of the plants to allow fast infection. Roots were sampled at 8, 24 and 48hpi and stored in 100% ethanol to undergo bleaching upon collection. A minimum of nine samples were taken for each variety at each time point (average: 17). Ethanol was then replaced with 10% potassium hydroxide and samples were incubated at

85°C for 1.5 hours. Samples were washed five times in phosphate buffer saline (PBS) pH7.4. Staining solution was prepared with 20µg/ml propidium iodide, 10µg/ml WGA-Alexa Fluor 488 conjugate (Thermo Fisher) and 0.1% (v/v) Tween-20 in PBS pH7.4. Propidium Iodide was used to stain plant cell walls and Alexa Fluor was used to stain fungal hyphae. Stain was added to the samples and vacuum infiltration was completed 3 times for 5 minutes each with 5 minute intervals between at atmospheric pressure. Samples were washed twice with PBS before visualisation with the Leica SP5 Confocal microscope (Leica Microsystems, Germany). This experiment was repeated with consistent results.

### 2.3.9 *Rhizoctonia solani* AG2-1 inoculation in compost

Seeds were surface sterilised and transferred to 50% MS pH 5.8 (Murashige and Skoog Basal Medium, Sigma-Aldrich, UK), 1% agar plates, cold stratified and grown vertically for eleven days. Seedlings were transplanted into 3x4 well trays containing a mix of M3 compost (Levington, Everris Limited, UK), vermiculite and perlite in a 4:2:1 ratio. Three days later, the plants were transferred into experimental trays with ten *R. solani* AG2-1 colonised or non-inoculated plugs added 3cm from the top of each well. Trays were watered once only at the start of the experiment to a depth of 1cm and then covered with clear plastic lids to maintain high humidity. Photographs were taken from above using a digital camera and the green area for each plant measured using ImageJ (Schneider, Rasband and Eliceiri, 2012). A ruler was

included in all photographs to set the scale for measurements. This experiment was repeated with consistent results.



**Figure 2-3: Photograph showing the experimental setup used for growing *Arabidopsis thaliana* plants under *Rhizoctonia solani* AG2-1 inoculation in compost.**

#### 2.3.10 Infection and imaging of Jas9:VENUS plants

*A. thaliana* Jas9:VENUS seeds were surface sterilised, cold stratified, and grown on 50% MS pH 5.8 1% agar plates for eight days. *R. solani* mycelium was then added close to the plant roots, and the plants were imaged 20h after inoculation. Images were taken using a Leica SP5 Confocal microscope (Leica Microsystems, Germany).



### 2.3.11 Infection and imaging of IAA2<sub>pro</sub>:GUS plants

*A. thaliana* Ws IAA2<sub>pro</sub>:GUS lines were surface sterilised, cold stratified, and grown on 50% MS pH 5.8 1% agar plates for seven days before AG2-1 inoculation. The plants were spaced at least 1cm apart and 3cm from the top of the plate. Plates were inoculated using plugs colonised with *R. solani* AG2-1. Three plugs were used per plate, spaced equally, 2cm from the bottom of the plate. The fungal growth was close to, but not touching the roots, by 3dpi. Sampling was attempted at later time points but after the fungus reached the plants, the roots were not able to be removed from the plates and stained effectively without breaking.

GUS buffer was prepared with 100mM pH7.0 sodium phosphate buffer, 0.5M EDTA, 1mM potassium ferricyanide, 1mM potassium ferrocyanide, 0.5% (w/v) 5-bromo-4-chloro-3-indolyl- $\beta$ -D-glucuronic acid (x-gluc; thermo scientific) dissolved in 1ml dimethylformamide (DMX) and 0.1% (v/v) Triton x-100. Whole plants were harvested and immediately placed in the prepared GUS buffer on ice until all samples were collected. Samples were incubated with GUS buffer at 37°C for 30 minutes wrapped in foil. Samples were transferred to fresh tubes with 25% ethanol overnight, before increasing the ethanol percentage over subsequent days (50%, 70%, 90%, 100%), then the samples were stored in 50% glycerol until microscopy. Samples were viewed using the Leica CTR5000 microscope (Leica Microsystems, Germany).

### 2.3.12 Statistical Analysis

Statistical analysis for all experiments were carried out using Genstat® Version 19 for windows (VSN International Ltd, UK). Analysis of Variance (ANOVA) was conducted on the data for the *B. napus* root and hypocotyl symptom scoring and root lengths. Both the variety and the treatment (AG2-1 inoculated or non-inoculated) were included as treatment factors. The plant leaf areas of the *A. thaliana* mutants were evaluated using *t*-tests to compare the AG2-1 inoculated to the non-inoculated plants for each genotype. Treatments were considered significantly different at  $p < 0.05$  with least significant difference (Lsd) of 5%.

## 2.4 Results

### 2.4.1 Phenotypic comparison of *Brassica napus* varieties

To compare the disease phenotypes of *B. napus* varieties under *R. solani* AG2-1 inoculation, differences in the symptom severity and total root length were determined at seven days post-inoculation (dpi). All varieties showed root and hypocotyl symptoms and a reduction in root length under inoculation, but plants of cv. Anastasia were most susceptible, showing extensive necrosis on both the root and hypocotyl (root: 4/4, hypocotyl: 3.5/4) and total root length reduction by 95% under inoculation (Figure 2-4). Campus showed the fewest symptoms on both the root and the hypocotyl (root: 2.75/4, hypocotyl: 1.25/4) with reduction of root length by 79% under inoculation. Skye exhibited more

severe symptoms than Campus (root: 3.25/4, hypocotyl: 2.25/4) but grew the longest roots under inoculation, despite an 85% reduction in length. Symptom severity on Saveo and Sensia were comparable to Anastasia and Skye, respectively.

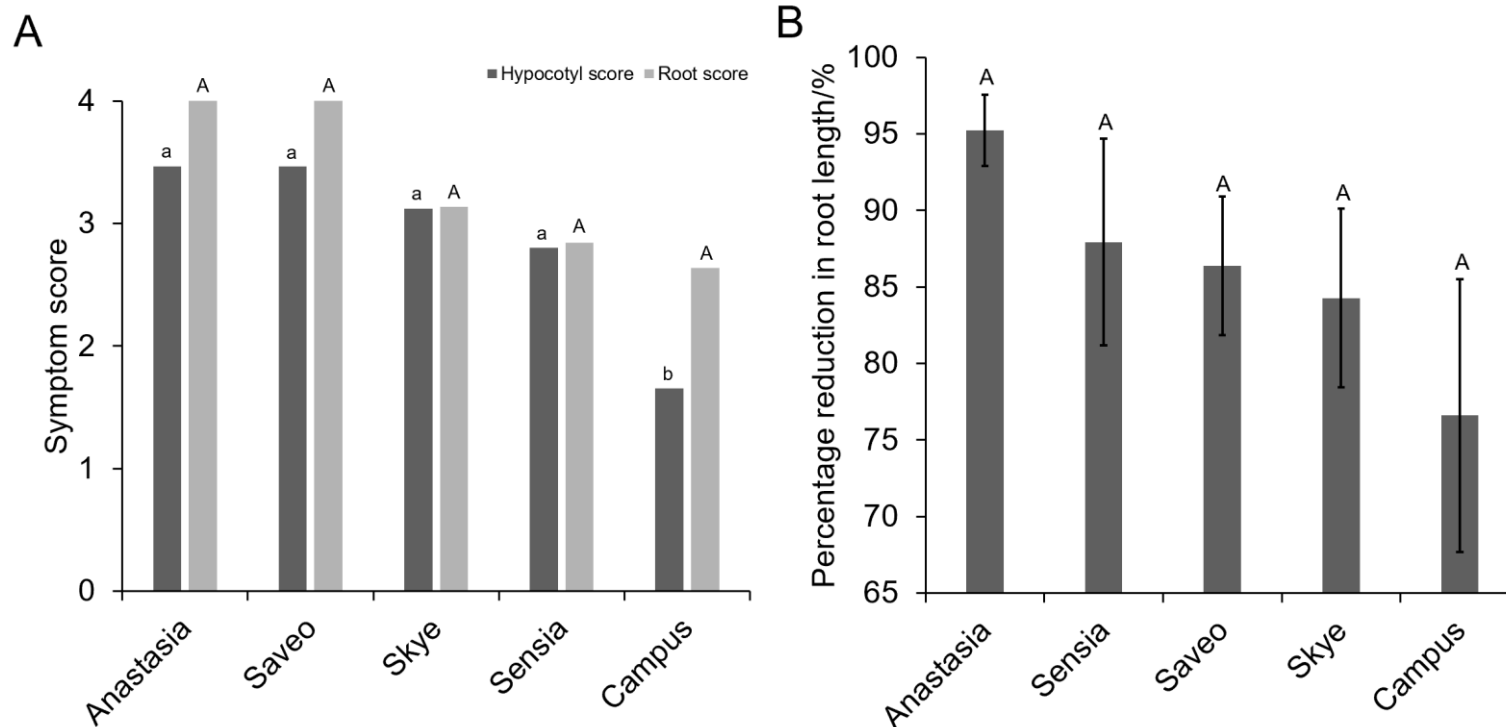


**Figure 2-4: *Brassica napus* symptom scores and percentage reductions in root length at seven days post inoculation with *Rhizoctonia solani* AG2-1. A) Average symptom scores for five commercially available *B. napus* varieties. Dark grey bars show average hypocotyl symptom scores and light grey bars show average root symptom scores. Non-inoculated data not shown as no individuals showed symptoms. B) Percentage reduction in root length measured using ImageJ and SmartRoot plugin. The total length included lateral roots. Tukey test was used to provide letters.**

Anastasia, Skye, and Campus were chosen for further investigation using confocal microscopy as these conventional genotypes represented contrasting disease severity phenotypes. Anastasia was identified as highly susceptible, Campus as most resistant and Skye was intermediate due to some tolerance to disease since root growth was least inhibited despite developing severe symptoms. To visualise the speed of infection and production of infection cushions on the contrasting varieties, Anastasia, Skye, and Campus roots were infected using *R. solani* AG2-1 sclerotia and stained using Propidium Iodide and Alexa Fluor Wheat Germ Agglutinin 488 (Figure 2-5). Propidium iodide showed plant cell walls, and the Alexa Fluor showed fungal hyphae. Sclerotia germinated and produced hyphae by 8 hours post-inoculation (hpi) on Anastasia, followed by rapid development of infection cushions by 24hpi and 48hpi. Hyphal growth was observed on Skye at 24hpi with smaller infection cushions than observed on Anastasia developing by 48hpi. Germination from sclerotia was rarely seen at 8hpi or 24hpi on Campus, and the most hyphal growth was observed at 48hpi. No infection cushions were observed in Campus at any time point of the microscopic investigation.

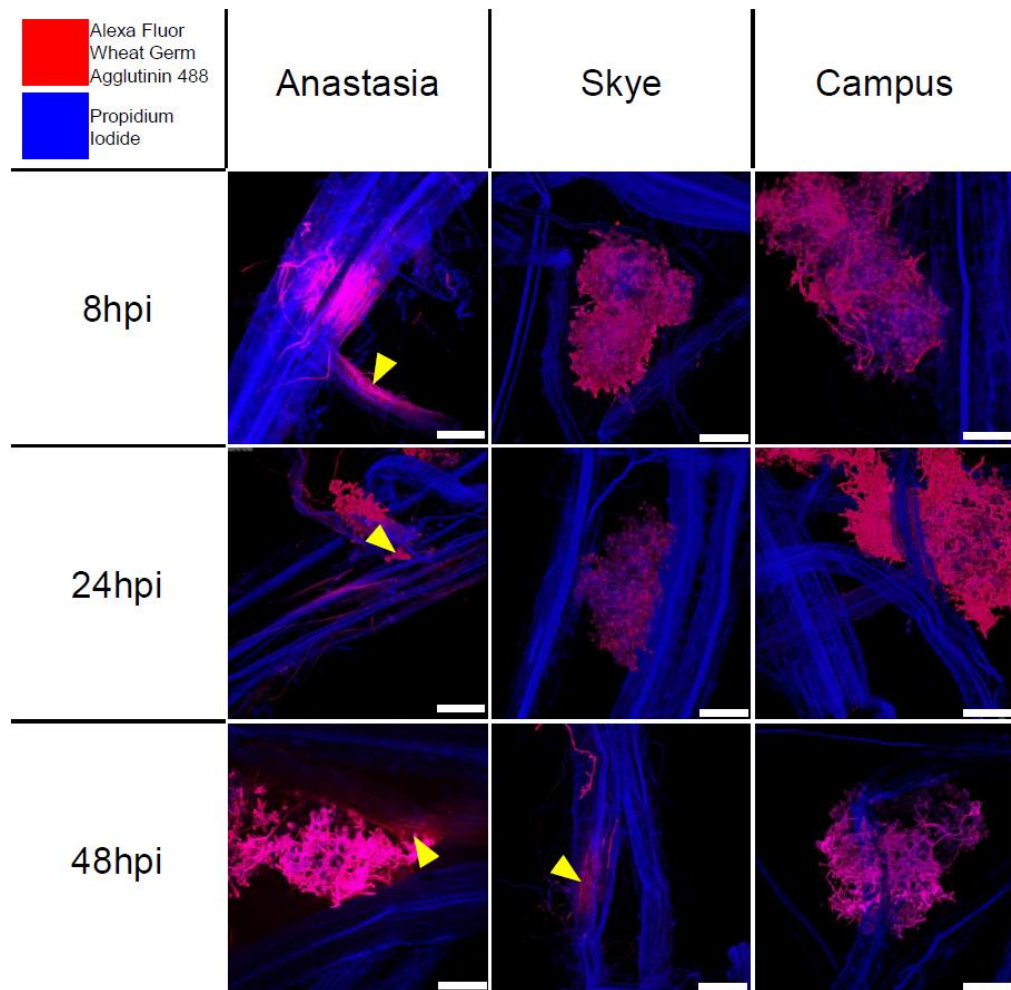


**Figure 2-5: Confocal microscopy images showing *Rhizoctonia solani* AG2-1 sclerotia infection on different *Brassica napus* varieties up to two days post-inoculation. Alexa Fluor Wheat Germ Agglutinin 488 and Propidium Iodide staining of *B. napus* showed differences in the development of infection structures in Anastasia, Skye, and Campus. Scale bars shown in the bottom right of each image represent 250 $\mu$ m. Yellow arrowheads indicate infection cushions. Red shows staining with Alexa Fluor Wheat Germ Agglutinin 488. Blue shows staining with Propidium Iodide. The images shown were chosen as representatives from a larger sample of infected roots for each variety.**

#### 2.4.2 Characterisation of defence and hormonal responses in *Brassica napus* by RT-qPCR

To understand which hormonal and defence pathways may be linked to the observed phenotypes of the *B. napus* varieties, RT-qPCRs were conducted using cDNA from whole plant RNA extractions, and log<sub>2</sub> fold changes of the relative gene expression were calculated. Differential gene expression is described in relation to the proposed defence diagram shown in Figure 2-6 **Error! Reference source not found.**. The relative expression of AUX1 (auxin transport), AXR1 and TIR1 (auxin signalling) was assessed first (Figure 2-7). AUX1 was upregulated in Campus at 8hpi then declined in expression over time, which contrasted with AXR1 showing increased expression by 48hpi. Skye and Anastasia had the greatest log<sub>2</sub> fold change of AUX1 and AXR1 at 24hpi, but the response was less in Skye and diminished by 48hpi. TIR1 and the auxin-responsive gene IAA7 had similar expression patterns, with Anastasia upregulating both genes significantly more than Campus or Skye at 24 or 48hpi. The least auxin gene responsive variety was Skye, showing repressed expression by 48hpi. These results showed that under inoculation, gene expression of auxin transport, signalling and response increased in the susceptible Anastasia compared to the other two more tolerant genotypes.

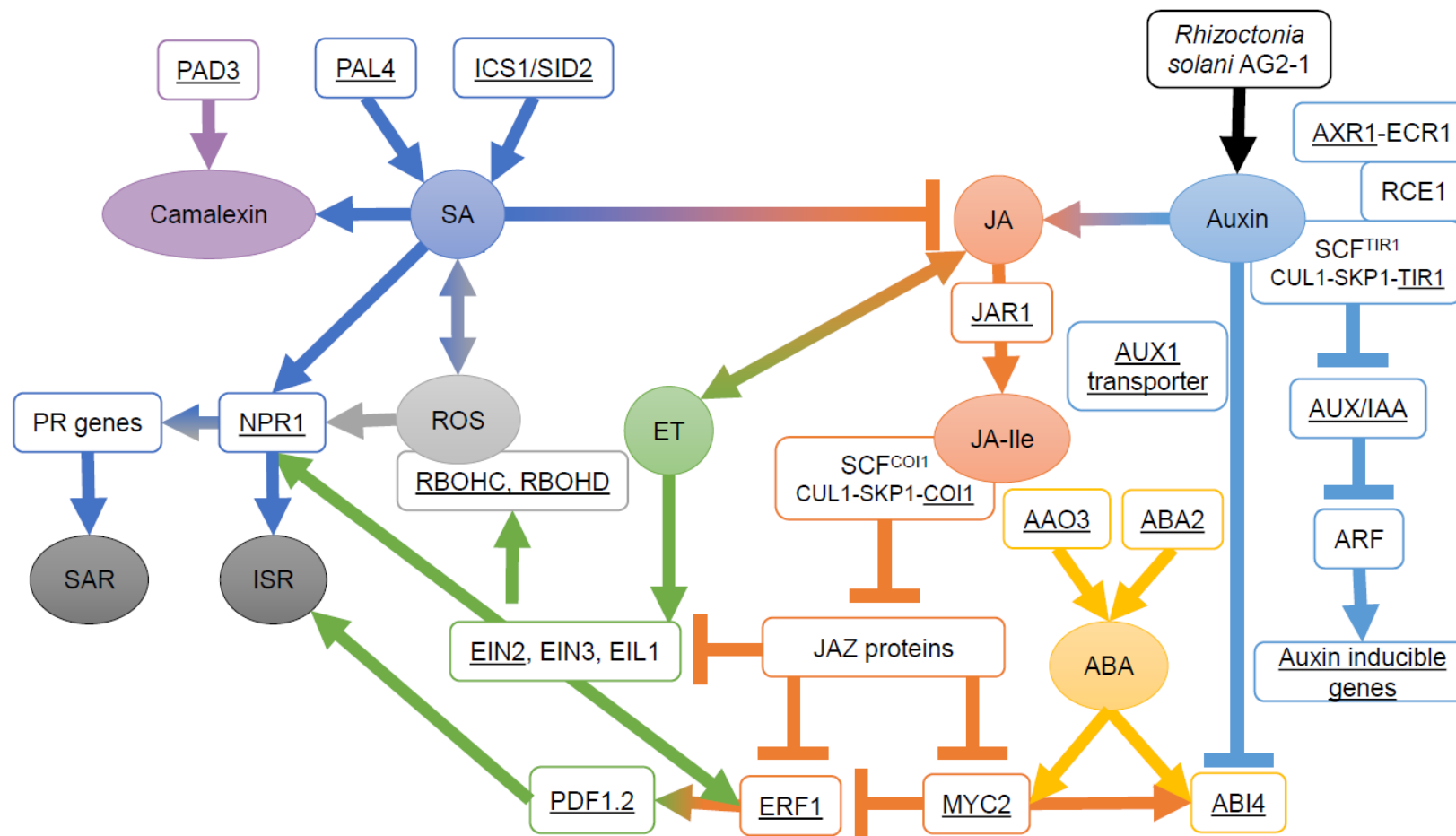
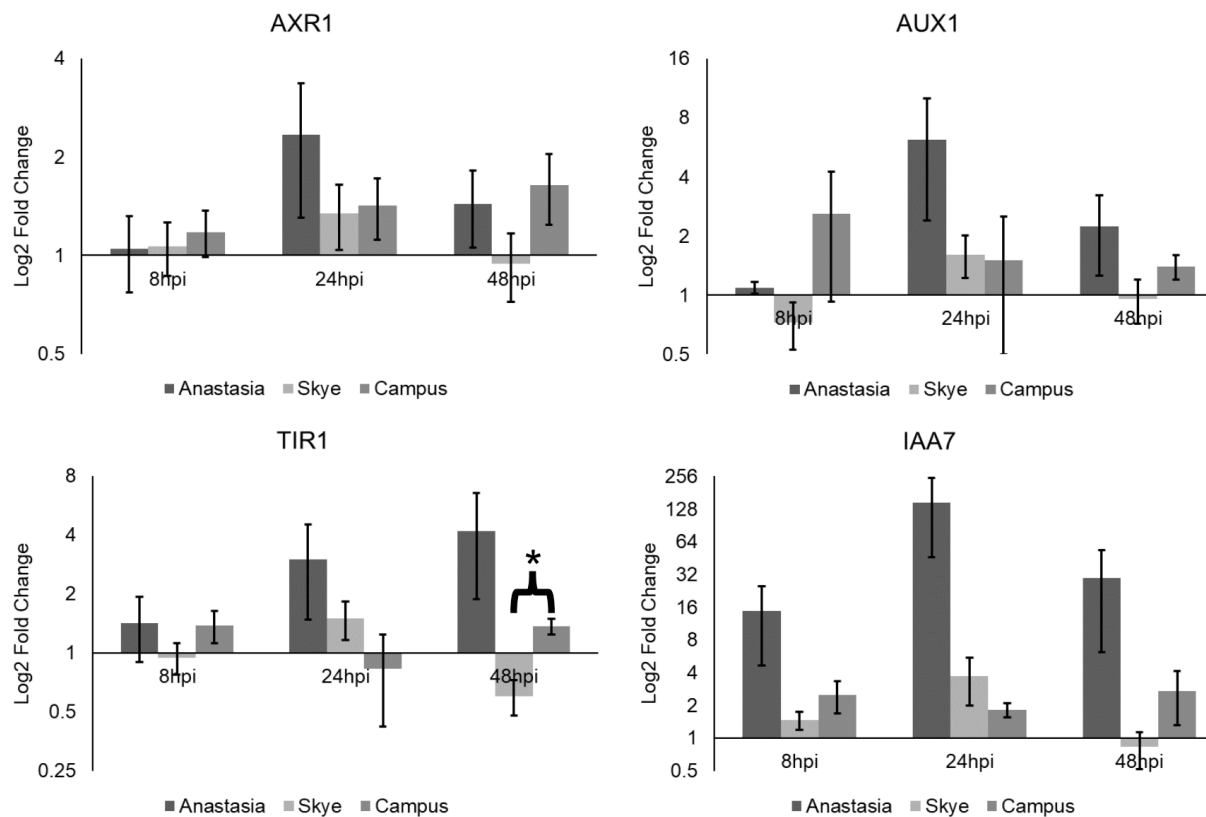


Figure 2-6: Proposed diagram of interactions between hormonal defence pathways.





**Figure 2-7: Differential gene expression of auxin genes in *Brassica napus* varieties following inoculation with *Rhizoctonia solani* AG2-1 at 8, 24 and 48 hours post inoculation. Significant differences between the varieties (t-test,  $p < 0.05$ ) are indicated by a bracket and \*.**

JAR1, which converts JA to its bioactive form JA-Ile, was first upregulated in Skye and Campus at 8hpi and 24hpi followed by a decrease in expression by 48hpi. This contrasted with Anastasia, which showed upregulated JAR1 at 48hpi. MYC2 regulates JA responses and was highly expressed in Anastasia at 24 and 48hpi compared to Campus and Skye (Figure 2-8), suggesting that the susceptible phenotype follows this branch of the JA signalling pathway.

AAO3 catalyses the final step of ABA biosynthesis and although downregulated at 8hpi in Anastasia, it showed an increasing log<sub>2</sub> fold change at 24 and 48hpi, with Campus and Skye showing lower expression at all time points (Figure 2-8). ABI4 is an ABA-regulated transcription factor, which has increased expression in the presence of ABA, but is repressed by auxin (Saini *et al.*, 2013). Anastasia had the greatest negative log<sub>2</sub> fold change of ABI4 at 8hpi, whilst Campus and Skye showed gene upregulation, however all varieties downregulated ABI4 by 48hpi (Figure 2-8).

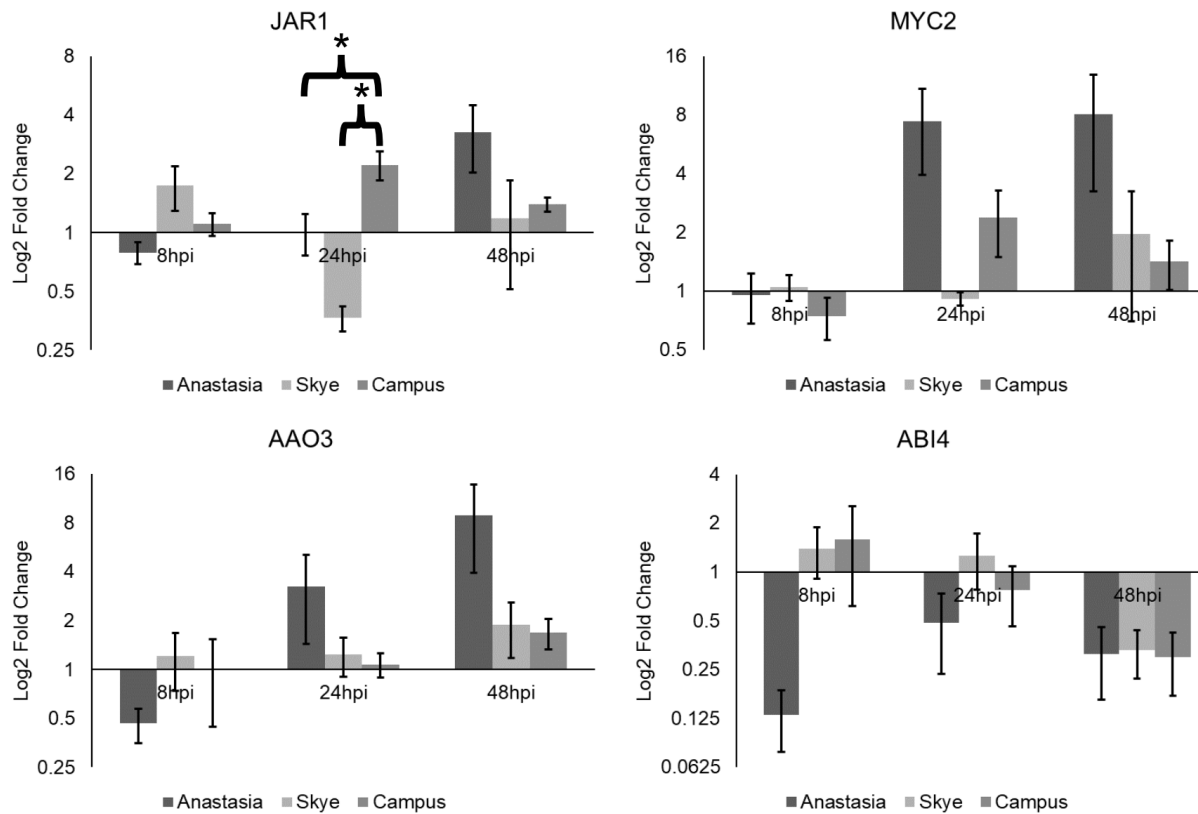


**Figure 2-8: Differential gene expression of jasmonate and abscisic acid genes in *Brassica napus* varieties following inoculation with *Rhizoctonia solani* AG2-1 at 8, 24 and 48 hours post inoculation. Significant differences between the varieties (t-test,  $p < 0.05$ ) are indicated by a bracket and \***

EIN2 activates ET signalling in high ET and showed the greatest upregulation in Anastasia (Figure 2-9). At 8hpi and 24hpi Anastasia also showed an increased expression of ERF1, which declined by 48hpi. In contrast, Skye and Campus increased expression over time with the greatest upregulation at 48hpi in Campus. PDF1.2, downstream of ERF1, showed an increased log<sub>2</sub> fold change in response to infection for Campus and Skye at 24hpi, and just for Campus at 48hpi. These results indicated that the ERF1 pathway contributed to defence against *R. solani* AG2-1.

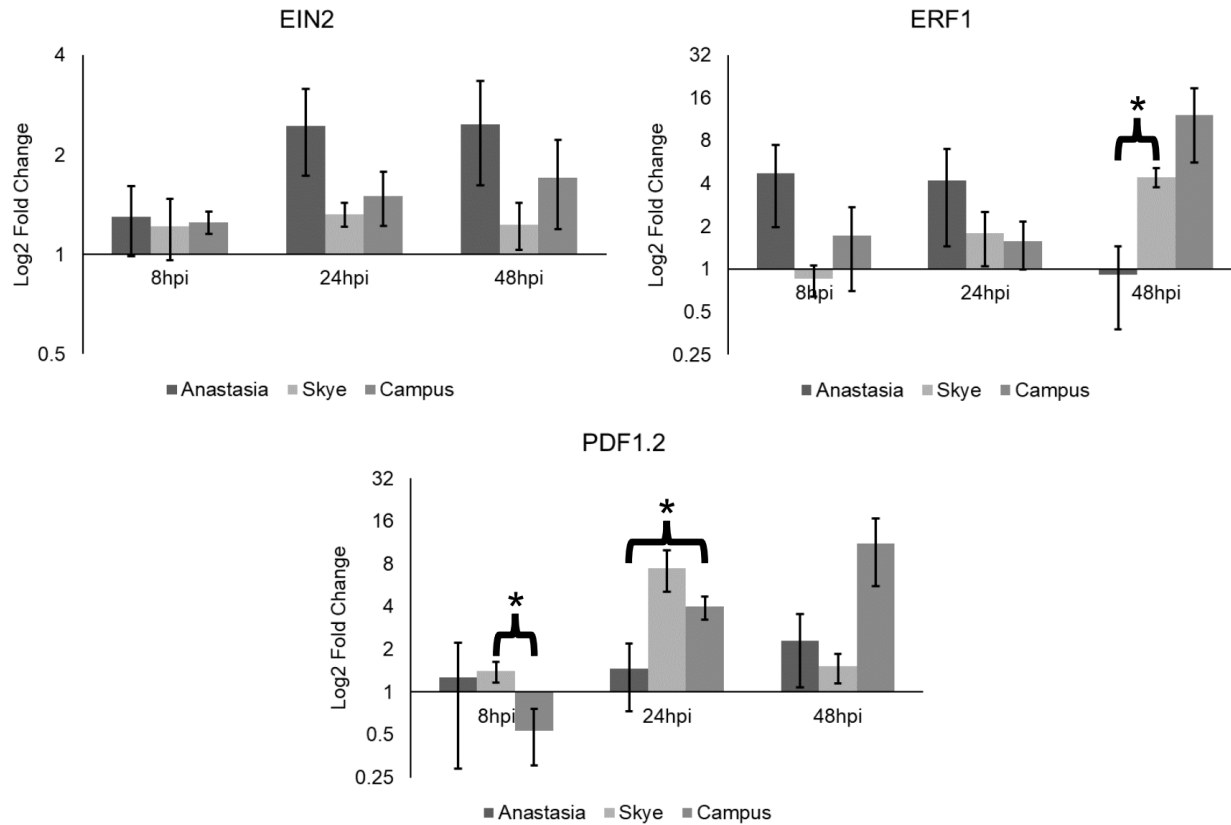


**Figure 2-9: Differential gene expression of ethylene genes in *Brassica napus* varieties following inoculation with *Rhizoctonia solani* AG2-1 at 8, 24 and 48 hours post inoculation. Significant differences between the varieties (t-test,  $p < 0.05$ ) are indicated by a bracket and \*.**

SA is synthesised via the ICS and PAL pathways (Lefevere, Bauters and Gheysen, 2020). ICS1 (also known as SID2) catalyses the first reaction of chorismate to isochorismate in the ICS pathway. PAL4 catalyses the reaction of phenylalanine to trans-cinnamic acid (tCA) that can also lead to lignin biosynthesis (Zheng, Koopmann and von Tiedemann, 2019; Lefevere, Bauters and Gheysen, 2020). In response to inoculation at 8hpi and in contrast to Campus, Anastasia downregulated both ICS1 and PAL4 (Figure 2-10). All varieties increased PAL4 expression beyond 24hpi. ICS1 was upregulated more in Anastasia than in Campus or Skye at 24 and 48hpi. NPR1 is required for the transcription of SA-responsive genes and is involved in both systemic acquired resistance (SAR) and induced systemic resistance (ISR) responses. Both Anastasia and Campus upregulated NPR1 in response to infection at 24 and 48hpi, in contrast to Skye, that showed no change in expression over time (Figure 2-10). The final step in the biosynthesis of the phytoalexin, camalexin, is catalysed by PAD3 (Zhou, Tootle and Glazebrook, 1999; Schuhegger *et al.*, 2006). In this work, PAD3 expression increased over time in Anastasia, with higher log<sub>2</sub> fold change observed in Anastasia compared to the other two varieties at 24 and 48hpi (Figure 2-10). Respiratory burst oxidase homologs (RBOHs), mediate signal transduction pathways via the production of reactive oxygen species (ROS) RBOHC expression increased in Anastasia at 8hpi and decreased slightly over time (Figure 2-10). In contrast, RBOHD was depressed in Anastasia at all time points. Campus was observed upregulating RBOHD at 48hpi.

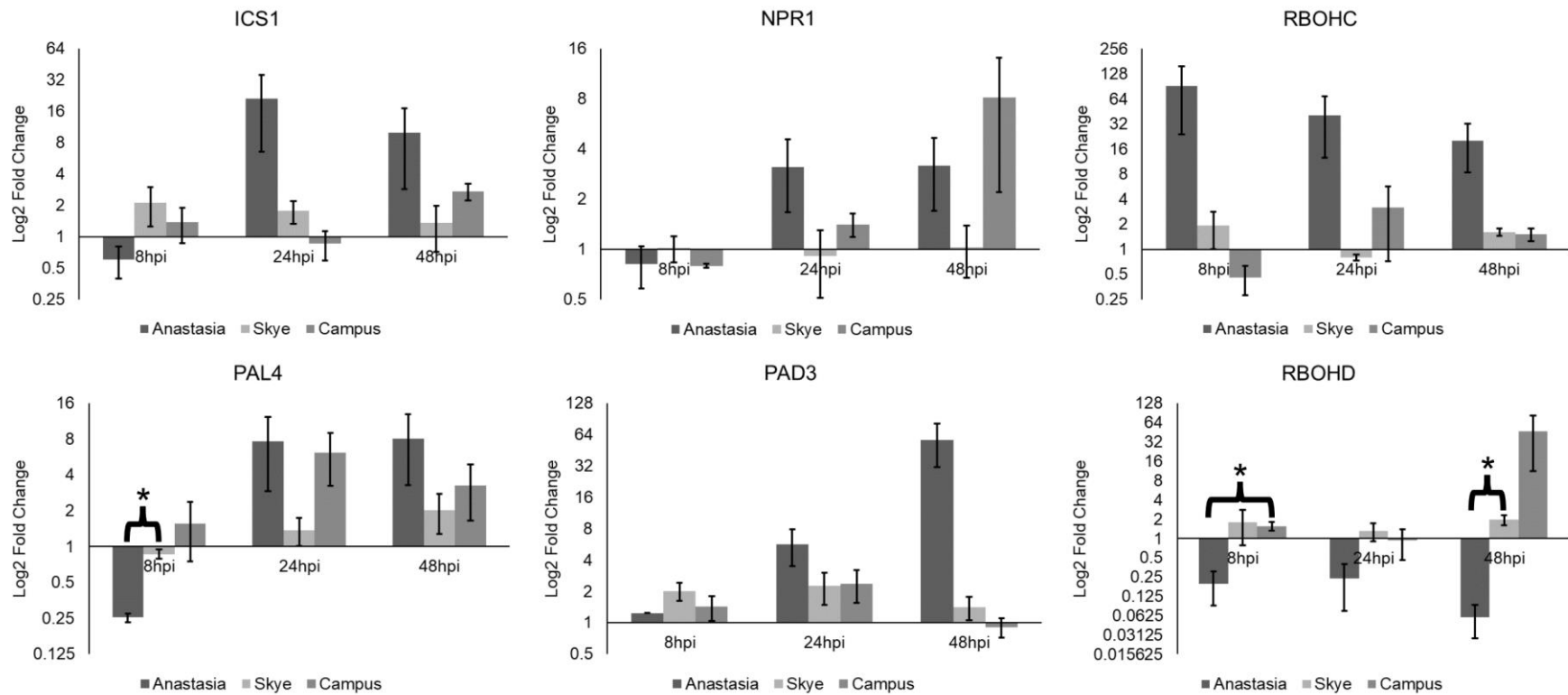


**Figure 2-10: Differential gene expression of salicylic acid and reactive oxygen species genes in *Brassica napus* varieties following inoculation with *Rhizoctonia solani* AG2-1 at 8, 24 and 48 hours post inoculation. Significant differences between the varieties (t-test,  $p < 0.05$ ) are indicated by a bracket and \*.**

### 2.4.3 Functional analysis and characterisation using *Arabidopsis thaliana*

To improve understanding of *R. solani* AG2-1 infection and its effect on regulating plant hormones as evidenced by the gene expression profiling of key genes involved in hormone signalling, a genetic approach was used. *R. solani* AG2-1 reduces the plant vigour, growth, and development of the model plant *A. thaliana* and this was exploited to functionally confirm hormonal defence responses. *A. thaliana* mutants were inoculated with *R. solani* AG2-1 in compost and assessed for disease effects on plant growth (Figure 2-11). At 11dpi, there was a significant difference in the size of the inoculated and non-inoculated wild-type (Col-0) plants (non-inoculated: 2.58cm<sup>2</sup>, inoculated: 0.51cm<sup>2</sup>; p<0.05). The mutant *aux1-21* (auxin transport) showed a significant reduction in growth under inoculation (non-inoculated: 9.57cm<sup>2</sup>, inoculated: 2.20cm<sup>2</sup>; p<0.01), in contrast to the auxin signalling mutants *axr1-22* (non-inoculated: 0.57cm<sup>2</sup>, inoculated: 0.21cm<sup>2</sup>; p=0.28) and *tir1* (non-inoculated: 3.54cm<sup>2</sup>, inoculated: 1.80cm<sup>2</sup>; p=0.20) that were not affected by inoculation, suggesting that auxin signalling, rather than transport, was involved in host susceptibility. Further evidence that auxin signalling increased in the susceptible hosts was provided by the *A. thaliana* IAA2<sub>pro</sub>:GUS lines showing more intense staining over the course of infection (Figure 2-12 **Error! Reference source not found.**).



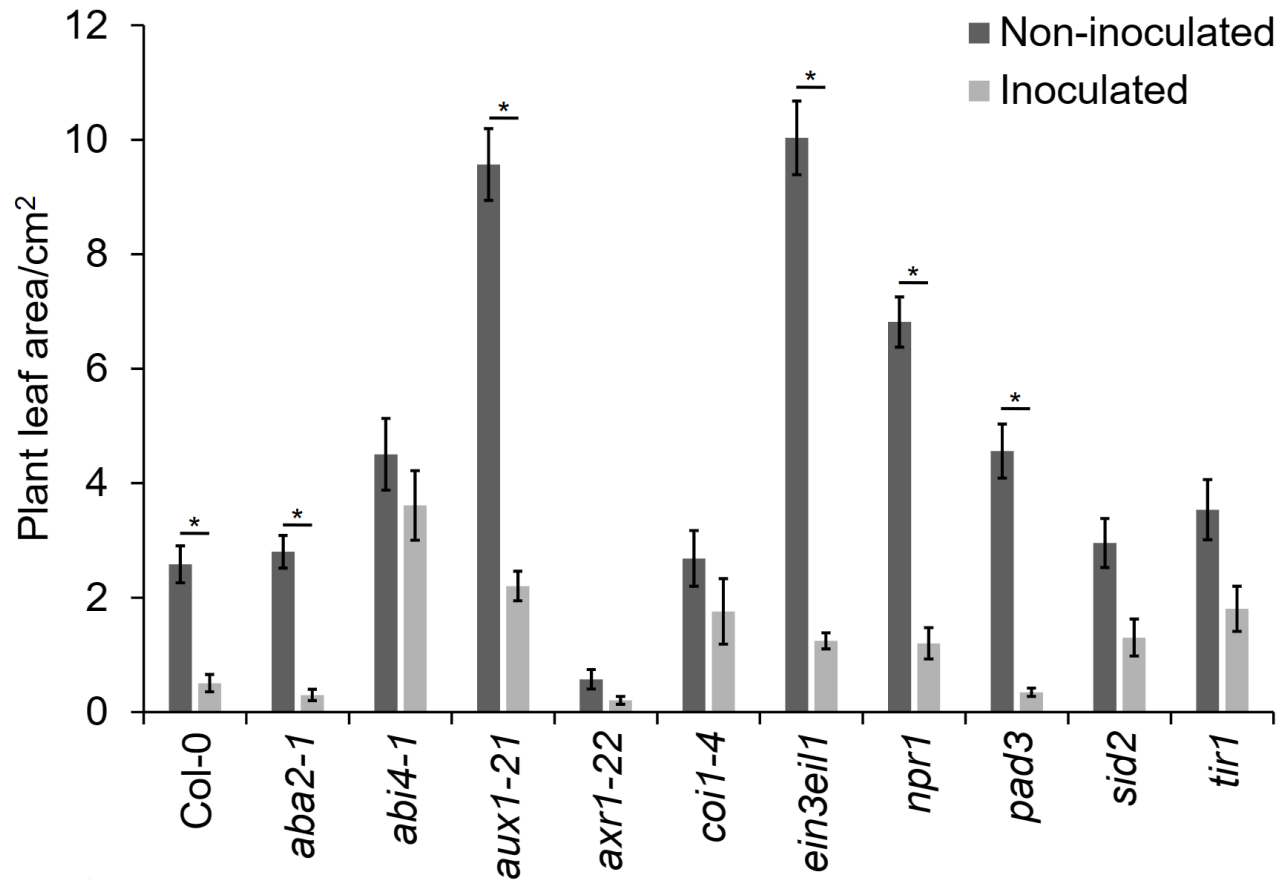
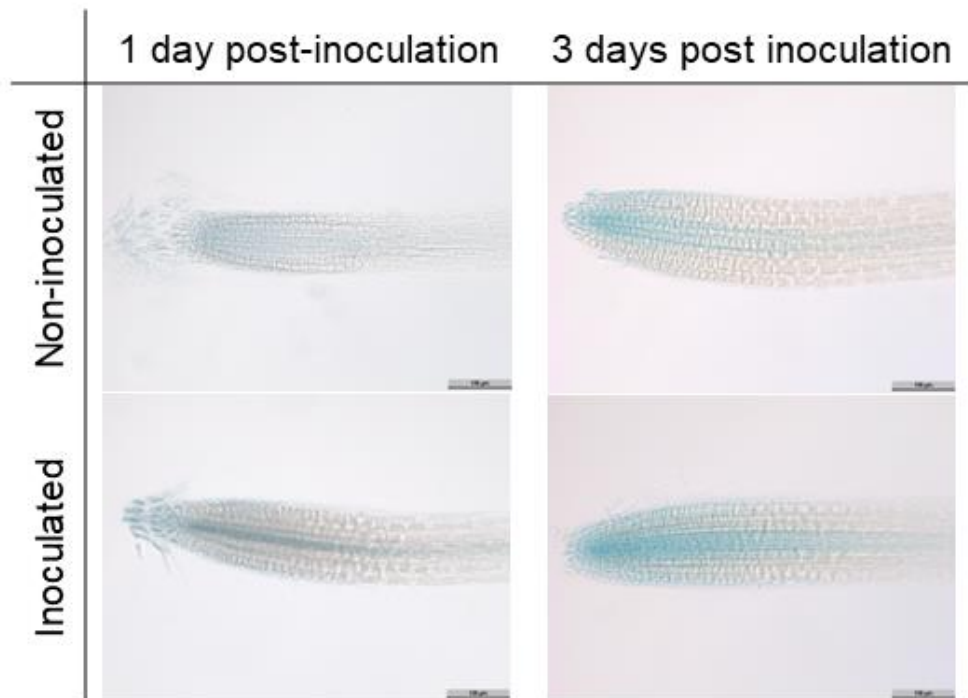


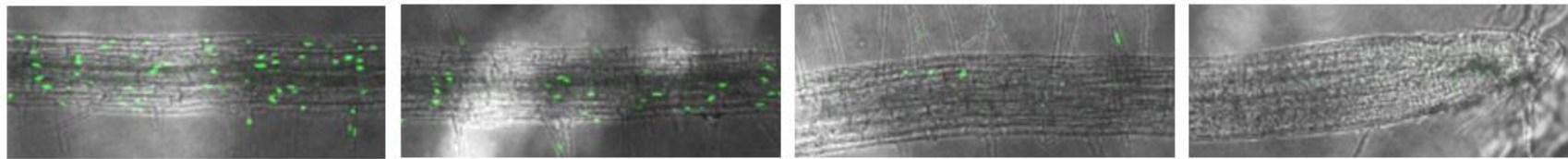
Figure 2-11: Total plant leaf areas of *Arabidopsis thaliana* mutant plants at 11 days post inoculation with *Rhizoctonia solani* AG2-1. Significant differences between the inoculated and non-inoculated plants (t-test, p<0.05) are indicated by a bar and \*.



**Figure 2-12: Response of *Arabidopsis thaliana* IAA2<sub>pro</sub>:GUS lines to *Rhizoctonia solani* AG2-1 at one and three days post-inoculation. Light microscopy images showing GUS staining in Ws IAA2<sub>pro</sub>:GUS plants. At the time of sampling, *R. solani* growth had not reached the root of plants. Scale bar represents 100µm.**

The *A. thaliana* mutant *coi1-4* (JA signalling) did not show a significant loss of growth under inoculation (non-inoculated: 2.68cm<sup>2</sup>, inoculated: 1.76cm<sup>2</sup>; p=0.36) (Figure 2-11), supporting the role of JA signalling in increasing susceptibility to *R. solani*. To visualise JA responses in the susceptible interaction, *A. thaliana* Jas9:VENUS lines were imaged under inoculation with AG2-1 (Figure 2-13**Error! Reference source not found.**) (Larrieu *et al.*, 2015). In the tissues near the root tip where *R. solani* had colonised, no fluorescence was observed, indicating the complete degradation of JAZ9 proteins. In root tissues further away from the infection, JAZ9 appears to be stabilised, indicating a reduction in JA activity.

Non-inoculated



Inoculated

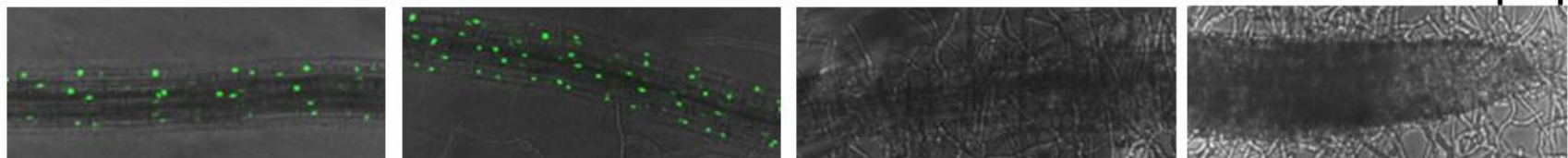


**Figure 2-13: Confocal microscopy images of *Arabidopsis thaliana* Jas9:VENUS seedlings showing JA response to *Rhizoctonia solani* AG2-1 inoculation. Images are ordered left to right reflecting their location within the taproot relative to the root tip, i.e. Most right is the root tip, and most left is furthest from the root tip. Fluorescence from the Jas9:VENUS biosensor is shown in green. Scale bar represents 100µm.**

The ABA biosynthesis mutant *aba2-1* showed a reduction in growth under inoculation (non-inoculated: 2.80cm<sup>2</sup>, inoculated: 0.30cm<sup>2</sup>; p<0.05) (Figure 2-11), suggesting that ABA biosynthesis via this pathway decreases susceptibility. *abi4-1* was not affected in growth by inoculation (non-inoculated: 4.50cm<sup>2</sup>, inoculated: 3.61cm<sup>2</sup>; p=0.38) (Figure 2-11), suggesting ABA signalling increased susceptibility to AG2-1. The ET signalling mutant *ein3eil1* showed a significant reduction in growth under inoculation (non-inoculated: 10.03cm<sup>2</sup>, inoculated: 1.25cm<sup>2</sup>; p<0.001) (Figure 2-11), suggesting that plants with reduced ET signalling were highly susceptible to *R. solani* AG2-1.

*sid2* (also known as *ics1*) did not show a significant reduction in growth under inoculation (non-inoculated: 2.96cm<sup>2</sup>, inoculated: 1.30cm<sup>2</sup>; p=0.18) (Figure 2-11), suggesting that SA biosynthesis via the ICS pathway increased susceptibility. *npr1* showed a significant reduction in growth under *R. solani* inoculation (non-inoculated: 6.81cm<sup>2</sup>, inoculated: 1.20cm<sup>2</sup>; p<0.01) (Figure 2-11) suggesting functional NPR1 reduces susceptibility to AG2-1 of *R. solani*. However, *pad3* showed a significant reduction in growth under inoculation (non-inoculated: 4.56cm<sup>2</sup>, inoculated: 0.35cm<sup>2</sup>; p<0.01) (Figure 2-11), suggesting that a reduction in camalexin biosynthesis increased susceptibility to AG2-1.

## 2.5 Discussion

This is the first study to molecularly characterise the defence response of OSR to its pathogen, *R. solani* AG2-1. The OSR varieties used here

showed contrasting disease phenotypes and use of defence pathways in their response to AG2-1. Using *A. thaliana* mutants, the functionality of key hormonal defence genes against *R. solani* AG2-1 was evaluated to support the gene expression studies. These results showed that auxin, JA and ABA signalling increased plant susceptibility to *R. solani* AG2-1, whilst ET signalling enhanced the resistance response.

Currently there are no *R. solani* AG2-1 resistant OSR varieties, however, it is shown here that some cultivar variation in susceptibility exists, with Anastasia being the most susceptible OSR variety used in this work, whilst Campus was the most resistant. This phenotype was also confirmed using microscopy to visualise the infection caused by *R. solani* sclerotia on *B. napus* roots. Infection cushions were observed developing quickly and more abundantly on the more susceptible hosts consistent with previous research (Verma, 1996) demonstrating that *R. solani* hyphae penetrated more rapidly in susceptible hosts. Indeed, the susceptible Anastasia exhibited severe root rot and death quickly, whereas necrotic lesions formed slowly on Campus and Skye, with the latter two genotypes continuing to grow despite the infection. The observed differences of faster seedling growth and development of the more tolerant genotypes, in contrast to Anastasia exhibiting the slowest root growth under non-inoculated conditions, has identified seedling vigour and growth as useful tolerance traits against the effects of *R. solani* AG2-1.

Molecular studies using RT-qPCRs showed differing defence responses amongst the OSR varieties, which was supported using functional studies with *Arabidopsis* mutants. These results showed a strong link between increased auxin signalling and susceptibility to *R. solani* AG2-1. IAA is synthesised from chorismate, via the tryptophan (Trp)-dependent or Trp-independent pathways (Mano and Nemoto, 2012) and functions through interactions with the E3-ligase complex SCF-TIR1, which promotes the ubiquitination of AUX/IAA proteins and their subsequent degradation (Sugawara *et al.*, 2015). This leads to the de-repression of ARFs and the transcription of auxin-responsive genes. LAX transporters, such as AUX1, are IAA influx carriers, and are vital for IAA concentration gradients (Sugawara *et al.*, 2015). The increased auxin signalling in susceptible hosts demonstrated here with increased expression of key auxin responsive genes, greater resistance of *Arabidopsis* mutants of these genes, and *A. thaliana* IAA2<sub>pro</sub>:GUS lines supports the hypothesis that an auxin produced by the fungus is likely to be involved in the modification of host development and defence. Previous work identified a link between the production of the auxin, phenyl acetic acid (PAA), by *R. solani* and pathogenicity (Bartz *et al.*, 2012). The role of PAA in plants is less studied than IAA, but it is known to be synthesised from phenylalanine, and is found at higher endogenous levels than IAA in various *A. thaliana* plant tissues (Sugawara *et al.*, 2015). In general, auxin-responsive genes can be regulated by both IAA and PAA (Sugawara *et al.*, 2015). It remains to be determined whether *R. solani* AG2-1 isolates produce auxins, and if

so, in what concentration. High auxin concentrations are toxic to plants, and so may function in virulence, but lower concentrations can stimulate growth. Alternatively, prior to colonisation, auxins may diffuse through a substrate to stimulate growth, but play a role in virulence when released in closer proximity.

The activation of auxin–TIR–AUX/IAA–ARF signalling also induces JA synthesis (Yang *et al.*, 2019). JAR1 converts JA to the bioactive JA-Ile with the latter promoting the ubiquitination and degradation of JAZ proteins via the E3-ligase complex SCF-COI1 (Wang *et al.*, 2021) causing the release of MYC2 and ERF1, forming two distinct, antagonistic signalling pathways (Kazan and Manners, 2013). MYC2 plays a substantial role in the crosstalk between growth and hormonal defence regulating pathways. For example, MYC2 is known to repress PLETHORA1 (PLT1) and PLT2 transcription factors, facilitating the interaction between JA and auxin to inhibit root growth (Chen *et al.*, 2011). This may have contributed to the almost complete inhibition of root growth in inoculated Anastasia plants. Furthermore, when using Jas9:VENUS lines under inoculation with AG2-1, increased JA responses were observed near the root tip where *R. solani* had colonised, indicated by the complete degradation of JAZ9 proteins. Based on the expression of the key genes of the JA signalling pathway and the functional analysis in *Arabidopsis*, the MYC2 branch of the pathway was shown to contribute to increased susceptibility to AG2-1.

The JAZs-MYC2 components play an important role in the crosstalk between JA and ABA signalling pathways, affecting plant growth and defence (Chen *et al.*, 2011). ABA enhances the interaction between PYRABACTIN RESISTANCE1-Like protein (PYL6) and JAZ, activating transcription of MYC2, which in turn activates the expression of the JA responsive gene VSP2 against herbivore damage, thus linking ABA and JA defence responses (Aleman *et al.*, 2016). However, this activity negatively regulates the ERF1/ORA59-PDF1.2 branch of the JA pathway required for pathogen defence (Kazan and Manners, 2013). The ABA biosynthesis mutants (*aao3* and *aba2*), as well as the ABA insensitive mutant (*abi4*) showed increased susceptibility to the soil-borne oomycete *Pythium irregulare*, however, these mutants were more resistant to the necrotroph *Botrytis cinerea* (Adie *et al.*, 2007). *abi4-1* showed no loss of growth under *R. solani* AG2-1 inoculation, in contrast to *aba2-1*, suggesting that ABA signalling, rather than biosynthesis, aided susceptibility to *R. solani* AG2-1 inoculation.

JAZs-MYC2 and EIN3/EIL1 of the JA and ET pathways, respectively, co-ordinate the plant defence response against necrotrophic or hemibiotrophic pathogens by activating the expression of the defence protein PDF1.2 through ERF1 and ORA59 (Yang *et al.*, 2019). ERF1 is a downstream component of both ET and JA pathways, and can be activated by both independently, or synergistically (Lorenzo *et al.*, 2003). ERF1 has previously been shown to regulate resistance to many necrotrophic fungi including *B. cinerea*, *Plectosphaerella cucumerina*, *Fusarium oxysporum* f. sp. *Conglutinans* and *F. oxysporum* f. sp.



*Lycopersici* (Berrocal-Lobo and Molina, 2004). Similarly in this work, the increased expression of ERF1 and PDF1.2 in Campus and Skye, in contrast to Anastasia, suggested the ET signalling pathway is a key regulator in the defence response of OSR to *R. solani* AG2-1.

Molecular genetics approaches have shown evidence that ET and NADPH oxidases act to co-ordinate plant responses to both abiotic and biotic stress (Xia *et al.*, 2015). In relation to biotic stress regulation, EIN2-mediated signalling has been shown to be required for flagellin-induced RBOHD-dependent ROS accumulation against bacterial pathogens (Xia *et al.*, 2015). RBOHD is a membrane protein, which undergoes conformational changes and phosphorylation during the influx of Ca<sup>2+</sup> after pathogen perception resulting in the production ROS (Lee *et al.*, 2020). The *A. thaliana* double mutant *rbohF rbohD* also exhibits almost complete loss of resistance to *R. solani* AG8 (Foley *et al.*, 2013). RBOHD can also be directly phosphorylated by DORN1 (Hu *et al.*, 2020), which has been previously shown to enhance the resistance of *A. thaliana* to *R. solani* AG8 (Kumar *et al.*, 2020). Taken together with these results showing upregulation of RBOHD in the more resistant variety Campus, ROS produced via RBOHD is likely to be an effective defence response to *R. solani*. In contrast, RBOHD was depressed in Anastasia at all time points, and instead RBOHC was upregulated. RBOHC, also known as RHD2, is a key regulator of ROS accumulation in the roots involved in root hair formation, and primary root elongation and development by regulating cell expansion (Chapman *et al.*, 2019; Hu *et al.*, 2020). The role of RBOHC in

resistance or susceptibility to soil-borne pathogens is unknown. Based on the expression of these contrasting varieties, RBOHC is not likely to be as effective as RBOHD in the defence to AG2-1. Further work using ROS staining to visualise the presence of ROS during the infection process will aid in understanding the role of ROS in defence.

SA, synthesised via the ICS and PAL pathways, also plays a key role in ROS production through the regulation of RBOH transcription, and can create a feedback loop where ROS also regulate SA signalling (Lukan and Coll, 2022). In this work ICS1 was upregulated more in Anastasia than in Campus or Skye at 24hpi and 48hpi and the *A. thaliana* mutant *sid2* resisted disease, suggesting that SA biosynthesis via the ICS pathway increased susceptibility. The differences in PAL4 expression were not consistent with the disease phenotypes of the varieties tested and therefore a confident inference of the influence of this gene on resistance to AG2-1 cannot be made. However, previously OsPAL4 was identified as contributing to resistance to *R. solani* AG2 (Tonnessen *et al.*, 2015) and BnPAL4 activity was increased in resistant OSR during *Verticillium longisporum* infection (Zheng, Koopmann and von Tiedemann, 2019). The role of PAL4 and secondary metabolism in the interaction with *R. solani* AG2-1 requires further investigation.

High cytosolic levels of SA lead to a redox change, causing cytosolic NPR1 oligomers to monomerise and translocate to the nucleus. There, NPR1 enables the transcription of SA-responsive genes enabling systemic acquired resistance (SAR) responses, and is then targeted for

degradation (Ding and Ding, 2020). NPR1 is also required for induced systemic resistance (ISR) independent of SA accumulation but requiring responsive JA or ET defence pathways (Withers and Dong, 2016). The importance of NPR1 for the response to *R. solani* or other soil-borne pathogens including *P. irregulare* (Adie *et al.*, 2007) has been demonstrated in various reports. For example, tissue-specific expression of AtNPR1 in rice has been shown in previous research to confer resistance to *R. solani* AG1-1A (Molla *et al.*, 2016). Similarly expression of BjNPR1 in mungbean also increased resistance to *R. solani* (AG not specified) (Vijayan and Kirti, 2012). However, here differences in NPR1 expression of OSR varieties and the growth phenotype of the *A. thaliana npr1* mutant under inoculation suggested that NPR1 may play a dual role in the disease response depending on the simultaneous activity of other hormones. Thus, the increased expression of NPR1 in the susceptible Anastasia was associated with NPR1 enabled transcription of SA-responsive genes for SAR (Ding and Ding, 2020) in contrast to Campus, where NPR1 functionality was required for ISR that is independent of SA accumulation, but dependant on responsive JA/ET defence pathways (Withers and Dong, 2016).

PAD3 encodes the cytochrome P450 enzyme CYP71B15 that catalyses the last step of camalexin biosynthesis, and camalexin plays an important role in both SAR and ISR (Nguyen *et al.*, 2022). SA, but not JA or ET, has been shown to be required for ISR associated with camalexin accumulation. Although greater PAD3 activity was observed in Anastasia, suggesting a link between camalexin production and

defence response, *Atpad3* mutants were susceptible to *R. solani*. *R. solani* AG2-1 has been shown to detoxify camalexin (Pedras and Liu, 2004), in part explaining these results, and suggesting a pathogen adaptation strategy rendering SAR or ISR involving camalexin ineffective against AG2-1.

A limitation of this work is the examination of only one *R. solani* AG2-1 isolate. *R. solani* is known to be a diverse species complex, and isolates vary in their virulence. Further work testing these OSR varieties with varied *R. solani* isolates would solidify the role of these pathways in defence. The production of toxins and virulence factors can vary between fungal isolates, and this is likely to play a role in plant defence responses. Further testing of a greater number of OSR varieties will also expand this work and may reveal varieties with greater resistance or tolerance than seen here. As with the variety Skye, some varieties may be able to tolerate *R. solani* AG2-1 damping-off disease if they have strong seedling vigour and are able to establish quickly, and this is worth identifying and investigating further.

In conclusion, these investigations have shown that susceptibility responses to *R. solani* AG2-1 vary among commercially available varieties of *B. napus*. Cv. Anastasia was most susceptible, Campus showed fewest symptoms, while Skye showed greatest root growth under inoculation. Further studies examining the genetic differences between these varieties can identify genes or markers that will inform breeding programs, and lead to the development of more resilient OSR

varieties. Investigating the relative expression of known defence pathway genes in the *B. napus* varieties has suggested that auxin signalling plays a role in susceptibility to *R. solani* AG2-1. Increased expression of genes in ABA signalling and the MYC2 component of JA signalling were also associated with increased susceptibility. In contrast, increased defence response was driven by ET signalling and RBOHD. The broad host range of *R. solani* AG2-1 makes these research findings important for other crops within the same family such as vegetable *Brassicas*. With limited chemical control options available, it is vital that *R. solani* resistant crops are developed to maintain future yields in fields with high inoculum.

## Chapter 3: Examining the role of auxins and

### *Rhizoctonia solani* AG2-1

#### 3.1 Abstract

The endogenous auxins indole-3-acetic acid (IAA) and phenyl acetic acid (PAA) play key roles in plant growth and development and can also influence plant immunity. Two Anastomosis Groups (AG3 and AG4) of the necrotrophic soil-borne pathogen *Rhizoctonia solani* have been previously shown to produce PAA, which may play a role in virulence. This chapter quantified the changes in the root architecture of *Arabidopsis thaliana* auxin resistant mutants *axr1* and *aux1* under *R. solani* AG2-1 inoculation and compared this with the effects of PAA and synthetic auxins 2,4-D and NAA, both with and without the presence of *R. solani*. The differences in root architecture for plants grown on plates at different distances from the pathogen showed that *R. solani* reduced the root length of WT plants at all distances from the pathogen, but not for *aux1* mutants, which also grew more agravitropically at the furthest distance from the pathogen. Quantifying the effects of auxins also led to the observations that PAA caused growth inhibition, increased lateral root number, and increased gravitropism in *aux1* plants. These results showed that PAA at low concentrations was able to stimulate *R. solani* AG2-1 growth but at high concentrations growth was inhibited almost completely. Finally, quantification of IAA and PAA from *R. solani* broth cultures showed that AG2-1 was able to produce both auxins *in vitro*.

Further experiments testing whether the isolates that produced the greatest concentration of auxins *in vitro* also cause the largest effects on root architecture will strengthen the hypothesis that auxin production by *R. solani* causes the changes in root architecture observed here. This work has provided insights into the relationship between PAA and auxin transport and signalling, as *aux1* mutants appear to be less resistant to PAA than *axr1* mutants.

### 3.2 Introduction

Auxins are vital to plant growth and development and play a role in defence against plant pathogens. Most auxin research has focussed on indole-3-acetic acid (IAA), but another endogenous auxin phenyl acetic acid (PAA), also functions in growth and defence. PAA naturally occurs at much higher concentrations than IAA (Wightman and Lighty, 1982; Morris and Johnson, 1987; Sugawara *et al.*, 2015) and is active at approximately 10-fold higher concentrations than IAA in *A. thaliana* (Sugawara *et al.*, 2015). Previous work has shown that IAA and PAA are both able to regulate auxin-responsive genes through the TIR1 pathway in *A. thaliana*, but have very different transport characteristics (Sugawara *et al.*, 2015).

The promoters of auxin-inducible genes contain Auxin Response Elements (AREs), which interact with AUXIN RESPONSE FACTOR (ARF) transcription factors (Paciorek and Friml, 2006). Aux/IAA transcriptional repressors interact with ARFs to prevent transcription of

auxin-inducible genes (Paciorek and Friml, 2006). The interaction of auxin with the SCF-type ubiquitin protein ligase E3 complex (SKP1-CUL1-TIR1/AFB-RBX1) transfers activated ubiquitin to Aux/IAA proteins, labelling them for degradation (Dharmasiri *et al.*, 2007). RUB-activating (AXR1 and ECR1) and RUB-conjugating enzymes (RCE1) mediate post-translational modifications of the CUL1 subunit (Dharmasiri *et al.*, 2007). *axr1* mutants show decreased plant height, irregularly shaped and curled rosette leaves, reduced fertility, shortened hypocotyls of dark-grown seedlings, reduced gravitropic responses and increased root elongation (Lincoln, Britton and Estelle, 1990; Leyser *et al.*, 1993). *axr1* plants are also resistant to the effects of exogenous 2,4-dichlorophenoxyacetic acid (2,4-D), IAA and 1-naphthalene acetic acid (NAA) (Yamamoto and Yamamoto, 1999). The degradation of Aux/IAA proteins de-represses ARF transcription factors, allowing transcription of auxin-inducible genes to take place. IAA and PAA may have different affinities for auxin co-receptors, but function through the same pathway, as shown by a pull-down assay where IAA enhanced the formation of TIR1-IAA3 and TIR1-IAA7 complexes, while PAA only enhanced TIR1-IAA7 complexes at the same concentrations (Sugawara *et al.*, 2015). A microarray analysis tested gene induction in *A. thaliana* after treatment with IAA or PAA and showed that many of the same genes are upregulated by both PAA and IAA, but not necessarily to the same degree (Sugawara *et al.*, 2015). A study testing every TIR/AFB with every AUX/IAA found that, overall, IAA had higher activity than PAA,



however IAA12 and IAA13 had a high sensitivity to PAA with TIR1 (Shimizu-Mitao and Kakimoto, 2014).

IAA exhibits polar transport which is facilitated by the asymmetric localisation of PIN-FORMED (PIN) and P-GLYCOPROTEIN (PGP) auxin efflux carriers and AUXIN1/LIKE-AUX1 (AUX/LAX) auxin influx carriers (Swarup and Péret, 2012). AUX1 functions as a carrier for IAA and 2,4-D and its mutant *aux1* displays an agravitropic phenotype, which can be restored by NAA (Marchant, 1999). *aux1* is similarly resistant to the effects of adding either IAA or 2,4-D (Yamamoto and Yamamoto, 1998) and depletes intracellular auxin levels, increasing root growth (Bennett *et al.*, 1996). Polar gradients and transmembrane transport carriers have not been observed for PAA, and it is not transported across long distances in the plant (Johnson and Morris, 1987; Morris and Johnson, 1987) although this has not been fully explored with PAA conjugates (Cook, 2019). PAA is readily taken up by the roots (Morris and Johnson, 1987), and is not affected by IAA chemical polar transport inhibitors (1-naphthylphthalamic acid: NPA, 2,3,5-triiodobenzoic acid: TIBA), suggesting that it is not a substrate for IAA carriers (Johnson and Morris, 1987). Work on maize seedlings showed that PAA is not transported actively or directionally (Sugawara *et al.*, 2015). Cook (2019) suggested that PAA biosynthesis and catabolism are the sole mechanisms for PAA regulation. However, PAA is able to inhibit IAA polar transport by blocking its efflux from cells, leading to the accumulation of IAA in cells with high PAA concentrations (Morris and Johnson, 1987). It has been suggested that an important

role for PAA may be to regulate the distribution and/or accumulation of IAA (Johnson and Morris, 1987).

Auxin interacts with other plant hormones including salicylic acid (SA) and jasmonic acid (JA), affecting defence responses to pathogens. The interaction between SA and auxin is mutually antagonistic and auxin can repress the expression of pathogenesis-related (PR) genes (Kazan and Manners, 2009). However, the signalling pathways of JA and auxin share many commonalities, and both can be involved in defence responses to necrotrophic pathogens (Kazan and Manners, 2009).

Previous studies have shown auxin mutants with increased resistance to *Fusarium oxysporum* (Kidd *et al.*, 2011), while mutants were more susceptible to *Plectosphaerella cucumerina*, *Botrytis cinerea* (Llorente *et al.*, 2008) and *Pythium irregulare* (Tiryaki and Staswick, 2002).

*Rhizoctonia solani* isolates from the Anastomosis Groups (AG) AG3 and AG4 have been shown to produce PAA and its derivatives when grown in culture, however this was inversely correlated with pathogenicity or virulence (Iacobellis and DeVay, 1987). High concentrations (1mM) of PAA and its derivatives were shown to inhibit the growth of tomato and bean seedlings, but lower concentrations of m-OH-PAA (0.01mM) were stimulatory (Iacobellis and DeVay, 1987). Another study identified PAA and its derivatives in *R. solani* AG3 cultures (along with one isolate for each of AG1-1A and AG4), and found that necrosis was induced in tomato seedlings grown in media containing PAA and its derivatives (Bartz *et al.*, 2012). A correlation was

also observed between high PAA producing isolates and high mortality for tomato seedlings (Bartz *et al.*, 2012). Root growth inhibition in rape seedlings can be seen above a 0.005% concentration of PAA and above 0.025% for m-OH-PAA (Aoki, Sassa and Tamura, 1963). PAA and p-OH-PAA were identified in sugar beet infected with *R. solani*, but m-OH-PAA was not (Aoki, Sassa and Tamura, 1963). m-OH-PAA and m-OMe-PAA were isolated from *R. solani* AG4 and were shown to inhibit root and hypocotyl growth in lettuce (Mandava *et al.*, 1980).

This chapter aimed to investigate the relationship between auxins and *Rhizoctonia solani* using *Arabidopsis thaliana*. The effects of 2,4-D, PAA and NAA on the root architecture of *A. thaliana* auxin mutants were quantified and compared with their growth in the presence of *R. solani*. The tested mutants were known to resist the effects of 2,4-D, but *axr1* mutants do not resist NAA. High quantities of PAA were hypothesised to induce changes in the root architecture of the auxin mutants, such as increased gravitropism and increased lateral root number due to its effects on IAA accumulation. Having observed increased auxin activity in OSR inoculated with *R. solani* AG2-1, it was hypothesised that there would be quantifiable effects of *R. solani* inoculation on root architecture, potentially due to the production of auxins by the pathogen. Plant root architecture was tested with the addition of both auxins and *R. solani* AG2-1 to identify whether an additive effect would be observed. It was hypothesised that AG2-1 isolates would produce PAA, similarly to previously tested AG3 and AG4 isolates, and that the concentration of PAA required for growth

inhibition of *R. solani* AG2-1 would be higher than that which was produced by the fungus or is found naturally in plants.

### 3.3 Methods







#### 3.3.1 Seed lines and preparation

*Arabidopsis thaliana aux1* and *axr1* seed lines were obtained from Dr Ranjan Swarup, University of Nottingham. Seeds were prepared with surface sterilisation using a 25% bleach solution for three minutes followed by three washes with sterile distilled water. They were plated on 0.5MS pH5.8 1% agar plates and cold stratified for three days at 4°C. Plates were moved to a controlled environment chamber with 16h light at 21°C and 8h night at 15°C.

#### 3.3.2 Growth of *Rhizoctonia solani*

*R. solani* AG2-1 isolates #1926, #1927, #1933, #1934, #1942 and 2076 from the University of Nottingham isolate collection were cultured on potato dextrose agar plates (PDA; Sigma-Aldrich, UK) at room temperature (18°C). Unless otherwise specified, isolate #1934 was used throughout, as 6 mm diameter plugs from seven-day old plates.

**Table 3-1: University of Nottingham *Rhizoctonia solani* AG2-1 isolates.**  
**Isolates were grown on PDA plates at room temperature.**

<u>Isolate identifier</u>	<u>Photograph</u>	<u>Additional information</u>
#1926		Originally obtained from FERA
#1927		Originally obtained from FERA
#1933		Originally obtained from FERA
#1934		Originally obtained from ADAS
#1942		Originally obtained from ADAS
#2076		Foreign Isolate from USA, obtained from Marc Cubeta

### 3.3.3 Inoculation of *Arabidopsis thaliana* auxin mutants with *Rhizoctonia solani* AG2-1 in compost

*Arabidopsis thaliana* WT, *aux1* and *axr1* seeds were sterilised and plated then grown for eleven days after cold stratification. They were transplanted into M3 compost, and then moved into experimental trays three days later. Experimental trays were prepared with 12-well trays, half filled with M3 compost, then ten inoculated or sterile PDA plugs added per well, then filled with M3 compost. Trays were watered once only at the start of the experiment to a depth of 1cm and covered with clear plastic lids to maintain high humidity. Experiments were designed as randomised blocks, with inoculated and non-inoculated 12-well trays to prevent cross contamination. These trays were grown for 17days at 20°C and 18°C with a 12hour photoperiod. Digital photographs were taken and the leaf area was calculated using ImageJ software (Schneider, Rasband and Eliceiri, 2012). A ruler was included in every photograph for scaling measurements.

### 3.3.4 Effects of the presence and location of *Rhizoctonia solani* AG2-1 on the root architecture of *Arabidopsis thaliana* auxin mutants

A factorial experimental design was used with the following factors: inoculation (levels: inoculated or non-inoculated), genotype (levels: WT, *aux1* or *axr1*) and plug position (levels: A, B or C) with a total of 18 treatment combinations replicated five times. The plug position variable was converted to the distance from the plug for the analysis (levels:

1.5cm, 3.5cm, 6.5cm and 8.5cm). Four plants were used per plate (with all plants of the same genotype on an individual plate), and the location of each plug was recorded, along with the distance from the plant to the plug. The experimental setup is shown as a diagram in Figure 3-1A and an example plate photograph is included in Figure 3-2A. Seeds were surface sterilised and plated, then cold stratified for four days. The plates were grown vertically for seven days, then the plugs were added. Photographs were taken using a digital camera with a black background six days post-inoculation (dpi). Two preliminary versions of this experiment were completed with plugs present in location B only, or locations A and C only. This experimental setup was completed once.

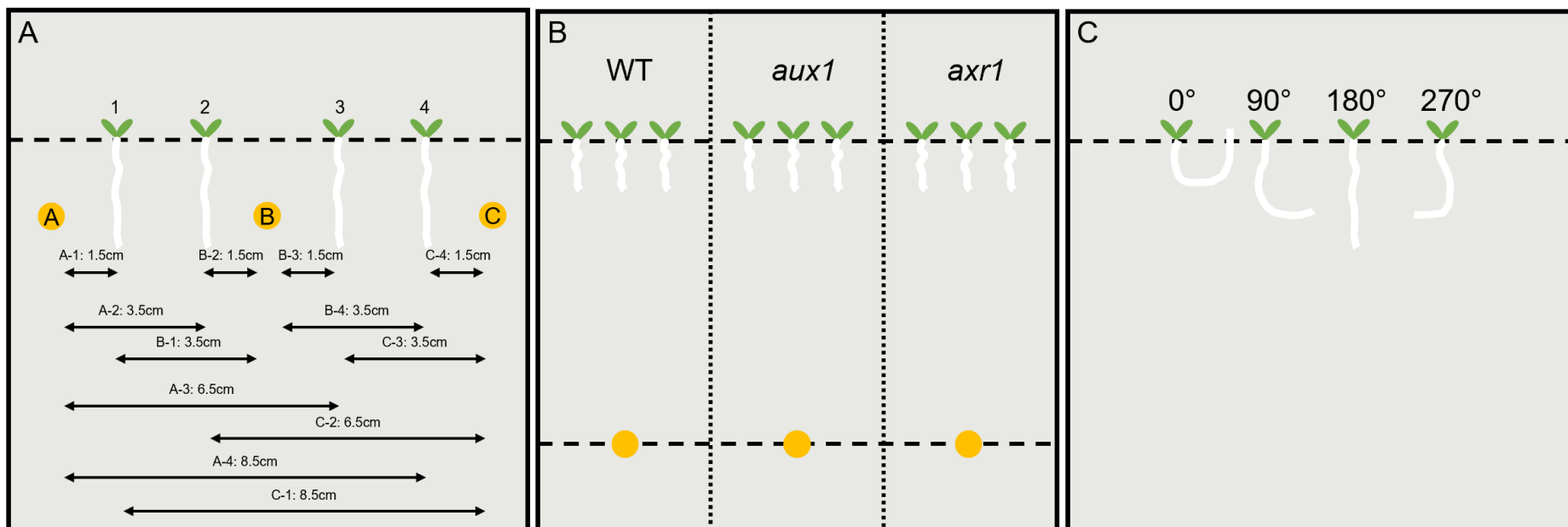


**Figure 3-1: Schematic diagrams showing the plate layouts and angle of root growth measurements. A) Plate layout used to test the effects of the presence and location of *Rhizoctonia solani* AG2-1 on *Arabidopsis thaliana* auxin mutants. Plants were grown in the locations marked 1-4 with one genotype used per plate. A sterile or *R. solani* inoculated plug was added at location A, B or C after the plants had grown for 7 days. Distances are shown between each plug-plant combination. B) Plate layout used for inoculation with *R. solani* and auxins. Media was supplemented with auxins or the same volume of DMSO, and *R. solani* inoculated or sterile plugs were added. C) Examples of root growth angle measurements. The angle was measured at the root tip, with 180° representing gravitropic growth.**



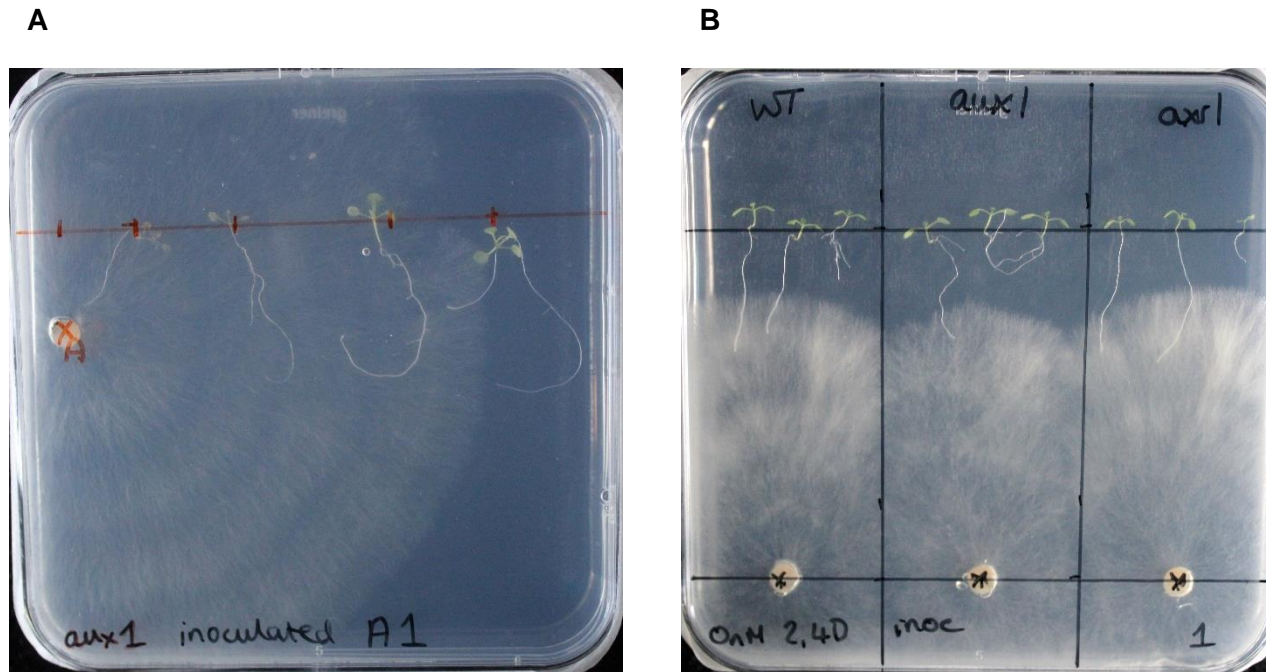


Figure 3-2: Photographs showing the experimental setup of A) testing the effects of the presence and location of *Rhizoctonia solani* AG2-1 on the root architecture of *Arabidopsis thaliana* auxin mutants, B) testing the effects of 2,4-D, PAA and NAA with *Rhizoctonia solani* AG2-1 inoculation on the root architecture of *Arabidopsis thaliana* auxin mutants.

### 3.3.5 Effects of 2,4-D, PAA and NAA on the root architecture of *Arabidopsis thaliana* auxin mutants

To determine the functional effects of 2,4-D, PAA and NAA on growth and root architecture of *A. thaliana aux1*, *axr1* mutants (defective in auxin transport and signalling respectively) and wildtype (WT, Col-0) plants were used. All auxins were obtained from Dr Ranjan Swarup, University of Nottingham. Auxins were dissolved in dimethyl sulfoxide (DMSO). For control plates (0M auxin concentration), the highest volume of DMSO was added. Seeds were surface sterilised, plated in a “nursery” set up, cold stratified and grown for four days. They were moved to the experimental plates with different concentrations of auxins and photographed nine days after the transfer. Preliminary experiments were used to determine the optimum auxin concentrations.

### 3.3.6 Effects of 2,4-D, PAA and NAA with *Rhizoctonia solani* AG2-1 inoculation on the root architecture of *Arabidopsis thaliana* auxin mutants

To test the effects of the presence of both the auxins and *R. solani* together, seeds were prepared as described in section 3.3.1 and were grown for four days before moving into experimental plates with a two-factor design: inoculation (levels: inoculated or non-inoculated), and presence of auxins (levels: high concentration of auxin or no auxins) (total: 4 treatments). Plates without high auxin concentration had the same volume of DMSO added, and non-inoculated plates had sterile

PDA plugs added. Three plants of each genotype were placed 1cm apart on each plate, and each treatment had 4 replicate plates (Figure 3-1B). The plates were photographed at five days post inoculation (dpi). Five dpi was the final time point used as after this time the fungus had grown to cover the entire plate, so the inoculated plants did not show further growth. Each experiment was repeated with consistent results.

### 3.3.7 Root architecture characteristics and image analysis

Photographs were taken using a digital camera with the plates face down, through the agar medium, onto a dark background for experiments described in sections 3.3.4, 3.3.5 and 3.3.6. Root characteristics were measured from the photographs using the SmartRoot plugin for ImageJ to quantify the root length, number of lateral roots, and the direction of root growth (Lobet, Pagès and Draye, 2011; Schneider, Rasband and Eliceiri, 2012). The direction of root growth was taken to be the angle measurement at the root tip. An angle of 180° represents roots growing downwards and any difference from this occurs when the roots are growing agravitropically (Figure 3-1C).

The absolute proportion of 180° was calculated using the following

formula: 
$$\left| \frac{\text{Angle of root growth} - 180^\circ}{180^\circ} \right|.$$

### 3.3.8 *Rhizoctonia solani* growth response to exogenous PAA

The growth response of *R. solani* isolate #1934 was tested following the method in Bartz *et al.* (2012). 100mL of Potato Dextrose Broth (PDB)

was added to 250mL conical flasks and sealed with non-absorbent cotton wool and foil before autoclaving. PAA was added to the media to give the following concentrations: 0.1, 0.5, 1.0, 3.0 and 7.5mM, plus 0mM PAA as a control. Three flasks were prepared per concentration. Flasks were inoculated with one plug of freshly cultured mycelium. Three further flasks were prepared at 0.5mM PAA with a plug of sterile PDA added as the non-inoculated control. Flasks were covered in foil to provide a dark environment and arranged in a randomised block design, then incubated at room temperature (18°C) for three weeks. Mycelium was separated from the broth using centrifugation, washed with sterile distilled water, and freeze-dried. This experiment was completed once.

### 3.3.9 Quantification of PAA and IAA from *Rhizoctonia solani* grown in liquid media

*Rhizoctonia solani* isolates (Table 3-1) were grown for analysis using the method described in Bartz *et al.* (2012). 250mL conical flasks were prepared with 100mL of Vogel's media (Vogel, 1956) (Supplementary Information 1), prepared without sucrose. One plug of freshly cultured mycelium was added to each flask, and three replicates were made per fungal isolate. Non-inoculated control flasks used sterile PDA plugs. Flasks were covered with foil to maintain darkness and incubated in a randomised block design at room temperature (18°C) for three weeks. Centrifugation was used to separate the mycelium and the broth. The mycelium was washed and freeze-dried, while the broth was stored at -

80°C until needed. 1mL aliquots of broth were prepared to minimise freezing and thawing.

### 3.3.10 LC-MS/MS analysis

Liquid-liquid extractions were used to prepare the broth samples for LC-MS/MS analysis. IAA and PAA standards (Sigma-Aldrich) were dissolved in 100% HPLC-grade MeOH. An internal standard solution was made with the deuterated standard 5µM PAA-d7 (Sigma-Aldrich) and 5µM IAA-d5 (Sigma-Aldrich) in 100% MeOH. 500µL ethyl acetate with 0.1% (v/v) acetic acid (acidified ethyl acetate) was added to 1mL of sample with 10µL internal standards solution. The tubes were mixed vigorously then allowed to separate and the upper fraction removed. This was repeated twice, and the three upper fractions merged. These were dried under nitrogen and reconstituted in 50µL 100% MeOH for liquid chromatography with tandem mass spectrometry (LC-MS/MS) analysis.

The HPLC Column used was Phenomenex Luna C18 100 Å LC 3µm (100x2mm, 3 µm particle size), maintained at 40°C in a Sciex ExionLC™ Series UHPLC (Applied Biosystem, Foster City, CA, USA). The programmed LC gradient was from 10% B to 99% B for four minutes, maintained at 99% B for another three minutes and then lowered to 10% B within 10 seconds followed by column re-equilibration for three minutes. The mobile phase A was 0.01% formic acid in 100% water and mobile phase B was 0.01% formic acid in methanol with a

flow rate of 0.45 mL/min. Injection volume was set to 10  $\mu$ L and samples were maintained at 4°C.

Mass spectrometry (MS) was performed using an Applied Biosystem MDS SCIEX 6500 Q-Trap hybrid triple-quadrupole–linear ion trap mass spectrometer (Applied Biosystem, Foster City, CA, USA) equipped with an electrospray ionisation (ESI) interface in multi-reaction monitoring (MRM) mode. The following conditions of detection were applied: an electrospray ionization (ESI) Turbo Spray source operating in negative mode at 450°C with the appropriate settings: curtain gas (nitrogen) 20psi, ion source gas 1 (GS1) 50psi, ion source gas 2 (GS2) 50psi, collision gas (nitrogen) at low position, ionization voltage –4000 V, MRM dwell time 25ms, pause between mass range 5ms and entrance potential (EP) –10V. For PAA and the deuterated PAA, the following transitions under optimal instrumental conditions of collision energy (CE), declustering potential (DP) and collision cell exit potential (CXP) were obtained: for PAA: 270.9 > 90.9 (CE = –24eV, DP = –45V, CXP = –15V), d7-PAA: 141.9 > 97.9 (CE = –12eV, DP = –75V, CXP = –11V). Chromatograms for the highest and lowest standard concentrations of both IAA and PAA are shown in Supplementary Information 2-5.

Quantification of each analyte was calculated using a fully extracted calibration standard curve. The peak area ratio of each analyte was used to calculate the molar concentration using the calibration standard curve. Quantification was performed using Analyst V.3.0.3 software. Analysis of the broth samples by LC-MS/MS was completed once.

### 3.3.11 Statistical analysis

All statistical analysis was carried out using Genstat® Version 22 for windows (VSN International Ltd, UK). Analysis of variance was carried out for the data in sections 3.3.4, 3.3.5 and 3.3.6 to determine significant terms and interactions. For section 3.3.4, analysis was carried for each genotype separately. For section 3.3.5 and 3.3.6, analysis was carried for each auxin separately. In section 3.3.5 root length was assessed as a proportion of the 0M auxin concentration control. For the growth response of *R. solani* AG2-1 to exogenous PAA (section 3.3.8), the freeze-dried sample weights were calculated as a proportion of the 0mM control, and a growth response curve plotted as a critical exponential standard curve.

## 3.4 Results

### 3.4.1 Disease phenotyping of *Arabidopsis thaliana* auxin mutants

The leaf area for plants grown in compost was measured in the presence and absence of *R. solani* AG2-1 inoculation (Figure 3-3). For the wild-type (Col-0) plants, *t*-tests showed a significant reduction in growth under inoculation ( $p=0.05$ ). For *aux1* mutants, plants did not show a significant reduction in growth under inoculation ( $p=0.21$ ), suggesting they have increased tolerance to disease. For *axr1*, plants showed a significant reduction in growth under inoculation ( $p=0.05$ ), however both the inoculated *axr1* and *aux1* plants were able to grow larger than the inoculated WT plants, though this was not significant.

Figure 3-3B shows representative images of the plants with and without inoculation.



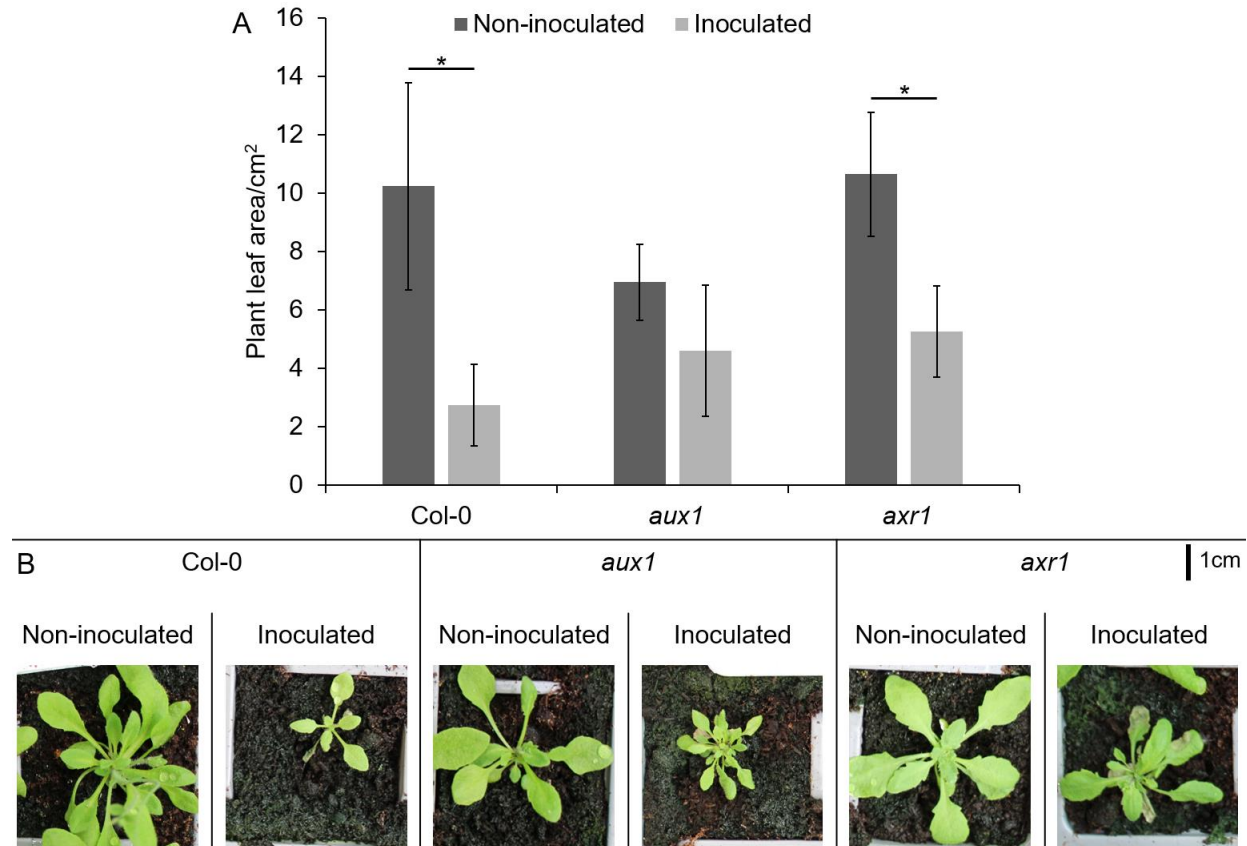


**Figure 3-3: A) Bar chart of the total plant leaf areas of *Arabidopsis thaliana* mutant plants at 17 days post inoculation with *Rhizoctonia solani* AG2-1. Standard error bars are shown. \* indicates a significant difference between the non-inoculated and inoculated plants ( $p=0.05$ ). B) Representative images of the same experiment. A 1cm scale bar is shown for the plant images.**

### 3.4.2 Effects of *Rhizoctonia solani* AG2-1 on the growth of *Arabidopsis thaliana* auxin mutants

Plant root architecture was measured six days after the inoculation of *A. thaliana* auxin mutants with a plug from *R. solani* AG2-1 inoculated or sterile PDA plates. This timepoint allowed for the maximum differences between the plants to be observed. Observed root lengths are shown in Figure 3-4. Inoculation reduced root length for WT plants irrespective of plug distance, however increasing the distance from the inoculated plug resulted in longer roots in *aux1* plants, although not beyond the non-inoculated root length. In contrast there were no differences due to inoculation for root length of *axr1*. Lateral root numbers increased in WT and *aux1* with increasing distance from the inoculated plug (Figure 3-5). Inoculated *axr1* plants did not grow any lateral roots at any distance while the non-inoculated *axr1* plants grew very few lateral roots. Analysis of the angle of root growth is shown in Figure 3-6. Although not significant, some differences were observed. The WT plants generally grew more gravitropically under inoculation. There was a significant interaction between inoculation and distance ( $p=0.027$ ) for *aux1* plants. Inoculated *aux1* plants were most agravitropic at 6.5cm away from the plug. *axr1* plants showed a similar degree of gravitropism for both inoculated and non-inoculated plants at all distances.

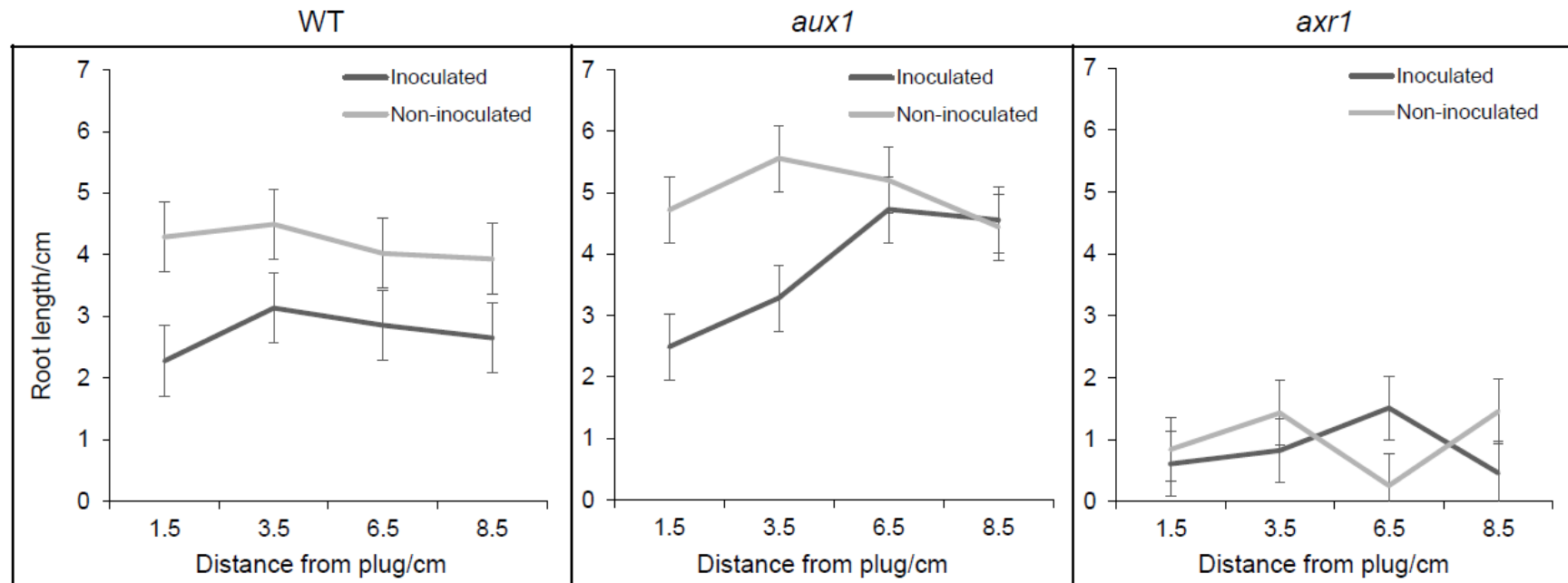


**Figure 3-4: Line graphs showing the effect of the presence of *Rhizoctonia solani* AG2-1 on the root length of *Arabidopsis thaliana* auxin mutants. Analysis of variance was carried out for each genotype separately. Standard error bars are shown. Inoculation had a significant effect on the root length of WT plants ( $p < 0.001$ ). Both inoculation ( $p < 0.001$ ) and distance ( $p = 0.004$ ) and the interaction between them ( $p = 0.003$ ) were significant for *aux1*. For *axr1*, the interaction between distance and inoculation was almost significant ( $p = 0.051$ ). Full analysis is shown in Supplementary Information 6-8. Growth was consistently inhibited, regardless of distance for WT plants, while the *aux1* mutant was only inhibited in growth close to the pathogen. Neither inoculation nor distance affected *axr1* growth.**

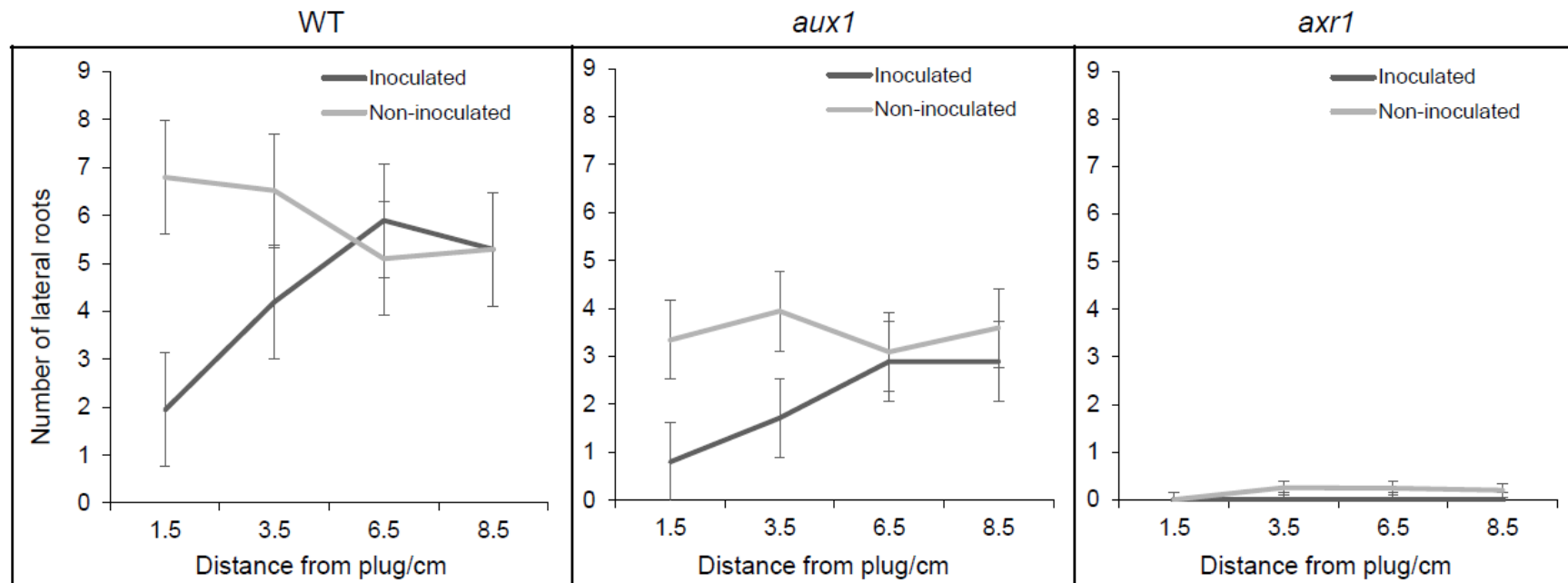


**Figure 3-5: Line graphs showing the effect of the presence of *Rhizoctonia solani* AG2-1 on the number of lateral roots of *Arabidopsis thaliana* auxin mutants. Analysis of variance was carried out for each genotype. Standard error bars are shown. The effect of inoculation ( $p < 0.001$ ) and the interaction between inoculation and distance ( $p = 0.003$ ) were significant for WT plants. Inoculation also had a significant effect on *aux1* ( $p < 0.001$ ) and *axr1* ( $p = 0.023$ ) lateral root numbers. Full analysis is shown in Supplementary Information 9-11. For both WT and *aux1* plants, the number of lateral roots was reduced close to the pathogen, while *axr1* plants grew few lateral roots under either inoculated or non-inoculated conditions.**

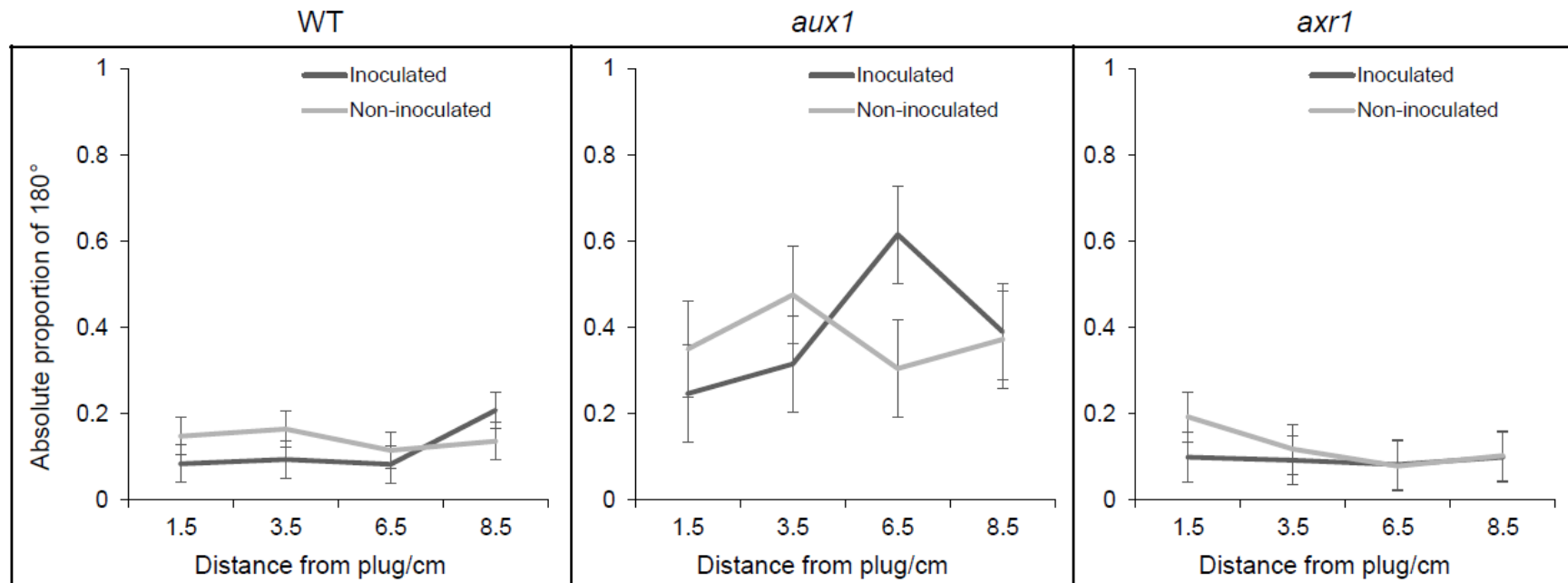


**Figure 3-6: Line graphs showing the effect of the presence of *Rhizoctonia solani* AG2-1 on the angle of root growth of *Arabidopsis thaliana* auxin mutants. Analysis of variance was carried out for each genotype separately. The absolute proportion of 180° was calculated, which is the angle of growth when the plant is growing towards the bottom of the plate. Standard error bars are shown. There were no significant effects of inoculation or distance for WT or *axr1* plants. For *aux1* plants, there was a significant interaction between inoculation and distance ( $p=0.027$ ). Full analysis is shown in Supplementary Information 12-14. Although the effects of inoculation and distance were not significant for WT and *axr1* plants, an increase in the straightness of WT and *axr1* roots was observed up to 6.5cm, while *aux1* roots were more gravitropic at 1.5cm and 3.5cm from the pathogen.**

### 3.4.3 Effects of 2,4-D, PAA and NAA on the growth of *Arabidopsis thaliana* auxin mutants

Plant root architecture was measured nine days after the transfer of *A. thaliana* auxin mutant plants onto media plates containing auxins at a range of concentrations. *Arabidopsis thaliana* WT plants showed root growth inhibition with increasing concentrations of 2,4-D, while both *aux1* and *axr1* mutants were resistant to the effects of 2,4-D (Figure 3-7). WT plants were also inhibited by PAA at all concentrations tested. *aux1* plants were stimulated by PAA at 2.5 $\mu$ M and showed growth inhibition at 10 $\mu$ M and 20 $\mu$ M. *axr1* was resistant to the PAA concentrations tested. WT root growth was stimulated at all but 500nM concentration of NAA. Similarly, *aux1* plants showed growth inhibition at 200nM and 500nM. *axr1* plants were inhibited at all NAA concentrations. Increasing 2,4-D concentrations led to decreases in the lateral root number for all genotypes, though the WT plants had more lateral roots than either mutant (Figure 3-8). PAA concentrations did not affect the lateral root number for WT plants or *axr1* plants but led to increased numbers of lateral roots for *aux1*. Increasing concentrations of NAA led to increases in lateral root number for all genotypes tested. It was observed that WT and *aux1* roots became less gravitropic at higher 2,4-D concentrations, though this was much more pronounced for *aux1* plants (Figure 3-9). *axr1* roots increased in straightness up to 100nM 2,4-D. WT and *axr1* roots grew gravitropically at all concentrations of PAA and *aux1* roots showed increased gravitropism from 5 $\mu$ M. WT roots grew gravitropically at all concentrations of NAA.

*axr1* roots increased in their gravitropism over the concentration range, while *aux1* increased its gravitropism up to 200nM NAA.

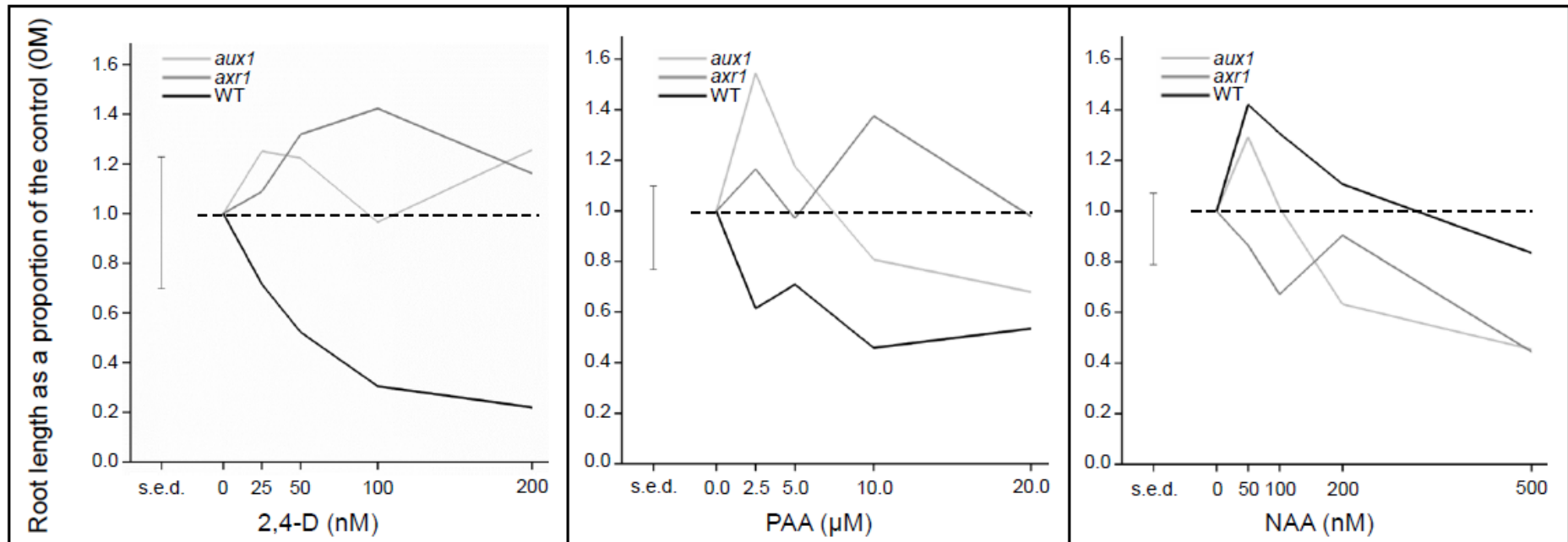
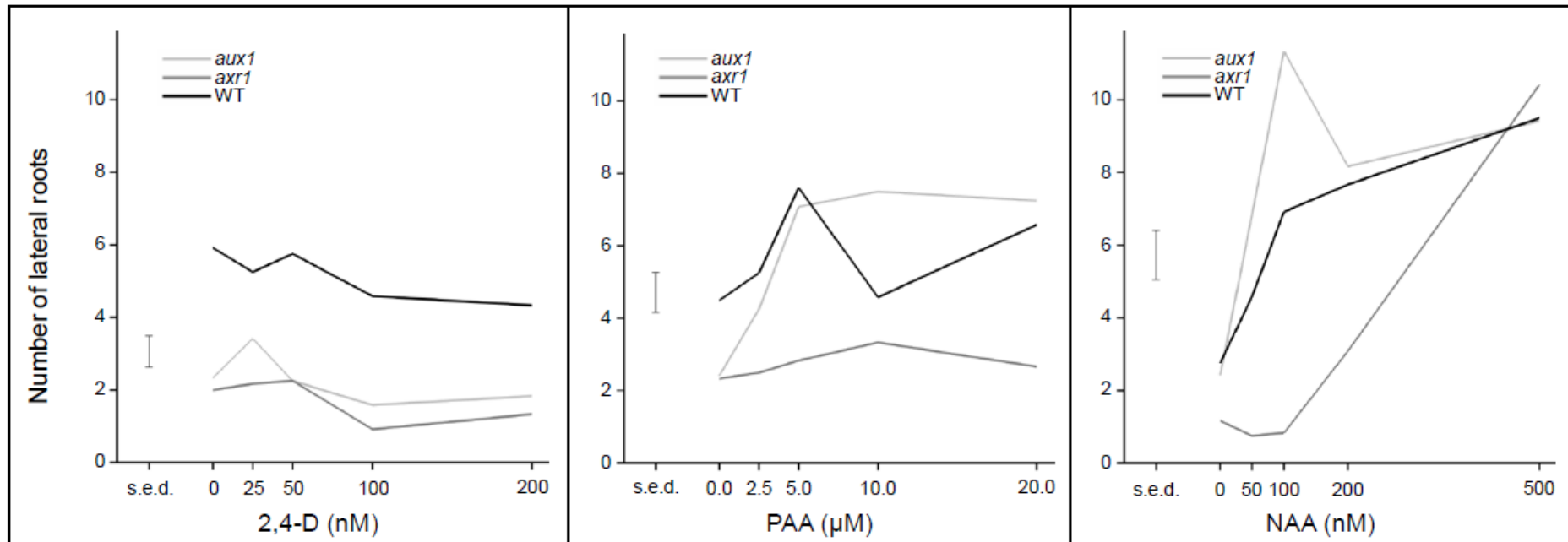


Figure 3-7: Line graphs showing the effect of 2,4-D, PAA and NAA auxin concentrations on the root length of *Arabidopsis thaliana* auxin mutants. Analysis of variance was carried out for each auxin separately. The standard errors of differences of means are shown. Analysis of the root length was calculated using proportions of the 0M auxin concentration control. Values on the graph that are greater than 1 represent an increase in root growth compared to the 0M control. The effect of genotype was significant for all auxins (2,4-D  $p=0.012$ , PAA  $p=0.01$ , NAA  $p=0.016$ ). The effect of NAA concentration was also significant ( $p=0.005$ ). Full analysis is shown in Supplementary Information 15-17.





**Figure 3-8: Line graphs showing the effect of 2,4-D, PAA and NAA auxin concentrations on the number of lateral roots of *Arabidopsis thaliana* auxin mutants. Analysis of variance was carried out for each auxin separately. The standard errors of differences of means are shown. The effect of genotype was significant for all auxins (2,4-D  $p < .001$ , PAA  $p < .001$ , NAA  $p < .001$ ). The effect of auxin concentration was also significant for all auxins (2,4-D  $p = 0.033$ , PAA  $p < .001$ , NAA  $p < .001$ ). There was an interaction between PAA concentration and genotype ( $p = 0.01$ ) and NAA concentration and genotype ( $p < .001$ ). Full analysis is shown in Supplementary Information 18-20.**

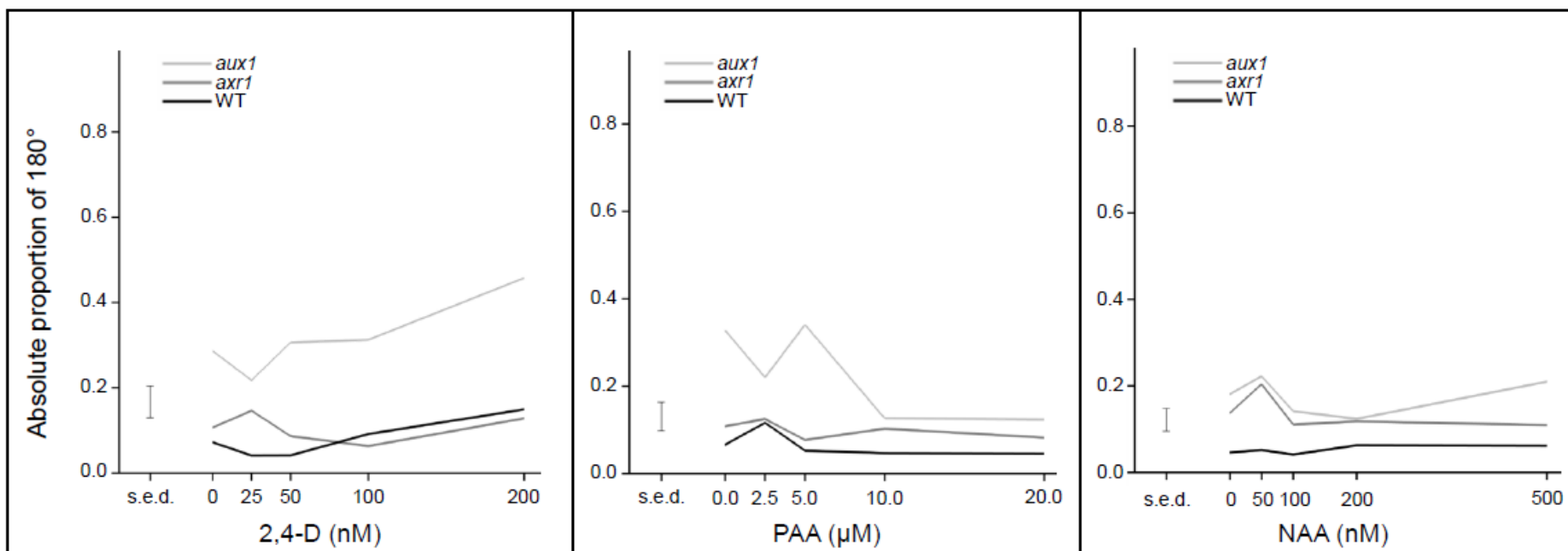
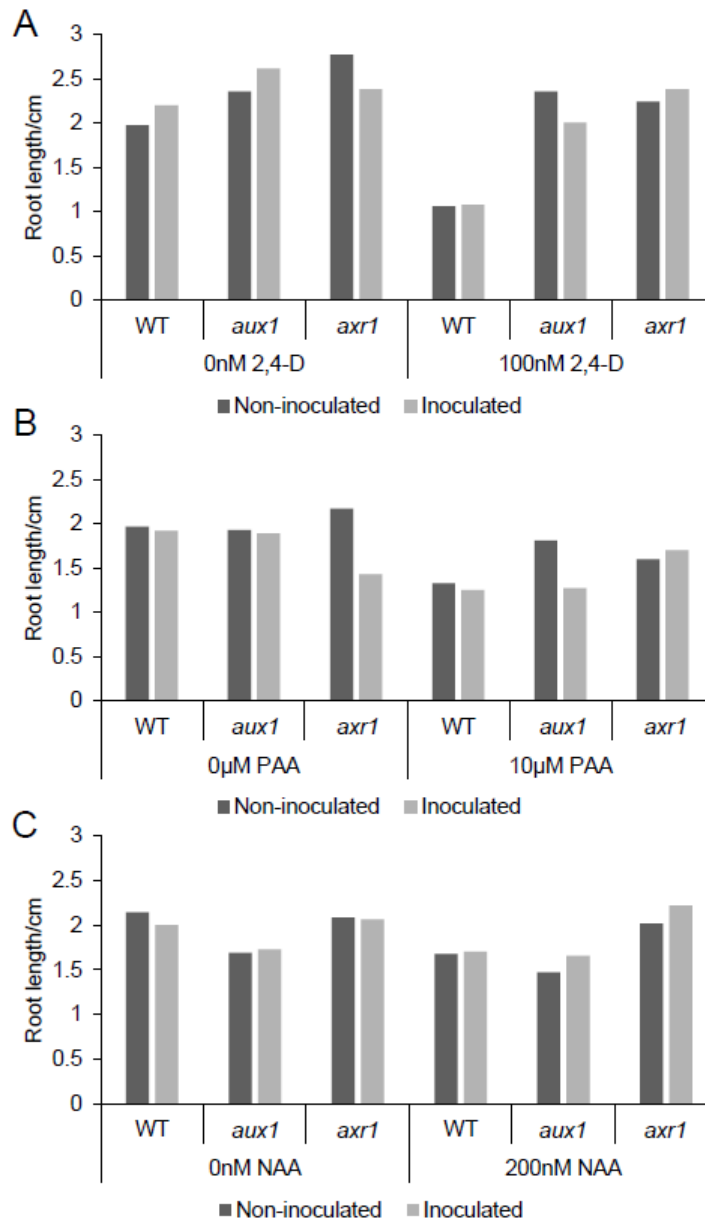


Figure 3-9: Line graphs showing the effect of 2,4-D, PAA and NAA auxin concentrations on the angle of root growth of *Arabidopsis thaliana* auxin mutants. Analysis of variance was carried out for each auxin separately. The standard errors of differences of means are shown. The angle of root growth was calculated using the absolute proportion of 180° (the angle at which plants are growing gravitropically). Values on the graph that are closer to 0 indicate that the root growth angle was growing gravitropically. The effect of genotype was significant for all auxins (2,4-D  $p < .001$ , PAA  $p < .001$ , NAA  $p < .001$ ). Full analysis is shown in Supplementary Information

21-23.

#### 3.4.4 Effects of 2,4-D, PAA and NAA with *R. solani* AG2-1 on the growth of *Arabidopsis thaliana* auxin mutants

The effects of exogenous auxins (2,4-D, PAA and NAA) and *R. solani* AG2-1 alone or simultaneously on the root architecture of *A. thaliana* auxin mutants at five days after the start of the experiment are shown in Figure 3-10, Figure 3-11 and Figure 3-12. The second highest auxin concentrations from the previous section (3.4.3) were chosen, as this concentration showed effects on root architecture, but did not inhibit root growth completely for any genotype. For root length, PAA was the only auxin to show a significant interaction between PAA, genotype and inoculation ( $p=0.03$ ). The effect of inoculation was also only significant for the PAA experiment. All three auxins had a significant effect on lateral root number, and there was a significant interaction between genotype and each auxin. Inoculation did not have a significant effect on lateral root number. NAA was shown to have a significant effect on the direction of root growth, but 2,4-D and PAA did not. Inoculation also did not have a significant effect.



**Figure 3-10: Bar charts showing the effect of high 2,4-D, PAA and NAA auxin concentrations with and without the presence of *Rhizoctonia solani* AG2-1 on the root length of *Arabidopsis thaliana* auxin mutants. Analysis of variance was carried out for each auxin separately. A) There was a significant effect of 2,4-D ( $p < .001$ ), genotype ( $p < .001$ ) and an interaction between them ( $p = 0.003$ ). B) There was a significant effect of PAA ( $p < .001$ ), inoculation ( $p = 0.034$ ) and an interaction between PAA, genotype and inoculation ( $p = 0.03$ ). C) There was a significant effect of genotype ( $p < .001$ ). Full analysis is shown in Supplementary Information 24-26.**

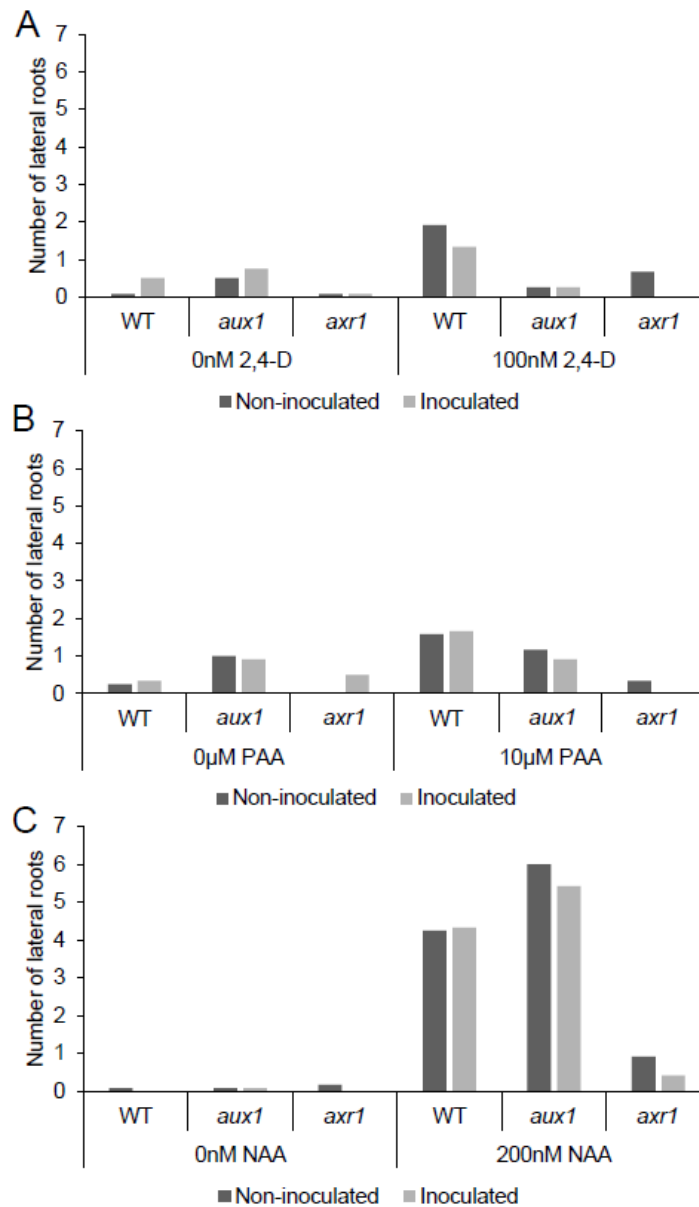


**Figure 3-11: Bar charts showing the effect of high 2,4-D, PAA and NAA auxin concentrations with and without the presence of *Rhizoctonia solani* AG2-1 on the number of lateral roots of *Arabidopsis thaliana* auxin mutants. Analysis of variance was carried out for each auxin separately. A) There was a significant effect of 2,4-D ( $p=0.016$ ), genotype ( $p=0.001$ ) and an interaction between them ( $p<.001$ ). B) There was a significant effect of PAA ( $p=0.023$ ), genotype ( $p=0.001$ ) and an interaction between them ( $p=0.006$ ). C) There was a significant effect of NAA ( $p<.001$ ), genotype ( $p<.001$ ) and an interaction between them ( $p<.001$ ). Full analysis is shown in Supplementary Information 27-29.**

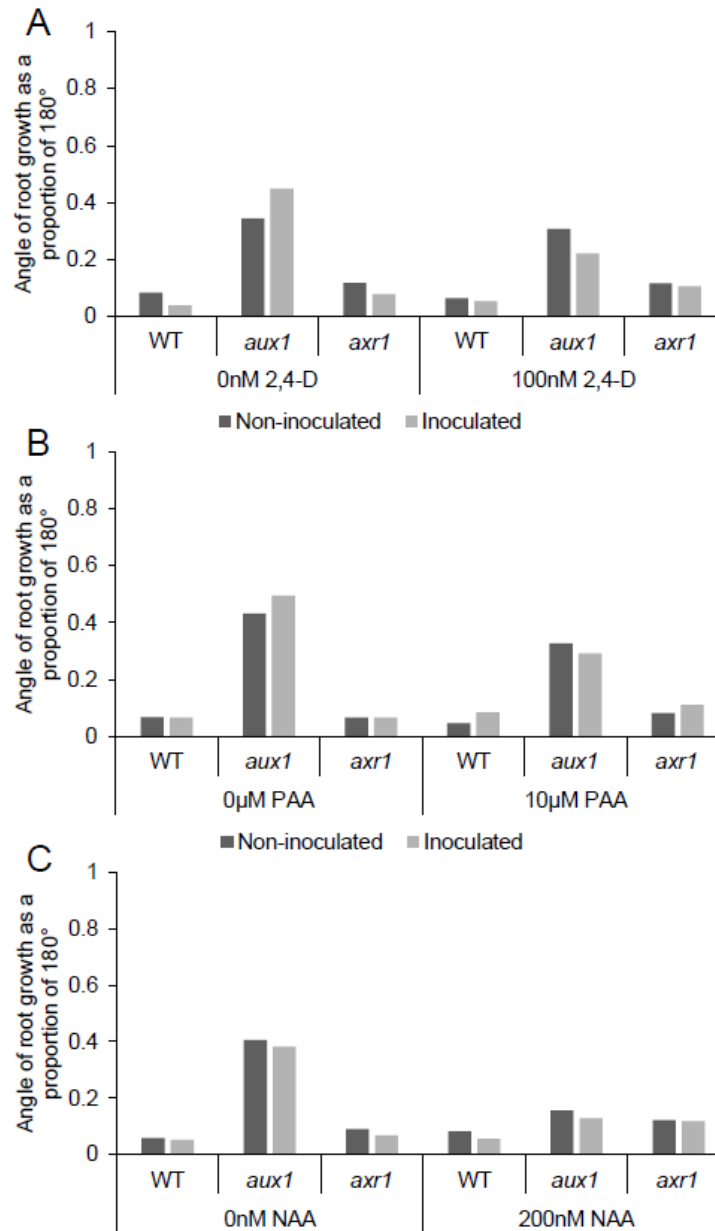


**Figure 3-12: Bar charts showing the effect of high 2,4-D, PAA and NAA auxin concentrations with and without the presence of *Rhizoctonia solani* AG2-1 angle of root growth of *Arabidopsis thaliana* auxin mutants.**

Analysis of variance was carried out for each auxin separately. The angle of root growth was calculated using the absolute proportion of 180° (the angle at which plants are growing gravitropically). Values on the graph that are closer to 0 indicate that the root growth angle was growing gravitropically. There was a significant effect of genotype for all auxins (2,4-D  $p < .001$ , PAA  $p < .001$ , NAA  $p < .001$ ). There was also a significant effect of NAA ( $p = 0.004$ ) and an interaction between NAA and genotype ( $p < .001$ ). Full analysis is shown in Supplementary Information

30-32.

### 3.4.5 Growth response of *Rhizoctonia solani* AG2-1 to exogenous PAA in liquid media

To test the effects of exogenous PAA on the growth of *R. solani* in liquid media, concentrations of PAA were added to flasks of PDB and *R. solani* was grown for three weeks. The resultant mycelium was freeze-dried and weighed, and non-linear regression analysis used to predict a critical exponential standard curve (fitted curve:  $A + (B + C \cdot X)^{(R \cdot X)}$ ,  $R < 1$ , parameter estimates:  $A=0.019$ ;  $B=1.053$ ;  $C=3.85$ ;  $R=0.192$ ) (Figure 3-13). The percentage variance accounted for was 83.7 and the standard error of observations was estimated to be 0.234. The F pr. value was  $<.001$ . At low concentrations (up to 0.5mM) of PAA, *R. solani* growth increased, and at high concentrations (above 3mM), growth was severely inhibited.

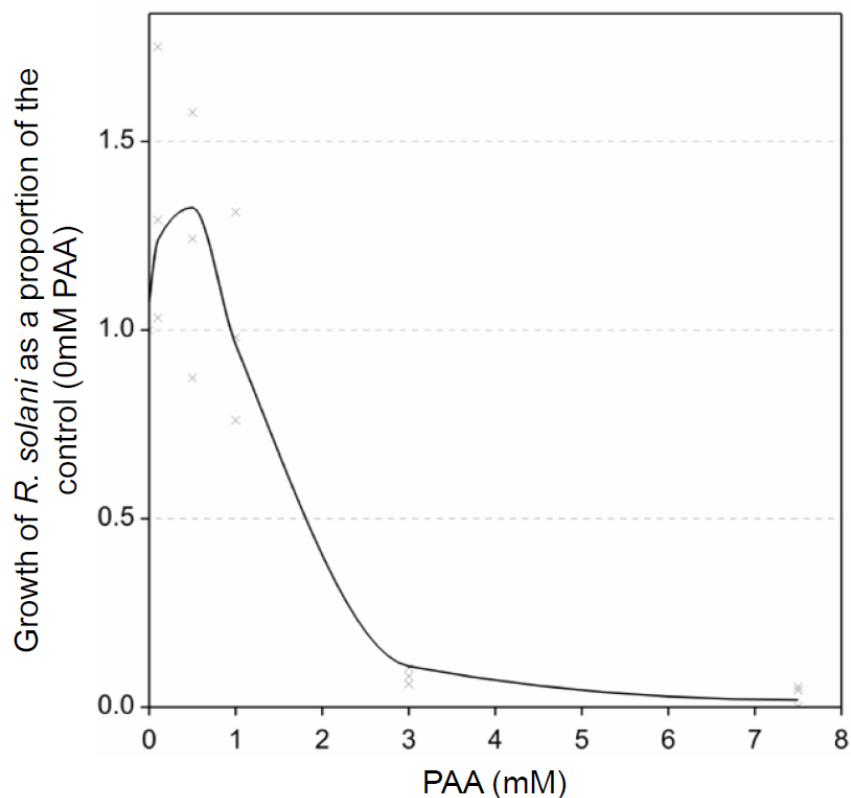


**Figure 3-13: Effect of exogenous PAA concentrations on the growth of *Rhizoctonia solani* AG2-1 in liquid media. The growth of *R. solani* was calculated as a proportion of the 0mM control and nonlinear regression analysis used to plot a critical exponential standard curve. The F pr. value was <.001. Full analysis is shown in Supplementary Information 33. Values above 1 represent growth stimulated by PAA.**

#### 3.4.6 Quantification of IAA and PAA in *Rhizoctonia solani* broth cultures

LC-MS/MS analysis was used to quantify the presence of auxins in broth samples in which *R. solani* AG2-1 isolates had been grown. Calibration of peak area ratios are shown in Figure 3-14 and the quantities of IAA and PAA found in the broth cultures are shown in Figure 3-15. Both IAA and PAA were identified in all isolates tested,



although in varying amounts. Isolate #2076, which originates from the USA, had both the highest IAA and PAA measured.

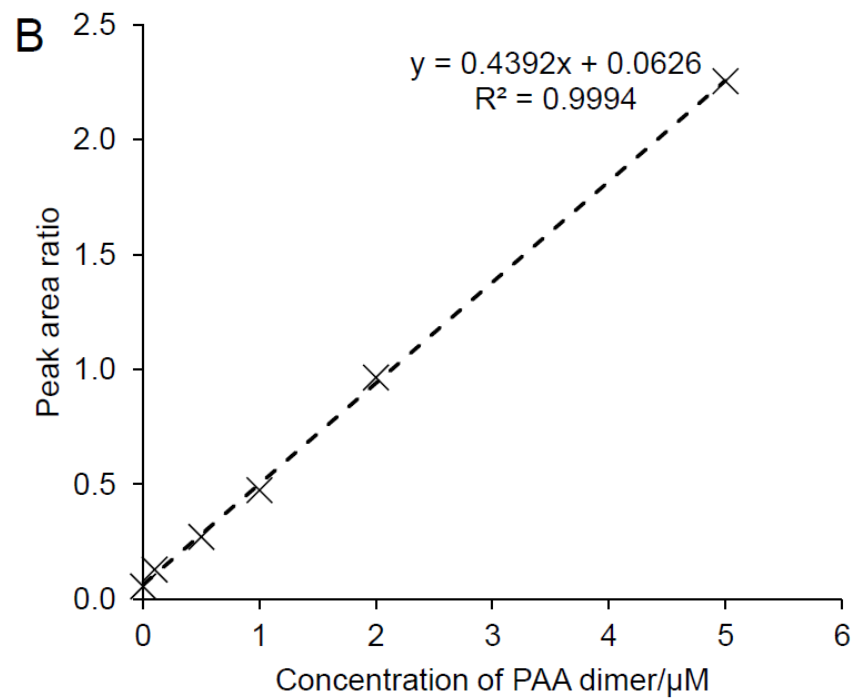
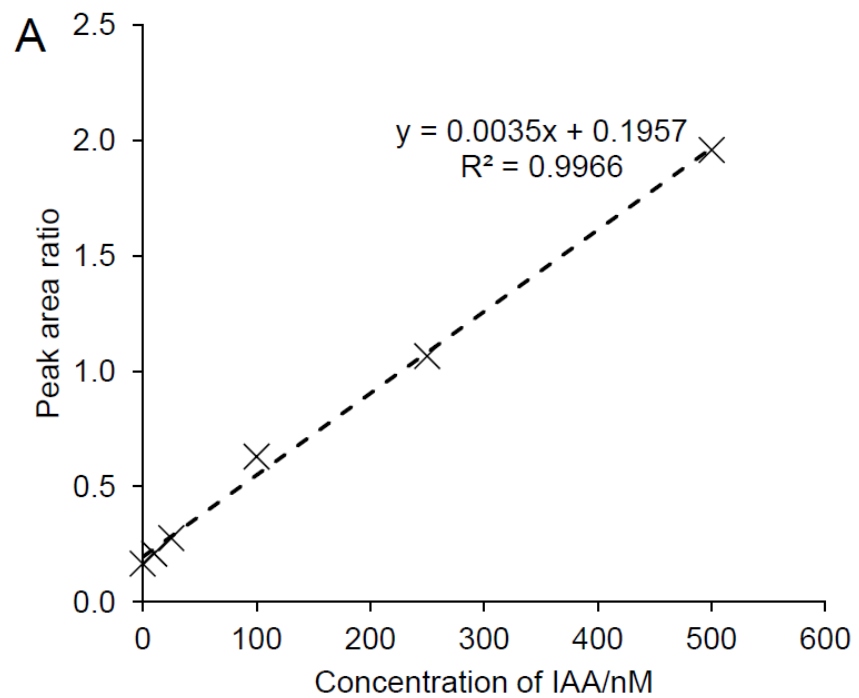


**Figure 3-14: LC-MS/MS peak area ratios obtained from testing A) IAA and B) PAA standards.**

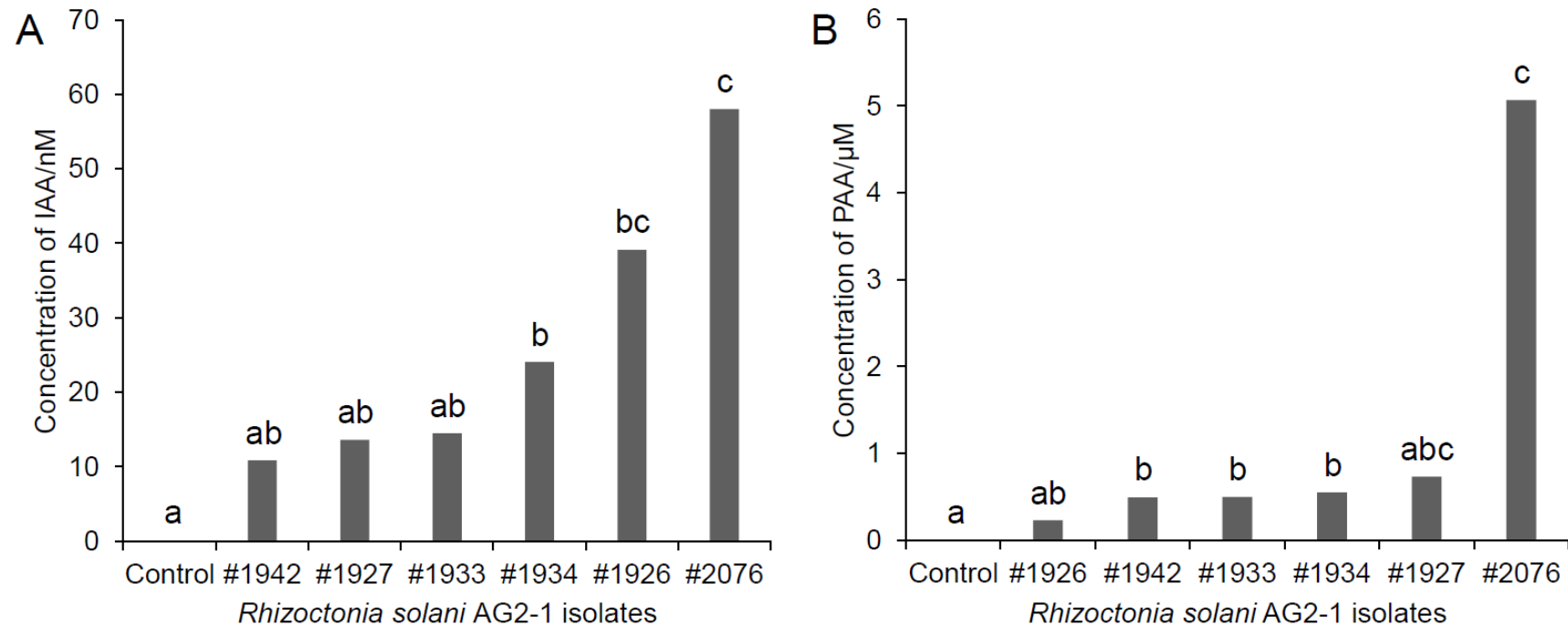


**Figure 3-15: Measured concentrations of A) IAA and B) PAA from *Rhizoctonia solani* AG2-1 isolate cultures. *R. solani* isolates were grown in Vogel's media for three weeks, then the mycelium separated from the broth. Liquid-liquid extractions were carried out on the broth samples, and they were prepared for LC-MS/MS analysis. Full analysis is shown in Supplementary Information 34-5.**

### 3.5 Discussion

Work carried out in chapter 2 showing a link between auxin and susceptibility to *R. solani* AG2-1 in OSR, along with previous work showing the production of PAA by *R. solani* AGs and the observation that *A. thaliana* auxin resistant mutants *aux1* and *axr1* showed increased tolerance to *R. solani* prompted further investigation into the effects of *R. solani* and auxins on roots. As a soil-borne pathogen, *R. solani* is likely to come into contact with plant roots in the first stages of infection, so the effects of *R. solani* AG2-1 on the root architecture of auxin mutants were investigated and compared with the effects of a range of known 2,4-D, NAA and PAA concentrations. It was shown that *R. solani* differentially affected *A. thaliana* auxin resistant mutants when grown at different distances from the pathogen, and the effects of 2,4-D, NAA and PAA on root growth, numbers of lateral roots and the direction of root growth were quantified. The effects of both auxins and *R. solani* simultaneously were also tested and significant interactions were observed for both root growth and the number of lateral roots. The growth of *R. solani* with high PAA concentrations in media was tested and *R. solani* culture samples were analysed for the presence of IAA and PAA. These results showed that *R. solani* AG2-1 isolates produced both PAA and IAA in broth culture, which is the first report of *R. solani* producing IAA and the first report of PAA for AG2-1.

With *R. solani* alone, WT plants showed root growth inhibition at all distances from the pathogen, while *aux1* plants only showed inhibition

at the closer distances, suggesting that compounds were released that inhibited the growth of WT plants to a greater degree than *aux1* plants. There was also an effect on the angle of root growth for the *aux1* plants. While the WT plants behaved more gravitropically under inoculation, *aux1* increased their agravitropism further from the pathogen (up to 6.5cm), although this was not significant.

Root architecture was modified by the concentrations of different auxins. NAA caused phenotypic changes at slightly higher concentrations (up to 500nM) than 2,4-D (up to 200nM), whilst a much higher concentration of PAA required (up to 20µM; 20 000nM) to show similar effects. This agrees with previous work that found that the active concentration of PAA was 10-times higher than IAA/2,4-D (Sugawara *et al.*, 2015; Cook, 2019). Generally, high concentrations of auxins inhibit root growth. 2,4-D is inhibitory for WT plants but has smaller effects on the auxin resistant mutants *aux1* and *axr1* (Yamamoto and Yamamoto, 1998, 1999). However, PAA caused a strong inhibition of root growth at all concentrations tested for WT plants, and higher concentrations (10µM and 20µM) showed inhibition for *aux1* plants. NAA caused inhibition of root growth for *axr1* at all concentrations, while *aux1* and WT plants were inhibited at the highest concentrations only (*aux1*: 200nM and 500nM, WT: 500nM only).

As well as inhibiting root growth, auxin promotes lateral root formation at low concentrations. *aux1* mutants form approximately 50% less lateral roots than WT plants, (Marchant *et al.*, 2002), and this was

reflected in the data presented here. Marchant *et al.* suggested that the reduced lateral root number in *aux1* may be a consequence of the reduced level of free IAA in the primary root apex of these mutants (2002). The addition of NAA restored the lateral root number and high concentrations of NAA led to a comparable number of lateral roots in both WT and auxin mutants in both these data and that of Marchant *et al.* (2002). PAA was also able to increase lateral root number for both the WT and *aux1* in these results, but not *axr1* plants. The greatest increases in lateral root number were seen under high NAA concentrations.

This work was consistent with previous studies observing that gravitropism was restored in *aux1* mutants with the addition of 300–1000nM NAA (Yamamoto and Yamamoto, 1998). It was shown that PAA can restore gravitropism in *aux1* mutants at 10 $\mu$ M and 20 $\mu$ M. However, increased agravitropism for *aux1* roots with increasing concentrations of 2,4-D was observed, which contrasts with Yamamoto and Yamamoto, who observed an increase in *aux1* gravitropism with IAA and 2,4-D, although not to the same extent as NAA (1998). WT plants showed increased agravitropism at the highest 2,4-D concentrations, which agrees with previous work showing high concentrations (1000nM) of 2,4-D caused WT plants to grow agravitropically (Yamamoto and Yamamoto, 1998). Due to the nature of *aux1* as an auxin influx carrier, *aux1* mutants have lower intracellular levels of auxin, which cannot be restored by the addition of 2,4-D, as it also requires AUX1 to enter the cell. The ability of NAA to restore

gravitropism (Yamamoto and Yamamoto, 1998) and lateral root number (Marchant *et al.*, 2002) in *aux1* reflects its lipophilic nature. These results showed that the addition of PAA also restored gravitropism and lateral root number, however this may have been due to the accumulation of IAA in cells caused by IAA efflux inhibition (Morris and Johnson, 1987).

The effects of *R. solani* inoculation with or without a high concentration of PAA on root growth were significant, however, this was not the case for 2,4-D and NAA. Small effects of inoculation were observed but varied between genotype and auxin tested. In some cases, *R. solani* inoculation led to increased root growth, and in other cases, root growth was more inhibited. All three experiments also showed significant interactions between the genotypes and respective auxins on the lateral root number, with the presence of auxins generally increasing the number of lateral roots observed. The only significant interaction between auxins and genotype when considering the effects on gravitropism was for NAA. A constraint of this experiment was that the plants could only be observed on the plates for five days before the fungus had colonised the whole plate, at which point, no further plant growth occurred. This was a short time period for the plants to grow and develop phenotypic differences in response to the auxins and *R. solani* inoculation before they were colonised. The use of larger plates where the fungus could be placed further away from the plants could improve this. The differences observed however, do suggest that *R. solani* may be releasing compounds that can differentially influence root

architecture depending on the presence of other auxins, and further testing would help clarify these responses.

Testing of the effect of exogenous PAA on the growth of *R. solani* AG2-1 in culture produced similar results to that obtained by Bartz *et al.* using AG3 (2012). Both experiments showed a significant reduction in mycelial growth at the highest concentrations, although Bartz *et al.* did not report an increase of growth at the lowest PAA concentration. The inhibition of fungal growth by PAA showed that it may be toxic to the fungus at high concentrations. This suggests an upper limit for any production of PAA by the *R. solani*, or that mechanisms may exist to prevent toxic effects in a localised manner during plant-pathogen interactions. The stimulation of growth under 0.5mM has not been previously observed but suggests there may be a role for PAA in fungal metabolism. This warrants further investigation with other *R. solani* isolates and a narrower range of PAA concentrations. It would also be interesting to test whether exogenous IAA (or 2,4-D) produces a similar effect on fungal growth. This has previously been tested for other fungal species (Fu *et al.*, 2015), but not for *R. solani*.

PAA and IAA were both quantified from *R. solani* broth cultures. This supports previous work quantifying PAA from AG3 and AG4 isolates (Iacobellis and DeVay, 1987; Bartz *et al.*, 2012), but is the first work to quantify PAA from AG2-1, and the first to include IAA. Quantification using LC-MS/MS analysis was challenging as the process of drying the samples under a nitrogen stream and re-suspending the extract has



previously been associated with a high loss of plant hormones (Müller and Munné-Bosch, 2011). Another potential issue was the instability of IAA and the tendency of indolic compounds to bind to glass (Barkawi *et al.*, 2010). The success of these initial quantifications provides the opportunity for further investigation quantifying the presence of PAA and IAA in plant-pathogen interactions. For example, future testing should investigate auxin levels from inoculated and non-inoculated seedlings. This could be done using the contrasting OSR varieties from chapter 2 to further define the role of auxins in highly susceptible and more tolerant interactions. The secretion of IAA by a pathogenic soil-borne fungus has been hypothesised to act via two potential mechanisms: either directly, by loosening the cell wall and inhibiting SA-dependent defence signalling; or indirectly by inducing IAA biosynthesis in the host plant, leading to amplified virulence (Fu *et al.*, 2015). Examination of *R. solani* genomes would also be beneficial to elucidating the production of auxins. The draft genome sequence of AG1 IA included a gene with 91% homology to the *AROM* gene, which is involved in PAA synthesis (Zheng *et al.*, 2013). The genome of AG2-1 has not yet been sequenced but will provide a future resource for developing this work.

Auxin resistant mutants have been shown to have increased tolerance to *R. solani* AG2-1. Although the role of auxins in plant immunity was not examined, auxin-signalling (*axr1*, *axr2*, *axr3* and *sgt1b* (SUPPRESSOR OF G2 ALLELE OF SKP1B)) and transport mutants (*aux1*, *axr4* and *pin2*) have been previously shown to have increased

resistance to the soilborne pathogen *Fusarium oxysporum* (Kidd *et al.*, 2011). However, there was a greater reduction in plant fresh weight under inoculation with the necrotrophic pathogen *Plectosphaerella cucumerina* in *axr1*, *axr2* and *axr6* mutants compared to wild-type plants, although *tir1* and *axr3* mutants did not differ from the wild-type (Llorente *et al.*, 2008). Plant decay also progressed more rapidly in *axr1* and *axr2* mutants under *Botrytis cinerea* infection compared to wild-type, *tir1* and *aux1* plants (Llorente *et al.*, 2008). *axr1-24* mutants were shown to be resistant to methyl jasmonate (MeJA) and showed increased susceptibility to *Pythium irregulare* (Tiryaki and Staswick, 2002). Further work is needed to understand the role of auxins in phytohormone immune signalling.

Due to time constraints, further experiments were planned but could not be completed. Once the work to quantify IAA and PAA in the cultured broth samples had been completed, it was planned to test the effects of adding the broth to agar plates and growing the same *A. thaliana* auxin mutants. Auxin quantification was required before this experiment could commence to calculate meaningful concentrations of broth to add to the agar. This experiment would be carried out using the same methods as described in section 3.3.5. This could also be tested with *Brassica napus* varieties to examine any differences in varietal susceptibility to the broth.

Testing of the effects of the same *R. solani* isolates on the *A. thaliana* auxin mutants was planned to ascertain whether the isolates which

produced the most PAA and IAA would have greater effects on the *A. thaliana* auxin mutants compared with the isolates producing the least PAA/IAA. Similar experiments have both found that PAA production in culture is correlated with high seedling mortality (Bartz *et al.*, 2012) and is unrelated to pathogenicity or virulence (Iacobellis and DeVay, 1987), however this has not been tested with *R. solani* AG2-1. The *R. solani* AG2-1 isolates could also be tested with the *B. napus* varieties from chapter 2 to examine whether the ones producing a greater quantity of auxins also caused the greatest symptom severity.

Another aspect that has not yet been tested is the severity of disease in the presence of IAA transport inhibitors such as NPA or TIBA. Treating *A. thaliana* leaves with IAA, 2,4-D or NAA solutions prior to root inoculation with *F. oxysporum* did not have a significant effect on disease development, however treatment with chemical inhibitors TIBA or NPA reduced disease development and increased resistance (Kidd *et al.*, 2011). Treating plants with TIBA prior to *P. cucumerina* inoculation increased the susceptibility of the wild-type plants to a comparable level as *axr1* and *axr2* plants without the addition of TIBA, though it did not increase the susceptibility of *axr1* and *axr2* plants further (Llorente *et al.*, 2008). Previous work has not considered the role of PAA, or involved fungal isolates known to produce PAA, so it would be interesting to see how interactions with *R. solani* are affected by the inhibitors.

In conclusion, this chapter adds new information about the effects of PAA and *R. solani* on auxin mutants. The role of auxins in plant disease is not yet fully understood, and it is unclear whether the release of auxins may be to manipulate host plants into increasing their biomass for the benefit of the pathogen, or whether this manipulates hormone signalling pathways to prevent defence signalling. Completing the experiments described here will support this work further to elucidate the role auxins play in *R. solani* interactions.

## Chapter 4: Identification and characterisation of candidate genes for resistance to *Rhizoctonia solani* AG2-1 in *Brassica napus* (Oilseed Rape)

### 4.1 Abstract

Many pathogens threaten Oilseed Rape (OSR) crop yields, including the soil-borne necrotroph *Rhizoctonia solani*, which can cause substantial establishment and yield losses. Isolates from the anastomosis group (AG) 2-1 are the most aggressive to OSR. There are currently no UK approved chemical seed treatments to prevent *R. solani* losses, and no varieties have been identified as resistant. A recent genome-wide association study (GWAS) (Ray *et al.*, 2020) identified a number of candidate genes associated with resistance or tolerance to *R. solani*. Analysis of the gene expression markers (GEMs) from the GWAS using gene ontology (GO) analysis and protein networks was carried out and provided links to ethylene, jasmonate and auxin response pathways. Candidate genes from the GWAS were preliminarily investigated by inoculating their *A. thaliana* mutants with *R. solani* AG2-1 under experimental conditions in a controlled environment room. Two of these genes, CIPK4 and NAA15, were taken forwards due to their reduced susceptibility under inoculation compared to wildtype *A. thaliana* plants and because they did not suffer a reduction in growth due to their mutations. RT-qPCRs were completed using *A. thaliana cipk4* and *naa15* mutants under inoculation to quantify the log<sub>2</sub>

fold change in the expression of defence pathway genes. For mutant plants that were more resistant to the pathogen, an increase in the signalling of key defence pathways was expected, but this would not be seen if the mutations increased tolerance. In order to investigate the role of CIPK4 and NAA15 in defence, *Brassica rapa* TILLING (Targeting Induced Local Lesions In Genomes) mutant variants were selected. TILLING is an approach that allows the generation and study of allelic series of mutations to evaluate their effects on gene expression, protein function and structure.

## 4.2 Introduction

The identification of resistance genes and the breeding of resistant crop varieties is vital to agricultural progress, and essential to maintain and improve yields. *Rhizoctonia solani* is a soil-borne plant pathogen with a global distribution, and the ability to affect numerous crop hosts, such as *Brassica napus* (Oilseed Rape; OSR). 1.2 million tonnes of OSR were produced in England in 2022 (Department for Environment Food and Rural Affairs, 2022). *Rhizoctonia solani* is divided into 13 reproductively isolated anastomosis groups (Carling, Kuninaga and Brainard, 2002), of which, anastomosis group (AG) 2-1 is the most aggressive to OSR (Babiker *et al.*, 2013). AG2-1 primarily affects the seedling growth stages of OSR, and causes hypocotyl and root rot, damping off, and wire-stem symptoms (Melzer *et al.*, 2016).

OSR breeding in the UK is driven in part by the AHDB recommended list (RL) criteria, which includes disease resistance to light leaf spot (*Pyrenopeziza brassicae*), phoma stem canker (*Leptosphaeria maculans* and *L. biglobosa*) and turnip yellows virus (TuYV), which is spread by the peach-potato aphid (*Myzus persicae*) (AHDB, 2022). Although *R. solani* is not currently an RL priority, inoculated field trials have shown establishment losses of 61% and yield losses of 41%, compared to non-inoculated control plots (Jayaweera and Ray, 2022). Management of *R. solani* on OSR includes recommendations to incorporate non-host crops in rotations and the use of tillage to disturb hyphal networks (Gill, Sivasithamparam and Smettem, 2001). However, *R. solani* AG2-1 can also cause significant damage to wheat root systems (Sturrock *et al.*, 2015), which is a common partner in OSR rotations. Furthermore, the UK Sustainable Farming Incentive pilot included incentives for using minimum tillage (min-till) and no tillage (no-till) cultivation to promote soil health (Department for Environment Food & Rural Affairs, 2022), which will increase the ability of soil-borne pathogens to survive in the soil and can also provide a “green bridge” environment, where the inoculum level is temporarily increased after herbicide sprays to manage weeds, before direct-sowing (Mahoney *et al.*, 2016).

Previous work has tested the susceptibility of *Brassica* spp. to *R. solani* AG2-1, AG8 and AG10, and found that all genotypes were susceptible to AG2-1 while three genotypes with some resistance to AG8 and AG10 were identified (Babiker *et al.*, 2013). Another study found that seedling

survival with AG2-1 was 51-69%, and 83-100% of seedlings showed root/hypocotyl rot, with all cultivars being highly susceptible (Lamprecht *et al.*, 2011). Research testing a range of *Brassica* genotypes with *R. solani* AG2-1 found differences within and between species, although no lines were immune (Yang and Verma, 1992). Most *Brassica juncea* genotypes, some *Brassica campestris* and some *B. napus* varieties had higher percentage emergence under inoculation than their control *B. napus* variety (Westar), while all *Brassica nigra*, *Brassica carinata* and *Brassica oleracea* varieties tested were more susceptible (Yang and Verma, 1992). Although resistance has not yet been identified, variation in the degree of susceptibility does exist and needs further investigation.

OSR is an allotetraploid crop, crossed from *Brassica rapa* (A genomes) and *Brassica oleracea* (C genomes). Genome-wide association studies (GWAS) have been used to identify promising loci for heritable traits including disease resistance. Raman *et al.* (2020) identified single nucleotide polymorphisms (SNPs) linked to quantitative resistance to *L. maculans* and Fikere *et al.* (2020) used a GWAS meta-analysis to provide resistance regions to *L. maculans*. Transcriptome analysis combined with GWAS have revealed candidate genes for resistance to *Sclerotinia sclerotiorum* stem rot disease in OSR (Wei *et al.*, 2016). Associative transcriptomics have been used to identify loci associated with resistance to clubroot (*Plasmodiophora brassicae*) (Hejna *et al.*, 2019). Due to the polyploid nature of *B. napus*, marker identification can be more challenging, so associative transcriptomics were developed,



which correlates measured trait variation with transcriptome sequencing to detect and score markers based on gene sequence variation and transcript abundance variation (Harper *et al.*, 2012). This was taken further by expanding the associative transcriptomics panel from 84 to 383 accessions to enable the analysis of more complex traits (Havlickova *et al.*, 2018).

GWAS and associative transcriptomics analysis can be used to study disease interactions for resistance, tolerance, and susceptibility markers. Resistance is defined as the ability of the host to limit pathogen multiplication, while tolerance as the ability of the host to reduce the effects of infection, without impacting the level of pathogen multiplication (Pagán and García-Arenal, 2018). Host susceptibility (S) genes are needed for compatible plant-pathogen interactions, and when mutated, prevent infection (van Schie and Takken, 2014). Host resistance is typically divided into qualitative and quantitative disease resistance. Qualitative resistance uses major resistance (R) genes, and typically follows the gene-for-gene relationship, where for each host R gene, there is a corresponding pathogen avirulence (Avr) gene (Flor, 1971). The largest class of R genes are nucleotide-binding site (NBS) – leucine rich repeat (LRR) genes (Zhang, Lubberstedt and Xu, 2013). This type of resistance has been successfully and frequently incorporated into breeding programs, but becomes ineffective to pathogen strains with evolved virulence genes (Flor, 1971). Quantitative resistance involves multiple genes, with each contributing to partial resistance, exerting less selection pressure on pathogens and is

therefore more durable (Zhang, Lubberstedt and Xu, 2013). Tolerance in crops has been described as the ability to suffer less loss in plant yield during pathogen infection, for which three groups of mechanisms have been proposed: compensation for lost photosynthetic activity, alteration of plant development and modification of the phytohormone balance (Pagán and García-Arenal, 2018). S genes present another option for breeding resistant crops and can function at different stages of the infection: pathogen establishment, host defence modulation and pathogen sustenance (van Schie and Takken, 2014). However, S genes require individual assessment as they play roles outside being a pathogen compatibility factor so cannot always be mutated without having other effects on fitness (van Schie and Takken, 2014).

*B. rapa* Targeting Induced Local Lesions In Genomes (TILLING) lines are a reverse genetics resource, which can be used to study gene function. The resource was generated using ethyl methane sulfonate (EMS), which produced a mutation density of approximately one mutation per 60kb (Stephenson *et al.*, 2010). After chemical mutagenesis, high-throughput screening for mutations was carried out and the resource made available through RevGenUK (<http://revgenuk.jic.ac.uk>). TILLING lines provide a valuable resource for plant breeding as they are not considered to be different from lines created by traditional mutation breeding, so genetically modified (GM) organism issues do not apply (Henikoff *et al.*, 2004).

Previously, Ray *et al.* (2020) carried out phenotypic screening of the ASSYST *B. napus* diversity set (454 accessions) under *R. solani* AG2-1 inoculation. Observations of disease on the hypocotyl, disease on the root, hypocotyl length, root length and plant survival were used for GWAS. Analysis of single nucleotide polymorphisms (SNPs) and gene expression markers (GEMs) was used to identify quantitative trait loci (QTL) associated with resistance and susceptibility responses, using the associative transcriptomics methods described by Havlickova *et al.* (2018). This chapter continued the analysis of the GEMs, to provide insight into the defence pathways changing expression during *R. solani* inoculation of *B. napus*. It was hypothesised that JA/ET pathways would be identified as associated with greater resistance, reflecting the RT-qPCR results in chapter 2 showing that ERF1 and PDF1.2 had increased relative expression in the more tolerant OSR varieties. Ray *et al.* (2020) identified several candidate genes, for which the *A. thaliana* mutants were tested with *R. solani* inoculation in compost to confirm functional phenotypes. The mutants of susceptibility genes were expected to show increased resistance or tolerance to *R. solani*. Two genes, CIPK4 and NAA15, were taken forwards, and the relative expression under inoculated and non-inoculated conditions of key defence pathways was examined using RT-qPCR analysis. This identified whether the mutations led to a resistance response to *R. solani*, or if the mutant's increased their tolerance through a different mechanism. *Brassica rapa* TILLING lines for CIPK4 and NAA15 were selected, genotyped and crossed to develop resources for further study.

## 4.3 Methods

### 4.3.1 Analysis of *Brassica napus* Gene Expression Markers (GEMs) under *Rhizoctonia solani* AG2-1 inoculation

Previously, Ray *et al.* (2020) carried out high throughput phenotypic screening of the ASSYST diversity set (454 accessions), using the inoculation in light expanded clay aggregates (LECA) method as described in Drizou *et al.* (2017). OSR seeds were pre-germinated then grown in trays filled with LECA particles, with *R. solani* inoculated or sterile PDA plugs placed at the bottom of each well. Disease scoring took place at seven days post inoculation, and disease indices were calculated for the hypocotyl (DIH%) and the root (DIR%). Trait data was used for genome wide association studies (GWAS) to provide information on single nucleotide polymorphism (SNPs) and gene expression markers (GEMs). GEMs data was provided by Prof. Ray, University of Nottingham. DIH% and DIR% were treated as separate datasets and were filtered to identify genes with a log<sub>10</sub>p value greater than 3. Genes were input into AgriGO (<http://bioinfo.cau.edu.cn/agriGO/>) using the Singular Enrichment Analysis and the TAIR9 background. The hypergeometric statistical test method was used, with Yekutieli multi-test adjustment method, a significance level of 0.05, a minimum number of mapping entries of 5 and “complete GO” gene ontology type.

Panther (<http://pantherdb.org/>) was used to carry out GO biological process complete statistical overrepresentation tests using the same datasets. The organism was listed as *Arabidopsis thaliana*, using the full *A. thaliana* reference list. The overrepresentation test was used with Fisher's exact test and the false discovery rate correction.

The STRING (<https://string-db.org/>) multiple proteins search tool was used to create a full STRING network with the required score as medium confidence (0.400) and FDR stringency as medium (5 percent). *A. thaliana* gene identifiers were used, and *A. thaliana* selected as the organism.

#### 4.3.2 Selection of genes for further testing

A Bonferroni-corrected threshold of  $P = 0.05$  ( $-\log_{10}P = 6.7$ ) was used to identify quantitative trait loci (QTL) with significant SNPs and GEMs across the chromosomes of the A (originating from *B. rapa*) and C (originating from *B. oleracea*) pan-genomes. The chromosomes with these QTLs are shown in Table 4-1. These SNPs have not yet been studied in detail, and no haplotype analysis was carried out. The annotated functions of the OSR genes allowed the identification of *A. thaliana* orthologues for the candidates with the highest significance threshold. Eleven of these genes were selected for further investigation and homozygous *A. thaliana* mutant seed lines (Table 4-2) were provided by Dr Dasuni Jayaweera, University of Nottingham.

**Table 4-1: Chromosome locations of the top SNPs and GEMS for disease responses identified with a  $-\log_{10}P > 6.7$  significance threshold (Ray *et al.*, 2020).**

<u><math>-\log_{10}P</math></u>	<u>Chromosome</u>
8.603	A09
7.914	C08
7.382	A02
7.353	A07
7.349	C01
7.326	C07
7.177	A05
7.143	C09
7.052	C05
6.910	C09
6.767	A06

**Table 4-2: Identification details for *Arabidopsis thaliana* mutants used in *Rhizoctonia solani* AG2-1 inoculation assay.**

<u><i>Arabidopsis thaliana</i> gene identifier</u>	<u><i>Arabidopsis thaliana</i> gene name</u>	<u>Mutant seed line identifier</u>	<u>Mutagen</u>	<u>Location of mutation</u>	<u>Phenotype</u>
AT1G22530	PATL2	SALK_086866C	T-DNA insertion	Coding region	Unknown
AT1G29720	RKFL1	SALK_013876	T-DNA insertion	Intron	Unknown
AT1G31770	ABCG14	SALK_036952C	T-DNA insertion	Unknown	Unknown
AT1G63740		SALKseq_8630	T-DNA insertion	Coding region	Unknown
AT1G80410	NAA15	SALK_012938C	T-DNA insertion	Promoter	Unknown
AT1G80450		SALK_110076	T-DNA insertion	Coding region	Unknown
AT2G01570	RGA24	rga-28	T-DNA insertion	Exon	No visible phenotype
AT3G21360		SALK_092692C	T-DNA insertion	Promoter	Unknown
AT4G14580	CIPK4	SALK_009893C	T-DNA insertion	Exon	Unknown
AT4G18010	5PTASE2	SALK_098943C	T-DNA insertion	Exon	Unknown
AT5G57940	CNGC5	SALK_053354C	T-DNA insertion	Promoter	Unknown

#### 4.3.3 *Arabidopsis thaliana* inoculation with *Rhizoctonia solani* AG2-1 in compost

Seeds were sown directly into M3 compost (Levington, Everris Limited, UK). A controlled environment chamber was used throughout the experiment, set at a constant 22°C temperature with a 16-hour photoperiod. After 12 days, seedlings were transplanted into experimental trays using a standard design with four biological repeats and 12 treatments (seed lines). Experimental 3x4 well trays contained a mix of M3 compost (Levington, Everris Limited, UK), vermiculite and perlite in a 4:2:1 ratio. Ten *R. solani* AG2-1 colonised or sterile 6mm diameter PDA plugs were added 3cm from the top of each well. Trays were watered once only at the start of the experiment to a depth of 1cm and then covered with clear plastic lids to maintain high humidity. Digital photographs were taken from above and ImageJ software (Schneider, Rasband and Eliceiri, 2012) was used to measure the green area of each plant. A ruler was included in every photograph to set the scale.

#### 4.3.4 *Arabidopsis thaliana* gene expression analysis

cDNA was prepared by Dr Dasuni Jayaweera, University of Nottingham, from RNA extractions of whole plant material from *A. thaliana* 8, 24 and 48 hours after *R. solani* AG2-1 inoculation. Quantitative reverse transcription PCR (RT-qPCR) was conducted using CFX96 Touch Real-Time PCR Detection System (BioRad) consisting of 95°C for 2 minutes 50 seconds, followed by 40 cycles with 15 seconds at 95°C and 30



seconds at 60°C. The primers used are listed in Table 4-3 and Sybr Green (Bio-Rad) was used as mastermix. Relative quantification was calculated using the  $2^{-\Delta\Delta C_T}$  method (Livak and Schmittgen, 2001). TUB9 was used as the reference gene and the non-inoculated samples were used as the control. Arithmetic means and standard errors were calculated with two biological (each with three technical) replicates per sample.

**Table 4-3: Primers used for RT-qPCR analysis. All primers were designed using NCBI Primer-BLAST, except the primers indicated by a \* which were taken from Sharon *et al.* (2011).**

<u>Gene</u>	<u>Gene name</u>	<u>Forward primer</u>	<u>Reverse primer</u>
AXR1	Auxin Resistant 1	TGGTCCGAGGCTTTGAAGA	AAGCTCTTGGAGAAACGCAC
CUL1	Cullin 1	GCCCTTTCATAGCAGCTCTC	TCAAGCTCTCCTCAACCTCG
COR13*	Coronatine Induced 1	ACTGGTTGGCTCACGCTAC	TCGGAGGGTTATTGTTTATCTGGAG
ERF1	Ethylene Responsive Factor 1	GGTCTCGGCGATTCTCAAT	TTCACGGAGCGGTGATCAAA
IAA7	Indole-3-Acetic Acid 7	TGGCCAAAATGTTTCAGCTCC	ACTCGGTAAGGTTTCATGAGTTT
LOX1*	Lipoxygenase 1	GACTATGCTTACTACAATGATTTAG	CGGTTCTTCCTCTTCTTG
LOX2	Lipoxygenase 2	GTTGGATCTTTTATCAACAC	CATACTTAACAACACCAGCT
NDR1*	Non race-specific disease resistance 1	CTATCAAGGACACAAGAAGAAG	AACAGCCGATCCATTAGG
NPR1	Nonexpresser of PR genes 1	TCGCCGAAATGAAGGGAACA	CGGGAAGAATCGTTTCCCGA
PAD3*	Phytoalexin Deficient 3	CGTGGTCAAGGAGACATTAAGG	CGCAGGAACATCGTAGCC
PAD4*	Phytoalexin Deficient 4	CTTATCCTCCGATGAACCTCTAC	ACCTAACAATTCCAATTCCAATCC
PDF1.2*	Plant Defensin 1.2	CACATACATCTATACATTGAAAAC	CAGCAAAGAGAACAAGAG
PR1	Pathogenesis-related gene 1	TTCTTCCCTCGAAAGCTCAA	AAGGCCACCAGAGTGTATG
PR5*	Pathogenesis-related gene 5	GTAACGGCGGGCGGAGTTC	TTGTAACCATCTACGAGGCTCAC
RBOHC	Respiratory Burst Oxidase Homolog C	ACCAATGAGCGGTGGTCAAT	TGCCGTACGTGTTCTCTGAC
RBOHD	Respiratory Burst Oxidase Homolog D	ACGTGCGTCCAAGAAAACG	GTCGTCCCTGATGTCTAGCG
TUB9*	Tubulin 9	TTTCGGTCTTCCCATCTC	ATACATTCATCAGCATTCTCAAC

#### 4.3.5 *Brassica rapa* TILLING lines

*Brassica rapa* yellow sarson (subsp. *trilocularis*) R-o-18 wildtype and *cipk4* (Bra036868 J130290-B, Bra036868 J131978-B, Bra036869 J131979-B, Bra036870 J130055-A, Bra096870 J132228-A) and *naa15* (Bra003565 J131739-B, Bra003565 J130605-B, Bra008474 J131384-B, Bra008474 J131025-B, Bra035184 J131449-A) mutant seeds were obtained from RevGenUK, John Innes Centre, UK (Stephenson *et al.*, 2010). There were three gene copies for each of CIPK4 (Bra036868, Bra036869 and Bra036870) and NAA15 (Bra003565, Bra008474 and Bra035184). Lines were chosen by looking for STOP gained mutations, and if these were unavailable, then missense mutations that involved a change in the amino acid classification (ie. aliphatic to aromatic). Mutations located within key domains, binding or interaction sites as identified using SMART protein domain prediction (Letunic and Bork, 2017) and NCBI conserved domains (Marchler-Bauer and Bryant, 2004) tools were preferred.

Protein alignments were made using the Clustal Omega Multiple Sequence Alignment tool (<https://www.ebi.ac.uk/Tools/msa/clustalo/>) to show differences and similarities between the *A. thaliana* and *B. rapa* lines. *Arabidopsis thaliana* protein sequences were obtained from TAIR (Huala *et al.*, 2001) and *B. rapa* sequences were obtained from Ensembl (Howe *et al.*, 2021). The output format was ClustalW with character counts and default settings were used.

The seeds were grown in a speed-breeding glasshouse chamber (Watson *et al.*, 2018), with 22 hours light (AP67 spectra) at 22°C and 2 hours dark at 17°C. Seeds were sown in M3 compost (Levington, Everris Limited, UK) in 12x8 trays and grown under fleece. At the five true leaf stage, they were transplanted into 1 litre pots using M3 compost with Exemptor insecticide (Bayer). Canes were used to support the plant, and plastic bag covers were put over the flowers to prevent cross-pollination. Plants were watered sufficiently to maintain optimum growth throughout. The first generation of plants were allowed to self-pollinate, and the seeds harvested. The next generation was grown, and the plants that were homozygous for the desired mutation were crossed with simultaneously grown wild type plants.

#### 4.3.6 Genotyping of *Brassica rapa* TILLING lines

Genomic extractions were carried out when the plants had 2-4 true leaves. Leaf samples were collected and stored on ice before 60µL extraction buffer (0.25M KCl, 10mM EDTA, 100mM Tris-HCl pH9.5 in sterile distilled water) was added and the tissue macerated thoroughly. Samples were heated at 95°C for ten minutes, then chilled on ice for five minutes. 60µL dilution buffer (3% bovine serum albumin) was added and the tubes inverted several times. Samples were centrifuged at 13 000rpm for three minutes and the supernatant was used for PCR reactions.

PCR reactions were carried out with 0.5 $\mu$ L of each primer (listed in Table 4-4), 10 $\mu$ L MangoMix (Meridian Bioscience), 0.75 $\mu$ L DNA and sterile distilled water to a total of 20 $\mu$ L. DMSO was added as indicated in Table 4-4. The cycle used included 3 minutes at 94°C, then 35 cycles of 1 minute at 94°C, 30 seconds at the annealing temperature (listed in Table 4-4), 1 minute at 72°C and a final 6 minutes at 72°C after the last cycle. Three sets of primers designed to amplify each of the regions containing the Bra003565 mutations (stop gained mutation at amino acid position 804 and missense mutation at amino acid location 1218) were tested under a range of conditions but none amplified the fragments successfully. After successful PCR amplification, QIAquick PCR purification kit (Qiagen) was used to purify the amplified fragment, and TubeSeq Service (Eurofins Genomics) was used for sequencing.

**Table 4-4: *Brassica rapa* TILLING lines primers and PCR details.**

<u>Mutation</u>	<u>Forward primer</u>	<u>Reverse primer</u>	<u>DMSO</u>	<u>Annealing temperature (°C)</u>
Bra036868 (CIPK4)	CCCAGAATCTCCTCCTCGAC	ACTCATCCTCCTCCTCCTCC	3%	66
Bra036869 (CIPK4)	TCCCTAGAAACCTCCGAGTT	ACGTCACTGTGCCATGAAAG	0%	61
Bra036870 (CIPK4)	GCTTTCCATCTCCATCATCACC	GAACGTAACCTGCGAGAAGTAC	0%	58
Bra008474.1 (NAA15)	GCCCAAGGATGATGCTGATG	ATGACGTTCCCCTTGTTCTT	0%	59
Bra008474.2 (NAA15)	TTGAGGAGTCCGGTGCTTTT	ACAGCCTCCTTAAACCTTTCA	0%	62
Bra035184 (NAA15)	CGCCGACAGTGATTGACCTA	TGAGTGCAATCGGTCTTGGA	0%	61

#### 4.3.7 Inoculation of *Brassica rapa* TILLING lines with *Rhizoctonia solani* AG2-1

Light expanded clay aggregate (LECA) particles were used to enable the clean extraction of roots from the substrate. A randomized block design with two factors (genotype and inoculation) resulting in six treatment combinations was used, with four replications. Wild-type *B. rapa*, Bra008474 (NAA15) with a homozygous missense mutation and Bra036868 (CIPK4) with a homozygous missense mutation were used. 9cm pots were filled one third with LECA particles (size 4-10mm; Saint-Gobain Weber Limited, UK) and five *R. solani* AG2-1 inoculated or non-inoculated 6mm diameter PDA plugs, before being filled with LECA particles. *Brassica rapa* seeds were pre-germinated in the dark for three days at room temperature (18°C) on filter paper in petri dishes with 5mL sterile distilled water. Three pre-germinated seedlings were added to each pot, and the pots supplemented with 25% Hoagland's (Sigma-Aldrich, UK) in 0.5 L of purified water in equal amounts once only at the start of the experiment. No further watering occurred. Clear plastic covers with the ventilation holes closed were kept over the trays for the duration of the experiment to maintain high humidity. Plants were kept in a controlled environment chamber at a constant 20°C temperature with a 12h photoperiod for seven days before being removed from the LECA and photographed on a white background. This experiment was completed once.

## 4.4 Results

### 4.4.1 Gene expression markers (GEMs) analysis

AgriGO was used to perform gene ontology enrichment analysis on the DIH% and DIR% GEMs datasets after being filtered to select only genes with a log<sub>10</sub>p value greater than 3. Biological processes analysis is shown in Figure 4-1 for the hypocotyl and Figure 4-2 for the root. As expected, there was a significant enrichment for the “response to stimulus” (GO:0050896) GO term, with 234/811 (p=0.00155) genes linked for the hypocotyl data and 220/730 (p=0.000405) genes for the root data. Both datasets also showed enrichment of the “cellular process” (GO:0009987; hypocotyl: p=1.84e-05; root: p=9.9e-06), “single-organism process” (GO:0044699; hypocotyl: p=1.84e-05; root: p=0.000405) and “metabolic process” (GO:0008152; hypocotyl: p=0.000294; root: p=0.000655) GO terms, however the hypocotyl dataset also showed enrichment of more specific terms including “organophosphate metabolic process” (GO:0090407; p=0.0185), “monocarboxylic acid metabolic process” (GO:0032787; p=0.0137) and “ion transport” (GO:0006811; p=0.0205). Cellular component analysis is shown in Figure 4-3 for the hypocotyl and Figure 4-4 for the root. The most significant interactions were for GO terms including “cytoplasmic part” (GO:0044444; hypocotyl: p=2.05e-12; root: p=1.65e-10) and “intracellular organelle part” (GO:0044446; hypocotyl: p=6.93e-12; root: p=7.12e-10), but more specific terms were also identified including “ribosome” (GO:0005840; hypocotyl: p=0.0158; root: p=0.000325),



“chloroplast” (GO:0009507; hypocotyl:  $p=8.39e-05$ ; root:  $p=0.000101$ ), “vacuole” (GO:0005773; hypocotyl:  $p=4.64e-07$ ; root:  $p=1.27e-6$ ) and “Golgi apparatus” (GO:0005794; hypocotyl:  $p=6.01e-06$ ; root:  $p=3.89e-05$ ). Molecular function analysis is shown in Figure 4-5 for the hypocotyl and Figure 4-6 for the root. The most significant terms for both datasets were “catalytic activity” (GO:0003824; hypocotyl:  $p=1.09e-06$ ; root:  $p=0.000891$ ), “protein binding” (GO:0005515; hypocotyl:  $p=4.52e-05$ ; root:  $p=0.00114$ ) and “mRNA binding” (GO:0003729; hypocotyl:  $p=8.12e-07$ ; root:  $p=0.000327$ ). The hypocotyl dataset also gave more specific terms including “NAD binding” (GO:0051287;  $p=0.035$ ), “ATP binding” (GO:0005524;  $p=0.00625$ ) and “cation-transporting ATPase activity” (GO:0019829;  $p=0.0214$ ). Many more GO terms were identified based on the DIH% dataset compared to the DIR% dataset, reflecting the fact that Ray *et al.* (2020) observed greater differences between the genotypes for the hypocotyl rot, but very few differences for root rot.

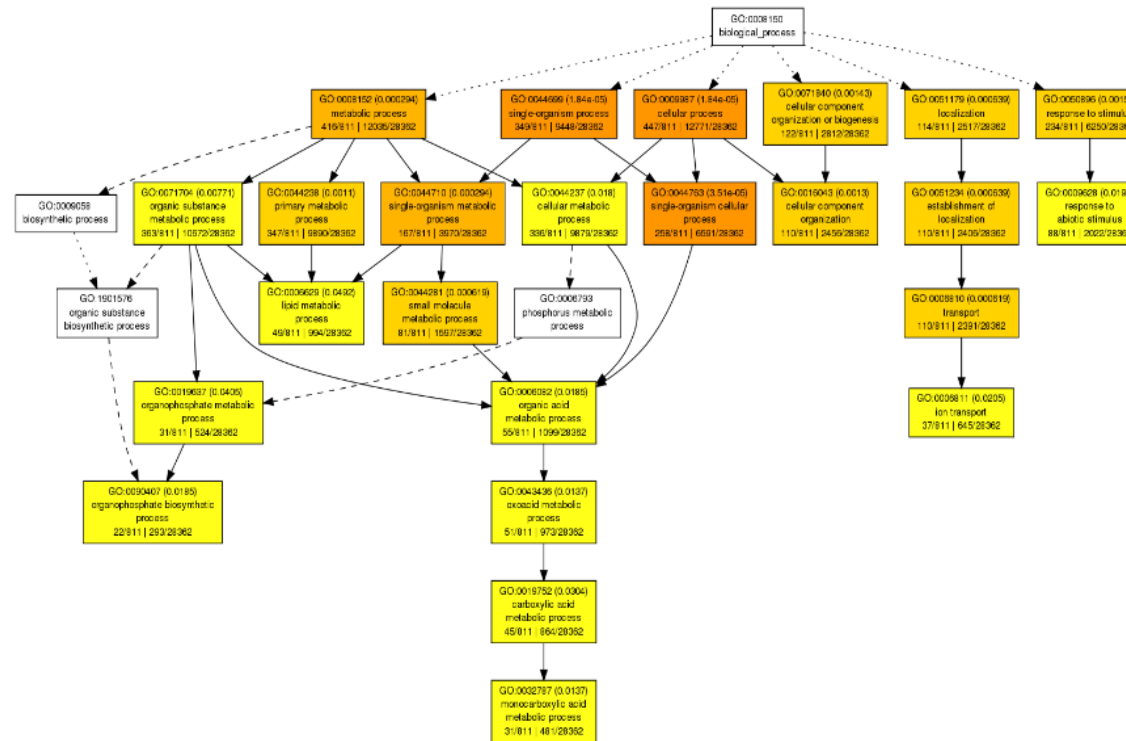
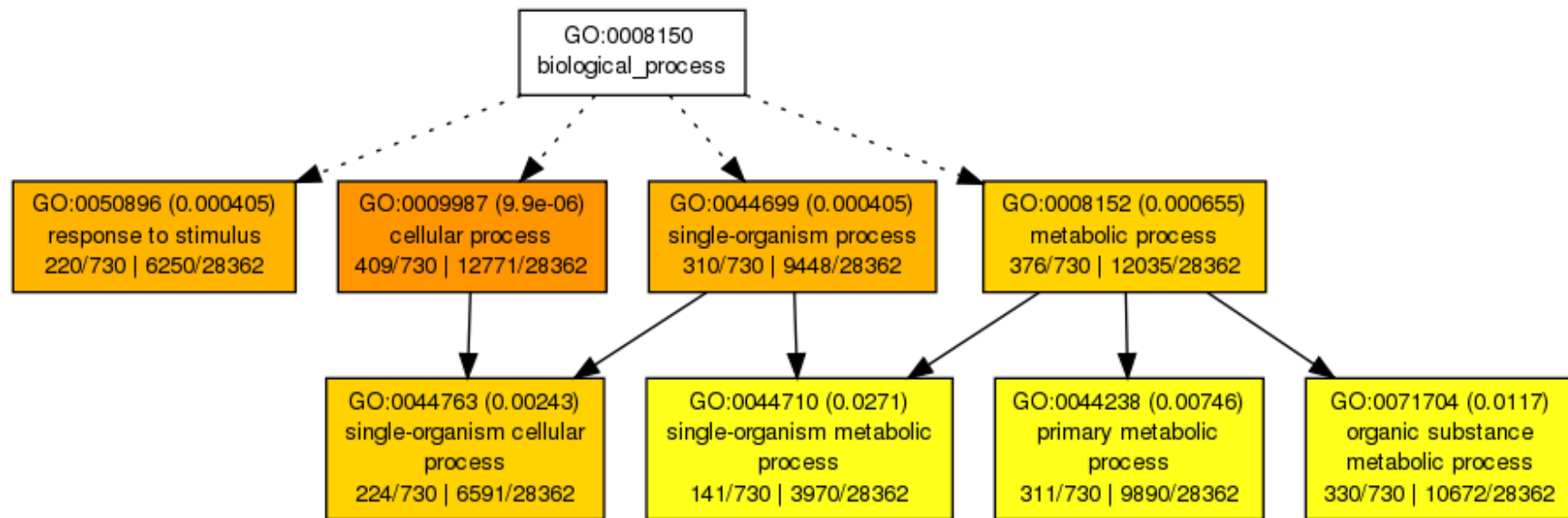
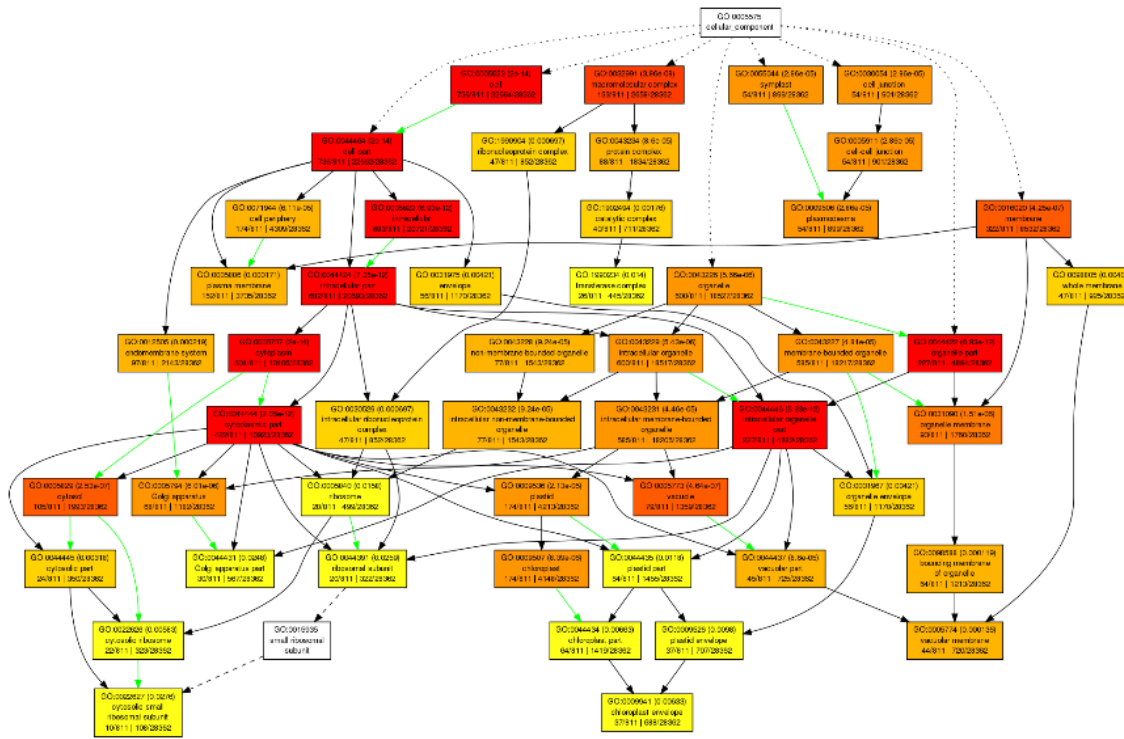


Figure 4-1: AgriGO gene ontology: biological processes analysis for the hypocotyl disease index data. Singular Enrichment Analysis was used with the TAIR9 background, hypergeometric statistical test method and Yekutieli multi-test adjustment method. The gene list used was filtered to only contain genes with a log<sub>10</sub>P greater than 3. Significant terms are shown by coloured boxes, where the degree of colour saturation is positively correlated with the term's enrichment level. Dotted, dashed and solid lines show zero, one and two enriched terms at both ends of the line.



**Figure 4-2: AgriGO gene ontology: biological processes analysis for the root disease index data. Singular Enrichment Analysis was used with the TAIR9 background, hypergeometric statistical test method and Yekutieli multi-test adjustment method. The gene list used was filtered to only contain genes with a log<sub>10</sub>P greater than 3. Significant terms are shown by coloured boxes, where the degree of colour saturation is positively correlated with the term's enrichment level. Dotted, dashed and solid lines show zero, one and two enriched terms at both ends of the line.**



**Figure 4-3: AgriGO gene ontology: cellular component analysis for the hypocotyl disease index data. Singular Enrichment Analysis was used with the TAIR9 background, hypergeometric statistical test method and Yekutieli multi-test adjustment method. The gene list used was filtered to only contain genes with a log<sub>10</sub>P greater than 3. Significant terms are shown by coloured boxes, where the degree of colour saturation is positively correlated with the term's enrichment level. Dotted, dashed and solid lines show zero, one and two regulated terms at both ends of the line. Green lines represent negative regulation.**

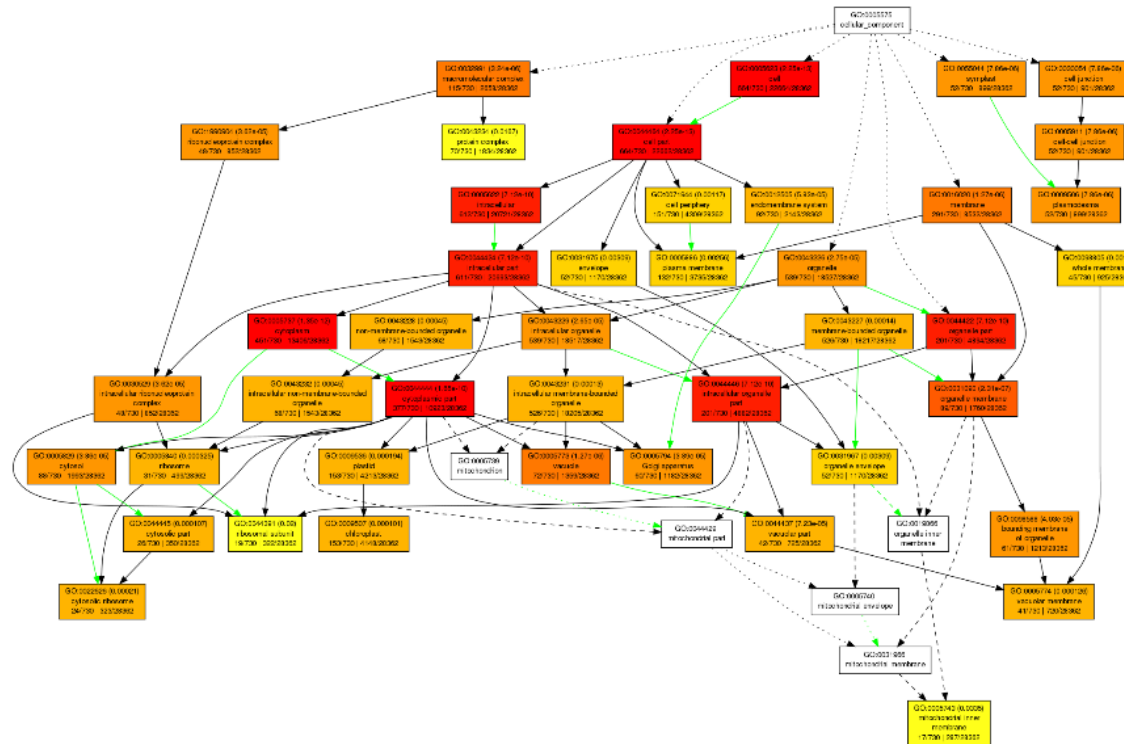


Figure 4-4: AgriGO gene ontology: cellular component analysis for the root disease index data. Singular Enrichment Analysis was used with the TAIR9 background, hypergeometric statistical test method and Yekutieli multi-test adjustment method. The gene list used was filtered to only contain genes with a log10P greater than 3. Significant terms are shown by coloured boxes, where the degree of colour saturation is positively correlated with the term's enrichment level. Dotted, dashed and solid lines show zero, one and two enriched terms at both ends of the line. Green lines represent negative regulation.

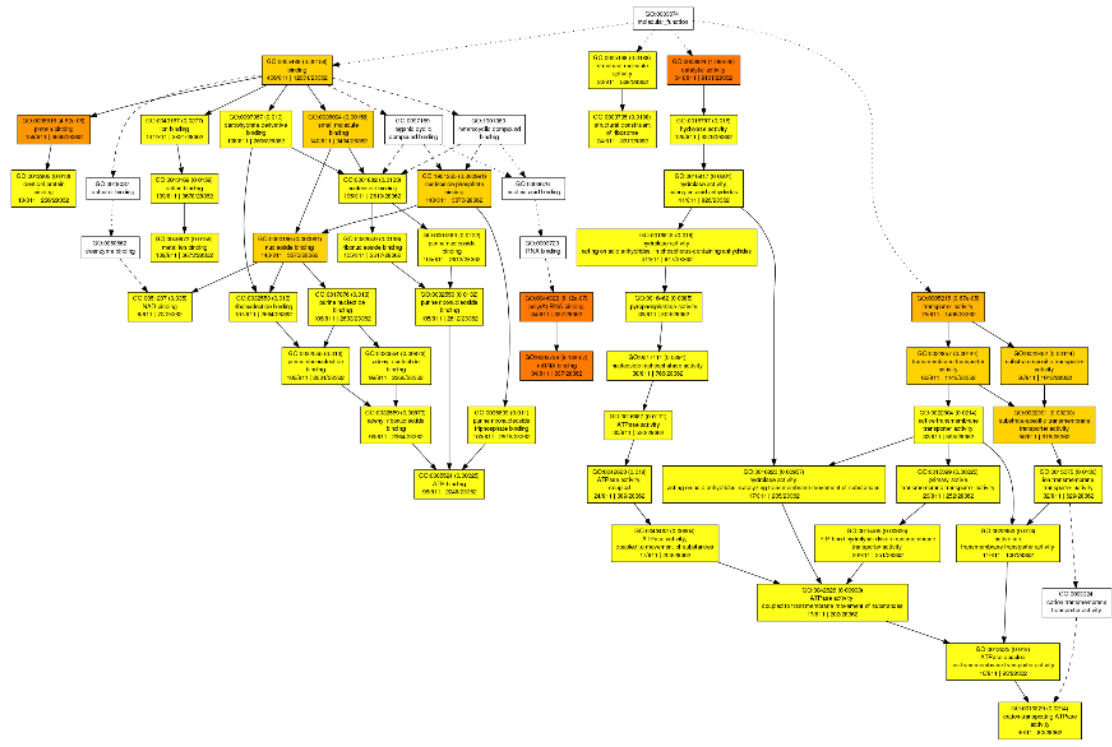
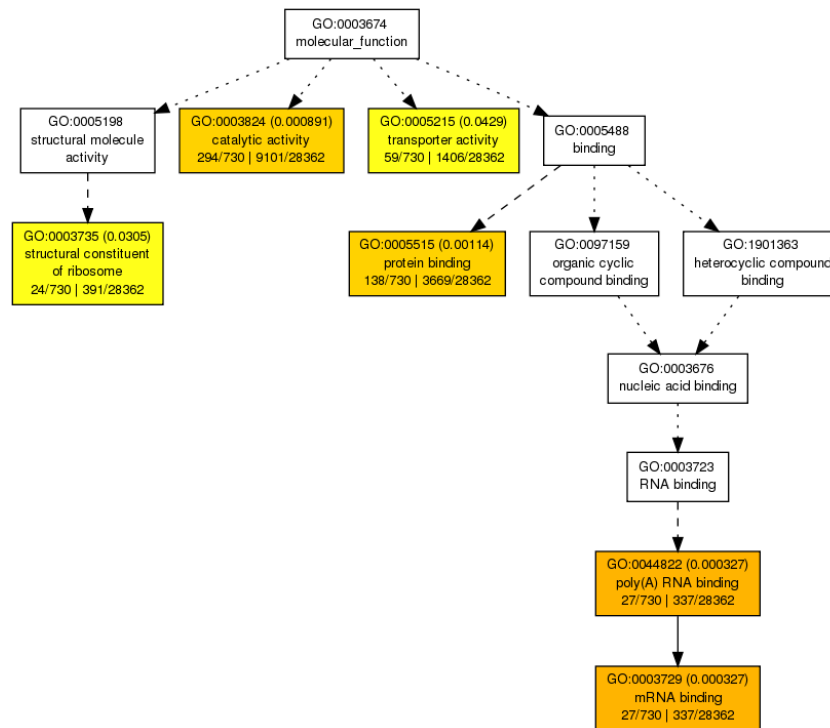


Figure 4-5: AgriGO gene ontology: molecular function analysis for the hypocotyl disease index data. Singular Enrichment Analysis was used with the TAIR9 background, hypergeometric statistical test method and Yekutieli multi-test adjustment method. The gene list used was filtered to only contain genes with a log10P greater than 3. Significant terms are shown by coloured boxes, where the degree of colour saturation is positively correlated with the term’s enrichment level. Dotted, dashed and solid lines show zero, one and two enriched terms at both ends of the line.



**Figure 4-6: AgriGO gene ontology: molecular function analysis for the root disease index data. Singular Enrichment Analysis was used with the TAIR9 background, hypergeometric statistical test method and Yekutieli multi-test adjustment method. The gene list used was filtered to only contain genes with a log10P greater than 3. Significant terms are shown by coloured boxes, where the degree of colour saturation is positively correlated with the term's enrichment level. Dotted, dashed and solid lines show zero, one and two enriched terms at both ends of the line.**

Overrepresentation tests were carried out using Panther for the same data, and the results are shown in Figure 4-7 and Figure 4-8. Both DIH% and DIR% datasets showed the “response to stimulus” (GO:0050896) GO term within the top five overrepresented terms. The DIH dataset also showed overrepresentation for GO terms including “developmental process” (GO:0032502), “multicellular organismal process” (GO:0032501), “multicellular organism development” (GO:0007275) and “protein metabolic process” (GO:0019538) while the DIR dataset showed overrepresentation for GO terms including “cellular macromolecule metabolic process” (GO:0044260), “catabolic process” (GO:0009056), “cellular component biogenesis” (GO:0044085) and “gene expression” (GO:0010467).



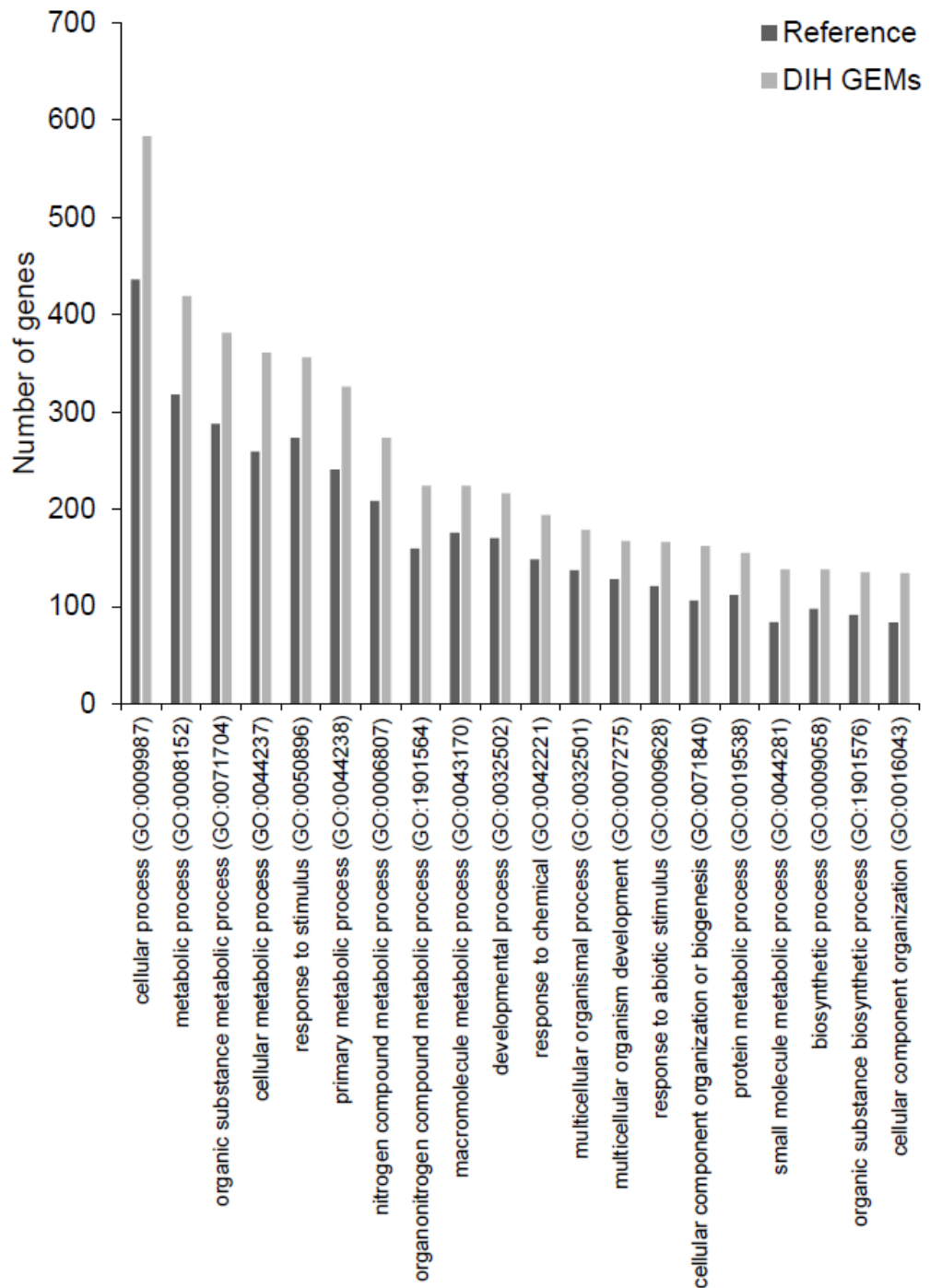


**Figure 4-7: Panther overrepresentation test showing the GO categories which were overrepresented in the hypocotyl disease index GEMs with  $\log_{10}p > 3$ . Fisher's exact test with false discovery rate (FDR) multiple test correction was used. The expected number of genes based on the *Arabidopsis thaliana* reference gene list is plotted (Reference) for comparison with the number of genes found in the GEMs (DIH GEMs). Only the top 20 categories are shown here.**

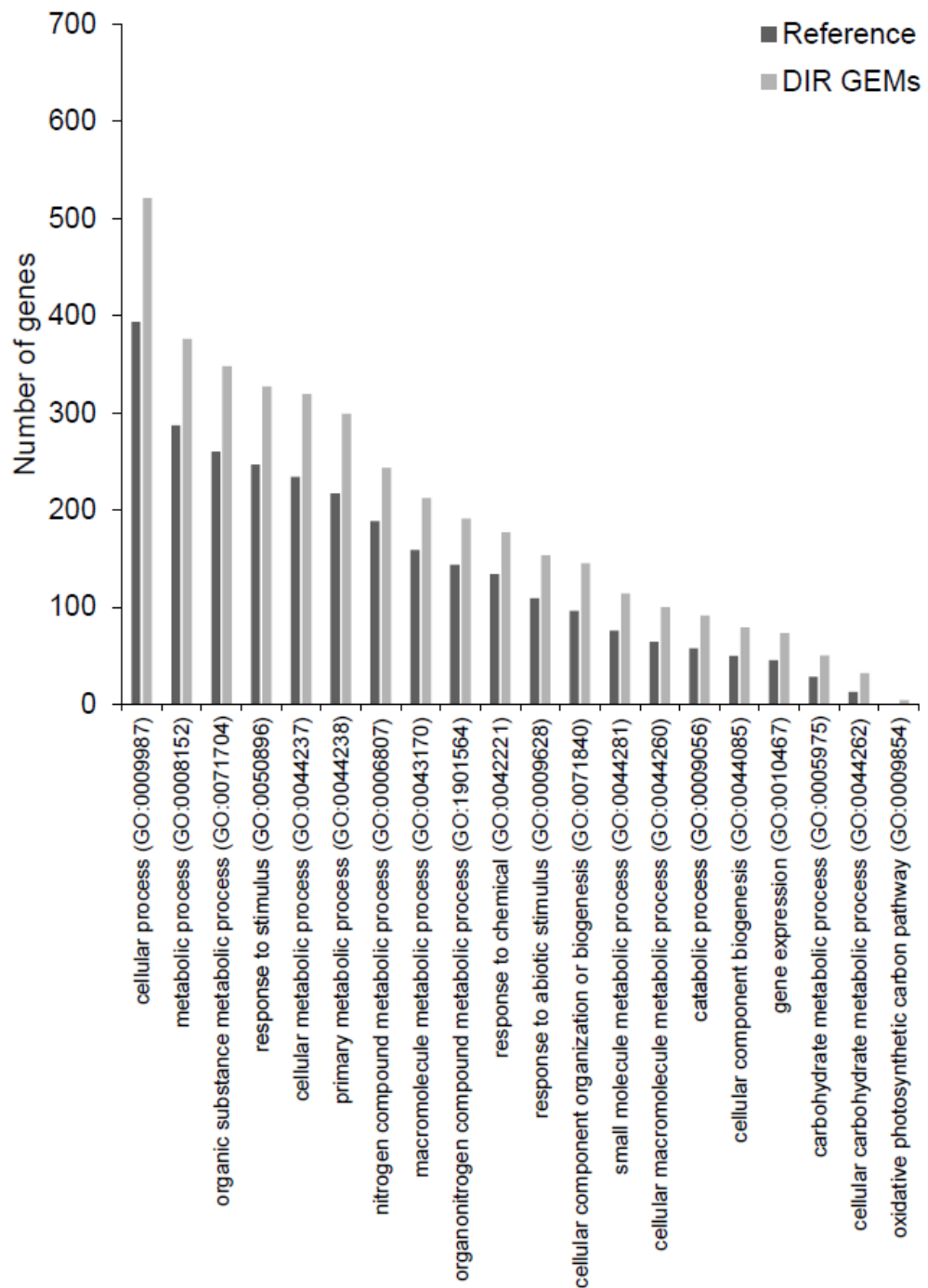


**Figure 4-8: Panther overrepresentation test showing the GO categories which were overrepresented in the root disease index GEMs with  $\log_{10}p > 3$ . Fisher's exact test with false discovery rate (FDR) multiple test correction was used. The expected number of genes based on the *Arabidopsis thaliana* reference gene list is plotted (Reference) for comparison with the number of genes found in the GEMs (DIR GEMs).**

Further investigation was carried out by selecting the genes that were linked to the “response to stimulus” (GO:0050896) category with a  $\log_{10}P > 2.5$  and  $Pr (>F) < 0.05$ . These genes were filtered to those that contained GO terms linked to plant defence, such as those related to phytohormones (jasmonic acid, salicylic acid, ethylene, auxin, and abscisic acid) or other key words relating to immune responses (kinase, receptor, transcription factor, immune and defence). Gene information was obtained using TAIR (Huala *et al.*, 2001) and a network was created using STRING (Figure 4-9). The full list of genes is given in Supplementary Information 36. This identified the involvement of several genes related to ethylene, jasmonic acid and auxin response pathways (EIL1, TPL, EIN3, IAA2 and EFE). Genes with receptor and/or kinase activity (UniProt) were also identified including RLK7, FER, HERK1, BARK1 and FLS2. Receptor-like kinases often play a key role in plant immunity and can function as pattern recognition receptors (PRRs) that detect pathogens and lead to pattern triggered immunity. Four genes with an NB-ARC (Pfam) domain (AT1G63740, AT3G51570, RPP8 and NRG1.1) were identified. These NLR (nucleotide-binding domain and leucine-rich repeats) genes detect the presence of effectors and trigger immune responses.

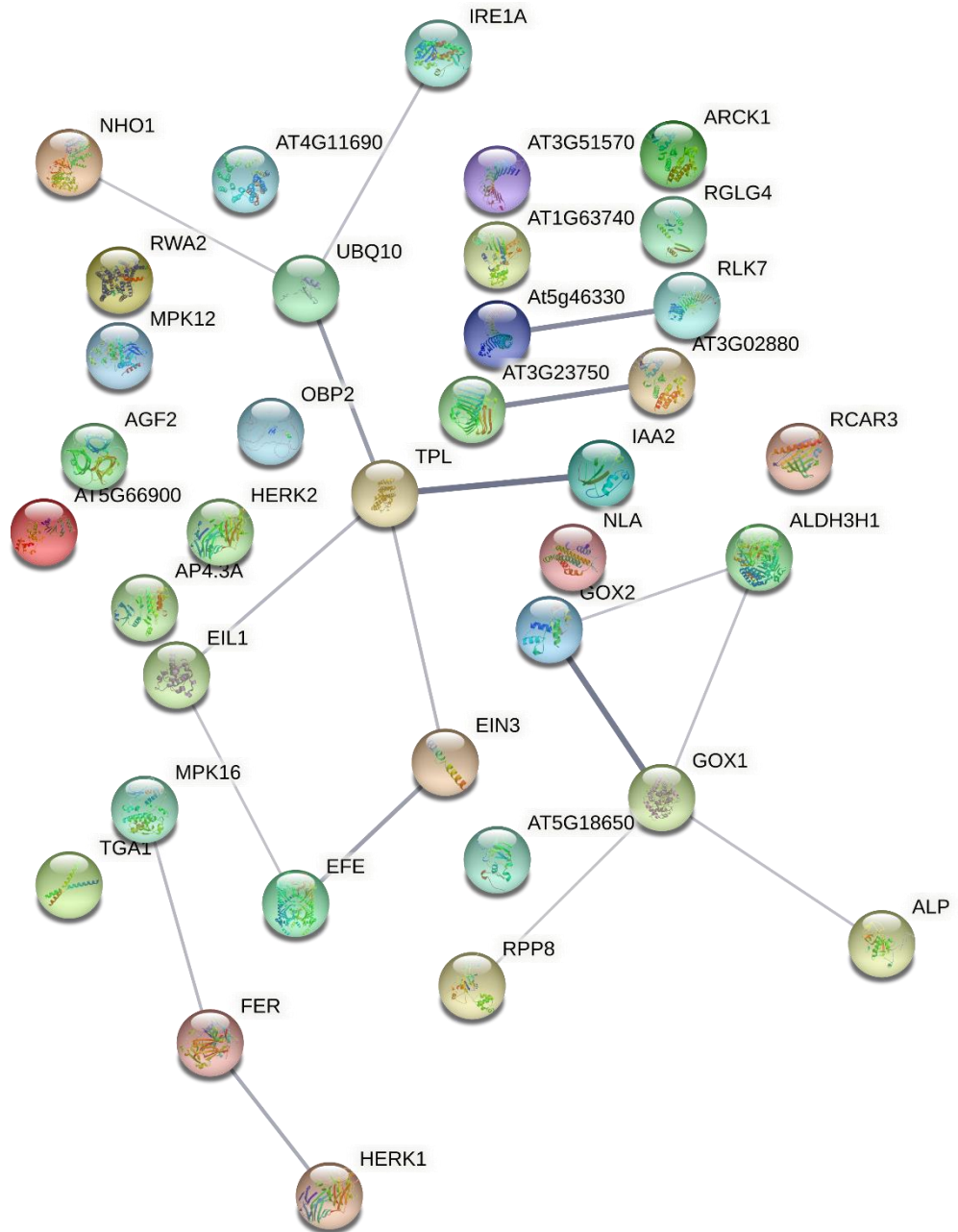


**Figure 4-9: STRING network showing significant GEMs with a role in defence. The required score was medium confidence (0.400) and FDR stringency was medium (5 percent). *Arabidopsis thaliana* gene identifiers were used. Line thickness shows the strength of data support for each interaction. The full list of genes is given in Supplementary Information 36.**

#### 4.4.2 Inoculation of *Arabidopsis thaliana* mutant candidate genes with *Rhizoctonia solani* in compost

Potential genes chosen as part of the ICAROS project (Ray *et al.*, 2020) were tested under inoculation using *A. thaliana* mutants. Table 4-5 and Supplementary Information 37 show information about the genes chosen. Plants were inoculated with *R. solani* AG2-1 in compost and their leaf area measured at 16dpi (Figure 4-10). Representative photographs of the inoculated plants are shown in Figure 4-11. Columbia-0 wild-type plants showed a significant reduction in their growth ( $p=0.020$ ) under *R. solani* AG2-1 inoculation, reflecting their susceptibility to the pathogen. Plants with mutations in the genes AT1G29720 (*rkl1*), AT1G80450, AT3G21360, AT4G18010 (*5ptase2*) and AT5G57940 (*cngc5*) also showed a significant reduction in their growth ( $p<0.050$ ). All other mutants tested did not show a significant reduction in growth, suggesting that the mutations reduced their susceptibility to the pathogen.

**Table 4-5: Gene information for genes selected from GWAS. Genes were matched to their *Arabidopsis thaliana* homolog and gene names, GO biological processes and additional descriptions were taken from TAIR (Huala *et al.*, 2001). Pr (>F) and log10P values for these genes are shown in Supplementary Information 37.**

<u><i>A. thaliana</i> identifier</u>	<u>Gene name</u>	<u>GO Biological process</u>	<u>Additional description</u>
AT1G22530	PATELLIN 2, PATL2	cellular response to auxin stimulus, protein localization involved in auxin polar transport	PATLs belong to a family of proteins having a Golgi dynamics (GOLD) domain in tandem with the Sec14p-like domain. PATLs are auxin regulated. Quadruple mutants ( <i>patl2456</i> ) show altered PIN1 lateralization in root endodermis cells.
AT1G29720	RKF-LIKE 1, RKFL1	protein phosphorylation	Encodes one of three RECEPTOR-LIKE KINASE IN FLOWERS 1 (RKF1) paralogues that is required in the stigmatic papillae and the female reproductive tract to promote compatible pollen grain hydration and pollen tube growth.
AT1G31770	ABCG14, ATP-BINDING CASSETTE G14	cytokinin transport, cytokinin-activated signaling pathway, defense response to bacterium, export across plasma membrane, export from cell, response to hydrogen peroxide, transmembrane transport	Transmembrane cytokinin transporter. Responsible for acropetal translocation of cytokinins.
AT1G63740		signal transduction	Disease resistance protein (TIR-NBS-LRR class) family

<u><i>A. thaliana</i></u> <u>identifier</u>	<u>Gene name</u>	<u>GO Biological process</u>	<u>Additional description</u>
AT1G80410	EMB2753, EMBRYO DEFECTIVE 2753, MUSE6, MUTANT, SNC1-ENHANCING 6, NAA15, OMA, OMISHA	N-terminal peptidyl-methionine acetylation	Encodes the catalytic subunit of a N-terminal acetyltransferase.
AT1G80450			VQ motif-containing protein
AT2G01570	REPRESSOR OF GA, REPRESSOR OF GA1-3 1, RGA, RGA1, RGA24	hyperosmotic salinity response, jasmonic acid mediated signaling pathway, negative regulation of gibberellic acid mediated signaling pathway, negative regulation of seed germination, positive regulation of DNA-templated transcription, regulation of DNA-templated transcription, regulation of reactive oxygen species metabolic process, regulation of seed dormancy process, regulation of seed germination, response to abscisic acid, response to cold, response to ethylene, salicylic acid mediated signaling pathway	Member of the VHIID/DELLA regulatory family. Contains homopolymeric serine and threonine residues, a putative nuclear localization signal, leucine heptad repeats, and an LXXLL motif. Putative transcriptional regulator repressing the gibberellin response and integration of phytohormone signalling. DELLAs repress cell proliferation and expansion that drives plant growth. The protein undergoes degradation in response to GA via the 26S proteasome. RGA1 binds to PIF3 and inhibits its DNA binding activity and thus affects the expression of PIF3 regulated genes. RGA may be involved in reducing ROS accumulation in response to stress by up-regulating the transcription of superoxide dismutases. Represses GA-induced vegetative growth and floral initiation. Rapidly degraded in response to GA. Involved in fruit and flower development.

<u>A. thaliana identifier</u>	<u>Gene name</u>	<u>GO Biological process</u>	<u>Additional description</u>
AT3G21360			2-oxoglutarate (2OG) and Fe(II)-dependent oxygenase superfamily protein
AT4G14580	CBL-INTERACTING PROTEIN KINASE 4, CIPK4, SNF1-RELATED PROTEIN KINASE 3.3, SNRK3.3	intracellular signal transduction, protein phosphorylation	CBL-interacting protein kinase
AT4G18010	5PTASE2, INOSITOL(1,4,5)P3 5-PHOSPHATASE II, IP5PII, MYO-INOSITOL POLYPHOSPHATE 5-PHOSPHATASE 2	inositol phosphate dephosphorylation, inositol trisphosphate metabolic process, phosphatidylinositol dephosphorylation, seedling development	Encodes an inositol polyphosphate 5-phosphatase that appears to have Type I activity. It can dephosphorylate IP3(inositol(1,4,5)P3) and IP4 (inositol(1,3,4,5)P4), but it does not appear to be active against phosphatidylinositol 4,5 bisphosphate. Overexpression of this gene renders plants insensitive to ABA in germination and growth assays.
AT5G57940	CNGC5, CYCLIC NUCLEOTIDE GATED CHANNEL 5		Encodes a cyclic GMP activated Ca <sup>2+</sup> -permeable cation channel in the plasma membrane of guard cells. Required for constitutive growth of root hairs as Ca <sup>2+</sup> -permeable channels.



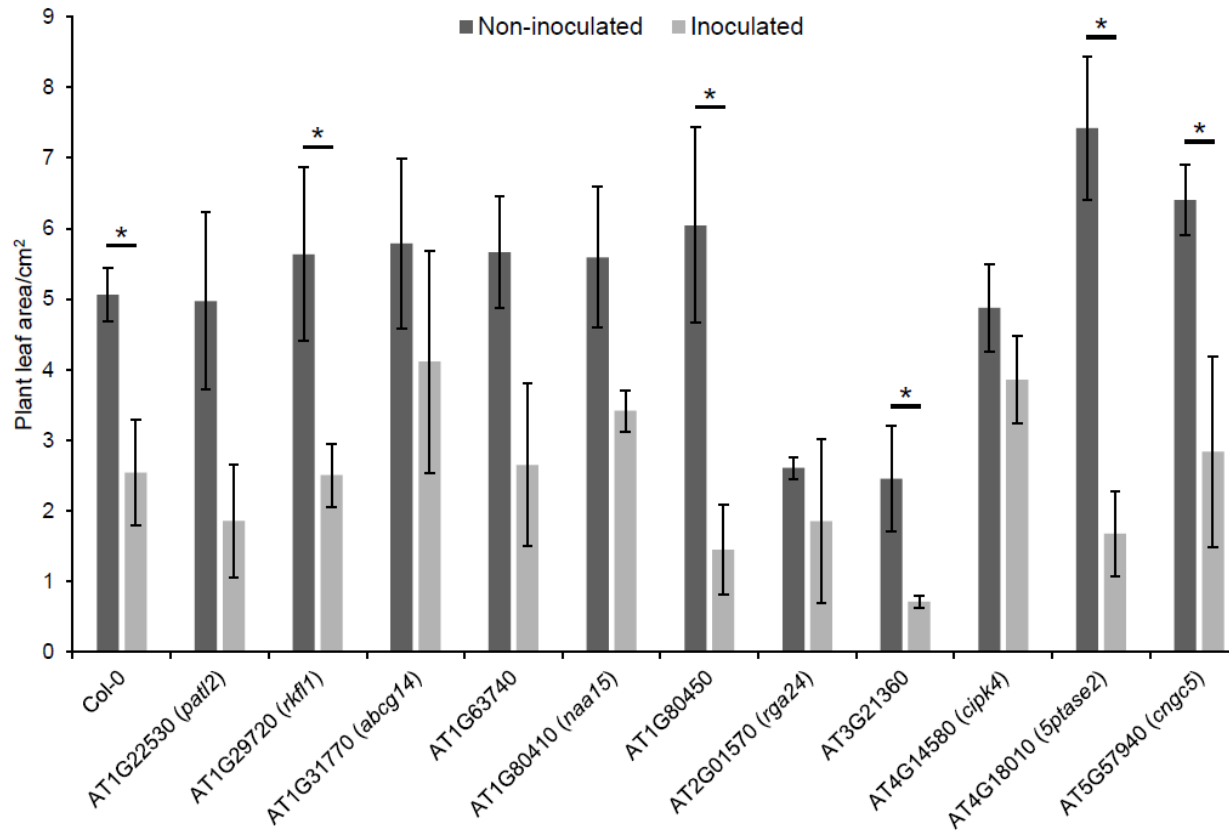


**Figure 4-10: *Arabidopsis thaliana* plant leaf areas at 16 days post *Rhizoctonia solani* AG2-1 inoculation. Genotypes with a significant difference (t-test,  $p < 0.05$ ) between the inoculated and non-inoculated plants are indicated by a bar and \*. Representative photographs of the inoculated plants are shown in Figure 4-11.**

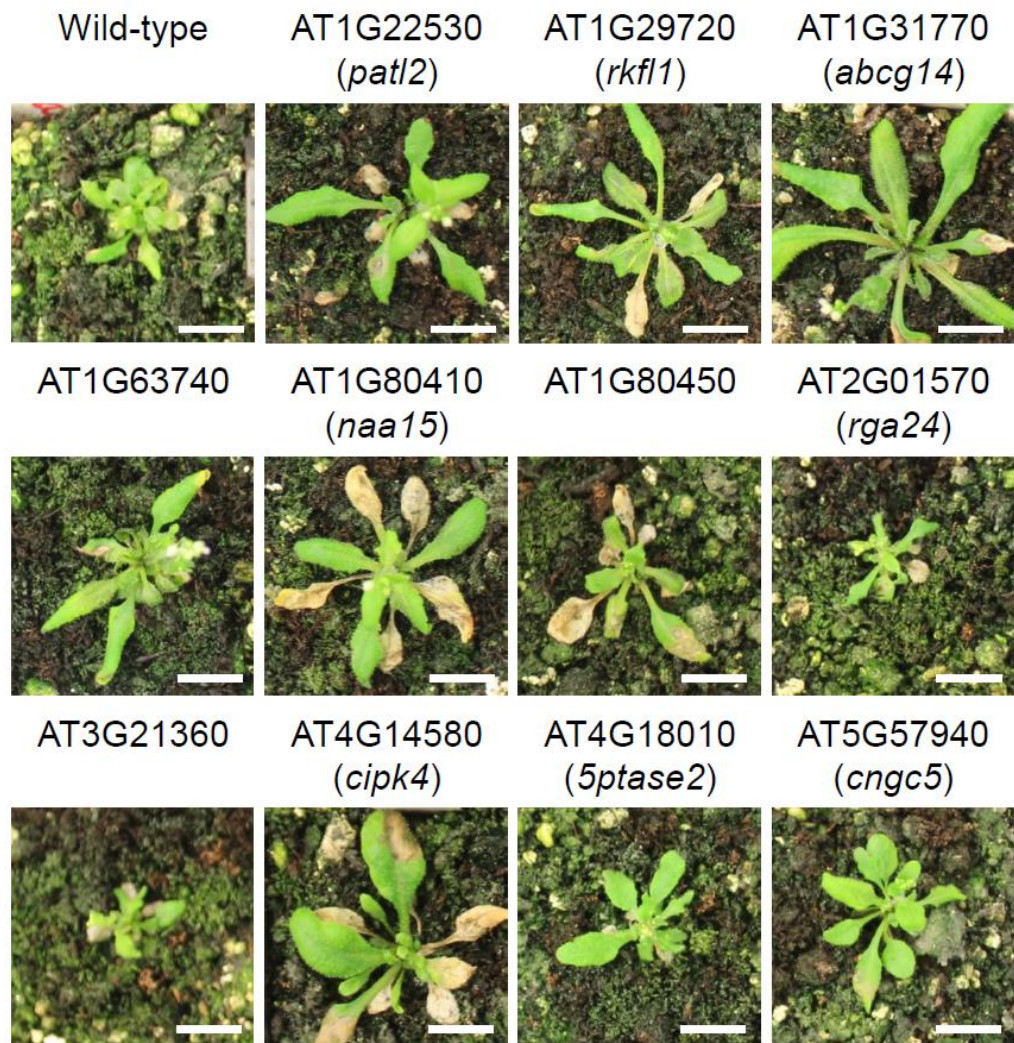


**Figure 4-11: Representative photographs of inoculated *Arabidopsis thaliana* plant leaf areas at 16 days post *Rhizoctonia solani* AG2-1 inoculation. Scale bar is shown in white in the bottom right corner of each image and represents 1cm.**

#### 4.4.3 Further investigation of CIPK4 and NAA15 in *Arabidopsis thaliana*

AT4G14580 (*cipk4*) and AT1G80410 (*naa15*) were selected for further investigation as these showed a smaller reduction in growth due to inoculation compared to WT plants, and did not show a reduction in growth due to their mutations.

CIPK4 is part of a family of calcineurin B-like (CBL)-interacting protein kinases, which interact with CBL Ca<sup>2+</sup> sensor proteins. These proteins are involved in stress responses, including biotic and abiotic stresses such as drought and salt stress (Mao *et al.*, 2016). Although research on CIPK4 is limited, the role of other CIPK genes in stress responses are better understood, such as CBL4 (SOS3) and CIPK24 (SOS2) (Mao *et al.*, 2016). CBL-CIPK proteins are also known to interact with ROS generation (Hu *et al.*, 2020). CIPK4 was shown to have associations with four functional partners: HOMOLOG OF YEAST SUCROSE NONFERMENTING 4 (SNF4), STARCH-EXCESS 4 (SEX4), LIKE SEX4 (LSF4) and AT2G20050 (Figure 4-12A). SNF4, SEX4 and LSF4 are involved in carbohydrate metabolism, with SEX4 and LSF1 being involved in the starch catabolic process and having carbohydrate phosphatase activity. LSF1 and SNF4 are located in the chloroplast starch grain. AT2G20050 is a possible interacting partner of CAP1, which is a membrane-localized receptor-like kinase involved in the regulation of root hair tip growth.

NAA15 is the auxiliary subunit of NatA (N-terminal acetyltransferase A) and interacts with the catalytic subunit NAA10 to catalyse protein N-terminal acetylation (NTA) (Feng *et al.*, 2016). This was previously shown to be essential for embryogenesis and NAA15 mutations produced an embryo-lethal phenotype (Feng *et al.*, 2016). NatA is downregulated by abscisic acid (ABA) and NTA decreases after drought stress (Linster *et al.*, 2015). NatA has been shown to contribute to the turnover of two nod-like receptor (NLR) immune receptors; suppressor

of NPR1, constitutive 1 (SNC1) and resistance to *P. syringae* pv *maculicola* 1 (RPM1) (Xu *et al.*, 2015). NAA15 showed a more complex network, with ten functional partners associated, many of which also associated with each other (Figure 4-12B). Five of these genes are also N-terminal acetyltransferases: AT5G13780 (NAA10), AT1G03150 (NAA20), AT5G58450 (NAA25), AT5G11340 (NAA50) and AT5G16800 (NAA60). Four genes are associated with N-terminal protein amino acid acetylation: MEIOTIC CONTROL OF CROSSOVERS1 (MCC1), NAA10, NAA25 and NAA20. Six genes have GNAT and acyl-CoA N-acyltransferase domains: MCC1, NAA10, NAA20, NAA50, NAA60, and AT1G03650. AT3G06610 (SUF1) is involved in the regulation of heat-stress induced protein ubiquitination. METHIONINE AMINOPEPTIDASE 2B (MAP2B) is involved in protein maturation and MAK10 encodes a non-functional homolog of yeast MAK10, which is a component of N-terminal acetyltransferase complex C.

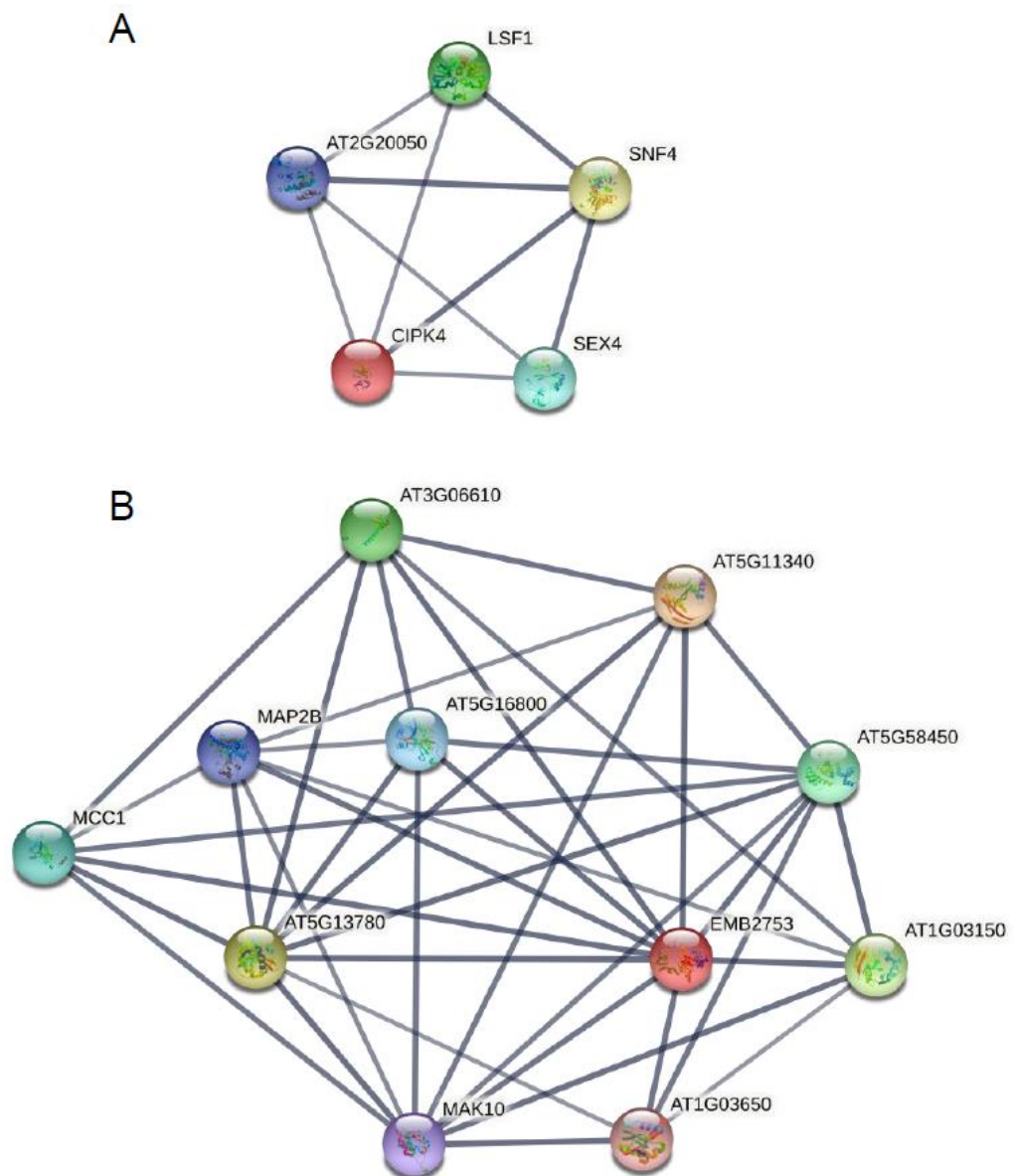


**Figure 4-12: Full STRING networks showing the functional partners of *Arabidopsis thaliana* A) CIPK4 and B) NAA15. The minimum required interaction score was high confidence (0.7) with a size cut-off of no more than 10 interactors. Line thickness shows the strength of data support for each interaction. NB. NAA15 is shown as EMB2753 in this diagram.**

RT-qPCRs were completed using cDNA from whole plant RNA extractions with log<sub>2</sub> fold changes of gene expression calculated for Col-0 (wild type), *cipk4* and *naa15* mutants at 8, 24 and 48hpi. Relative gene expression was calculated from inoculated and non-inoculated values, with TUB9 used as the control. Genes were selected for testing

based on the assessment of resistance pathways induced by *R. solani* in *A. thaliana* by Sharon *et al.* (2011). These can be divided into two sections, assessing the involvement of systemic acquired resistance (SAR) (Figure 4-13) and induced systemic resistance (ISR) (Figure 4-14). SAR is an inducible broad-spectrum defence mechanism which requires SA signalling through NPR1, whereas ISR is triggered independently of SA and responds to JA and ET (Withers and Dong, 2016).

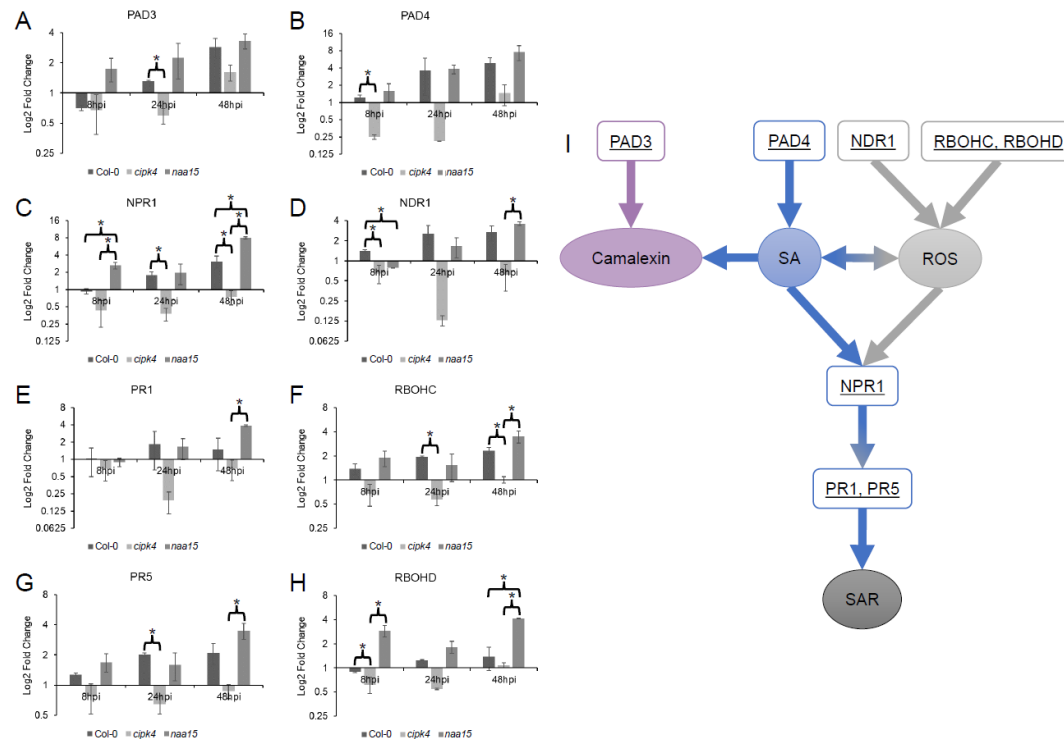


**Figure 4-13: Graphs showing the log<sub>2</sub> fold change of differential gene expression of *Arabidopsis thaliana* wild-type, *cipk4* and *naa15* plants following inoculation with *Rhizoctonia solani* AG2-1 at 8, 24 and 48 hours post inoculation and network of genes relating to systemic acquired resistance (SAR). *naa15* mutants and wild-type plants show increased expression under inoculation of many genes involved in SAR, while reduced expression was seen in *cipk4* plants. Brackets and a \* show significant differences between the genotypes at each time point.**

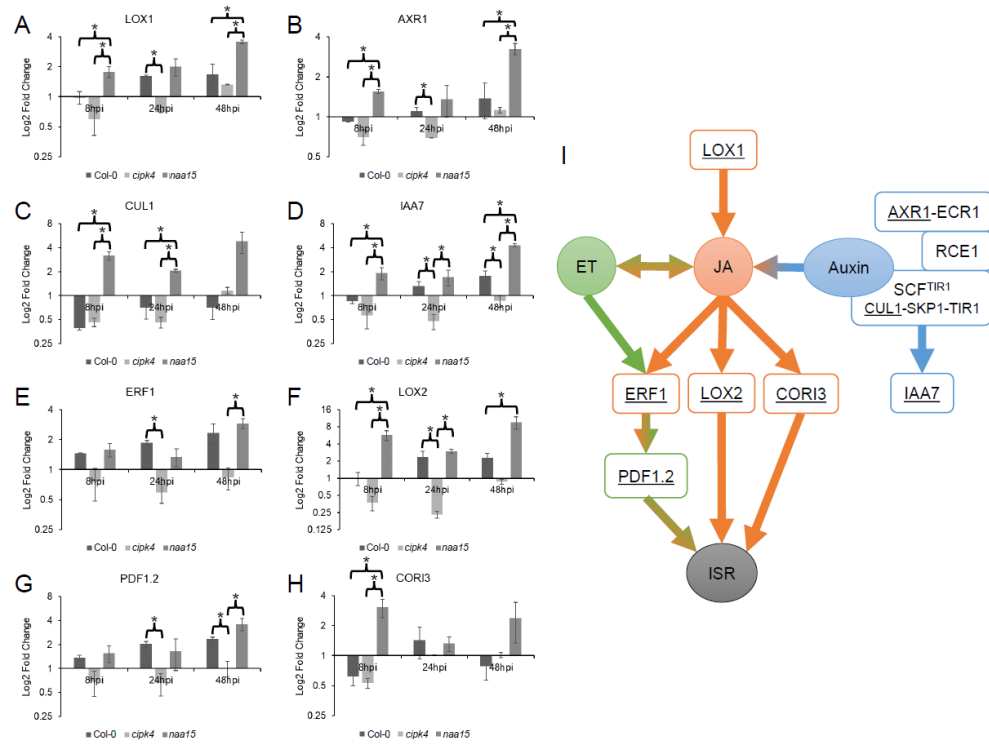


**Figure 4-14: Graphs showing the log<sub>2</sub> fold change of differential gene expression of *Arabidopsis thaliana* wild-type, *cipk4* and *naa15* plants following inoculation with *Rhizoctonia solani* AG2-1 at 8, 24 and 48 hours post inoculation and network of genes relating to induced systemic resistance (ISR). *naa15* mutants show the greatest increase in expression under inoculation, while *cipk4* often showed a reduction in expression and the responses for the wild-type plants were more variable. Brackets and a \* show significant differences between the genotypes at each time point.**



PAD3 is required for camalexin biosynthesis (Zhou, Tootle and Glazebrook, 1999) and showed increased expression under inoculation at all time points for *naa15*, and at the later timepoints for Col-0 and *cipk4* (Figure 4-13A). PAD4 is involved in camalexin biosynthesis, but also functions upstream of SA signalling and pathogenesis related (PR) genes (Zhou, Tootle and Glazebrook, 1999) and showed increased expression in Col-0 and *naa15* but reduced expression at 8hpi and 24hpi for *cipk4* (Figure 4-13B). NPR1 plays a key role in SA signalling and is required for both systemic acquire resistance (SAR) and induced systemic resistance (ISR) (Withers and Dong, 2016). NPR1 showed increased expression under inoculation at the later timepoints for Col-0 and all timepoints for *naa15* but showed reduced expression for all timepoints in *cipk4* (Figure 4-13C). PR genes function downstream of SA and PR1 and PR5 showed increased expression in Col-0 and *naa15*, and decreased expression in *cipk4* (Figure 4-13E, Figure 4-13G). These results suggested that Col-0 and *naa15* both had increased SAR activity under inoculation, though this was not the case for *cipk4*.

NDR1 is involved in both PAMP triggered immunity (PTI) and effector triggered immunity (ETI) responses and is required for the activation of CC-NLR resistance proteins (Knepper, Savory and Day, 2011).

Increased NDR1 expression was observed in Col-0 and at the later timepoints for *naa15* but decreased expression was observed at all timepoints for *cipk4* (Figure 4-13D). Respiratory burst oxidase homologs (RBOH) or NADPH oxidases are key ROS producers, which

function in signalling during stress responses (Hu *et al.*, 2020). RBOHC showed increasing relative expression for Col-0 and also showed increased expression at all timepoints for *naa15* but showed decreased expression at 8hpi and 24hpi for *cipk4* (Figure 4-13F). For RBOHD, increased expression was seen at the later timepoints for Col-0, and at all timepoints for *naa15*, while *cipk4* showed decreased expression for RBOHD at 8hpi and 24hpi but was slightly increased at 48hpi (Figure 4-13H). This suggested that reactive oxygen species (ROS) may play a role in responses in Col-0 and *naa15* but are unlikely in *cipk4*.

Lipoxygenases are oxidoreductase enzymes, of which, LOX1 is involved in pathogen resistance and LOX2 is involved in jasmonic acid (JA) biosynthesis (Singh *et al.*, 2022). Both LOX genes show similar expression patterns with Col-0 plants showing increased expression at 24hpi and 48hpi, while *naa15* plants showed an increase at all timepoints. *cipk4* plants showed decreased expression under inoculation at all timepoints for LOX2 and in LOX1 at 8hpi and 24hpi, with an increase for LOX1 at 48hpi (Figure 4-14A and Figure 4-14F). LOX2 and CORI3 are both downstream of JA and are linked to ISR. CORI3 has been linked with responses to JA, ABA and wounding (Castillo *et al.*, 2004). CORI3 increased its expression under inoculation in Col-0 at 24hpi and decreased at 8hpi and 48hpi, while in *naa15* it increased at all timepoints (Figure 4-14H). *cipk4* showed decreased expression at 8hpi but showed no change at 24hpi and 48hpi.

ERF1 can be upregulated by both ethylene (ET) and JA, and PDF1.2 functions downstream of ERF1 (Lorenzo *et al.*, 2003). Similar expression patterns were seen for both genes (Figure 4-14E, Figure 4-14G), with increased expression over time for Col-0 and *naa15*, and decreased expression for *cipk4* at 8hpi and 24hpi. This suggested that ISR and JA and ET responsive genes may be involved in Col-0 and *naa15* responses but not *cipk4*.

AXR1 and CUL1 are both required for auxin signalling and IAA7 is an auxin-responsive gene (Paciorek and Friml, 2006). AXR1 showed a slight increase in expression in Col-0 at 48hpi, and increased expression at all timepoints for *naa15*, but decreased expression for 8hpi and 24hpi in *cipk4* (Figure 4-14B). For CUL1, all timepoints showed decreased expression in Col-0 and 8hpi and 24hpi also decreased for *cipk4* (Figure 4-14C). *naa15* showed increased expression of CUL1 at all timepoints. Finally, Col-0 showed increased expression of IAA7 under inoculation at 24hpi and 48hpi and was increased at all timepoints for *naa15* (Figure 4-14D). *cipk4* showed decreased expression for IAA7 at all timepoints.

Overall, *naa15* and Col-0 show similar expression patterns in the defence genes tested here, suggesting that any increased tolerance to the pathogen is due to other mechanisms. *cipk4* however, shows very different expression patterns from Col-0, with most genes being downregulated under inoculation. This could suggest that *R. solani* is manipulating host immunity to cause susceptibility in the wild-type

plants, and the reduced susceptibility seen in the *cipk4* mutant is due to a lack of immune signalling. The mutant's increased tolerance may be linked to its ability to invest resources in growth and development.

#### 4.4.4 Phenotyping CIPK4 and NAA15 using *Brassica rapa* TILLING lines

For both CIPK4 and NAA15, there are three copies of the genes in *B. rapa*, all of which have multiple TILLING lines available. Protein alignments for each gene are shown in Figure 4-15 for CIPK4 and Figure 4-16 for NAA15. For CIPK4, Bra036868 is most similar to *A. thaliana*, while Bra036870 only has the first half of the protein, and Bra036869 only had the second half. For NAA15, Bra003565 has a long section at the start of the protein, which is only shared in part by Bra008474.

Bra036869.1	-----	0
Bra036868.1	MLPPSTSPRQPSSHHMDLPTPQSPDKSPATILLGKYELGRLLGSGSFAKVHVARSIETE	60
AT4G14580.1	-----MESPYPKSPEKITGTVLLGKYELGRLLGSGSFAKVHVARSIISTGE	45
Bra036870.1	-----MGFPSPSSPEKSPGTILLGKYELGRLLGSGSFAKVHVARSIIEAGE	45
Bra036869.1	-----	0
Bra036868.1	LLAVKIIDKKRTATAGMEPMIIREIEAMRRLQHHPNVLTIHEVMATKTKIYLVMELAAGG	120
AT4G14580.1	LVAIKIIDKQKTIDSGMEPRIIREIEAMRRLHHPNVLKIHVMATKSKIYLVVEYAAGG	105
Bra036870.1	LVAVKIIDKKKTADAGMEPRIIREIEAMRRLHHPNVLKIHVMATKTKIYLVMELAAGG	105
		Leu to Phe missense mutation
Bra036869.1	-----	0
Bra036868.1	EIYTKIRDSGRLKEEARRYFQQLVSALTFCHREGIAHRDVKPQNLLLDNEGNLKVSDFG	180
AT4G14580.1	ELFTKLIIRFGRNLNESAARRYFQQLASALSFCCHRDIHRDVKPQNLLLDKQGNLKVSDFG	165
Bra036870.1	ELFTRIRRSGRLQESAARRYFQQLASALTFCHREGIAHRDVKPQNLLLDKQGNLKVSDFG	165
		Asp to Asn missense mutation
Bra036869.1	-----	0
Bra036868.1	LSALPEDRRSTGMLHTACGTPAYTAPEVIAHRHYDGAKADSMSCGVFLFVLLAGYVPFND	240
AT4G14580.1	LSALPEHRSNGLLHTACGTPAYTAPEVIAQRGYDGAKADAWSCGVFLFVLLAGYVPFDD	225
Bra036870.1	LSALPEHRSSTGLLQTSCTPAYTAPEVIAQKSYDGAKADSWSCGVFLFVLLAGYVPFED	225
		STOP mutation
Bra036869.1	-----MSIEAVTETKWFKKSLTSE	20
Bra036868.1	CHIVLHYRKIQGRDYKFPNWSKPARSIIYKLLDPNPETRMSEAVTETKWFKKSLKTSE	300
AT4G14580.1	ANIVAMYRKIHKRDYRFPSPWISKPARSIIYKLLDPNPETRMSEAVMGTVWFQKSLEISE	285
Bra036870.1	SNVVTHYRKIQRRDYKFPNGISKQARSIIYNNVVESNQPEI-KINAKQSQL-----	274
		* * *
		Ser to Leu missense mutation
Bra036869.1	FKPNVLESDDRIG--KLRSDTITAFDLISAGLDLSGLFERRKRKTRFTATVSAEGVV	78
Bra036868.1	FKPNVLESDERLIG--PLRSDTITAFDLISLSTEWDLSGLFERRKMKRTRFTARVSVEGVV	358
AT4G14580.1	FQSSVFEIDRFLEKEAKSSNAITAFDLISLSSGLDLSGLFERRKRKEKRFTARVSAERVV	345
Bra036870.1	-----	274
Bra036869.1	EKAKTIGEKLGYRVEKKEEAMALGLGKGRITVMEAVELVEGLVVAEVKVEGE---EEE	135
Bra036868.1	EKAKAIGEKLGFVRVKESEARVVALSKGRITVVVEAVELVEGLVVAEMKVVEGVE---EEE	416
AT4G14580.1	EKAGMIGEKLGFVRVEKKEETKVVGLGKGRITAVVVEVVEFAEGLVVDVVKVVEGEVEEEE	405
Bra036870.1	-----	274
Bra036869.1	EESYWSELIVEFEEIIVLSNHSDVSVKVESDLA-----	167
Bra036868.1	DESHWSEITVGLEEIVLAWHHDVDTVAYYLSVLKPLFPNGINVLFMFTGISGGEVALHHL	476
AT4G14580.1	VESHWSELIVELEEIVLSNHN-----	426
Bra036870.1	-----	274
Bra036869.1	-----	167
Bra036868.1	QIPMKTVVSVVEISV	490
AT4G14580.1	-----	426
Bra036870.1	-----	274

**Figure 4-15: Protein alignment for CIPK4 genes in *Arabidopsis thaliana* and *Brassica rapa*. Protein sequences were obtained from TAIR (Huala *et al.*, 2001) and Ensembl (Howe *et al.*, 2021) and the Multiple Sequence Alignment tool used in Clustal Omega (<https://www.ebi.ac.uk/Tools/msa/clustalo/>). Mutations for TILLING lines were chosen as indicated.**

Bra003565.1	MNGEITYLLSDEKTDNTRKKKKARWRFRNwVfVIPGDEAQQQVDVKREKDNMEVYENMVQ	60
Bra008474.1	-----	0
AT1G80410.2	-----	0
Bra035184.1	-----	0
Bra003565.1	YHENCYQLFNTLHVLNKRFFELIFTKKKNGKTKLEYTWVEINPELVLTCLRRHRKVRGIC	120
Bra008474.1	-----	0
AT1G80410.2	-----	0
Bra035184.1	-----	0
Bra003565.1	EKLKRSKQYPQALDVSQWITEHKICSLVPEDYTTDFHLIKNVLVFEEVEKFLKVPENLR	180
Bra008474.1	-----	0
AT1G80410.2	-----	0
Bra035184.1	-----	0
Bra003565.1	NKSMYTVLILKYAESGKKDIDRTEDVFKMRELGLLLKPSPFSSIMSLYISVGNRVKQVDE	240
Bra008474.1	-----	0
AT1G80410.2	-----	0
Bra035184.1	-----	0
Bra003565.1	ILREMKENNVKVDSLTMAKAYLRVGSKREAREMLLGTTELNDPMLM-SLYGEAGDREDV	299
Bra008474.1	-----MSQKRNLPSWI-SSRDPHPHPQPEKPKKDDADDE	36
AT1G80410.2	-----	0
Bra035184.1	-----	0
Bra003565.1	YRIRNLYKKTREQDNDGFLTLNFDVCNRAAVMYNEYEWSLEFDIRIPTMVVSGFRKRK	359
Bra008474.1	HNIRNAPQ-----SSSTTMDFSKLLE-----GVVFLSGFVNPE	70
AT1G80410.2	-----	0
Bra035184.1	-----	0
Bra003565.1	N--FQRADILMNKTLRNIKFGNKSFTLSPEEWGKIERNQVKPSELRLDIKNFQDSTQFPK	417
Bra008474.1	RSTLRSQALSMGAT-----YQPDWNSD-----STLLICAFPNTPKFRQ	108
AT1G80410.2	-----	0
Bra035184.1	-----	0
Bra003565.1	-----ALEPSWJLCDQEVISLFLEDYANRFDLTKVLFKEAQNESDAKENMMSLSLGNK	471
Bra008474.1	VQSNSTIVSKDIAECYTKKLV-----DI-----	134
AT1G80410.2	-----	0
Bra035184.1	-----	0
Bra003565.1	IKHLVGGHTLMADRMWPCGFELYDWKYYKQMESFINQGPVVEEILKVKVLQVSDIYGSY	531
Bra008474.1	----EQYLLHAGKPWRKTSAPQNT-----TIRE-KKKQLSIKSEENQVETKPGTR	179
AT1G80410.2	-----	0
Bra035184.1	-----	0
Bra003565.1	GCKETSVTTSLLNGVFTHETYPLADKL-YL--HANELEVWHEKIKISNDANICKRLREQV	588
Bra008474.1	GTSSASSKNRPACN-TVEEPFSVTEVKKWARDDLTETISWLESQEEKPAPGDIKRIAAEG	238
AT1G80410.2	-----	0
Bra035184.1	-----	0
Bra003565.1	LLRIM-----STEKHKRYRRAWKFKFMSKNLIGVCTSRRRYFDPGITKLFREILVYA	640
Bra008474.1	VLTCQDAIDSLEQKDVGSVTELWSFVPRVKELGKMESSKTEN-----	284
AT1G80410.2	-----	0
Bra035184.1	-----	0
Bra003565.1	AVSTMRFEAAAEIC----LIWAHSSRRLIRRNEPEI---KRLHEMRSSMSLKTSS----	688
Bra008474.1	-----STASKDQLCKQAKSWKKIYEAEQAQKGESEEAASRRTSGVASGYDSDETVEMTE	339
AT1G80410.2	-----	0
Bra035184.1	-----	0

Asp to Asn missense mutation

Bra003565.1	-EMAFILHEIGSETVESI---IGQNRGSALELQRNENTPHVWHRWKNRVGKQAVYKS	743
Bra008474.1	EEIEHAYRNVSVDKVEANSTPSSLSSASSASSLSCPRTMGAP---LPPKEANLFKLIIVKS	395
AT1G80410.2	-----MGAS-----LPPKEANLFKLIIVKS	19
Bra035184.1	-----MGAS-----LPTKEANLFKLIIVKS	19
	STOP mutation	:: :... :: : **
Bra003565.1	YETKQYKKGKKAADAILKKFPSHGGETLSMKGLTLNCMDRKTAEYELVRLGVKNDIKSHVC	803
Bra008474.1	YETKQYKKGKKAADAILKKFPSHGGETLSMKGLTLNCMDRKTAEYELVRLGVKNDIKSHVC	455
AT1G80410.2	YETKQYKKGKKAADAILKKFPHGGETLSMKGLTLNCMDRKTAEYELVRLGVKNDIKSHVC	79
Bra035184.1	YETKQYKKGKKAADAILKKFPSHGGETLSMKGLTLNCMDRKTAEYELVRLGVKNDIKSHVC	79
*****		
Bra003565.1	WHVFLGLLYRSREYREAIKCYRNALRIDPENLEILRDLSLLQAQMRDLSGFVETRQQLLT	863
Bra008474.1	WHVYGLLYRSREYREAIKCYRNALRIDPDNLEILRDLSLLQAQMRDLSGFVETRQQLLT	515
AT1G80410.2	WHVLGLLYRSREYREAIKCYRNALRIDPDNLEILRDLSLLQAQMRDLSGFVETRQQLLT	139
Bra035184.1	WHVLGLLYRSREYREAIKCYRNALRIDPDNLEILRDLSLLQAQMRDLSGFVETRQQLLT	139
*****		
Bra003565.1	LKPNHRMNNWIGFAVSQHLNANASKAVEILEAFEGTLEDDYPPENELCEHEMILYKVSLL	923
Bra008474.1	LKPNHRMNNWIGFAVSQHLNANASKAVEILEAFEGTLEDDYPPENELCEHEMIMYKVSLL	575
AT1G80410.2	LKPNHRMNNWIGFAVSQHLNANASKAVEILEAFEGTLEDDYPPENELIEHEMILYKVSLL	199
Bra035184.1	LKPNHRMNNWIGFAVSQHLNANASKAVEILEAFEGTLEDDYPPENELCEHEMILYKVSLL	199
*****		
Bra003565.1	EEIGAFDKALEELHKKEPKIVDKLSYKELEVSLLSKLGRPAEADKLYRVLLSMNPDNRYR	983
Bra008474.1	EESGAFGKALEELHKNEPKIVDKLSYKEQAYLLWKLGRPAEASKLYRVLLSMNPDNRYR	635
AT1G80410.2	EESGAFDKALEELHKKEPKIVDKLSYKEQEVSLSKVGRLEEANKLYRVLLSMNPDNRYR	259
Bra035184.1	EESGAFDKALEELHKKEPKIVDKLSYKEQEVSLSKLGRLEEAKKLYRVLLSMNPDNRYR	259
** *, * ***** * ***** * ** *,** * *****		
	STOP mutation	
Bra003565.1	YEGLOKCFGLYSESGQYSSDKIEKLNALYQSLSEQYTRSSAVKRIPLDFLQDESFKEAVA	1043
Bra008474.1	YEGLOKCFGLYSESGQYSSDRIEKLNALYQSLSEQYTRSSAVKRIPLDFLQDERFKEAVA	695
AT1G80410.2	HEGLQKCLGLYSESGQYSSDQIEKLNALYQSLSEQYTRSSAVKRIPLDFLQDENFKEAVA	319
Bra035184.1	YEGLOKCLELYSENGQYSSDQIEKLNALYQSLSEQYTRSSAVKRIPLDFLQDESFKEA VG	319
:*****: *****:*****:*****:*****:*****:*****:*****		
Bra003565.1	KYIKPLLTKGVPSLFDLSSLYDHPKPDILEQVVMEMHSIRTTGSYPGSDVKPEPSTL	1103
Bra008474.1	KYIKPLLTKGVPSLFDLCSLYDHPKPDILEQVVMEMHSVRTTGSYPGSDVKPEPSTL	755
AT1G80410.2	KYIKPLLTKGVPSLFDLSSLYDHPKPDILEQVVMEMKHSIGTTGSYPGSDVKPEPSTL	379
Bra035184.1	KYIKPLLTKGVPSLFDLSSLYDHPKPDILEQLLEMENSIKTTRSYPGSDVKPEPSTL	379
*****:*****:*****:*****:*****:*****:*****:*****		
Bra003565.1	LWTLFFLAQHYDKRGQYDVALGKIDEAIAHTPTVIDLYSVKSRIMKHAGDLTAAALADE	1163
Bra008474.1	LWTLFFLAQHYDKRGQYDVALGKIDEAIAHTPTVIDLYSVKSRIMKHAGDLTAAALADE	815
AT1G80410.2	LWTLFFLAQHYDRRGQYDVALCKIDEAIAHTPTVIDLYSVKSRIMKHAGDLTAAALADE	439
Bra035184.1	LWTLFFLAQHYDKRGQYDVALGKIDEAIAHTPTVIDLYSVKSRIMKHAGDLTAAALADE	439
*****:*****:*****:*****:*****:*****:*****:*****		
Bra003565.1	ARCMDLADRYINSECVKRMQLQADQVTLAEKTAFLFTKEGDQINNLDHMQCMWYDLASGDS	1223
Bra008474.1	ARCMDLADRYINSECVKRLQADQVASAETAFLFTKEGDQLNSLDHMQCMWYDLASGDS	875
AT1G80410.2	ARGMDLADRYINSECVKRMQLQADQVPLAEKTAFLFTKEGDQLNLDHMQCMWYDLASGDS	499
Bra035184.1	ARCMDLADRYINSECVKRMQLQADQVTLAEKTAFLFTKEGDQINNLDHMQCMWYDLASGDS	499
** *****:*****:*****:*****:*****:*****:*****:*****		
	Ala to Thr missense mutation	
Bra003565.1	YFRQGDGRALKRFLAVEKHYTDISEDQDFDHSYCLRKMTLRSYVDMLKFQDRLHSFPYF	1283
Bra008474.1	YFRQGDGRALKRFLAVEKHYSDISEDQDFDHSYCLRKMTLRSYVGMKLFEDRLHSFPYF	935
AT1G80410.2	YFRQGDGRALKRFLAVEKHYADISEDQDFDHSYCLRKMTLRSYVDMLKFQDRLHSFPYF	559
Bra035184.1	YFRQGDGRALKRFLAVEKHYSDIHEDQDFDHSYCLRKMTLRSYVDMLKFQDRLHSFPYF	559
* *****:*****:*****:*****:*****:*****:*****:*****		
Bra003565.1	HKAAIRAIRCYLKLHDSPKSTAEEDGMSKMAPAQKKMKKQKAEARAKKEAESKSEEST	1343
Bra008474.1	HKAAIRAIRCYLKLHDTPKSTAEEDMSKMAPAQKKMKKQKAEARAKKEAESKSEEST	995
AT1G80410.2	HKAAIRAIRCYLKLHDSPKSTAGEDEMSKMAPAQKKMKKQKAEARAKKEAESKSEEST	619
Bra035184.1	HKAAVKAIRCYLKLHDSPKSTAEEDMSKMAPAQKKMKKQKAEARAKKEAESKSEEST	619
***:*****:*****:*****:*****:*****:*****:*****		
Bra003565.1	ASGVSKSGKNNKVPDPPHGGKLIQVEPMAEASKYLRLQKHSPNSLETHLVSFEVNM	1403
Bra008474.1	ATGVSKSGKNNKVPDPPHGGKLIQVEDPMAEASKYLRLQKHSPNSLETHLSFEVNM	1055
AT1G80410.2	ASGASKSGKNNKVPDPPHGGKLIQVEPMAEASKYLRLQKHSPNSLETHLSFEVNM	679
Bra035184.1	ASVSKSGKNNKVPDPPHGGKLIQVEPMAEASKYLRLQKHSPNSLETHLSFEVNM	679
*: *****:*****:*****:*****:*****:*****:*****:*****		

```

Bra003565.1   RKQKFLAFQAVKQMLKLD AENPDSHRS LKFFLNTESTSAPTTEAEKLRWSVLEAERPS   1463
Bra008474.1   RKEKFLAFQAVKQLKLD AENPDSHRS LVKFFLKTGSTSAPTTEAEKLRCSVLEAERPS   1115
AT1G80410.2   RKQKFLAFQAVKQLKLD AENPDSHRS LVKFFLMTESISAPTTEAEKLRWRVLEAERPS   739
Bra035184.1   RKQKFLAFQAVKQLKLD AENPDSHRS LKFFSLKTGSTSAPTTEAEKLRWSVLEAERPS   739
**;*****;*:*:*:*:*:*:*:*:*:*:*:*:*:*:*:*:*

Bra003565.1   ISQLLNKSLVEVNE DFLGRHKDSL VHRAAYAEMLYLLDPSKKT EAIKTIEDSTNKVVQTN   1523
Bra008474.1   ISQLQNKSLVEANKE FFLGRHEDSL VHRAAYAEMMCLLDPSKKT EAIKLIEDSTNKVVQQT   1175
AT1G80410.2   ISQLQNKSLMEANKE FFLGRHEDSL VHRAAYAEMLYLLDPSKKT EAIKIIEDSTNKVVQ-T   798
Bra035184.1   ISQLQNKSLVEANKE FLARHEVSL VHRAAYAEMLYRLDPSKKT ESIKVIEDSTKVVQ-P   798
**** **;*:*:*:*:*:*:*:*:*:*:*:*:*:*:*:*:*

Bra003565.1   ---GAQIEWLKD C IAVHKL LDTVLLDSE AASRWKSRCAEYFPCSTYFEGKRSSVMPDS   1579
Bra008474.1   NGALGVAREW LKDC IAVHKL LLETVFLDSE AASRWKSRCAEYFPFSTHFEGKRSSVMPDS   1235
AT1G80410.2   NEALGQAREW LKDC IAVHTL LDTVLLD SQAASRWKSRCAEYFPCSTHFEGKHCSLMPDS   858
Bra035184.1   NGALGLAREW LKDC IAVHKL LDTVLLDSE AASRWKTRCAEYFPCSTYFEGKHSSMIPDS   858
* *****;*:*:*:*:*:*:*:*:*:*:*:*:*:*:*:*

Bra003565.1   VYNSSRKSNDNGD APNHPMGQTEMSD GQVEAFKSLSVST----- 1618
Bra008474.1   VYNSSLKSNENG DTPNHPMGQTE LNDGQLEAFKSLTVST----- 1274
AT1G80410.2   VYNSSRKSNDNG DTPNHPMGQTE LSDGQLEAFKSLSKMFWSCNMPWVYNCFSI   911
Bra035184.1   VYNSSRKSNDNG DTPSHPMGQTE FSDGQLEAIKSLSVST----- 897
**** **;*:*:*:*:*:*:*:*:*:*:*:*:*:*:*

```

**Figure 4-16: Protein alignment for NAA15 genes in *Arabidopsis thaliana* and *Brassica rapa*. Protein sequences were obtained from TAIR (Huala et al., 2001) and Ensembl (Howe et al., 2021) and the Multiple Sequence Alignment tool used in Clustal Omega (<https://www.ebi.ac.uk/Tools/msa/clustalo/>). Mutations for TILLING lines were chosen as indicated.**

Gene maps are presented for each copy of the gene (Figure 4-17, Figure 4-18, Figure 4-19, Figure 4-20, Figure 4-21 and Figure 4-22), and the mutations selected for the TILLING lines are indicated on the maps and in Table 4-6. For Bra036868 (CIPK4), a stop gained mutation at amino acid position 222 and a missense mutation (Ser to Leu) at amino acid position 327 were selected. For Bra036869 (CIPK4), a missense mutation (Ser to Leu) at amino acid position 47 was selected. For Bra036870 (CIPK4), a missense mutation (Leu to Phe) at amino acid position 101 and a missense mutation (Asp to Asn) at amino acid position 163 were selected. For Bra003565 (NAA15), a stop gained mutation at amino acid position 804 and a missense mutation (Leu to Phe) at amino acid position 1218 were selected. For Bra008474 (NAA15), a missense mutation (Asp to Asn) at amino acid position 120



and a stop gained mutation at amino acid position 640 were selected. For Bra035184 (NAA15), a missense mutation (Ala to Thr) at amino acid position 467 was selected.

**Table 4-6: Information about the selected *Brassica rapa* TILLING lines.**

<u>Gene name</u>	<u>Mutation name</u>	<u>Mutation type</u>	<u>Mutation location</u>
CIPK4	Bra036868 J130290-B	Stop gained	Amino acid 222 Within the S_TKc domain
CIPK4	Bra036868 J131978-B	Missense: Serine to Leucine (Hydroxylic to Aliphatic)	Amino acid 327 Within a CBL interaction site of the NAF domain
CIPK4	Bra036869 J131979-B	Missense: Serine to Leucine (Hydroxylic to Aliphatic)	Amino acid 47 Within a CBL interaction site of the NAF domain
CIPK4	Bra036870 J130055-A	Missense: Leucine to Phenylalanine (Aliphatic to Aromatic)	Amino acid 101 Within an ATP binding site of the S_TKc domain
CIPK4	Bra096870 J132228-A	Missense: Aspartic acid to Asparagine (Acidic to Amidic)	Amino acid 163 Within an ATP binding site of the S_TKc domain
NAA15	Bra003565 J131739-B	Stop gained	Amino acid 804 Within a TPR repeat
NAA15	Bra003565 J130605-B	Missense: Leucine to Phenylalanine (Aliphatic to Aromatic)	Amino acid 1218 Within the NARP1 domain
NAA15	Bra008474 J131384-B	Missense: Aspartic acid to Asparagine (Acidic to Amidic)	Amino acid 120 Within the BRCT domain
NAA15	Bra008474 J131025-B	Stop gained	Amino acid 640 Within the NARP1 domain
NAA15	Bra035184 J131449-A	Missense: Alanine to Threonine (Aliphatic to hydroxylic)	Amino acid 467 Within the NARP1 domain

The same gene maps also show key domains and features, as listed in the SMART (Letunic and Bork, 2017) and NCBI conserved domains (Marchler-Bauer and Bryant, 2004) databases. The NAF domain is both necessary and sufficient to mediate interactions between CIPK and CBL proteins and is found in Bra036868 and Bra036869 but not Bra036870, suggesting that Bra036870 may not function in a CIPK-CBL interaction. Both Bra036868 and Bra036870 have a tyrosine kinase domain, which may be key for signal transduction, but Bra036869 does not have this domain. Bra003565, Bra008474 and Bra035184 all have tetratricopeptide repeat (TPR) regions, which are structural motifs that mediate protein-protein interactions. NMDA receptor-regulated protein 1 (NARP1) domains were also identified in Bra003565, Bra008474 and Bra035184 and are found in association with TPR1 and TPR2 and are homologues for a mammalian cell cycle acetyltransferase. The BRCT domain, which was found in Bra008474 only, is predominantly found in proteins involved in DNA checkpoint controls and DNA repair. Selecting mutations within these domains was expected to prevent the proteins from functioning normally and give a mutant phenotype.

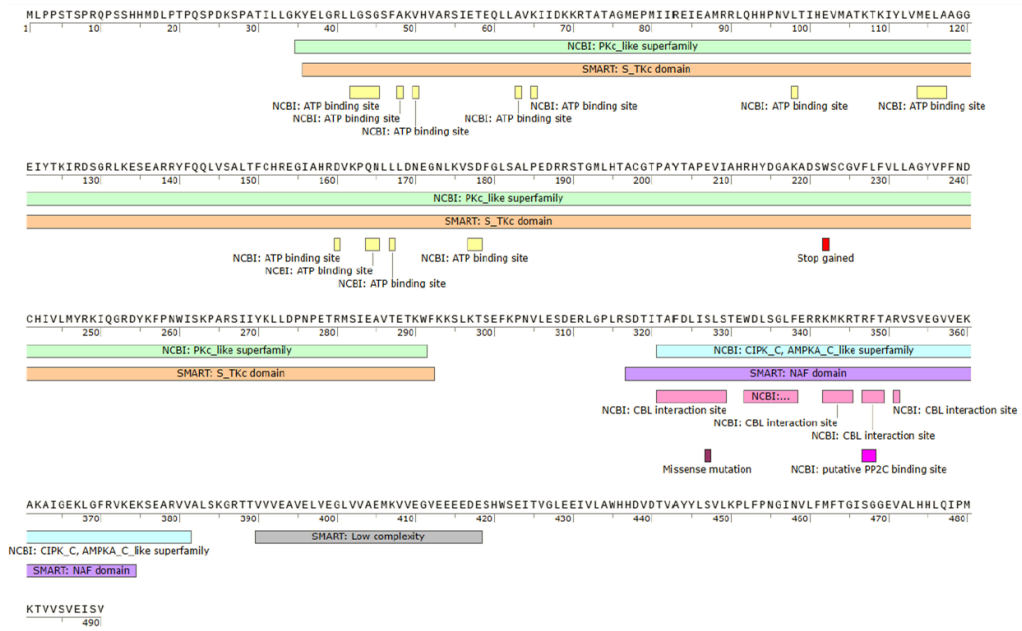


**Figure 4-17: Bra036868 gene map showing the mutation locations and key features for the TILLING lines. Information shown was gathered from SMART (Letunic and Bork, 2017) and NCBI conserved domains (Marchler-Bauer and Bryant, 2004) tools. Gene maps were created using SnapGene software.**

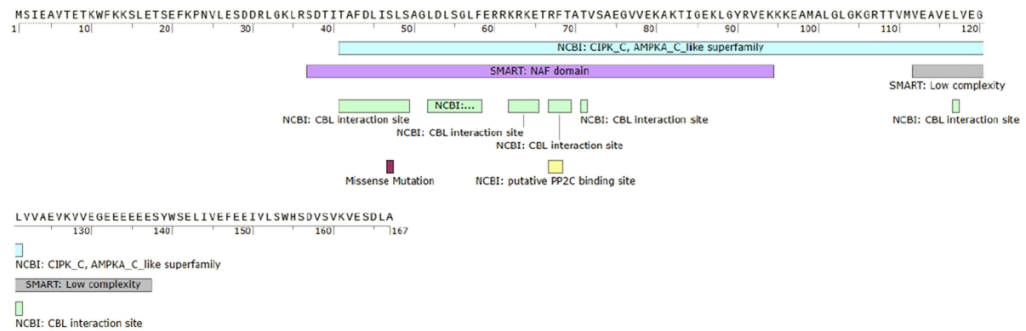


**Figure 4-18: Bra036869 gene map showing the mutation locations and key features for the TILLING lines. Information shown was gathered from SMART (Letunic and Bork, 2017) and NCBI conserved domains (Marchler-Bauer and Bryant, 2004) tools. Gene maps were created using SnapGene software.**

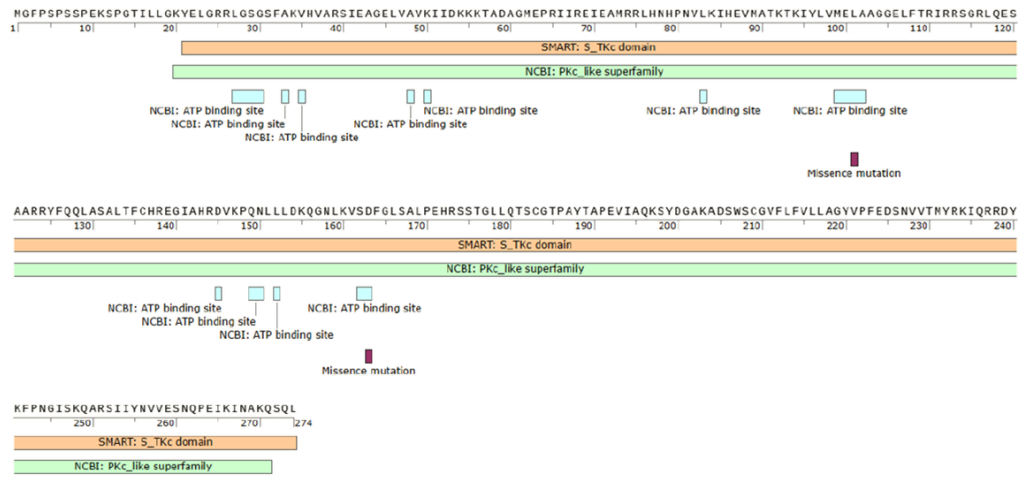


**Figure 4-19: Bra036870 gene map showing the mutation locations and key features for the TILLING lines. Information shown was gathered from SMART (Letunic and Bork, 2017) and NCBI conserved domains (Marchler-Bauer and Bryant, 2004) tools. Gene maps were created using SnapGene software.**

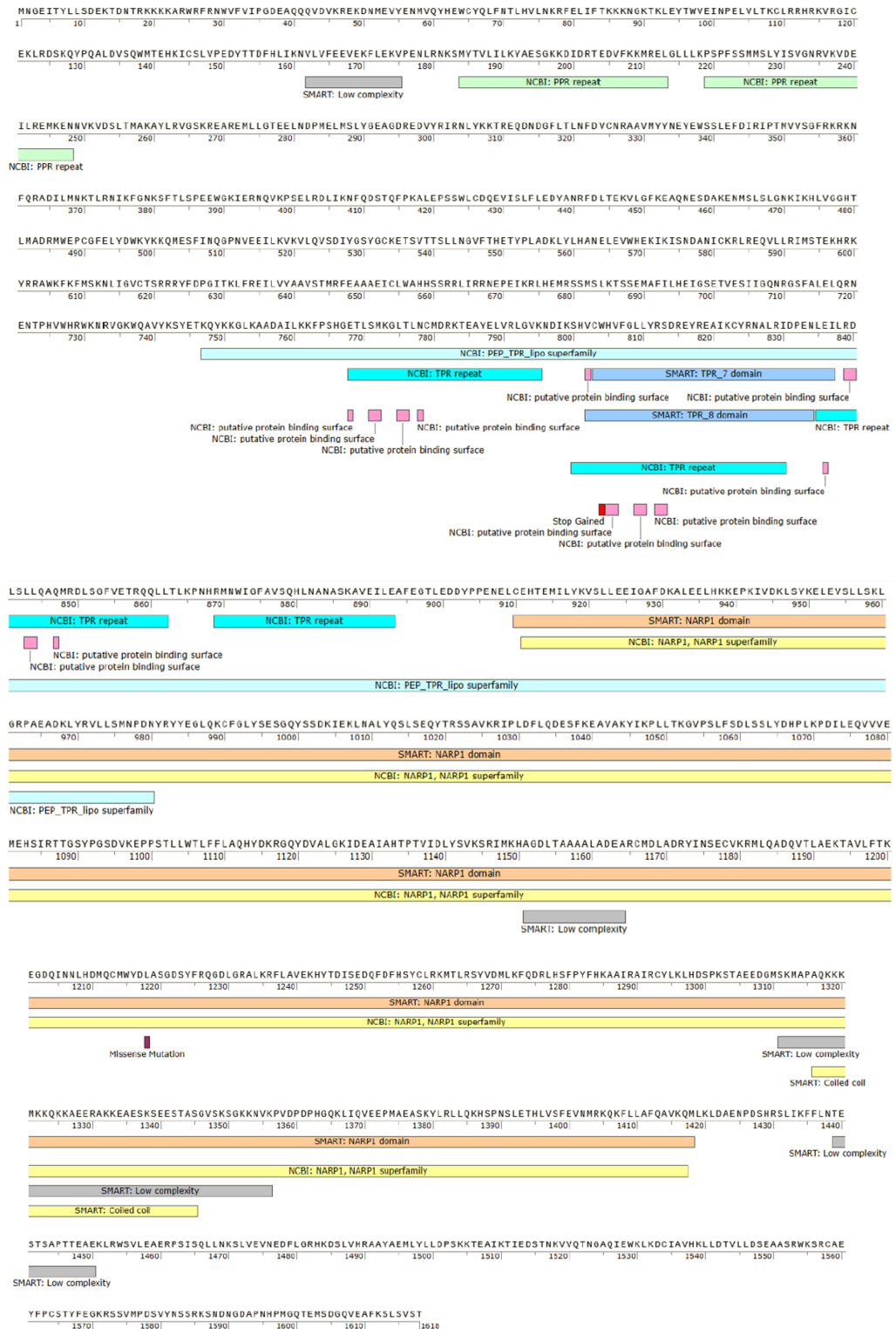


**Figure 4-20: Bra003565 gene map showing the mutation locations and key features for the TILLING lines. Information shown was gathered from SMART (Letunic and Bork, 2017) and NCBI conserved domains (Marchler-Bauer and Bryant, 2004) tools. Gene maps were created using SnapGene software.**

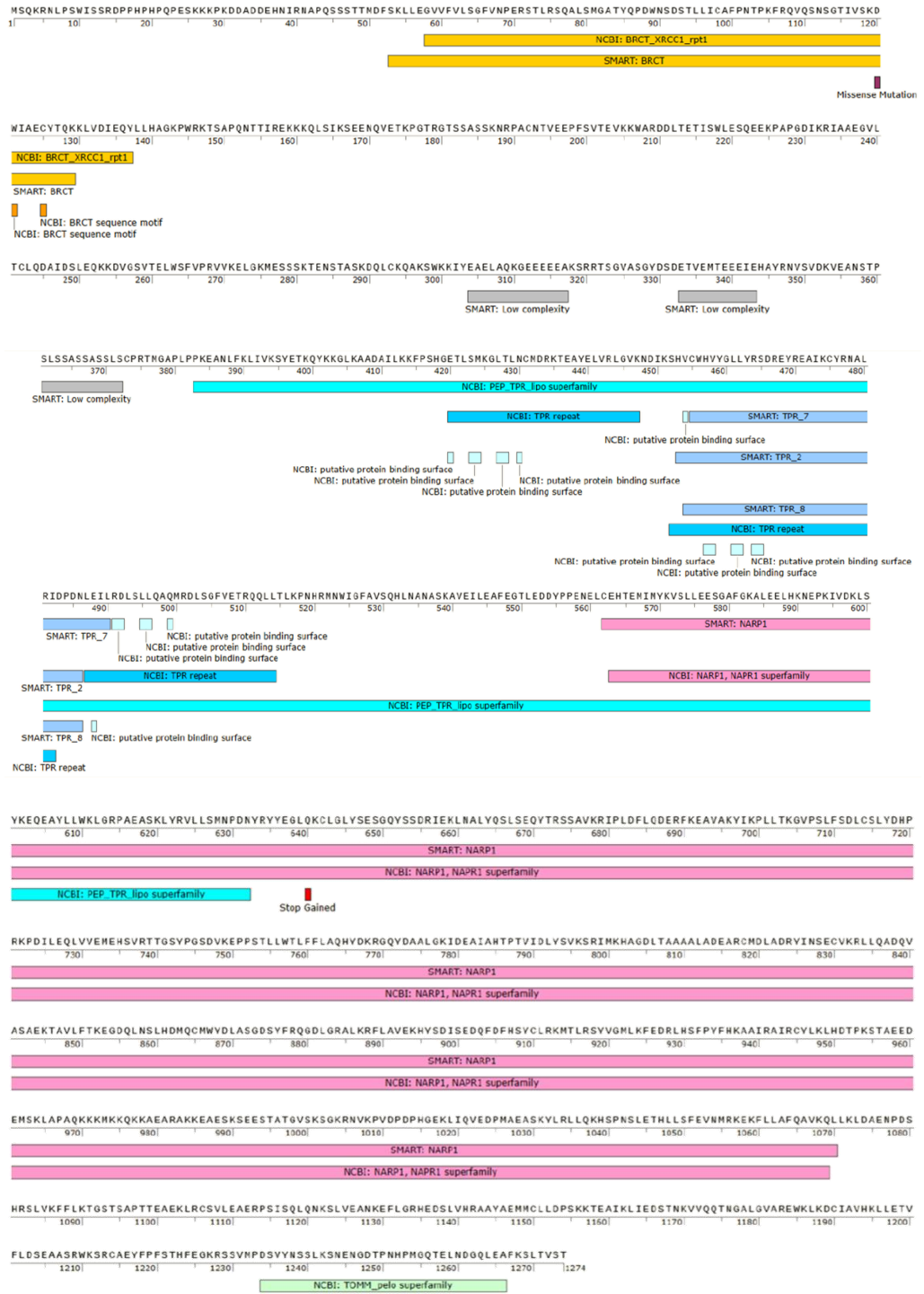


**Figure 4-21: Bra008474 gene map showing the mutation locations and key features for the TILLING lines. Information shown was gathered from SMART (Letunic and Bork, 2017) and NCBI conserved domains (Marchler-Bauer and Bryant, 2004) tools. Gene maps were created using SnapGene software.**

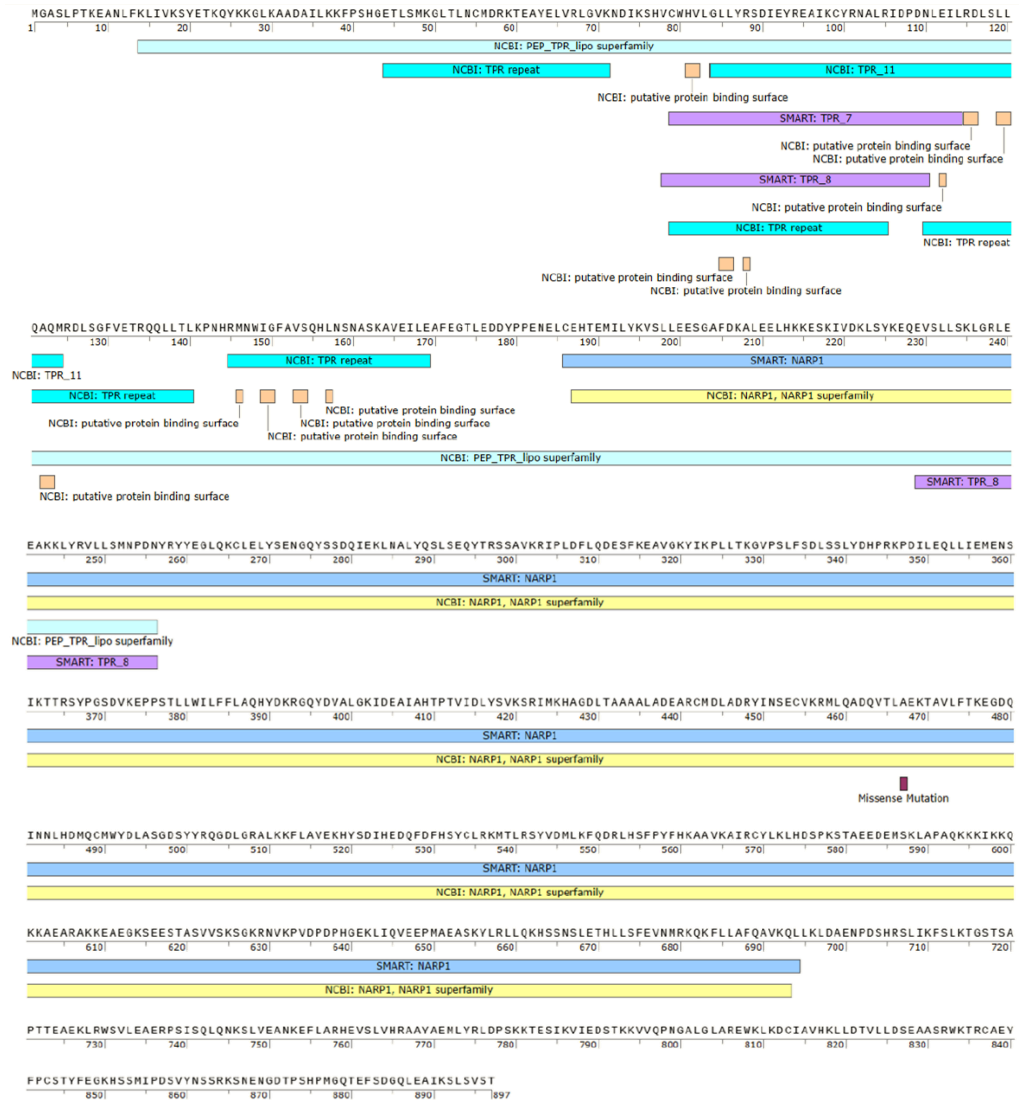


**Figure 4-22: Bra035184 gene map showing the mutation locations and key features for the TILLING lines. Information shown was gathered from SMART (Letunic and Bork, 2017) and NCBI conserved domains (Marchler-Bauer and Bryant, 2004) tools. Gene maps were created using SnapGene software.**

#### 4.4.5 Inoculation of TILLING lines

Wild-type *B. rapa*, Bra008474 (NAA15) with a homozygous missense mutation and Bra036868 (CIPK4) with a homozygous missense mutation were inoculated with *R. solani* AG2-1 in LECA particles to examine disease symptoms. Due to low humidity, several inoculated

and non-inoculated plants died before the pathogen could infect and cause symptoms. Images of successfully inoculated plants are presented in Figure 4-23. Necrosis can be seen on the roots but *cipk4* appears to be able to grow more lateral roots, and *naa15* plants have less necrosis than the WT plants.

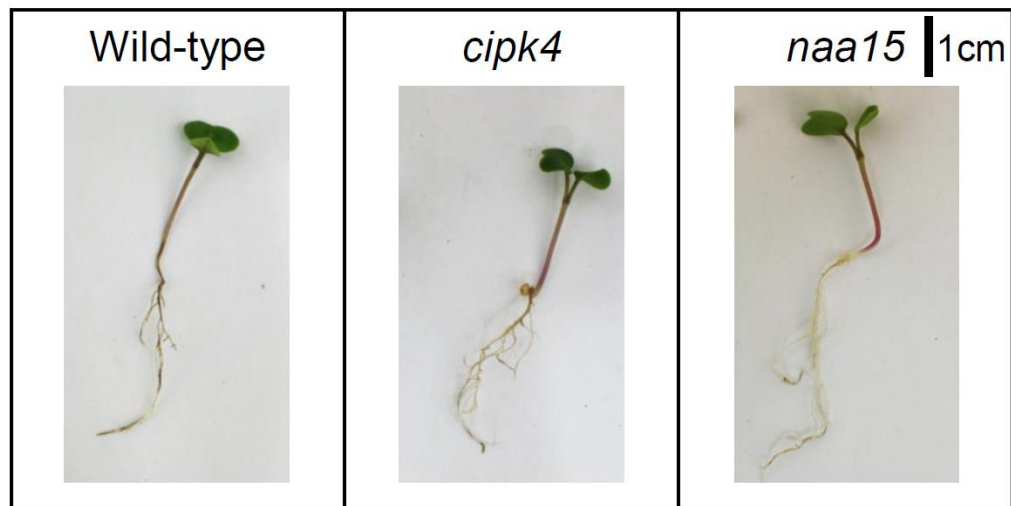


**Figure 4-23: Inoculation of *Brassica rapa* TILLING lines with *Rhizoctonia solani* AG2-1. Plants were pre-germinated then inoculated in LECA particles to enable them to be removed cleanly for photographing the root symptoms. Photographs of inoculated plants at 7dpi. Scale bar indicates 1cm.**

#### 4.5 Discussion

This work progresses understanding of candidate resistance genes to *R. solani* AG2-1 in OSR. Examination of GEMs from the GWAS has revealed several key defence genes which indicate the involvement of hormone pathways and immune responses. The characterisation of CIPK4 and NAA15 and the development of *B. rapa* TILLING lines will



enable further research to understand the role of these genes in responses to *R. solani* AG2-1.

The genes listed in Supplementary Information 36 provide insights into the pathways and genes activated during *R. solani* infection.

Nucleotide-binding leucine-rich repeat (NLR) proteins are key for the recognition of pathogen effectors. Two TIR-type NLR genes were identified (AT1G63740 and AT3G51570), a CC-NLR gene (RPP8) and the RPW8-NLR gene, NRG1.1, which is required for the signal transduction of TIR-NLRs. Genes that are hypothesised to be involved in pathogen recognition and resistance responses are difficult to study as mutants with *R. solani*, as they are likely to be extremely susceptible to the disease.

Genes related to jasmonic acid (JA), ethylene (ET), abscisic acid (ABA) and auxin pathways were also identified. TOPLESS (TPL) and RING DOMAIN LIGASE 4 (RGLG4) are both involved in JA signalling. ETHYLENE-INSENSITIVE3-LIKE 1 (EIL1) and ETHYLENE-INSENSITIVE3 (EIN3) are both involved in responses to ethylene and IAA2 is an auxin inducible gene. The mitogen-activated protein kinase (MAPK) MPK12 was identified, and is known to negatively regulate auxin signalling by being inactivated by the MAPK phosphatase IBR5 (Lee *et al.*, 2009). MPK16 was also identified. ABA- AND OSMOTIC-STRESS-INDUCIBLE RECEPTOR-LIKE CYTOSOLIC KINASE1 (ARCK1), which negatively controls ABA and osmotic stress signal transduction and ABA OVERLY SENSITIVE MUTANT (ABO8) were

also identified. REGULATORY COMPONENTS OF ABA RECEPTOR 3 (RCAR3) is a regulatory component of an ABA receptor and interacts with ABI1 and ABI2 and stimulates ABA signalling. ALDH4 encodes ALDEHYDE DEHYDROGENASE 4, which is induced by ABA.

Time constraints meant that not every promising candidate gene could be taken forwards for further investigation. One such candidate was the receptor-like kinase (RLK) protein, FERONIA (FER), which promotes the association between BAK1 and FLS2 (Duan *et al.*, 2022), while mediating the inhibition of plant immunity by acting as a RALF-regulated scaffold (Stegmann *et al.*, 2017). FER has also been shown to phosphorylate and destabilise the JA signalling transcription factor MYC2, positively regulating plant immunity (Guo *et al.*, 2018). A negative feedback mechanism exists between FER and ABA signalling whereby FER-mediated signalling can inhibit the ABA pathway, and FER signalling is inhibited by ABI2 (Hu *et al.*, 2020). Greater resistance to powdery mildew (*Golovinomyces orontii*) was observed in *fer* mutants, but FER appears to play different roles in response to different pathogen lifestyles (Duan *et al.*, 2022). A recent integrated omics study revealed that FER regulates the expression, abundance and phosphorylation of thousands of transcripts and proteins (Wang *et al.*, 2022) so is likely to be a key regulator in plant responses. GO enrichment confirmed the upregulation of transcripts and proteins relating to JA and ABA, and downregulation for auxin (Wang *et al.*, 2022).

Two other genes from the same subfamily of kinases were also identified: HERCULES RECEPTOR KINASE (HERK1) and HERK2. These are induced by brassinosteroids (BR) and play a role in BR-mediated cell elongation (Guo *et al.*, 2009). Several receptor kinases with known links to pathogen perception were identified including RLK7, BARK1, KIN7, FLS2 and LECRK-S.2. Together with the genes discussed above, it appears that responses to *R. solani* may be linked through the BAK1 signalling hub as described by Bürger and Chory in their Figure 4C (2019) (Figure 4-24). This links the activity of BAK1 as a co-receptor for FLS2 and BRI1 with RALF and FER. RALFs inhibit root growth and induce MAPK activation. Further investigation to understand the role of this signalling hub in *OSR-R. solani* interactions is needed. Gene expression studies should be carried out to examine the role of BAK1, as well as the contribution of brassinosteroids, which has not previously been examined.

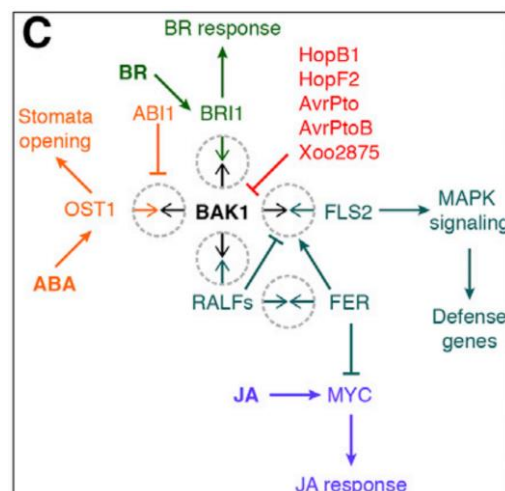


**Figure 4-24: Defence signalling hub centred on BAK1 (Figure 4C: Bürger and Chory, 2019). BAK1 integrates signals from BR, JA, ABA and peptide immune signalling pathways. Encircled arrows represent protein-protein interactions.**

The gene maps for CIPK4 showed tyrosine kinase and NAF domains. However, while Bra036868 contained both these domains, Bra036869 only contained the NAF domain and Bra036870 only contained the tyrosine kinase domain. All three *B. rapa* genes were found close together on chromosome A01. This arrangement may have arisen from a duplication event, and it may be that Bra036868 is the only functional protein as it was the only one with both domains intact. Further work using RT-qPCRs to quantify the relative expression of all three genes would help to clarify this. The gene structures of NAA15 genes Bra003565 and Bra035184 were largely the same, but Bra008474 contained an additional BRCT domain. Bra003565 and Bra035184 were found on chromosome A07 and Bra008474 was found on chromosome A02. The  $\log_{10}P$  values shown in Supplementary Information 37 were higher for GEMS associated with NAA15 on A07 compared to A02, and both hypocotyl and root disease scores were significant, rather than only root for the A02 GEM. The higher GEMS scores suggests that the genes on A07 play a greater role in responses to *R. solani* than their A02 counterparts.

CIPK and CBL proteins work together in calcium signalling. CIPK26 with CBL1 and CBL9 have been shown to interact with RBOHF, providing a direct connection between CBL-CIPK  $Ca^{2+}$  and ROS signalling (Drerup *et al.*, 2013). CBL10 and CIPK6 were identified in *Nicotiana benthamiana* and *Solanum lycopersicum* (tomato) as required for programmed cell death triggered by resistance genes and effectors (de la Torre *et al.*, 2013). CBL10 and CIPK6 contributed to ROS

generated during effector triggered immunity and were shown to interact with RBOHB (de la Torre *et al.*, 2013). The link between CBL-CIPK proteins and ROS in immunity requires further investigation. Quantification and staining (such as using DAB to visualise H<sub>2</sub>O<sub>2</sub> accumulation) of ROS, and relative expression of RBOH genes should be tested in CIPK mutants and wild-type plants to assess the contribution of ROS.

Although this work makes progress towards the characterisation of CIPK4 and NAA15 in *B. rapa*, further investigation is needed. Successful PCR amplifications could not be achieved for the two Bra003565 mutations (stop gained mutation at amino acid position 804 and missense mutation at amino acid location 1218), possibly due to the large numbers of introns in these genes. Each plant created through TILLING was predicted to have on average 10 000 mutations in total (Stephenson *et al.*, 2010) so the background mutations must be removed from the TILLING lines via several backcrossing events with the WT line. The first round of backcrossing was carried out, but extreme weather conditions meant that seeds were unable to be recovered as the plants suffered too much heat stress. The lines then need to be crossed with each other to generate triple mutants and ensure that all copies of the respective genes are knocked out. During this process, RT-qPCRs should be performed to check that expression of the mutated genes is zero. Once achieved, inoculation experiments can be carried out similarly to those described here. Initial phenotyping suggested that CIPK4 plants may be able to develop more complex root

structures, and NAA15 may be able to resist necrotic lesions better than the wildtype plants, but this requires more in-depth investigation using the backcrossed triple mutants.

It is hoped that further investigation into the genes described here will provide genetic markers that can be used in OSR breeding to develop *R. solani* resistant varieties. These are greatly needed as resistance has not been identified previously, and losses from *R. solani* are likely to increase due to changing soil management approaches and the lack of approved chemical seed treatments. The development of resources in *B. rapa* is particularly useful as studies using *A. thaliana*, while useful, cannot fully explore the host-pathogen relationship, and cannot be tested in field environments. Additionally, the exploration of genes involved in tolerance may provide useful markers as traits such as vigour and quicker establishment also help to minimise the impact of damping-off disease.

## General discussion

This PhD aimed to investigate *Rhizoctonia solani* AG2-1 interactions with *Brassica napus* and *Arabidopsis thaliana*, which was divided into three objectives. It has been shown here that not all OSR varieties respond in the same way to *R. solani*. Auxin, ABA signalling and the MYC2 branch of JA signalling were linked to susceptibility, while RBOHD, ET signalling and the ERF branch of JA signalling were linked to increased tolerance. This was supported by gene expression data from OSR varieties, *A. thaliana* mutants and microscopy in chapter 2. Analysis of GEMs from a recent GWAS also supported the involvement of JA, ET, ABA, and auxin in OSR responses in chapter 4. The genes identified through the GWAS prompted a link to the BAK1 signalling hub. Further study on the role of this hub is required to understand its involvement in *R. solani* resistance responses.

Examination of *R. solani* AG2-1 broth cultures showed the production of both IAA and PAA auxins. In chapter 3 it was demonstrated that *R. solani* AG2-1 affects the root architecture of *A. thaliana* auxin mutants prior to colonisation and it was hypothesised that this may be due to the release of auxins. Further experiments are needed to confirm this, but it prompts several pertinent questions. Is *R. solani* releasing auxin to act as a toxin to the plants, as it has been shown that high quantities of auxin inhibited plant growth? Or is it using it to manipulate the plant, either to increase plant biomass prior to colonisation, as auxins were shown to promote lateral root formation, or to affect defence responses

and trigger pathways which increase susceptibility rather than resistance to the pathogen? The expression of auxin related genes including AXR1, TIR1, AUX1 and IAA7 was shown to be increased to a greater degree in the most susceptible OSR variety Anastasia under inoculation and the *A. thaliana* auxin mutants (*aux1*, *axr1* and *tir1*) showed greater tolerance under inoculation compared to wild-type plants in chapter 2. IAA2<sub>pro</sub>:GUS lines also showed increased auxin activity under *R. solani* inoculation. Characterisation of the root architecture of auxin mutants under inoculation showed that *R. solani* inhibited root growth for WT plants, while *aux1* plants grew roots of comparable length with or without inoculation only at the furthest distance from the pathogen. It was also observed that the presence of *R. solani* increased gravitropism for WT roots, but gravitropism decreased at the furthest distance from the pathogen for *aux1* roots. *axr1* plants showed fewer changes under inoculation, suggesting that *R. solani* was able to affect the transport mutant more than the signalling mutant. Characterisation of the root architecture of *A. thaliana* auxin mutants agreed with previous research using 2,4-D and NAA but has provided new insights for PAA. PAA restored gravitropism, increased lateral root number, and inhibited root growth in *aux1* plants, while *axr1* plants were resistant. Experiments using the *R. solani* broth cultures will help to elucidate the effects of compounds being released by *R. solani* and identify any differences in varietal responses to these compounds. It will be important to quantify the production of auxins within an *R. solani*-OSR interaction, as currently this so far has only



been measured using broth cultures, which are likely to be different from interactions with the plant host. Further investigations with different *R. solani* isolates will also be useful due to the diversity within AG2-1. Additionally, the treatment of plants with auxins and auxin transport inhibitors prior to inoculation has been shown to affect the resistance of plants to diseases, but this has not yet been investigated with *R. solani*. Understanding the role that PAA plays in plant defence is vital to understanding the relationship between plants and pathogens that produce PAA and requires further investigation.

Work on *B. rapa* TILLING resources was commenced in chapter 4 for two candidate genes, but these still need to be backcrossed with the WT line to remove unwanted mutations and then crossed together to form triple mutants. The resulting lines can then be investigated for their levels of resistance or tolerance to *R. solani* AG2-1. Other genes from the GWAS could also be investigated using TILLING lines and will provide insights into *R. solani* resistance and tolerance mechanisms. It is vital to investigate these genes in *B. rapa* as they can provide greater elucidation in OSR-*R. solani* interactions than *A. thaliana*.

*R. solani* disease research is crucial for the future of farming due to its nature as a long-lived soil-borne pathogen. It is likely to be causing greater yield and establishment losses than is generally appreciated, and sustainable farming approaches such as reduced tillage may increase inoculum levels in the soil. This means that understanding defence responses and the identification of resistance or tolerance is

critical to ensuring OSR yields into the future. Work presented here helps lay the foundations for further work exploring these host-pathogen interactions and provide the initial analysis of a GWAS which can lead to the identification of genetic markers for use in breeding.

## Bibliography

Adie, B. A. T. *et al.* (2007) 'ABA is an essential signal for plant resistance to pathogens affecting JA biosynthesis and the activation of defenses in Arabidopsis', *Plant Cell*, 19(5), pp. 1665–1681. doi: 10.1105/tpc.106.048041.

Aggeli, F. *et al.* (2020) 'Novel biocontrol agents against *Rhizoctonia solani* and *Sclerotinia sclerotiorum* in lettuce', *BioControl*. Springer Netherlands, 65(6), pp. 763–773. doi: 10.1007/s10526-020-10043-w.

Agrios, G. N. (2005) *Plant pathology*. 5th ed. Burlington, MA Burlington, Mass. ; London: Burlington, MA : Elsevier Academic Press.

AHDB (2022) *Recommended Lists for Cereals and Oilseeds*. Available at: <https://ahdb.org.uk/knowledge-library/recommended-lists-for-cereals-and-oilseeds-rl>.

Ajayi-Oyetunde, O. O. and Bradley, C. A. (2018) 'Rhizoctonia solani: taxonomy, population biology and management of rhizoctonia seedling disease of soybean', *Plant Pathology*, 67(1), pp. 3–17. doi: 10.1111/ppa.12733.

Ajayi-Oyetunde, O. O., Butts-Wilmsmeyer, C. J. and Bradley, C. A. (2017) 'Sensitivity of *Rhizoctonia solani* to succinate dehydrogenase inhibitor and demethylation inhibitor fungicides', *Plant Disease*, 101(3), pp. 487–495. doi: 10.1094/PDIS-07-16-1015-RE.

Ajigboye, O. O. *et al.* (2021) 'The role of photoprotection in defence of two wheat genotypes against *Zymoseptoria tritici*', *Plant Pathology*, 70(6), pp. 1421–1435. doi: 10.1111/ppa.13392.

Aleman, F. *et al.* (2016) 'An ABA-increased interaction of the PYL6 ABA receptor with MYC2 Transcription Factor: A putative link of ABA and JA

signaling', *Scientific Reports*. Nature Publishing Group, 6(June), pp. 1–7. doi: 10.1038/srep28941.

Almeida, F. B. D. R. *et al.* (2007) 'Mycoparasitism studies of *Trichoderma harzianum* strains against *Rhizoctonia solani*: Evaluation of coiling and hydrolytic enzyme production', *Biotechnology Letters*, 29(8), pp. 1189–1193. doi: 10.1007/s10529-007-9372-z.

Anderson, J. P. *et al.* (2016) 'Proteomic analysis of *Rhizoctonia solani* identifies infection-specific, redox associated proteins and insight into adaptation to different plant hosts', *Molecular and Cellular Proteomics*, 15(4), pp. 1188–1203. doi: 10.1074/mcp.M115.054502.

Aoki, H., Sassa, T. and Tamura, T. (1963) 'Phytotoxic Metabolites of *Rhizoctonia solani*', *Nature*, (200), p. 575.

Araujo, R. *et al.* (2019) 'Decoding wheat endosphere–rhizosphere microbiomes in *Rhizoctonia solani*–infested soils challenged by *Streptomyces* biocontrol agents', *Frontiers in Plant Science*, 10(August). doi: 10.3389/fpls.2019.01038.

Armentrout, V. N. (1987) 'Infection Cushion Development by *Rhizoctonia solani* on Cotton', *Phytopathology*, p. 619. doi: 10.1094/phyto-77-619.

Atanasova, L. *et al.* (2013) 'Comparative transcriptomics reveals different strategies of *Trichoderma* mycoparasitism', *BMC Genomics*, 14(1). doi: 10.1186/1471-2164-14-121.

Babiker, E. M. *et al.* (2013) 'Evaluation of Brassica species for resistance to *Rhizoctonia solani* and binucleate *Rhizoctonia* (*Ceratobasidium* spp.) under controlled environment conditions', *European Journal of Plant Pathology*, 136(4), pp. 763–772. doi: 10.1007/s10658-013-0205-8.

Backer, R., Naidoo, S. and van den Berg, N. (2019) 'The NONEXPRESSOR OF PATHOGENESIS-RELATED GENES 1 (NPR1) and Related Family: Mechanistic Insights in Plant Disease Resistance', *Frontiers in Plant Science*, 10(February), pp. 1–21. doi: 10.3389/fpls.2019.00102.

Barkawi, L. S. *et al.* (2010) 'A high-throughput method for the quantitative analysis of auxins', *Nature Protocols*. Nature Publishing Group, 5(10), pp. 1609–1618. doi: 10.1038/nprot.2010.118.

Barnett, S. J., Roget, D. K. and Ryder, M. H. (2006) 'Suppression of *Rhizoctonia solani* AG-8 induced disease on wheat by the interaction between *Pantoea*, *Exiguobacterium*, and *Microbacteria*', *Australian Journal of Soil Research*, 44(4), pp. 331–342. doi: 10.1071/SR05113.

Bartz, F. E. *et al.* (2012) 'Elucidating the role of the phenylacetic acid metabolic complex in the pathogenic activity of *Rhizoctonia solani* anastomosis group 3', *Mycologia*, 104(4), pp. 793–803. doi: 10.3852/11-084.

Benhamou, N. and Chet, I. (1993) 'Hyphal interactions between *Trichoderma harzianum* and *Rhizoctonia solani*: Ultrastructure and gold cytochemistry of the mycoparasitic process', *Phytopathology*, pp. 1062–1071. doi: 10.1094/Phyto-83-1062.

Bennett, M. J. *et al.* (1996) 'Arabidopsis AUX1 gene: A permease-like regulator of root gravitropism', *Science*, 273(5277), pp. 948–950. doi: 10.1126/science.273.5277.948.

Berrocal-Lobo, M. and Molina, A. (2004) 'Ethylene Response Factor 1 Mediates Arabidopsis Resistance to the Soilborne Fungus *Fusarium oxysporum*', *Molecular Plant-Microbe Interactions*, 17(7), pp. 763–770. doi: 10.1094/mpmi.2004.17.7.763.

Berrocal-Lobo, M., Molina, A. and Solano, R. (2002) 'Constitutive

expression of Ethylene-Response-Factor1 in arabidopsis confers resistance to several necrotrophic fungi', *Plant Journal*, 29(1), pp. 23–32. doi: 10.1046/j.1365-313x.2002.01191.x.

Berry, P. *et al.* (2018) 'Oilseed rape guide', *AHDB Cereals & Oilseed*, (January), p. 32.

Broders, K. D. *et al.* (2014) 'Phylogenetic diversity of *Rhizoctonia solani* associated with canola and wheat in Alberta, Manitoba, and Saskatchewan', *Plant Disease*, 98(12), pp. 1695–1701. doi: 10.1094/PDIS-02-14-0146-RE.

Brown, M. *et al.* (2020) 'Population dynamics of *Rhizoctonia*, *Oculimacula*, and *Microdochium* species in soil, roots, and stems of English wheat crops', *Plant Pathology*, 70(November), pp. 862–874. doi: 10.1111/ppa.13329.

Bürger, M. and Chory, J. (2019) 'Stressed Out About Hormones: How Plants Orchestrate Immunity', *Cell Host and Microbe*, 26(2), pp. 163–172. doi: 10.1016/j.chom.2019.07.006.

Carling, D. E., Kuninaga, S. and Brainard, K. A. (2002) 'Hyphal anastomosis reactions, rDNA-internal transcribed spacer sequences, and virulence levels among subsets of *Rhizoctonia solani* anastomosis group-2 (AG-2) and AG-B1', *Phytopathology*, 92(1), pp. 43–50. doi: 10.1094/PHYTO.2002.92.1.43.

Castillo, M. C. *et al.* (2004) 'Gene-specific involvement of  $\beta$ -oxidation in wound-activated responses in *Arabidopsis*', *Plant Physiology*, 135(1), pp. 85–94. doi: 10.1104/pp.104.039925.

Chapelle, E. *et al.* (2016) 'Fungal invasion of the rhizosphere microbiome', *ISME Journal*. Nature Publishing Group, 10(1), pp. 265–268. doi: 10.1038/ismej.2015.82.

Chapman, J. M. *et al.* (2019) 'RBOH-Dependent ROS Synthesis and ROS Scavenging by Plant Specialized Metabolites to Modulate Plant Development and Stress Responses', *Chemical Research in Toxicology*, pp. 370–396. doi: 10.1021/acs.chemrestox.9b00028.

Chen, L. *et al.* (2016) 'Induced maize salt tolerance by rhizosphere inoculation of *Bacillus amyloliquefaciens* SQR9', *Physiologia plantarum*, 158(1), pp. 34–44. doi: 10.1111/ppl.12441.

Chen, Q. *et al.* (2011) 'The Basic Helix-Loop-Helix Transcription Factor MYC2 Directly Represses PLETHORA Expression during Jasmonate-Mediated Modulation of the Root Stem Cell Niche in Arabidopsis', *The Plant Cell*, 23, pp. 3335–3352.

Chowdhury, S. P. *et al.* (2013) 'Effects of *Bacillus amyloliquefaciens* FZB42 on Lettuce Growth and Health under Pathogen Pressure and Its Impact on the Rhizosphere Bacterial Community', *PLoS ONE*, 8(7), pp. 1–10. doi: 10.1371/journal.pone.0068818.

Commission Implementing Regulation (EU) 2017/2091 (2017) 'Concerning the non-renewal of approval of the active substance iprodione', *Official Journal of the European Union*, 297(25), pp. 1–3. doi: 10.2903/j.efsa.2016.4609.L.

Commission Implementing Regulation (EU) 2018/1500 (2018) 'Concerning the non-renewal of approval of the active substance thiram, and prohibiting the use and sale of seeds treated with plant protection products containing thiram', *Official Journal of the European Union*, 254(1), pp. 1–3.

Commission Implementing Regulation (EU) 2020/617 (2020) 'Renewing the approval of the active substance metalaxyl-M, and restricting the use of seeds treated with plant protection products containing it', *Official Journal of the European Union*, 143(6), pp. 1–5. doi:

10.2903/j.efsa.2018.5311.

Cook, S. D. (2019) 'An Historical Review of Phenylacetic Acid', *Plant and Cell Physiology*, 60(2), pp. 243–254. doi: 10.1093/pcp/pcz004.

Cordovez, V. *et al.* (2017) 'Plant phenotypic and transcriptional changes induced by volatiles from the fungal root pathogen *Rhizoctonia solani*', *Frontiers in Plant Science*, 8(July), pp. 1–14. doi: 10.3389/fpls.2017.01262.

Cubeta, M. A. *et al.* (2014) 'Draft genome sequence of the plant-pathogenic soil fungus *Rhizoctonia solani* anastomosis group 3 strain Rhs1AP', *Genome Announcements*, 2(5), p. 2014. doi: 10.1128/genomeA.01072-14.

Dahiya, J. S. and Woods, D. L. (1987) 'Control of *Rhizoctonia solani*, causal agent of brown girdling root rot of canola/rapeseed by *Pseudomonas fluorescens*', *Canadian Journal of Plant Pathology*, 9, pp. 275–276.

Davey, R. S. *et al.* (2021) 'Potential for suppression of *Rhizoctonia* root rot is influenced by nutrient (N and P) and carbon inputs in a highly calcareous coarse-textured topsoil', *Soil Research*, (C). doi: 10.1071/SR20247.

Dempsey, D. A. *et al.* (2011) 'Salicylic Acid Biosynthesis and Metabolism', *The Arabidopsis Book*, 9, p. e0156. doi: 10.1199/tab.0156.

Denancé, N. *et al.* (2013) 'Disease resistance or growth: the role of plant hormones in balancing immune responses and fitness costs', *Frontiers in Plant Science*, 4(May), pp. 1–12. doi: 10.3389/fpls.2013.00155.

Department for Environment Food & Rural Affairs (2022) *Sustainable Farming Incentive pilot guidance*, *Future Farming Blog*. Available at:



<https://defraframing.blog.gov.uk/sustainable-farming-incentive-pilot-guidance/>.

Department for Environment Food and Rural Affairs (2022) *Cereal and oilseed rape production, National Statistics*. Available at: <https://www.gov.uk/government/statistics/cereal-and-oilseed-rape-production>.

Depotter, J. R. L. *et al.* (2016) 'Verticillium longisporum, the invisible threat to oilseed rape and other brassicaceous plant hosts', *Molecular plant pathology*, 17(7), pp. 1004–1016. doi: 10.1111/mpp.12350.

Derbyshire, M. C. and Denton-Giles, M. (2016) 'The control of sclerotinia stem rot on oilseed rape (*Brassica napus*): current practices and future opportunities', *Plant Pathology*, 65(6), pp. 859–877. doi: 10.1111/ppa.12517.

Dewage, C. S. K. *et al.* (2018) 'Host-pathogen interactions in relation to management of light leaf spot disease (caused by *Pyrenopeziza brassicae*) on *Brassica* species', *Crop and Pasture Science*, 69(1), pp. 9–19. doi: 10.1071/CP16445.

Dharmasiri, N. *et al.* (2007) 'AXL and AXR1 have redundant functions in RUB conjugation and growth and development in *Arabidopsis*', *Plant Journal*, 52(1), pp. 114–123. doi: 10.1111/j.1365-313X.2007.03211.x.

Ding, P. and Ding, Y. (2020) 'Stories of Salicylic Acid: A Plant Defense Hormone', *Trends in Plant Science*. Elsevier Ltd, 25(6), pp. 549–565. doi: 10.1016/j.tplants.2020.01.004.

Donn, S. *et al.* (2014) 'Rhizosphere microbial communities associated with *Rhizoctonia* damage at the field and disease patch scale', *Applied Soil Ecology*. Elsevier B.V., 78, pp. 37–47. doi: 10.1016/j.apsoil.2014.02.001.

Dörffling, K. *et al.* (1984) 'Abscisic Acid in Phytopathogenic Fungi of the Genera *Botrytis*, *Ceratocystis*, *Fusarium*, and *Rhizoctonia*', *Z. Naturforsch.*, 39c, pp. 683–684.

Drerup, M. M. *et al.* (2013) 'The calcineurin B-like calcium sensors CBL1 and CBL9 together with their interacting protein kinase CIPK26 regulate the arabidopsis NADPH oxidase RBOHF', *Molecular Plant*, 6(2), pp. 559–569. doi: 10.1093/mp/sst009.

Drizou, F. *et al.* (2017) 'Development of high-throughput methods to screen disease caused by *Rhizoctonia solani* AG 2-1 in oilseed rape', *Plant Methods*. BioMed Central, 13(1), pp. 1–14. doi: 10.1186/s13007-017-0195-1.

Duan, Z. *et al.* (2022) 'Regulation of immune complex formation and signalling by FERONIA, a busy goddess in plant–microbe interactions', *Molecular Plant Pathology*, (June), pp. 1695–1700. doi: 10.1111/mpp.13256.

Dutton, M. V. and Evans, C. S. (1996) 'Oxalate production by fungi: Its role in pathogenicity and ecology in the soil environment', *Canadian Journal of Microbiology*, 42(9), pp. 881–895. doi: 10.1139/m96-114.

Erlacher, A. *et al.* (2014) 'The impact of the pathogen *Rhizoctonia solani* and its beneficial counterpart *Bacillus amyloliquefaciens* on the indigenous lettuce microbiome', *Frontiers in Microbiology*, 5(APR), pp. 1–8. doi: 10.3389/fmicb.2014.00175.

Eyal, J. *et al.* (1997) 'Large-scale production of chlamydozoospores of *Gliocladium virens* strain GL-21 in submerged culture', *Journal of Industrial Microbiology and Biotechnology*, 19(3), pp. 163–168. doi: 10.1038/sj.jim.2900430.

Feng, J. *et al.* (2016) 'Protein N-terminal acetylation is required for embryogenesis in *Arabidopsis*', *Journal of Experimental Botany*, 67(15),

pp. 4779–4789. doi: 10.1093/jxb/erw257.

Fikere, M. *et al.* (2020) 'Meta-analysis of GWAS in canola blackleg (*Leptosphaeria maculans*) disease traits demonstrates increased power from imputed whole-genome sequence', *Scientific Reports*. Nature Publishing Group UK, 10(1), pp. 1–15. doi: 10.1038/s41598-020-71274-6.

Fitt, B. D. L. *et al.* (2006) 'World-wide importance of phoma stem canker (*Leptosphaeria maculans* and *L. biglobosa*) on oilseed Rape (*Brassica napus*)', *European Journal of Plant Pathology*, 114(1), pp. 3–15. doi: 10.1007/s10658-005-2233-5.

Flor, H. H. (1971) 'Current status of the gene-for-gene concept', *Annual Review of Phytopathology*, 9, pp. 275–296. doi: doi.org/10.1146/annurev.py.09.090171.001423.

Foley, R. C. *et al.* (2013) 'Genetic and Genomic Analysis of *Rhizoctonia solani* Interactions with *Arabidopsis*; Evidence of Resistance Mediated through NADPH Oxidases', *PLoS ONE*, 8(2). doi: 10.1371/journal.pone.0056814.

Foley, R. C. *et al.* (2016) 'Reactive oxygen species play a role in the infection of the necrotrophic fungi, *Rhizoctonia solani* in wheat', *PLoS ONE*, 11(3), pp. 1–16. doi: 10.1371/journal.pone.0152548.

Food and Agriculture Organisation of the United Nations (2022) *FAOSTAT*. Available at: <https://www.fao.org/faostat/en/#data>.

Fu, S.-F. *et al.* (2015) 'Indole-3-acetic acid: A widespread physiological code in interactions of fungi with other organisms', *Plant Signaling and Behavior*, 10(8). doi: <http://dx.doi.org/10.1080/15592324.2015.1048052>.

Gill, J. S., Sivasithamparam, K. and Smettem, K. R. J. (2000) 'Soil types with different textures affects development of *Rhizoctonia* root rot of

wheat seedlings', *Plant and Soil*, 221, pp. 113–120. doi: 10.1023/A:1010394119522.

Gill, J. S., Sivasithamparam, K. and Smettem, K. R. J. (2001) 'Influence of depth of soil disturbance on root growth dynamics of wheat seedlings associated with *Rhizoctonia solani* AG-8 disease severity in sandy and loamy sand soils of Western Australia', *Soil and Tillage Research*, pp. 73–83. doi: 10.1016/S0167-1987(01)00217-3.

Gnanamanickam, S. S. *et al.* (2008) 'Taegro: A biofungicide with broad spectrum of activity towards soilborne or foliar fungal and bacterial pathogens', in *APS Centennial Meeting*, p. 98:S60. Available at: [https://www.apsnet.org/meetings/Documents/2008\\_Meeting\\_Abstracts/a08ma287.htm](https://www.apsnet.org/meetings/Documents/2008_Meeting_Abstracts/a08ma287.htm).

Goll, M. B. *et al.* (2014) 'Survey on the prevalence of *Rhizoctonia* spp. in European soils and determination of the baseline sensitivity towards sedaxane', *Plant Pathology*, 63(1), pp. 148–154. doi: 10.1111/ppa.12063.

Gugel, R. K., Verma, P. R. and Kaminski, D. A. (1986) 'Protection of canola seedlings from *Rhizoctonia solani* infection by a nonpathogenic, binucleate *Rhizoctonia*-like isolate', *Canadian Journal of Plant Pathology*, 8, p. 349.

Guo, H. *et al.* (2009) 'Three related receptor-like kinases are required for optimal cell elongation in *Arabidopsis thaliana*', *Proceedings of the National Academy of Sciences of the United States of America*, 106(18), pp. 7648–7653. doi: 10.1073/pnas.0812346106.

Guo, H. *et al.* (2018) 'FERONIA Receptor Kinase Contributes to Plant Immunity by Suppressing Jasmonic Acid Signaling in *Arabidopsis thaliana*', *Current Biology*. Elsevier Ltd., 28(20), pp. 3316-3324.e6. doi: 10.1016/j.cub.2018.07.078.

Hane, J. K. *et al.* (2014) 'Genome Sequencing and Comparative Genomics of the Broad Host-Range Pathogen *Rhizoctonia solani* AG8', 10(5), pp. 11–12. doi: 10.1371/journal.pgen.1004281.

Hannukkala, A. O. *et al.* (2016) 'Rhizoctonia solani injuries in oilseed crops in Finland and impacts of different crop management practices on disease incidence and severity', *Annals of Applied Biology*, 169(2), pp. 257–273. doi: 10.1111/aab.12293.

Harper, A. L. *et al.* (2012) 'Associative transcriptomics of traits in the polyploid crop species *Brassica napus*', *Nature Biotechnology*. Nature Publishing Group, 30(8), pp. 798–802. doi: 10.1038/nbt.2302.

Harries, E. *et al.* (2020) 'Soil properties related to suppression of *Rhizoctonia solani* on tobacco fields from northwest Argentina', *Plant Pathology*, 69(1), pp. 77–86. doi: 10.1111/ppa.13106.

Havlickova, L. *et al.* (2018) 'Validation of an updated Associative Transcriptomics platform for the polyploid crop species *Brassica napus* by dissection of the genetic architecture of erucic acid and tocopherol isoform variation in seeds', *Plant Journal*, 93(1), pp. 181–192. doi: 10.1111/tpj.13767.

Hayden, H. L. *et al.* (2019) 'Metabolomics approaches for the discrimination of disease suppressive soils for *Rhizoctonia solani* AG8 in cereal crops using 1H NMR and LC-MS', *Science of the Total Environment*. Elsevier B.V., 651, pp. 1627–1638. doi: 10.1016/j.scitotenv.2018.09.249.

Hejna, O. *et al.* (2019) 'Analysing the genetic architecture of clubroot resistance variation in *Brassica napus* by associative transcriptomics', *Molecular Breeding*, 39(8). doi: 10.1007/s11032-019-1021-4.

Henikoff, S. *et al.* (2004) 'Perspectives on Translational Biology TILLING . Traditional Mutagenesis Meets Functional Genomics',

*Cancer Research*, 135(June), pp. 630–636. doi:  
10.1104/pp.104.041061.630.

Howe, K. L. *et al.* (2021) 'Ensembl 2021', *Nucleic Acids Research*,  
49(D1), pp. D884–D891. doi: 10.1093/nar/gkaa942.

Howell, C. R. *et al.* (2000) 'Induction of Terpenoid Synthesis in Cotton  
Roots and Control of *Rhizoctonia solani* by Seed Treatment with  
*Trichoderma virens*', *Phytopathology*, 90(3), pp. 248–252.

Hu, C. H. *et al.* (2020) 'NADPH Oxidases: The Vital Performers and  
Center Hubs during Plant Growth and Signaling', *Cells*, 9(2), pp. 1–41.  
doi: 10.3390/cells9020437.

Huala, E. *et al.* (2001) 'The Arabidopsis Information Resource (TAIR): A  
comprehensive database and web-based information retrieval, analysis,  
and visualization system for a model plant', *Nucleic Acids Research*,  
29(1), pp. 102–105. doi: 10.1093/nar/29.1.102.

Hwang, S. F. *et al.* (2014) 'The effect of seed size, seed treatment,  
seeding date and depth on *Rhizoctonia* seedling blight of canola',  
*Canadian Journal of Plant Science*, 94(2), pp. 311–321. doi:  
10.4141/CJPS2013-294.

Iacobellis, N. S. and DeVay, J. E. (1987) 'Studies on pathogenesis of  
*Rhizoctonia solani* in beans: an evaluation of the possible roles of  
phenylacetic acid and its hydroxy derivatives as phytotoxins',  
*Physiological and Molecular Plant Pathology*, 30(3), pp. 421–432. doi:  
10.1016/0885-5765(87)90021-X.

Jayaweera, D. P. and Ray, R. V. (2022) 'Yield loss and integrated  
disease control of *Rhizoctonia solani* AG2-1 using seed treatment and  
sowing rate of oilseed rape', *Plant Disease*, pp. 1–25. doi:  
10.1094/PDIS-08-22-1817-RE.

Johnson, C. F. and Morris, D. A. (1987) 'Regulation of auxin transport in pea (*Pisum sativum* L.) by phenylacetic acid: effects on the components of transmembrane transport of indol-3yl-acetic acid', *Planta*, 172(3), pp. 400–407. doi: 10.1007/BF00398670.

Kataria, H. R. and Verma, P. R. (1992) 'Rhizoctonia solani damping-off and root rot in oilseed rape and canola', *Crop Protection*, 11(1), pp. 8–13. doi: 10.1016/0261-2194(92)90072-D.

Kazan, K. and Manners, J. M. (2009) 'Linking development to defense: auxin in plant-pathogen interactions', *Trends in Plant Science*, 14(7), pp. 373–382. doi: 10.1016/j.tplants.2009.04.005.

Kazan, K. and Manners, J. M. (2013) 'MYC2: The master in action', *Molecular Plant*. © The Authors. All rights reserved., 6(3), pp. 686–703. doi: 10.1093/mp/sss128.

Keijer, J. (1996) 'The Initial Steps of the Infection Process in *Rhizoctonia Solani*', in *Rhizoctonia Species: Taxonomy, Molecular Biology, Ecology, Pathology and Disease Control*. Dordrecht: Springer Netherlands, pp. 149–162. doi: 10.1007/978-94-017-2901-7\_13.

Khangura, R. K., Barbetti, M. J. and Sweetingham, M. W. (1999) 'Characterization and Pathogenicity of *Rhizoctonia* Species on Canola', *Plant Disease*, 83(8), pp. 714–721. doi: 10.1094/pdis.1999.83.8.714.

Kidd, B. N. *et al.* (2011) 'Auxin Signaling and Transport Promote Susceptibility to the Root-Infecting Fungal Pathogen *Fusarium oxysporum* in *Arabidopsis*', 24(6), pp. 733–748.

Kidd, B. N. *et al.* (2021) 'Foliar resistance to *Rhizoctonia solani* in *Arabidopsis* is compromised by simultaneous loss of ethylene, jasmonate and PEN2 mediated defense pathways', *Scientific Reports*. Nature Publishing Group UK, 11(1), pp. 1–14. doi: 10.1038/s41598-021-81858-5.

Klein-Gebbinck, H. W. and Woods, D. L. (2002) 'Yield loss assessment in canola: Effects of brown girdling root rot and maggot damage on single plant yield', *Plant Disease*, 86(9), pp. 1005–1010. doi: 10.1094/PDIS.2002.86.9.1005.

Knecht, K. *et al.* (2010) ' Expression of BvGLP-1 Encoding a Germin-Like Protein from Sugar Beet in *Arabidopsis thaliana* Leads to Resistance Against Phytopathogenic Fungi ', *Molecular Plant-Microbe Interactions*, 23(4), pp. 446–457. doi: 10.1094/mpmi-23-4-0446.

Knepper, C., Savory, E. A. and Day, B. (2011) 'The role of NDR1 in pathogen perception and plant defense signaling', *Plant Signaling and Behavior*, 6(8), pp. 1114–1116. doi: 10.4161/psb.6.8.15843.

Koh, J. C. O. *et al.* (2017) 'A multiplex PCR for rapid identification of Brassica species in the triangle of U', *Plant Methods*. BioMed Central, 13(1), pp. 1–8. doi: 10.1186/s13007-017-0200-8.

Kumar, S. *et al.* (2020) 'Purinoreceptor P2K1/DORN1 Enhances Plant Resistance Against a Soilborne Fungal Pathogen, *Rhizoctonia solani*', *Frontiers in Plant Science*, 11(September), pp. 1–10. doi: 10.3389/fpls.2020.572920.

de la Torre, F. *et al.* (2013) 'The tomato calcium sensor Cbl10 and its interacting protein kinase cipk6 define a signaling pathway in plant immunity', *Plant Cell*, 25(7), pp. 2748–2764. doi: 10.1105/tpc.113.113530.

Lagerlof, J. *et al.* (2011) 'Interaction between a fungal disease, fungivorous nematodes and compost suppressiveness', *Acta Agriculturae Scandinavica, Section B — Soil & Plant Science*, 61(4), pp. 372–377.

Lakshman, D. K. *et al.* (2006) 'Characterization of the *arom* gene in *Rhizoctonia solani*, and transcription patterns under stable and induced



hypovirulence conditions', *Current Genetics*, 49(3), pp. 166–177. doi: 10.1007/s00294-005-0005-6.

Lamichhane, J. R. *et al.* (2017) 'Integrated management of damping-off diseases. A review', *Agronomy for Sustainable Development*. *Agronomy for Sustainable Development*, 37(2). doi: 10.1007/s13593-017-0417-y.

Lamprecht, S. C. *et al.* (2011) 'Evaluation of strategies for the control of canola and lupin seedling diseases caused by *Rhizoctonia* anastomosis groups', *European Journal of Plant Pathology*, 130(3), pp. 427–439. doi: 10.1007/s10658-011-9764-8.

Larrieu, A. *et al.* (2015) 'A fluorescent hormone biosensor reveals the dynamics of jasmonate signalling in plants', *Nature Communications*, 6(May 2014), pp. 1–9. doi: 10.1038/ncomms7043.

Lee, D. H. *et al.* (2020) 'Regulation of reactive oxygen species during plant immunity through phosphorylation and ubiquitination of RBOHD', *Nature communications*. Springer US, 11(1), p. 1838. doi: 10.1038/s41467-020-15601-5.

Lee, J. S. *et al.* (2009) 'Arabidopsis mitogen-activated protein kinase MPK12 interacts with the MAPK phosphatase IBR5 and regulates auxin signaling', *Plant Journal*, 57(6), pp. 975–985. doi: 10.1111/j.1365-313X.2008.03741.x.

Lefevre, H., Bauters, L. and Gheysen, G. (2020) 'Salicylic Acid Biosynthesis in Plants', *Frontiers in Plant Science*, 11(April), pp. 1–7. doi: 10.3389/fpls.2020.00338.

Letunic, I. and Bork, P. (2017) '20 years of the SMART protein domain annotation resource', *Nucleic Acids Research*. Oxford University Press, pp. 1–4. doi: 10.1093/nar/gkx922.

Lewis, J. A. and Papavizas, G. C. (1992) 'Potential of *Laetisaria arvalis* for the biocontrol of *Rhizoctonia solani*', *Soil Biology and Biochemistry*, 24(11), pp. 1075–1079.

Leyser, H. M. O. *et al.* (1993) 'Arabidopsis auxin-resistance gene AXR1 encodes a protein related to ubiquitin-activating enzyme E1', *Nature*, 364, pp. 161–4. Available at: <https://www.nature.com/articles/364161a0.pdf>.

Liang, X. *et al.* (2015) 'Oxaloacetate acetylhydrolase gene mutants of *Sclerotinia sclerotiorum* do not accumulate oxalic acid, but do produce limited lesions on host plants', *Molecular Plant Pathology*, 16(6), pp. 559–571. doi: 10.1111/mpp.12211.

Lincoln, C., Britton, J. H. and Estelle, M. (1990) 'Growth and development of the *axr1* mutants of *arabidopsis*', *Plant Cell*, 2(11), pp. 1071–1080. doi: 10.1105/tpc.2.11.1071.

Linster, E. *et al.* (2015) 'Downregulation of N-terminal acetylation triggers ABA-mediated drought responses in *Arabidopsis*', *Nature Communications*, 6(May). doi: 10.1038/ncomms8640.

Livak, K. J. and Schmittgen, T. D. (2001) 'Analysis of relative gene expression data using real-time quantitative PCR and the  $2^{-\Delta\Delta CT}$  method', *Methods*, 25(4), pp. 402–408. doi: 10.1006/meth.2001.1262.

Llorente, F. *et al.* (2008) 'Repression of the auxin response pathway increases *Arabidopsis* susceptibility to necrotrophic fungi', *Molecular Plant*, 1(3), pp. 496–509. doi: 10.1093/mp/ssn025.

Lobet, G., Pagès, L. and Draye, X. (2011) 'A novel image-analysis toolbox enabling quantitative analysis of root system architecture', *Plant Physiology*, 157(1), pp. 29–39. doi: 10.1104/pp.111.179895.

Lorenzo, O. *et al.* (2003) 'ETHYLENE RESPONSE FACTOR1

integrates signals from Ethylene and Jasmonate pathways in plant defense', 15, pp. 165–178. doi: 10.1105/tpc.007468.signaling.

Lukan, T. and Coll, A. (2022) 'Intertwined Roles of Reactive Oxygen Species and Salicylic Acid Signaling Are Crucial for the Plant Response to Biotic Stress', *International Journal of Molecular Sciences*, 23(10). doi: 10.3390/ijms23105568.

MacNish, G. C. *et al.* (1995) 'Characterisation of Anastomosis Group-10 (AG-10) of *Rhizoctonia solani*', *Australasian Plant Pathology*, 24(4), pp. 252–260.

Mahoney, A. K. *et al.* (2016) 'Characterizing and mapping resistance in synthetic-derived wheat to *Rhizoctonia* root rot in a green bridge environment', *Phytopathology*, 106(10), pp. 1170–1176. doi: 10.1094/PHYTO-02-16-0055-FI.

Mandava, N. B. *et al.* (1980) 'Phytotoxins in *Rhizoctonia Solani*: Isolation and Biological Activity of m-Hydroxy-and m-Methoxyphenylacetic Acids', *Journal of Agricultural and Food Chemistry*, 28(1), pp. 71–75. doi: 10.1021/jf60227a009.

Mano, Y. and Nemoto, K. (2012) 'The pathway of auxin biosynthesis in plants', *Journal of Experimental Botany*, 63(8), pp. 2853–2872. doi: 10.1093/jxb/ers091.

Mao, J. *et al.* (2016) 'Mechanisms and physiological roles of the CBL-CIPK networking system in *Arabidopsis thaliana*', *Genes*, 7(9), pp. 1–15. doi: 10.3390/genes7090062.

Marchant, A. (1999) 'AUX1 regulates root gravitropism in *Arabidopsis* by facilitating auxin uptake within root apical tissues', *The EMBO Journal*, 18(8), pp. 2066–2073. doi: 10.1093/emboj/18.8.2066.

Marchant, A. *et al.* (2002) 'AUX1 promotes lateral root formation by

facilitating indole-3-acetic acid distribution between sink and source tissues in the Arabidopsis seedling', *Plant Cell*, 14(3), pp. 589–597. doi: 10.1105/tpc.010354.

Marchler-Bauer, A. and Bryant, S. H. (2004) 'CD-Search: Protein domain annotations on the fly', *Nucleic Acids Research*, 32(WEB SERVER ISS.), pp. 327–331. doi: 10.1093/nar/gkh454.

Matsuura, K. (1986) ' Scanning Electron Microscopy of the Infection Process of *Rhizoctonia solani* in Leaf Sheaths of Rice Plants ', *Phytopathology*, p. 811. doi: 10.1094/phyto-76-811.

Melzer, M. S. *et al.* (2016) 'Characterization and pathogenicity of *Rhizoctonia* spp. from field crops in Canada', *Canadian Journal of Plant Pathology*. Taylor & Francis, 38(3), pp. 367–374. doi: 10.1080/07060661.2016.1199596.

Molla, K. A. *et al.* (2016) 'Tissue-specific expression of Arabidopsis NPR1 gene in rice for sheath blight resistance without compromising phenotypic cost', *Plant Science*. Elsevier Ireland Ltd, 250, pp. 105–114. doi: 10.1016/j.plantsci.2016.06.005.

Morris, D. A. and Johnson, C. F. (1987) 'Regulation of auxin transport in pea (*Pisum sativum* L.) by phenylacetic acid: inhibition of polar auxin transport in intact plants and stem segments', *Planta*, 172(3), pp. 408–416. doi: 10.1007/BF00398671.

Müller, M. and Munné-Bosch, S. (2011) 'Rapid and sensitive hormonal profiling of complex plant samples by liquid chromatography coupled to electrospray ionization tandem mass spectrometry', *Plant Methods*, 7(1), pp. 1–11. doi: 10.1186/1746-4811-7-37.

Nadarajah, K. *et al.* (2017) 'Draft genome sequence of *Rhizoctonia solani* anastomosis group 1 subgroup 1A strain 1802/KB isolated from rice', *Genome Announcements*, 5(43), pp. 10–11. doi:

10.1128/genomeA.01188-17.

Nguyen, N. H. *et al.* (2022) 'Priming of camalexin accumulation in induced systemic resistance by beneficial bacteria against *Botrytis cinerea* and *Pseudomonas syringae* pv. *tomato* DC3000', *Journal of Experimental Botany*, 73(11), pp. 3743–3757. doi: 10.1093/jxb/erac070.

Ogoshi, A. (1996) 'Introduction The Genus *Rhizoctonia*', in Sneh, B. *et al.* (eds) *Rhizoctonia Species: Taxonomy, Molecular Biology, Ecology, Pathology and Disease Control*. Dordrecht: Springer Netherlands, pp. 1–9. doi: 10.1007/978-94-017-2901-7\_1.

Oladzad, A. *et al.* (2019) 'Genotypes and Genomic Regions Associated With *Rhizoctonia solani* Resistance in Common Bean', *Frontiers in Plant Science*, 10(July), pp. 1–14. doi: 10.3389/fpls.2019.00956.

Otten, W. *et al.* (2001) 'Soil physics, fungal epidemiology and the spread of *Rhizoctonia solani*', *New Phytologist*, 151(2), pp. 459–468. doi: 10.1046/j.0028-646X.2001.00190.x.

Otten, W. *et al.* (2004) 'Preferential spread of the pathogenic fungus *Rhizoctonia solani* through structured soil', *Soil Biology and Biochemistry*, 36(2), pp. 203–210. doi: 10.1016/j.soilbio.2003.09.006.

Paciorek, T. and Friml, J. (2006) 'Auxin signaling', *Journal of Cell Science*, 119(7), pp. 1199–1202. doi: 10.1242/jcs.02910.

Pagán, I. and García-Arenal, F. (2018) 'Tolerance to plant pathogens: Theory and experimental evidence', *International Journal of Molecular Sciences*, 19(3). doi: 10.3390/ijms19030810.

Paulitz, T. C. (2006) 'Low input no-till cereal production in the Pacific Northwest of the U.S.: The challenges of root diseases', *European Journal of Plant Pathology*, 115(3), pp. 271–281. doi: 10.1007/s10658-006-9023-6.

Paulitz, T. C., Schroeder, K. L. and Schillinger, W. F. (2010) 'Soilborne pathogens of cereals in an irrigated cropping system: Effects of tillage, residue management, and crop rotation', *Plant Disease*, 94(1), pp. 61–68. doi: 10.1094/PDIS-94-1-0061.

Pedras, M. S. C. and Liu, J. (2004) 'Designer phytoalexins : probing camalexin detoxification pathways in the phytopathogen *Rhizoctonia solani* †', pp. 1–7.

Pedras, M. S. C., Montaut, S. and Suchy, M. (2004) 'Phytoalexins from the crucifer rutabaga: Structures, syntheses, biosyntheses, and antifungal activity', *Journal of Organic Chemistry*, 69(13), pp. 4471–4476. doi: 10.1021/jo049648a.

Pedras, M. S. C., Zheng, Q. and Sarma-Mamillapalle, V. K. (2007) 'The Phytoalexins from Brassicaceae: Structure, Biological Activity, Synthesis and Biosynthesis', *Natural Product Communications*, 2(3), pp. 319–330.

Ploetz, R. C. and Mitchell, D. J. (1985) 'Influence of water potential on the survival and saprophytic activity of *Rhizoctonia solani* AG4 in natural soil', *Canadian Journal of Botany*, 63(12), pp. 2364–2368.

Poromarto, S. H., Nelson, B. D. and Freeman, T. P. (1998) 'Association of binucleate *Rhizoctonia* with soybean and mechanism of biocontrol of *Rhizoctonia solani*', *Phytopathology*, 88(10), pp. 1056–1067. doi: 10.1094/PHYTO.1998.88.10.1056.

Qiu, M. *et al.* (2014) 'Comparative proteomics analysis of *Bacillus amyloliquefaciens* SQR9 revealed the key proteins involved in in situ root colonization', *Journal of Proteome Research*, 13(12), pp. 5581–5591. doi: 10.1021/pr500565m.

Raman, H. *et al.* (2020) 'Genome-Wide Association Mapping Identifies Novel Loci for Quantitative Resistance to Blackleg Disease in Canola',

*Frontiers in Plant Science*, 11(August). doi: 10.3389/fpls.2020.01184.

Ray, R. *et al.* (2020) *Project Report No. 616 Integrating Control strategies Against soilborne Rhizoctonia solani in OilSeed rape (ICAROS)*.

Redkar, A., Jaeger, E. and Doehlemann, G. (2018) 'Visualization of Growth and Morphology of Fungal Hyphae in planta Using WGA-AF488 and Propidium Iodide Co-staining', *Bio-Protocol*, 8(14), pp. 1–7. doi: 10.21769/bioprotoc.2942.

Ritchie, F., Bain, R. and Mcquilken, M. (2013) 'Survival of Sclerotia of *Rhizoctonia solani* AG3PT and Effect of Soil-Borne Inoculum Density on Disease Development on Potato', *Journal of Phytopathology*, 161(3), pp. 180–189. doi: 10.1111/jph.12052.

Sagi, M. and Fluhr, R. (2006) 'Production of Reactive Oxygen Species by Plant NADPH Oxidases', *Plant Physiology*, 141(June), pp. 336–340. doi: 10.1104/pp.106.078089.336.

Saini, S. *et al.* (2013) 'Auxin: A master regulator in plant root development', *Plant Cell Reports*, 32(6), pp. 741–757. doi: 10.1007/s00299-013-1430-5.

van Schie, C. C. N. and Takken, F. L. W. (2014) 'Susceptibility Genes 101: How to Be a Good Host', *Annual Review of Phytopathology*, 52(1), pp. 551–581. doi: 10.1146/annurev-phyto-102313-045854.

Schillinger, W. F. and Paulitz, T. C. (2006) 'Reduction of *Rhizoctonia* bare patch in wheat with barley rotations', *Plant Disease*, 90(3), pp. 302–306. doi: 10.1094/PD-90-0302.

Schlatter, D. *et al.* (2017) 'Disease suppressive soils: New insights from the soil microbiome', *Phytopathology*, 107(11), pp. 1284–1297. doi: 10.1094/PHYTO-03-17-0111-RVW.

Schneider, C. A., Rasband, W. S. and Eliceiri, K. W. (2012) 'NIH Image to ImageJ: 25 years of Image Analysis', *Nat Methods*, 9(7), pp. 671–675. doi: 10.1007/978-1-84882-087-6\_9.

Schuhegger, R. *et al.* (2006) 'CYP71B15 (PAD3) catalyzes the final step in camalexin biosynthesis', *Plant Physiology*, 141(4), pp. 1248–1254. doi: 10.1104/pp.106.082024.

Sharon, M., Freeman, S. and Sneh, B. (2011) 'Assessment of resistance pathways induced in *Arabidopsis thaliana* by hypovirulent *Rhizoctonia* spp. isolates', *Phytopathology*, 101(7), pp. 828–838. doi: 10.1094/phyto-09-10-0247.

Shimizu-Mitao, Y. and Kakimoto, T. (2014) 'Auxin sensitivities of all *Arabidopsis* aux/IAAs for degradation in the presence of every TIR1/AFB', *Plant and Cell Physiology*, 55(8), pp. 1450–1459. doi: 10.1093/pcp/pcu077.

Singh, P. *et al.* (2022) 'Specific Roles of Lipxygenases in Development and Responses to Stress in Plants', *Plants*, 11(7), pp. 1–18. doi: 10.3390/plants11070979.

Smiley, R. W. and Uddin, W. (1993) 'Influence of soil temperature on *Rhizoctonia* root rot (*R. solani* AG-8 and *R. oryzae*) of winter wheat', *Phytopathology*, p. 777. doi: 10.1094/phyto-83-777.

Sneh, B., Burpee, L. and Ogoshi, A. (1991) *Identification of Rhizoctonia species*. St. Paul, Minn.: APS Press.

Stegmann, M. *et al.* (2017) 'The receptor kinase FER is a RALF-regulated scaffold controlling plant immune signaling', *Science*, 355(6322), pp. 287–289. doi: 10.1126/science.aal2541.

Stephenson, P. *et al.* (2010) 'A rich TILLING resource for studying gene function in *Brassica rapa*', *BMC Plant Biology*, 10, pp. 1–10. doi:



10.1186/1471-2229-10-62.

Struck, C., Rüsck, S. and Strehlow, B. (2022) 'Control Strategies of Clubroot Disease Caused by *Plasmodiophora brassicae*', *Microorganisms*, 10(3), pp. 1–13. doi: 10.3390/microorganisms10030620.

Sturrock, C. J. *et al.* (2015) 'Effects of damping-off caused by *Rhizoctonia solani* anastomosis group 2-1 on roots of wheat and oil seed rape quantified using X-ray Computed Tomography and real-time PCR', *Frontiers in Plant Science*, 6(June), pp. 1–11. doi: 10.3389/fpls.2015.00461.

Sugawara, S. *et al.* (2015) 'Distinct characteristics of indole-3-acetic acid and phenylacetic acid, two common auxins in plants', *Plant and Cell Physiology*, 56(8), pp. 1641–1654. doi: 10.1093/pcp/pcv088.

Swarup, R. and Péret, B. (2012) 'AUX/LAX family of auxin influx carriers-An overview', *Frontiers in Plant Science*, 3(OCT), pp. 1–11. doi: 10.3389/fpls.2012.00225.

Teo, B. K. *et al.* (1988) 'Influence of soil moisture, seeding date and *Rhizoctonia solani* isolates (AG2-1 and AG4) on disease incidence and yield in canola', *Canadian Journal of Plant Pathology*, 10(2), pp. 151–158. doi: 10.1080/07060668809501747.

Tewoldemedhin, Y. T. *et al.* (2006) 'Characterization of *Rhizoctonia* spp. recovered from crop plants used in rotational cropping systems in the Western Cape province of South Africa', *Plant Disease*, 90(11), pp. 1399–1406. doi: 10.1094/PD-90-1399.

The Royal Botanic Gardens Kew, Landare Research-NZ and Chinese Academy of Science (2022) *Index Fungorum*. Available at: <http://www.indexfungorum.org/Index.htm>.

Tiryaki, I. and Staswick, P. E. (2002) 'An Arabidopsis mutant defective in jasmonate response is allelic to the auxin-signaling mutant axr1', *Plant Physiology*, 130(2), pp. 887–894. doi: 10.1104/pp.005272.

Tonnessen, B. W. *et al.* (2015) 'Rice phenylalanine ammonia-lyase gene OsPAL4 is associated with broad spectrum disease resistance', *Plant Molecular Biology*, 87(3), pp. 273–286. doi: 10.1007/s11103-014-0275-9.

U, N. (1935) 'Genome analysis in Brassica with special reference to the experimental formation of *B. napus* and peculiar mode of fertilization', *Japanese Journal of Botany*, 7, pp. 389–452.

Verma, P. R. (1996) 'Biology and control of *Rhizoctonia solani* on rapeseed : A review', *Phytoprotection*, 77(3), pp. 99–111. doi: 10.7202/706106ar.

Vijayan, S. and Kirti, P. B. (2012) 'Mungbean plants expressing BjNPR1 exhibit enhanced resistance against the seedling rot pathogen, *Rhizoctonia solani*', *Transgenic Research*, 21(1), pp. 193–200. doi: 10.1007/s11248-011-9521-y.

Vogel, H. J. (1956) 'A convenient growth medium for *Neurospora* (Medium N)', *Microbial Genetics Bulletin*, 13, pp. 42–43.

VSN International (2019) 'GenStat for Windows 20th Edition'. Hemel Hempstead, UK. Available at: [Genstat.co.uk](http://Genstat.co.uk).

Wang, P. *et al.* (2022) 'Integrated omics reveal novel functions and underlying mechanisms of the receptor kinase FERONIA in *Arabidopsis thaliana*', *The Plant cell*, 34(7), pp. 2594–2614. doi: 10.1093/plcell/koac111.

Wang, Y. *et al.* (2021) 'Function and Mechanism of Jasmonic Acid in Plant Responses to Abiotic and Biotic Stresses', *International Journal of*

*Molecular Sciences*, 22(8568). doi: <https://doi.org/10.3390/ijms22168568>.

Wang, Y. J. *et al.* (2016) 'The fundamental role of NOX family proteins in plant immunity and their regulation', *International Journal of Molecular Sciences*, 17(6). doi: 10.3390/ijms17060805.

Watson, A. *et al.* (2018) 'Speed breeding is a powerful tool to accelerate crop research and breeding', *Nature Plants*. Springer US, 4(1), pp. 23–29. doi: 10.1038/s41477-017-0083-8.

Wei, L. *et al.* (2016) 'Genome-wide association analysis and differential expression analysis of resistance to Sclerotinia stem rot in Brassica napus', *Plant Biotechnology Journal*, 14(6), pp. 1368–1380. doi: 10.1111/pbi.12501.

Westrick, N. M., Smith, D. L. and Kabbage, M. (2021) 'Disarming the Host: Detoxification of Plant Defense Compounds During Fungal Necrotrophy', *Frontiers in Plant Science*, 12(April), pp. 1–18. doi: 10.3389/fpls.2021.651716.

Wibberg, D. *et al.* (2013) 'Establishment and interpretation of the genome sequence of the phytopathogenic fungus *Rhizoctonia solani* AG1-IB isolate 7/3/14', *Journal of Biotechnology*. Elsevier B.V., 167(2), pp. 142–155. doi: 10.1016/j.jbiotec.2012.12.010.

Wibberg, D. *et al.* (2016) 'Genome analysis of the sugar beet pathogen *Rhizoctonia solani* AG2-2IIIB revealed high numbers in secreted proteins and cell wall degrading enzymes', *BMC Genomics*. BMC Genomics, 17(1), pp. 1–12. doi: 10.1186/s12864-016-2561-1.

Wightman, F. and Lighty, D. L. (1982) 'Identification of phenylacetic acid as a natural auxin in the shoots of higher plants', *Physiologia Plantarum*, 55(1), pp. 17–24. doi: 10.1111/j.1399-3054.1982.tb00278.x.

Windels, C. E., Kuznia, R. A. and Call, J. (1997) 'Characterization and pathogenicity of *Thanatephorus cucumeris* from sugar beet in Minnesota', *Plant Disease*, 81(3), pp. 245–249. doi: 10.1094/PDIS.1997.81.3.245.

Withers, J. and Dong, X. (2016) 'Posttranslational Modifications of NPR1: A Single Protein Playing Multiple Roles in Plant Immunity and Physiology', *PLoS Pathogens*, 12(8), pp. 1–9. doi: 10.1371/journal.ppat.1005707.

Xia, X. J. *et al.* (2015) 'Interplay between reactive oxygen species and hormones in the control of plant development and stress tolerance', *Journal of Experimental Botany*, 66(10), pp. 2839–2856. doi: 10.1093/jxb/erv089.

Xu, F. *et al.* (2015) 'Two N-terminal acetyltransferases antagonistically regulate the stability of a nod-like receptor in arabidopsis', *Plant Cell*, 27(5), pp. 1547–1562. doi: 10.1105/tpc.15.00173.

Xue, A. G. *et al.* (2007) 'Effect of seed treatments on emergence, yield, and root rot severity of soybean under *Rhizoctonia solani* inoculated field conditions in Ontario', *Canadian Journal of Plant Science*, 87(1), pp. 167–173. doi: 10.4141/p05-192.

Xue, C. Y. *et al.* (2018) 'Cell-wall-degrading enzymes produced in vitro and in vivo by *Rhizoctonia solani*, the causative fungus of peanut sheath blight', *PeerJ*, 2018(9). doi: 10.7717/peerj.5580.

Yamamoto, M. and Yamamoto, K. T. (1998) 'Differential effects of 1-naphthaleneacetic acid, indole-3-acetic acid and 2,4-dichlorophenoxyacetic acid on the gravitropic response of roots in an auxin-resistant mutant of *Arabidopsis*, *aux1*', *Plant and Cell Physiology*, 39(6), pp. 660–664. doi: 10.1093/oxfordjournals.pcp.a029419.

Yamamoto, M. and Yamamoto, K. T. (1999) 'Effects of natural and

synthetic auxins on the gravitropic growth habit of roots in two auxin-resistant mutants of Arabidopsis, *axr1* and *axr4*: Evidence for defects in the Auxin influx mechanism of *axr4*', *Journal of Plant Research*, 112(4), pp. 391–396. doi: 10.1007/pl00013892.

Yang, J. *et al.* (2019) 'The Crosstalks Between Jasmonic Acid and Other Plant Hormone Signaling Highlight the Involvement of Jasmonic Acid as a Core Component in Plant Response to Biotic and Abiotic Stresses', *Frontiers in Plant Science*. doi: 10.3389/fpls.2019.01349.

Yang, J., Tewari, J. P. and Verma, P. R. (1993) 'Calcium oxalate crystal formation in *Rhizoctonia solani* AG 2-1 culture and infected crucifer tissue: relationship between host calcium and resistance', *Mycological Research*, 97(12), pp. 1516–1522. doi: 10.1016/S0953-7562(09)80227-X.

Yang, J. and Verma, P. R. (1992) 'Screening genotypes for resistance to pre-emergence damping-off and postemergence seedling root rot of oilseed rape and canola caused by *Rhizoctonia solani* AG-2-1', *Crop Protection*, 11(5), pp. 443–448. doi: 10.1016/0261-2194(92)90028-4.

Yin, C. *et al.* (2013) 'Role of bacterial communities in the natural suppression of *Rhizoctonia solani* bare patch disease of wheat (*Triticum aestivum* L.)', *Applied and Environmental Microbiology*, 79(23), pp. 7428–7438. doi: 10.1128/AEM.01610-13.

Yulianti, T., Sivasithamparam, K. and Turner, D. W. (2006) 'Saprophytic growth of *Rhizoctonia solani* Kühn AG2-1 (ZG5) in soil amended with fresh green manures affects the severity of damping-off in canola', *Soil Biology and Biochemistry*, 38(5), pp. 923–930. doi: 10.1016/j.soilbio.2005.07.014.

Zeun, R., Scalliet, G. and Oostendorp, M. (2013) 'Biological activity of sedaxane - a novel broad-spectrum fungicide for seed treatment', *Pest*

*Management Science*, 69(4), pp. 527–534. doi: 10.1002/ps.3405.

Zhang, Y. *et al.* (2020) 'Fungi–nematode interactions: Diversity, ecology, and biocontrol prospects in agriculture', *Journal of Fungi*, 6(4), pp. 1–24. doi: 10.3390/jof6040206.

Zhang, Y., Lubberstedt, T. and Xu, M. (2013) 'The Genetic and Molecular Basis of Plant Resistance to Pathogens', *Journal of Genetics and Genomics*. Elsevier Limited and Science Press, 40(1), pp. 23–35. doi: 10.1016/j.jgg.2012.11.003.

Zhang, Z. *et al.* (2021) 'Genome Sequence of *Rhizoctonia solani* Anastomosis Group 4 Strain Rhs4ca, a Widespread Pathomycete in Field Crops', *Molecular Plant-Microbe Interactions*®, August(MPMI12200362A). doi: 10.1094/mpmi-12-20-0362-a.

Zheng, A. *et al.* (2013) 'The evolution and pathogenic mechanisms of the rice sheath blight pathogen', *Nature Communications*. Nature Publishing Group, 4(May 2012), pp. 1410–1424. doi: 10.1038/ncomms2427.

Zheng, X., Koopmann, B. and von Tiedemann, A. (2019) 'Role of salicylic acid and components of the phenylpropanoid pathway in basal and cultivar-related resistance of oilseed rape (*Brassica napus*) to *Verticillium longisporum*', *Plants*, 8(11). doi: 10.3390/plants8110491.

Zhou, N., Tootle, T. L. and Glazebrook, J. (1999) 'Arabidopsis PAD3, a gene required for camalexin biosynthesis, encodes a putative cytochrome P450 monooxygenase', *Plant Cell*, 11(12), pp. 2419–2428. doi: 10.1105/tpc.11.12.2419.

Zhou, Q. *et al.* (2014) 'Effect of inoculum density and quantitative PCR-based detection of *Rhizoctonia solani* AG-2-1 and *Fusarium avenaceum* on canola', *Crop Protection*, 59, pp. 71–77. doi: 10.1016/j.cropro.2014.01.015.

## Supplementary Information

### Supplementary Information 1: Preparation of Vogel's media

<u>Trace element solution</u>		~100ml	~50ml
H <sub>2</sub> O	Distilled water	95ml	47.5ml
Citric acid.1H <sub>2</sub> O	Citric acid	5g	2.5g
ZnSO <sub>4</sub> .7H <sub>2</sub> O	Zinc sulphate heptahydrate	5g	2.5g
Fe(NH <sub>4</sub> ) <sub>2</sub> (SO <sub>4</sub> ) <sub>2</sub> .6H <sub>2</sub> O	Ammonium iron (II) sulphate hexahydrate	1g	0.5g
CuSO <sub>4</sub> .5H <sub>2</sub> O	Copper sulphate pentahydrate Copper (II) sulphate	0.25g	0.125g
MnSO <sub>4</sub> .1H <sub>2</sub> O	Manganese sulphate monohydrate Manganese (II) sulphate	0.05g	0.025g
H <sub>3</sub> BO <sub>3</sub> (anhydrous)	Boric acid	0.05g	0.025g
Na <sub>2</sub> MoO <sub>4</sub> .2H <sub>2</sub> O	Sodium molybdate dihydrate	0.05g	0.025g
CHCl <sub>3</sub>	Chloroform (preservative) Trichloromethane	1ml	0.5ml

1. Dissolve the components successively in water while stirring at room temperature.
2. Store in a stoppered bottle at room temperature, with chloroform added as preservative.
3. The same formula may be used also for other synthetic media.  
Trivial quantitative differences in published trace element recipes may reflect differences in hydration of the constituents and can be ignored.
4. Biotin solution
  - a. Dissolve 5mg biotin in 50ml water.
  - b. Aliquot into 2.5ml tubes aliquots and store at -20°C.

<u>50x salts solution</u>		1litre	500ml	Final conc. per litre
H <sub>2</sub> O	Water	750ml	375ml	
Na <sub>3</sub> citrate.2H <sub>2</sub> O	Tri sodium citrate Sodium citrate dihydrate	150g	75g	3g
KH <sub>2</sub> PO <sub>4</sub> anhydrous	Monopotassium phosphate Potassium dihydrogen phosphate	250g	125g	5g
NH <sub>4</sub> NO <sub>3</sub> anhydrous	Ammonium nitrate	100g	50g	2g
MgSO <sub>4</sub> .7H <sub>2</sub> O	Magnesium sulphate heptahydrate Epsomite	10g	5g	0.2g
CaCl <sub>2</sub> .2H <sub>2</sub> O (dissolved)	Calcium chloride dihydrate	5g	2.5g	0.1g
Trace element solution	See below	5ml	2.5ml	0.1ml
Biotin stock solution	See below	2.5ml	1.25ml	0.05ml
CHCl <sub>3</sub>	Chloroform (preservative) Trichloromethane	2ml	1ml	0.04ml

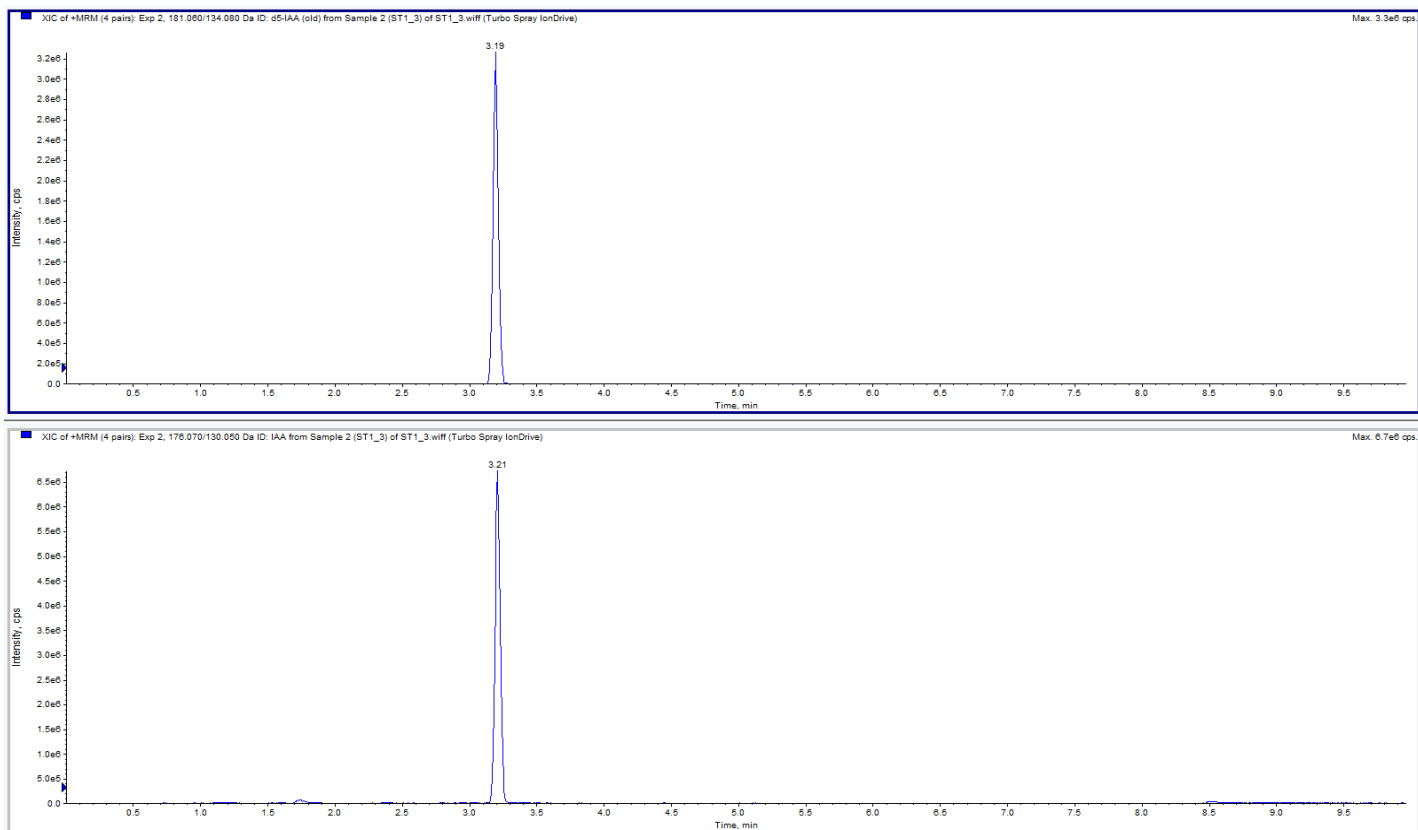
This solution has been shown to be stable for at least 6months.

1. Prepare in a large Erlenmeyer flask with a magnetic stirrer. Add 730ml distilled water.
2. Dissolve the components in the order listed above with stirring, and make sure that everything is fully dissolved before moving on to the next component.
3. Moderate heating can help in dissolving the citrate and phosphate.
4. Dissolve the calcium chloride separately in 20ml water and add the solution slowly. (Alternatively, powdered calcium chloride can be added slowly, but this takes longer.)

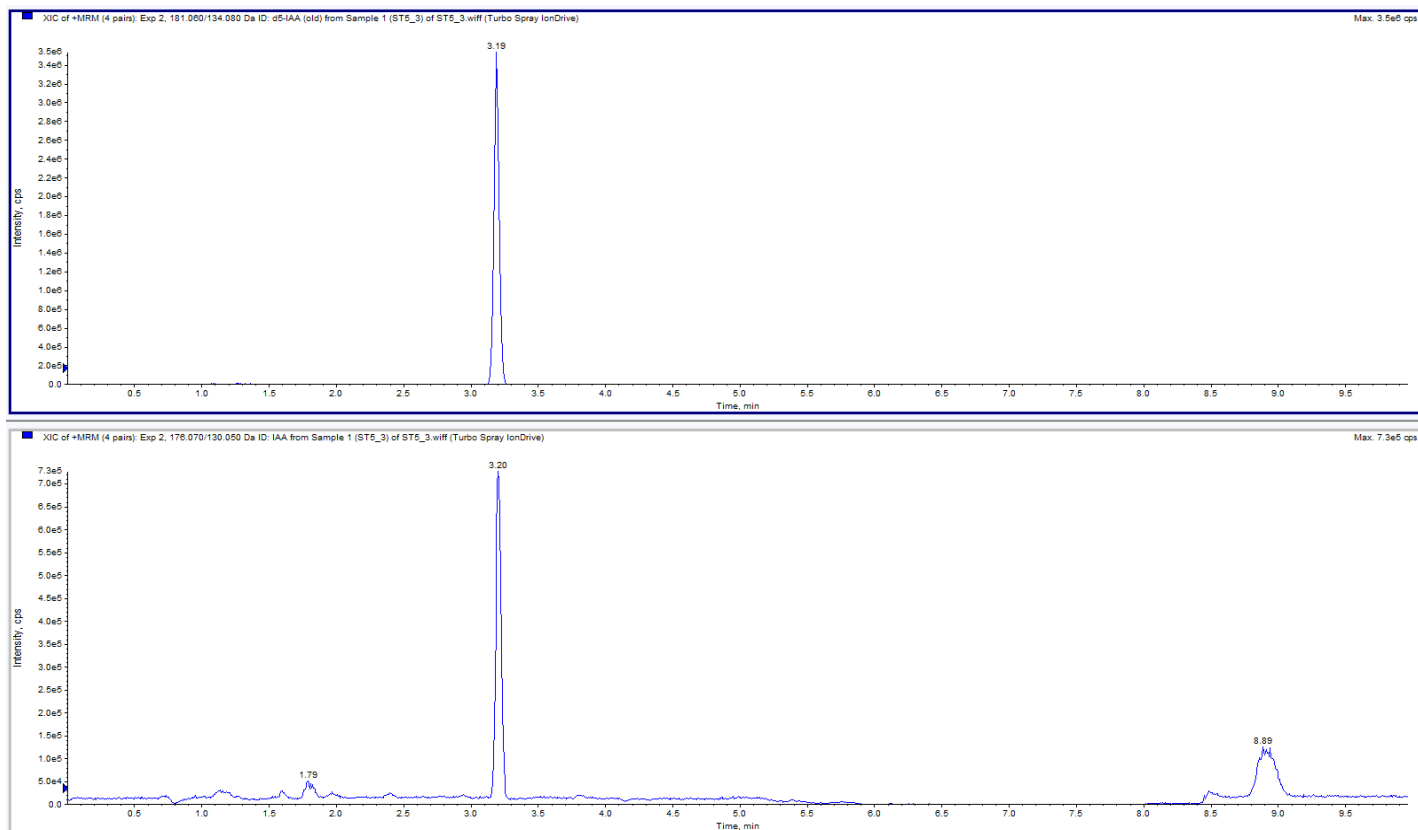


5. Add 2ml Chloroform as preservative and store the 50x stock solution at room temperature.
6. To make 500ml, add 10ml of the salts solution to 490ml of distilled water (1litre = 980ml+20ml).
7. The pH of the medium should be ~5.8, no adjustment is necessary.
8. 1-2% sucrose can be added at this stage.
9. 1.5% agar can be added at this stage.
10. Autoclave the solution to sterilise.

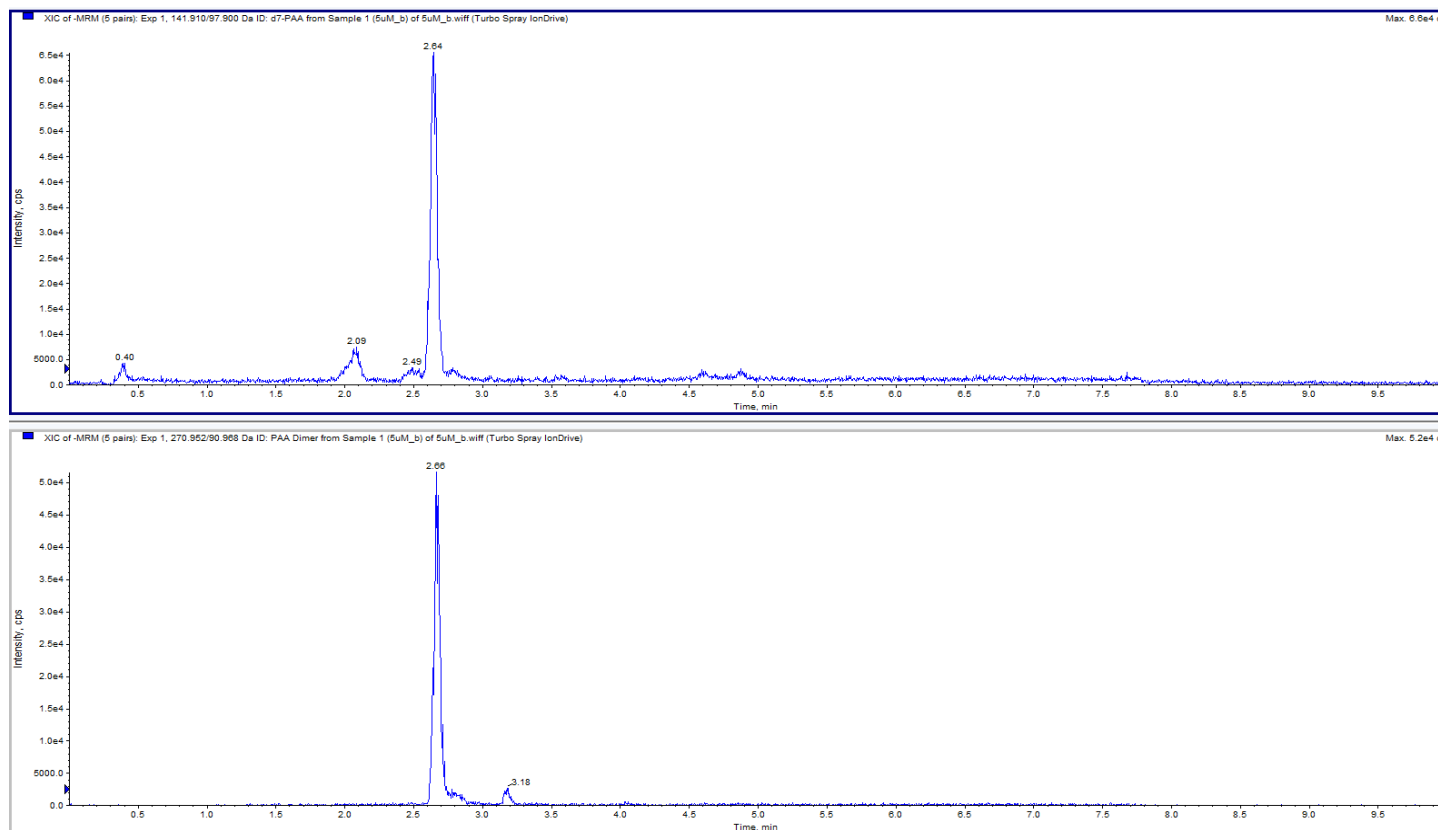
**Supplementary Information 2: Chromatogram showing peaks for d5-IAA (top) and IAA (bottom). These were extracted from samples with known concentrations of 500nM for IAA and 5000nM for d5-IAA.**



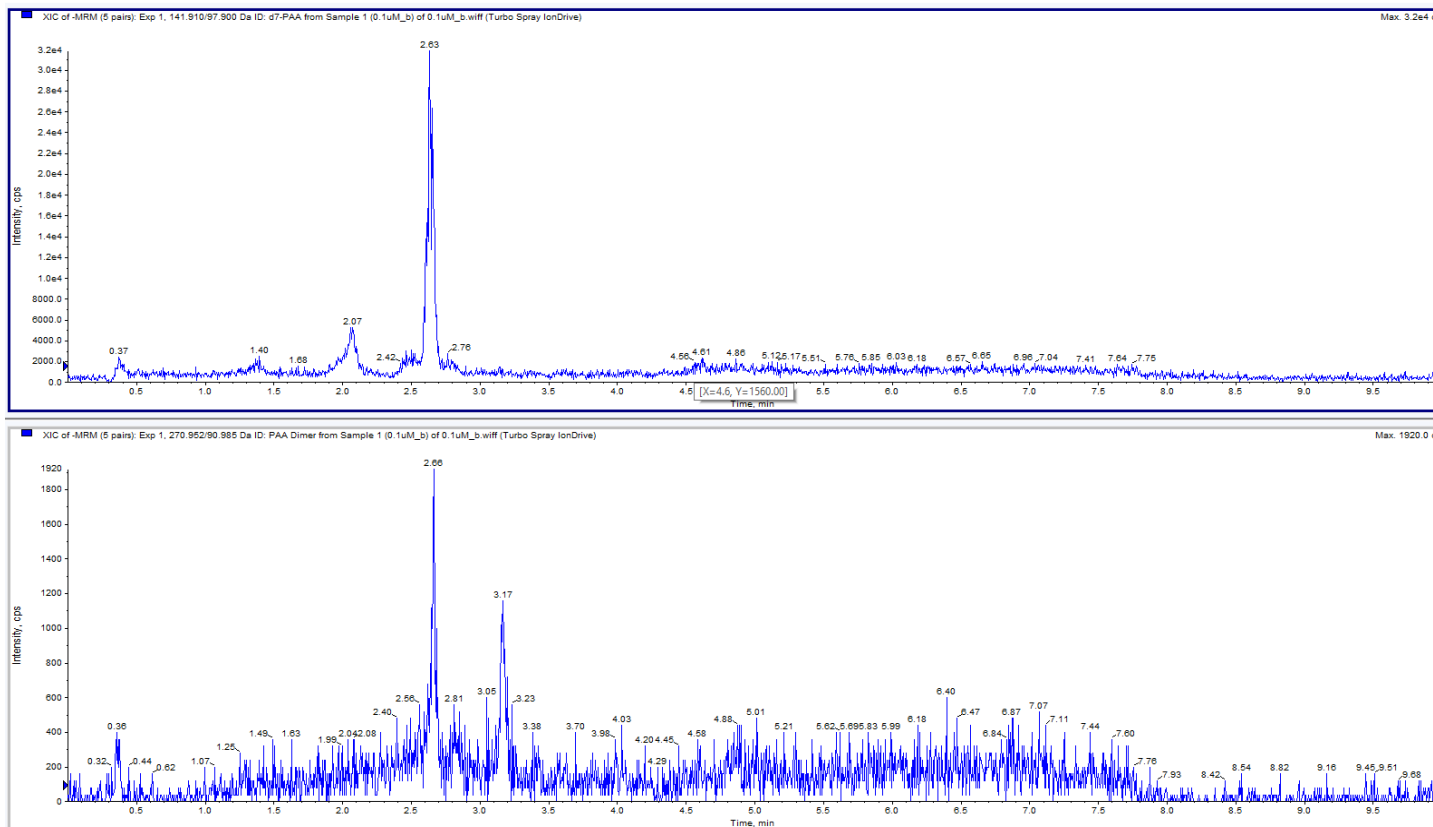
**Supplementary Information 3: Chromatogram showing peaks for d5-IAA (top) and IAA (bottom). These were extracted from samples with known concentrations of 10nM for IAA and 5000nM for d5-IAA.**



**Supplementary Information 4: Chromatogram showing peaks for d7-PAA (top) and PAA dimer (bottom). These were extracted from samples with known concentrations of 5000nM for PAA and 5000nM for d7-PAA.**



**Supplementary Information 5: Chromatogram showing peaks for d7-PAA (top) and PAA dimer (bottom). These were extracted from samples with known concentrations of 100nM for PAA and 5000nM for d7-PAA.**



**Supplementary Information 6: Analysis of the effects of *Rhizoctonia solani* AG2-1 on the root length of *Arabidopsis thaliana* Col-0 (wild type) plants.**

## Analysis of an unbalanced design using Genstat regression

Variate: length

### Accumulated analysis of variance

Change	d.f. v.r.	s.s. F pr.	m.s.
+ plate_rep	4 0.55	4.756 0.702	1.189
+ distance	3 0.93	6.042 0.431	2.014
+ inoculation	1 31.40	68.288 <.001	68.288
+ distance.inoculation	3 0.53	3.487 0.660	1.162
Residual	105	228.361	2.175
Total	116	310.934	2.680

### Grand mean

3.463

### Predictions from regression model

Response variate: length

distance	Prediction
1.5	3.257
3.5	3.797
6.5	3.424
8.5	3.274

Minimum standard error of difference	0.3365
Average standard error of difference	0.4050
Maximum standard error of difference	0.4665

### Predictions from regression model

Response variate: length

inoculation	Prediction
inoc	2.719
non-inoc	4.248

Standard error of differences between predicted means 0.2729

## Predictions from regression model

Response variate: length

inoculation distance	Prediction	
	inoc	non-inoc
1.5	2.278	4.288
3.5	3.136	4.493
6.5	2.854	4.023
8.5	2.651	3.931

Minimum standard error of difference 0.4664  
Average standard error of difference 0.5720  
Maximum standard error of difference 0.6595

### Supplementary Information 7: Analysis of the effects of *Rhizoctonia solani* AG2-1 on the root length of *Arabidopsis thaliana aux1* plants.

## Analysis of an unbalanced design using Genstat regression

Variate: length

### Accumulated analysis of variance

Change	d.f. v.r.	s.s. F pr.	m.s.
+ plate_rep	4	25.041	6.260
+ distance	3	27.725	9.242
+ inoculation	1	70.676	70.676
+ distance.inoculation	3	29.217	9.739
Residual	106	204.483	1.929
Total	117	357.141	3.052

## Grand mean

4.279

## Predictions from regression model

Response variate: length

distance	Prediction
1.5	3.626
3.5	4.444

6.5	4.971
8.5	4.500

Minimum standard error of difference	0.3147
Average standard error of difference	0.3804
Maximum standard error of difference	0.4393

## Predictions from regression model

Response variate: length

	Prediction
inoculation	
inoc	3.485
non-inoc	5.034

Standard error of differences between predicted means      0.2558

## Predictions from regression model

Response variate: length

inoculation	Prediction	
distance	inoc	non-inoc
1.5	2.494	4.721
3.5	3.287	5.563
6.5	4.731	5.203
8.5	4.557	4.445

Minimum standard error of difference	0.4392
Average standard error of difference	0.5373
Maximum standard error of difference	0.6211

### **Supplementary Information 8: Analysis of the effects of *Rhizoctonia solani* AG2-1 on the root length of *Arabidopsis thaliana axr1* plants.**

## Analysis of an unbalanced design using Genstat regression

Variate: length

### Accumulated analysis of variance

Change	d.f.	s.s.	m.s.
	v.r.	F pr.	
+ plate_rep	4	6.609	1.652
	0.95	0.441	
+ distance	3	3.286	1.095
	0.63	0.599	
+ inoculation	1	2.062	2.062
	1.18	0.280	
+ distance.inoculation	3	14.049	4.683
	2.68	0.051	
Residual	106	185.166	1.747



Total	117	211.173	1.805
-------	-----	---------	-------

## Grand mean

0.9371

## Predictions from regression model

Response variate: length

	Prediction
distance	
1.5	0.7236
3.5	1.1243
6.5	0.8951
8.5	0.9519

Minimum standard error of difference	0.2956
Average standard error of difference	0.3673
Maximum standard error of difference	0.4308

## Predictions from regression model

Response variate: length

	Prediction
inoculation	
inoc	0.7960
non-inoc	1.0570

Standard error of differences between predicted means	0.2436
---	--------

## Predictions from regression model

Response variate: length

	Prediction	
inoculation	inoc	non-inoc
distance		
1.5	0.6100	0.8412
3.5	0.8265	1.4323
6.5	1.5114	0.2576
8.5	0.4631	1.4575

Minimum standard error of difference	0.4180
Average standard error of difference	0.5187
Maximum standard error of difference	0.6281

**Supplementary Information 9: Analysis of the effects of *Rhizoctonia solani* AG2-1 on the number of lateral roots of *Arabidopsis thaliana* Col-0 (wild type) plants.**

## Analysis of an unbalanced design using Genstat regression

Variate: n\_child

## Accumulated analysis of variance

Change	d.f. v.r.	s.s. F pr.	m.s.
+ plate_rep	4	71.678	17.919
	1.92	0.113	
+ distance	3	28.719	9.573
	1.02	0.385	
+ inoculation	1	145.803	145.803
	15.59	<.001	
+ distance.inoculation	3	137.691	45.897
	4.91	0.003	
Residual	105	982.109	9.353
Total	116	1366.000	11.776

## Grand mean

5.000

## Predictions from regression model

Response variate: n\_child

	Prediction
distance	
1.5	4.307
3.5	5.327
6.5	5.504
8.5	5.294

Minimum standard error of difference 0.6978  
Average standard error of difference 0.8398  
Maximum standard error of difference 0.9674

## Predictions from regression model

Response variate: n\_child

	Prediction
inoculation	
inoc	3.923
non-inoc	6.158

Standard error of differences between predicted means 0.5659

## Predictions from regression model

Response variate: n\_child

	Prediction	
inoculation	inoc	non-inoc
distance		
1.5	1.944	6.794

3.5	4.194	6.520
6.5	5.894	5.094
8.5	5.294	5.294

Minimum standard error of difference	0.967
Average standard error of difference	1.186
Maximum standard error of difference	1.368

**Supplementary Information 10: Analysis of the effects of *Rhizoctonia solani* AG2-1 on the number of lateral roots of *Arabidopsis thaliana aux1* plants.**

## Analysis of an unbalanced design using Genstat regression

Variate: n\_child

### Accumulated analysis of variance

Change	d.f. v.r.	s.s. F pr.	m.s.
+ plate_rep	4	58.051	14.513
	3.19	0.016	
+ distance	3	22.412	7.471
	1.64	0.184	
+ inoculation	1	88.339	88.339
	19.42	<.001	
+ distance.inoculation	3	25.947	8.649
	1.90	0.134	
Residual	106	482.267	4.550
Total	117	677.017	5.786

### Grand mean

2.695

### Predictions from regression model

Response variate: n\_child

distance	Prediction
1.5	2.091
3.5	2.845
6.5	2.994
8.5	3.248

Minimum standard error of difference	0.4833
Average standard error of difference	0.5842
Maximum standard error of difference	0.6746

### Predictions from regression model

Response variate: n\_child

	Prediction
inoculation	
inoc	1.809
non-inoc	3.541

Standard error of differences between predicted means 0.3929

## Predictions from regression model

Response variate: n\_child

inoculation	Prediction	
distance	inoc	non-inoc
1.5	0.797	3.342
3.5	1.710	3.942
6.5	2.892	3.092
8.5	2.892	3.592

Minimum standard error of difference 0.6745  
Average standard error of difference 0.8251  
Maximum standard error of difference 0.9539

### **Supplementary Information 11: Analysis of the effects of *Rhizoctonia solani* AG2-1 on the number of lateral roots of *Arabidopsis thaliana axr1* plants.**

## Analysis of an unbalanced design using Genstat regression

Variate: n\_child

### Accumulated analysis of variance

Change	d.f.	s.s.	m.s.
	v.r.	F pr.	
+ plate_rep	4	0.6088	0.1522
	1.13	0.346	
+ distance	3	0.3565	0.1188
	0.88	0.452	
+ inoculation	1	0.7116	0.7116
	5.29	0.023	
+ distance.inoculation	3	0.3749	0.1250
	0.93	0.430	
Residual	106	14.2616	0.1345
Total	117	16.3136	0.1394

### Grand mean

0.07627

## Predictions from regression model

Response variate: n\_child

	Prediction
distance	
1.5	0.00047
3.5	0.12336
6.5	0.11992
8.5	0.09878

Minimum standard error of difference 0.0820  
Average standard error of difference 0.1019  
Maximum standard error of difference 0.1196

## Predictions from regression model

Response variate: n\_child

	Prediction
inoculation	
inoc	0.00047
non-inoc	0.15619

Standard error of differences between predicted means 0.06762

## Predictions from regression model

Response variate: n\_child

	Prediction	
inoculation	inoc	non-inoc
distance		
1.5	0.00047	0.00047
3.5	0.00047	0.25047
6.5	0.00047	0.24348
8.5	0.00047	0.20047

Minimum standard error of difference 0.1160  
Average standard error of difference 0.1440  
Maximum standard error of difference 0.1743

**Supplementary Information 12: Analysis of the effects of *Rhizoctonia solani* AG2-1 on the absolute proportion of 180° of *Arabidopsis thaliana* Col-0 (wild type) plants.**

## Analysis of an unbalanced design using Genstat regression

Variate: proportion\_of\_180

### Accumulated analysis of variance

Change	d.f. v.r.	s.s. F pr.	m.s.
--------	--------------	---------------	------

+ rep	4	0.06413	0.01603
	1.30	0.276	
+ distance	3	0.06196	0.02065
	1.67	0.178	
+ inoculation	1	0.04129	0.04129
	3.34	0.070	
+ distance.inoculation	3	0.07662	0.02554
	2.07	0.109	
Residual	105	1.29793	0.01236
Total	116	1.54194	0.01329

## Grand mean

0.1265

## Predictions from regression model

Response variate: proportion\_of\_180

	Prediction
distance	
1.5	0.1156
3.5	0.1287
6.5	0.0989
8.5	0.1735

Minimum standard error of difference 0.02537  
Average standard error of difference 0.03053  
Maximum standard error of difference 0.03517

## Predictions from regression model

Response variate: proportion\_of\_180

	Prediction
inoculation	
inoc	0.1086
non-inoc	0.1462

Standard error of differences between predicted means 0.02057

## Predictions from regression model

Response variate: proportion\_of\_180

	Prediction	
inoculation	inoc	non-inoc
distance		
1.5	0.0843	0.1485
3.5	0.0944	0.1648
6.5	0.0830	0.1157
8.5	0.2083	0.1369

Minimum standard error of difference 0.03516  
Average standard error of difference 0.04312  
Maximum standard error of difference 0.04972

**Supplementary Information 13: Analysis of the effects of *Rhizoctonia solani* AG2-1 on the absolute proportion of 180° of *Arabidopsis thaliana aux1* plants.**

## Analysis of an unbalanced design using Genstat regression

Variate: proportion\_of\_180

### Accumulated analysis of variance

Change	d.f.	s.s.	m.s.
	v.r.	F pr.	
+ rep	4	0.18837	0.04709
	0.56	0.695	
+ distance	3	0.38449	0.12816
	1.51	0.216	
+ inoculation	1	0.02912	0.02912
	0.34	0.559	
+ distance.inoculation	3	0.80768	0.26923
	3.18	0.027	
Residual	106	8.98467	0.08476
Total	117	10.39433	0.08884

### Grand mean

0.3735

### Predictions from regression model

Response variate: proportion\_of\_180

	Prediction
distance	
1.5	0.2998
3.5	0.3972
6.5	0.4578
8.5	0.3814

Minimum standard error of difference	0.06597
Average standard error of difference	0.07974
Maximum standard error of difference	0.09208

### Predictions from regression model

Response variate: proportion\_of\_180

	Prediction
inoculation	
inoc	0.3566
non-inoc	0.3881

Standard error of differences between predicted means 0.05363

## Predictions from regression model

Response variate: proportion\_of\_180

inoculation distance	Prediction	
	inoc	non-inoc
1.5	0.2474	0.3505
3.5	0.3158	0.4760
6.5	0.6156	0.3052
8.5	0.3903	0.3728

Minimum standard error of difference 0.0921  
Average standard error of difference 0.1126  
Maximum standard error of difference 0.1302

### **Supplementary Information 14: Analysis of the effects of *Rhizoctonia solani* AG2-1 on the absolute proportion of 180° of *Arabidopsis thaliana* *axr1* plants.**

## Analysis of an unbalanced design using Genstat regression

Variate: proportion\_of\_180

### Accumulated analysis of variance

Change	d.f.	s.s.	m.s.
	v.r.	F pr.	
+ rep	4	0.05359	0.01340
	0.63	0.645	
+ distance	3	0.06754	0.02251
	1.05	0.372	
+ inoculation	1	0.04858	0.04858
	2.27	0.135	
+ distance.inoculation	3	0.04558	0.01519
	0.71	0.548	
Residual	106	2.26635	0.02138
Total	117	2.48165	0.02121

## Grand mean

0.1151

## Predictions from regression model

Response variate: proportion\_of\_180

distance	Prediction
	1.5



3.5	0.1052
6.5	0.0811
8.5	0.1016

Minimum standard error of difference	0.03270
Average standard error of difference	0.04064
Maximum standard error of difference	0.04767

## Predictions from regression model

Response variate: proportion\_of\_180

Prediction	
inoculation	
inoc	0.0948
non-inoc	0.1353

Standard error of differences between predicted means 0.02695

## Predictions from regression model

Response variate: proportion\_of\_180

Prediction		
inoculation	inoc	non-inoc
distance		
1.5	0.0999	0.1933
3.5	0.0925	0.1183
6.5	0.0829	0.0793
8.5	0.0998	0.1035

Minimum standard error of difference	0.04624
Average standard error of difference	0.05739
Maximum standard error of difference	0.06948

### Supplementary Information 15: Analysis of the effects of 2,4-D concentration on the root length proportion of *Arabidopsis thaliana* auxin mutant plants.

## Analysis of variance

Variate: length\_proportion

Source of variation	d.f.	s.s.	m.s.	v.r.	F pr.
plate_rep stratum	3	15.367	5.122	3.06	
plate_rep.*Units* stratum					
%2_4_D_concentration_nM	4	0.691	0.173	0.10	0.981
genotype	2	15.286	7.643	4.56	0.012
%2_4_D_concentration_nM.genotype	8	6.515	0.814	0.49	0.865
Residual	162	271.550	1.676		
Total	179	309.408			

*Message: the following units have large residuals.*

plate_rep 1 *units* 10	4.570	s.e. 1.228
plate_rep 1 *units* 28	3.735	s.e. 1.228
plate_rep 1 *units* 37	6.444	s.e. 1.228
plate_rep 3 *units* 22	6.094	s.e. 1.228
plate_rep 3 *units* 31	8.136	s.e. 1.228
plate_rep 3 *units* 40	5.559	s.e. 1.228

## Tables of means

Variate: length\_proportion

Grand mean 0.963

%2_4_D_concentration_nM	0	25	50	100	200
	1.000	1.018	1.022	0.898	0.879

genotype	aux1	axr1	WT
	1.139	1.198	0.553

%2_4_D_concentration_nM	genotype	aux1	axr1	WT
0		1.000	1.000	1.000
25		1.251	1.088	0.716
50		1.223	1.319	0.523
100		0.965	1.423	0.305
200		1.256	1.161	0.220

## Standard errors of differences of means

Table	%2_4_D_concentration_nM	genotype
rep.	36	60
d.f.	162	162
s.e.d.	0.3052	0.2364

Table	%2_4_D_concentration_nM	genotype
rep.	12	
d.f.	162	
s.e.d.	0.5286	

**Supplementary Information 16: Analysis of the effects of PAA concentration on the root length proportion of *Arabidopsis thaliana* auxin mutant plants.**

## Analysis of an unbalanced design using Genstat regression

Variate: length\_proportion

### Accumulated analysis of variance

Change	d.f.	s.s.	m.s.
	v.r.	F pr.	
+ plate_rep	3	18.1240	6.0413
	9.37	<.001	

+ PAA_concentration_uM	4	2.8717	0.7179
	1.11	0.352	
+ genotype	2	6.5853	3.2926
	5.11	0.007	
+ PAA_concentration_uM.genotype	8	6.2396	0.7800
	1.21	0.296	
Residual	160	103.1162	0.6445
Total	177	136.9368	0.7737

## Grand mean

0.9366

## Predictions from regression model

Response variate: length\_proportion

PAA_concentration_uM	Prediction
0.0	0.9987
2.5	1.1142
5.0	0.9546
10.0	0.8852
20.0	0.7330

Minimum standard error of difference 0.1892  
Average standard error of difference 0.1905  
Maximum standard error of difference 0.1923

## Predictions from regression model

Response variate: length\_proportion

genotype	Prediction
aux1	1.0400
axr1	1.0993
WT	0.6625

Minimum standard error of difference 0.1466  
Average standard error of difference 0.1475  
Maximum standard error of difference 0.1480

## Predictions from regression model

Response variate: length\_proportion

PAA_concentration_uM	Prediction		
	aux1	axr1	WT
0.0	0.9987	0.9987	0.9987
2.5	1.5455	1.1661	0.6143
5.0	1.1760	0.9705	0.7092
10.0	0.8077	1.3757	0.4581
20.0	0.6794	0.9783	0.5348

Minimum standard error of difference	0.3277
Average standard error of difference	0.3299
Maximum standard error of difference	0.3439

**Supplementary Information 17: Analysis of the effects of NAA concentration on the root length proportion of *Arabidopsis thaliana* auxin mutant plants.**

## Analysis of variance

Variate: length\_proportion

Source of variation	d.f.	s.s.	m.s.	v.r.	F pr.
plate_rep stratum	3	9.2196	3.0732	6.45	
plate_rep.*Units* stratum					
NAA_concentration_nM	4	7.3938	1.8484	3.88	0.005
genotype	2	4.0581	2.0290	4.26	0.016
NAA_concentration_nM.genotype	8	2.9607	0.3701	0.78	0.624
Residual	162	77.1847	0.4764		
Total	179	100.8168			

*Message: the following units have large residuals.*

plate_rep 2 *units* 11	2.520	s.e. 0.655
plate_rep 3 *units* 25	1.990	s.e. 0.655
plate_rep 4 *units* 16	2.911	s.e. 0.655
plate_rep 4 *units* 25	2.115	s.e. 0.655
plate_rep 4 *units* 34	2.713	s.e. 0.655
plate_rep 4 *units* 43	2.341	s.e. 0.655

## Tables of means

Variate: length\_proportion

Grand mean 0.930

NAA_concentration_nM	0	50	100	200	500
	1.000	1.193	0.997	0.881	0.577

genotype	aux1	axr1	WT
	0.879	0.777	1.134

NAA_concentration_nM	genotype	aux1	axr1	WT
0		1.000	1.000	1.000
50		1.294	0.865	1.421
100		1.014	0.671	1.307
200		0.632	0.904	1.106
500		0.454	0.444	0.835

## Standard errors of differences of means

Table	NAA_concentration_nM	genotype
-------	----------------------	----------

rep.	36	60
d.f.	162	162
s.e.d.	0.1627	0.1260

Table	NAA_concentration_nM
	genotype
rep.	12
d.f.	162
s.e.d.	0.2818

**Supplementary Information 18: Analysis of the effects of 2,4-D concentration on the number of lateral roots of *Arabidopsis thaliana* auxin mutant plants.**

## Analysis of variance

Variate: no\_of\_laterals

Source of variation	d.f.	s.s.	m.s.	v.r.	F pr.
plate_rep stratum	3	10.950	3.650	0.80	
plate_rep.*Units* stratum					
%2_4_D_concentration_nM	4	48.967	12.242	2.69	0.033
genotype	2	408.078	204.039	44.91	<.001
%2_4_D_concentration_nM.genotype	8	14.367	1.796	0.40	0.922
Residual	162	735.967	4.543		
Total	179	1218.328			

*Message: the following units have large residuals.*

plate_rep 2 *units* 27	-5.98	s.e. 2.02
plate_rep 3 *units* 2	5.57	s.e. 2.02
plate_rep 3 *units* 14	5.74	s.e. 2.02

## Tables of means

Variate: no\_of\_laterals

Grand mean 3.06

%2_4_D_concentration_nM		0	25	50	100	200
		3.42	3.61	3.42	2.36	2.50
genotype		aux1	axr1	WT		
		2.28	1.73	5.17		
%2_4_D_concentration_nM	genotype	aux1	axr1	WT		
0		2.33	2.00	5.92		
25		3.42	2.17	5.25		
50		2.25	2.25	5.75		
100		1.58	0.92	4.58		
200		1.83	1.33	4.33		

## Standard errors of differences of means

Table	%2_4_D_concentration_nM	genotype
rep.	36	60
d.f.	162	162
s.e.d.	0.502	0.389

Table	%2_4_D_concentration_nM	genotype
rep.	12	
d.f.	162	
s.e.d.	0.870	

### Supplementary Information 19: Analysis of the effects of PAA concentration on the number of lateral roots of *Arabidopsis thaliana* auxin mutant plants.

## Analysis of an unbalanced design using Genstat regression

Variate: no\_of\_laterals

### Accumulated analysis of variance

Change	d.f.	s.s.	m.s.
	v.r.	F pr.	
+ plate_rep	3	57.699	19.233
	2.69	0.048	
+ PAA_concentration_uM	4	178.108	44.527
	6.23	<.001	
+ genotype	2	347.239	173.620
	24.28	<.001	
+ PAA_concentration_uM.genotype	8	150.133	18.767
	2.62	0.010	
Residual	160	1143.922	7.150
Total	177	1877.101	10.605

## Grand mean

4.674

## Predictions from regression model

Response variate: no\_of\_laterals

PAA_concentration_uM	Prediction
0.0	3.061
2.5	3.980
5.0	5.815
10.0	5.139
20.0	5.482

Minimum standard error of difference 0.6303  
 Average standard error of difference 0.6344  
 Maximum standard error of difference 0.6404

## Predictions from regression model

Response variate: no\_of\_laterals

genotype	Prediction
aux1	5.678
axr1	2.726
WT	5.677

Minimum standard error of difference 0.4883  
 Average standard error of difference 0.4913  
 Maximum standard error of difference 0.4928

## Predictions from regression model

Response variate: no\_of\_laterals

PAA_concentration_uM	Prediction		
	genotype aux1	axr1	WT
0.0	2.411	2.327	4.494
2.5	4.244	2.494	5.244
5.0	7.077	2.827	7.601
10.0	7.494	3.327	4.577
20.0	7.244	2.661	6.577

Minimum standard error of difference 1.092  
 Average standard error of difference 1.099  
 Maximum standard error of difference 1.146

### Supplementary Information 20: Analysis of the effects of NAA concentration on the number of lateral roots of *Arabidopsis thaliana* auxin mutant plants.

## Analysis of variance

Variate: no\_of\_laterals

Source of variation	d.f.	s.s.	m.s.	v.r.	F pr.
plate_rep stratum	3	2.69	0.90	0.08	
plate_rep.*Units* stratum					
NAA_concentration_nM	4	1188.50	297.13	27.25	<.001
genotype	2	604.74	302.37	27.73	<.001
NAA_concentration_nM.genotype	8	501.87	62.73	5.75	<.001
Residual	162	1766.31	10.90		
Total	179	4064.11			

Message: the following units have large residuals.

plate_rep 1 *units* 19	8.79	s.e. 3.13
plate_rep 3 *units* 19	11.79	s.e. 3.13
plate_rep 4 *units* 26	9.96	s.e. 3.13
plate_rep 4 *units* 34	9.21	s.e. 3.13

## Tables of means

Variate: no\_of\_laterals

Grand mean 5.72

NAA_concentration_nM	0	50	100	200	500
	2.11	4.06	6.36	6.31	9.78
genotype	aux1	axr1	WT		
	7.63	3.25	6.28		
NAA_concentration_nM	genotype	aux1	axr1	WT	
0		2.42	1.17	2.75	
50		6.83	0.75	4.58	
100		11.33	0.83	6.92	
200		8.17	3.08	7.67	
500		9.42	10.42	9.50	

## Standard errors of differences of means

Table	NAA_concentration_nM	genotype
rep.	36	60
d.f.	162	162
s.e.d.	0.778	0.603

Table	NAA_concentration_nM	genotype
rep.	12	
d.f.	162	
s.e.d.	1.348	

### Supplementary Information 21: Analysis of the effects of 2,4-D concentration on the angle of root growth as an absolute proportion of 180° of *Arabidopsis thaliana* auxin mutant plants.

## Analysis of variance

Variate: abs\_prop\_direction

Source of variation	d.f.	s.s.	m.s.	v.r.	F pr.
plate_rep stratum	3	0.04893	0.01631	0.49	
plate_rep.*Units* stratum					
%2_4_D_concentration_nM	4	0.28330	0.07083	2.15	0.078
genotype	2	2.01735	1.00867	30.55	<.001
%2_4_D_concentration_nM.genotype	8	0.23236	0.02905	0.88	0.535
Residual	162	5.34889	0.03302		



Total 179 7.93084

*Message: the following units have large residuals.*

plate_rep 1 *units* 20	0.522	s.e. 0.172
plate_rep 2 *units* 2	0.686	s.e. 0.172
plate_rep 3 *units* 30	0.644	s.e. 0.172
plate_rep 3 *units* 44	0.623	s.e. 0.172

## Tables of means

Variate: abs\_prop\_direction

Grand mean 0.167

%2_4_D_concentration_nM	0	25	50	100	200
	0.155	0.135	0.145	0.156	0.245

genotype	aux1	axr1	WT
	0.316	0.106	0.079

%2_4_D_concentration_nM	genotype	aux1	axr1	WT
0		0.287	0.107	0.072
25		0.218	0.146	0.041
50		0.307	0.087	0.042
100		0.313	0.064	0.092
200		0.458	0.129	0.149

## Standard errors of differences of means

Table	%2_4_D_concentration_nM	genotype
rep.	36	60
d.f.	162	162
s.e.d.	0.0428	0.0332

Table	%2_4_D_concentration_nM	genotype
rep.	12	
d.f.	162	
s.e.d.	0.0742	

**Supplementary Information 22: Analysis of the effects of PAA concentration on the angle of root growth as an absolute proportion of 180° of *Arabidopsis thaliana* auxin mutant plants.**

## Analysis of an unbalanced design using Genstat regression

Variate: abs\_prop\_direction

## Accumulated analysis of variance

Change	d.f.	s.s.	m.s.
	v.r.	F pr.	

+ plate_rep	3	0.08497	0.02832
	1.12	0.344	
+ PAA_concentration_uM	4	0.23628	0.05907
	2.33	0.058	
+ genotype	2	0.85929	0.42964
	16.96	<.001	
+ PAA_concentration_uM.genotype	8	0.36029	0.04504
	1.78	0.085	
Residual	160	4.05414	0.02534
Total	177	5.59498	0.03161

## Grand mean

0.1315

## Predictions from regression model

Response variate: abs\_prop\_direction

PAA_concentration_uM	Prediction
0.0	0.1685
2.5	0.1540
5.0	0.1579
10.0	0.0923
20.0	0.0842

Minimum standard error of difference 0.03752  
Average standard error of difference 0.03776  
Maximum standard error of difference 0.03812

## Predictions from regression model

Response variate: abs\_prop\_direction

genotype	Prediction
aux1	0.2263
axr1	0.0992
WT	0.0656

Minimum standard error of difference 0.02907  
Average standard error of difference 0.02925  
Maximum standard error of difference 0.02934

## Predictions from regression model

Response variate: abs\_prop\_direction

PAA_concentration_uM	Prediction			
	genotype aux1	axr1	WT	
0.0	0.3277	0.1083	0.0660	
2.5	0.2197	0.1248	0.1163	
5.0	0.3409	0.0768	0.0525	

10.0	0.1260	0.1026	0.0467
20.0	0.1235	0.0821	0.0455

Minimum standard error of difference 0.06499  
Average standard error of difference 0.06541  
Maximum standard error of difference 0.06820

**Supplementary Information 23: Analysis of the effects of NAA concentration on the angle of root growth as an absolute proportion of 180° of *Arabidopsis thaliana* auxin mutant plants.**

## Analysis of variance

Variate: abs\_prop\_direction

Source of variation	d.f.	(m.v.)	s.s.	m.s.	v.r.
	F	pr.			
plate_rep stratum	3		0.07169	0.02390	1.43
plate_rep.*Units* stratum					
NAA_concentration_nM	3	(1)	0.08739	0.02913	1.75
0.160					
genotype	2		0.47236	0.23618	14.17
	<.001				
NAA_concentration_nM.genotype	6	(2)	0.07951	0.01325	0.80
0.575					
Residual	129	(33)	2.14947	0.01666	
Total	143	(36)	2.73231		

*Message: the following units have large residuals.*

plate_rep 1 *units* 38	0.3052	s.e. 0.1093
plate_rep 1 *units* 39	0.7003	s.e. 0.1093
plate_rep 4 *units* 14	0.7189	s.e. 0.1093

## Tables of means

Variate: abs\_prop\_direction

Grand mean 0.1215

NAA_concentration_nM	0	50	100	200	500
	0.1215	0.1595	0.0979	0.1016	0.1270

genotype	aux1	axr1	WT
	0.1757	0.1360	0.0528

NAA_concentration_nM	genotype	aux1	axr1	WT
0		0.1810	0.1374	0.0461
50		0.2224	0.2042	0.0519
100		0.1416	0.1107	0.0414
200		0.1237	0.1181	0.0629

500                      0.2099      0.1096      0.0617

## Standard errors of differences of means

Table	NAA_concentration_nM	genotype
rep.	36	60
d.f.	129	129
s.e.d.	0.03043	0.02357

Table	NAA_concentration_nM	genotype
rep.	12	
d.f.	129	
s.e.d.	0.05270	

(Not adjusted for missing values)

### Supplementary Information 24: Analysis of the effects of 2,4-D and *Rhizoctonia solani* AG2-1 inoculation on the root growth of *Arabidopsis thaliana* auxin mutant plants.

## Analysis of variance

Variate: length

Source of variation	d.f.	s.s.	m.s.	v.r.	F pr.
Plate_rep stratum	3	2.1521	0.7174	2.06	
Plate_rep.*Units* stratum					
%24D_Concentration_nM	1	10.1046	10.1046	29.06	<.001
Genotype	2	21.2588	10.6294	30.57	<.001
Inoculation	1	0.0113	0.0113	0.03	0.857
%24D_Concentration_nM.Genotype	2	4.2791	2.1395	6.15	0.003
%24D_Concentration_nM.Inoculation	1	0.0832	0.0832	0.24	0.625
Genotype.Inoculation	2	0.3747	0.1874	0.54	0.585
%24D_Concentration_nM.Genotype.Inoculation	2	2.0151	1.0075	2.90	0.059
Residual	129	44.8556	0.3477		
Total	143	85.1345			

*Message: the following units have large residuals.*

Plate_rep 1 *units* 15	-1.692	s.e. 0.558
Plate_rep 2 *units* 5	-1.677	s.e. 0.558
Plate_rep 3 *units* 23	-1.522	s.e. 0.558
Plate_rep 4 *units* 33	-1.992	s.e. 0.558

## Tables of means

Variate: length

Grand mean 2.120

%24D_Concentration_nM	0	100
	2.385	1.855

Genotype	aux1	axr1	WT
	2.334	2.445	1.580

Inoculation	inoc	non-inoc
	2.111	2.129

%24D_Concentration_nM	Genotype	aux1	axr1	WT
0		2.488	2.578	2.089
100		2.180	2.313	1.072

%24D_Concentration_nM	Inoculation	inoc	non-inoc
0		2.400	2.369
100		1.822	1.888

Genotype	Inoculation	inoc	non-inoc
aux1		2.310	2.357
axr1		2.382	2.508
WT		1.640	1.521

%24D_Concentration_nM	Genotype	Inoculation	inoc	non-inoc
0	aux1		2.617	2.358
	axr1		2.382	2.773
	WT		2.200	1.977
100	aux1		2.004	2.356
	axr1		2.383	2.243
	WT		1.080	1.064

## Standard errors of differences of means

Table	%24D_Concentration_nM	Genotype
rep.	72	48
d.f.	129	129
s.e.d.	0.0983	0.1204

Table	Inoculation	%24D_Concentration_nM
rep.	72	Genotype
d.f.	129	24
s.e.d.	0.0983	129
		0.1702

Table	%24D_Concentration_nM	Genotype
rep.	Inoculation	Inoculation
d.f.	36	24
s.e.d.	129	129
	0.1390	0.1702

Table	%24D_Concentration_nM
rep.	Genotype
d.f.	Inoculation
s.e.d.	12
	129
	0.2407

**Supplementary Information 25: Analysis of the effects of PAA and *Rhizoctonia solani* AG2-1 inoculation on the root growth of *Arabidopsis thaliana* auxin mutant plants.**

## Analysis of variance

Variate: length

Source of variation	d.f.	s.s.	m.s.	v.r.	F pr.
Plate_rep stratum	3	1.9391	0.6464	1.67	
Plate_rep.*Units* stratum					
PAA_concentration_uM	1	5.5153	5.5153	14.28	<.001
Genotype	2	0.3691	0.1846	0.48	0.621
Inoculation	1	1.7798	1.7798	4.61	0.034
PAA_concentration_uM.Genotype	2	1.5306	0.7653	1.98	0.142
PAA_concentration_uM.Inoculation	1	0.0997	0.0997	0.26	0.612
Genotype.Inoculation	2	0.4786	0.2393	0.62	0.540
PAA_concentration_uM.Genotype.Inoculation	2	2.7767	1.3884	3.60	0.030
Residual	129	49.8176	0.3862		
Total	143	64.3067			

*Message: the following units have large residuals.*

Plate_rep 1 *units* 6	-1.659	s.e. 0.588
Plate_rep 1 *units* 14	1.741	s.e. 0.588

## Tables of means

Variate: length

Grand mean 1.690

PAA_concentration_uM	0	10			
	1.886	1.495			
Genotype	aux1	axr1	WT		
	1.726	1.726	1.619		
Inoculation	inoc	non-inoc			
	1.579	1.802			
PAA_concentration_uM	Genotype	aux1	axr1	WT	
	0	1.911	1.802	1.946	
	10	1.542	1.651	1.292	
PAA_concentration_uM	Inoculation	inoc	non-inoc		
	0	1.749	2.024		
	10	1.410	1.580		
Genotype	Inoculation	inoc	non-inoc		
	aux1	1.583	1.870		
	axr1	1.567	1.886		

	WT	1.589	1.649		
PAA_concentration_uM	Genotype	Inoculation	inoc	non-inoc	
0	aux1		1.891	1.930	
	axr1		1.431	2.172	
	WT		1.923	1.969	
10	aux1		1.274	1.810	
	axr1		1.702	1.600	
	WT		1.254	1.329	

## Standard errors of differences of means

Table	PAA_concentration_uM	Genotype
rep.	72	48
d.f.	129	129
s.e.d.	0.1036	0.1269

Table	Inoculation	PAA_concentration_uM
rep.	72	24
d.f.	129	129
s.e.d.	0.1036	0.1794

Table	PAA_concentration_uM	Genotype
rep.	Inoculation	Inoculation
d.f.	36	24
s.e.d.	129	129
	0.1465	0.1794

Table	PAA_concentration_uM
rep.	Genotype
d.f.	Inoculation
s.e.d.	12
	129
	0.2537

### Supplementary Information 26: Analysis of the effects of NAA and *Rhizoctonia solani* AG2-1 inoculation on the root growth of *Arabidopsis thaliana* auxin mutant plants.

## Analysis of variance

Variate: length

Source of variation	d.f.	s.s.	m.s.	v.r.	F pr.
plate_rep stratum	3	0.7637	0.2546	0.88	
plate_rep.*Units* stratum					
NAA_concentration_nM	1	0.9388	0.9388	3.25	0.074
genotype	2	5.0607	2.5304	8.77	<.001
inoculation	1	0.0822	0.0822	0.29	0.594
NAA_concentration_nM.genotype	2	1.1055	0.5527	1.92	0.151
NAA_concentration_nM.inoculation	1	0.2812	0.2812	0.97	0.325
genotype.inoculation	2	0.2089	0.1044	0.36	0.697

NAA_concentration_nM.genotype.inoculation	2	0.0092	0.0046	0.02	0.984
Residual	129	37.2051	0.2884		
Total	143	45.6551			

*Message: the following units have large residuals.*

plate_rep 1 *units* 14	-1.378	s.e. 0.508
plate_rep 2 *units* 23	-1.415	s.e. 0.508
plate_rep 3 *units* 31	-1.443	s.e. 0.508

## Tables of means

Variate: length

Grand mean 1.870

NAA_concentration_nM	0	200			
	1.950	1.789			
genotype	aux1	axr1	WT		
	1.635	2.094	1.880		
inoculation	inoc	non-inoc			
	1.894	1.846			
NAA_concentration_nM	genotype	aux1	axr1	WT	
0		1.708	2.072	2.072	
200		1.563	2.116	1.688	
NAA_concentration_nM	inoculation	inoc	non-inoc		
0		1.930	1.971		
200		1.857	1.721		
genotype	inoculation	inoc	non-inoc		
aux1		1.692	1.578		
axr1		2.138	2.050		
WT		1.851	1.910		
NAA_concentration_nM	genotype	inoculation	inoc	non-inoc	
0	aux1		1.729	1.686	
	axr1		2.061	2.083	
	WT		2.001	2.143	
200	aux1		1.656	1.470	
	axr1		2.215	2.017	
	WT		1.701	1.676	

## Standard errors of differences of means

Table	NAA_concentration_nM	genotype
rep.	72	48
d.f.	129	129
s.e.d.	0.0895	0.1096

Table	inoculation	NAA_concentration_nM
rep.	72	genotype
d.f.	129	24
		129



s.e.d.		0.0895		0.1550
Table	NAA_concentration_nM		genotype	
	inoculation		inoculation	
rep.		36		24
d.f.		129		129
s.e.d.		0.1266		0.1550
Table	NAA_concentration_nM		genotype	
	inoculation		inoculation	
rep.		12		
d.f.		129		
s.e.d.		0.2192		

**Supplementary Information 27: Analysis of the effects of 2,4-D and *Rhizoctonia solani* AG2-1 inoculation on the number of lateral roots of *Arabidopsis thaliana* auxin mutant plants.**

## Analysis of variance

Variate: n\_child

Source of variation	d.f.	s.s.	m.s.	v.r.	F pr.
Plate_rep stratum	3	3.4097	1.1366	1.16	
Plate_rep.*Units* stratum					
%24D_Concentration_nM	1	5.8403	5.8403	5.96	0.016
Genotype	2	14.1806	7.0903	7.24	0.001
Inoculation	1	0.3403	0.3403	0.35	0.557
%24D_Concentration_nM.Genotype	2	17.9306	8.9653	9.15	<.001
%24D_Concentration_nM.Inoculation	1	3.6736	3.6736	3.75	0.055
Genotype.Inoculation	2	1.2639	0.6319	0.65	0.526
%24D_Concentration_nM.Genotype.Inoculation	2	0.8472	0.4236	0.43	0.650
Residual	129	126.3403	0.9794		
Total	143	173.8264			

*Message: the following units have large residuals.*

Plate_rep 1 *units* 18	3.285	s.e. 0.937
Plate_rep 1 *units* 24	3.118	s.e. 0.937
Plate_rep 3 *units* 23	3.257	s.e. 0.937
Plate_rep 3 *units* 36	3.590	s.e. 0.937
Plate_rep 4 *units* 27	4.229	s.e. 0.937

## Tables of means

Variate: n\_child

Grand mean 0.535

%24D_Concentration_nM	0	100
-----------------------	---	-----

		0.333	0.736		
Genotype	aux1	axr1	WT		
	0.438	0.208	0.958		
Inoculation	inoc	non-inoc			
	0.486	0.583			
%24D_Concentration_nM	Genotype	aux1	axr1	WT	
	0	0.625	0.083	0.292	
	100	0.250	0.333	1.625	
%24D_Concentration_nM	Inoculation	inoc	non-inoc		
	0	0.444	0.222		
	100	0.528	0.944		
Genotype	Inoculation	inoc	non-inoc		
aux1		0.500	0.375		
axr1		0.042	0.375		
WT		0.917	1.000		
%24D_Concentration_nM	Genotype	Inoculation	inoc	non-inoc	
	0	aux1	0.750	0.500	
		axr1	0.083	0.083	
		WT	0.500	0.083	
	100	aux1	0.250	0.250	
		axr1	0.000	0.667	
		WT	1.333	1.917	

### Standard errors of differences of means

Table	%24D_Concentration_nM	Genotype
rep.	72	48
d.f.	129	129
s.e.d.	0.1649	0.2020

Table	Inoculation	%24D_Concentration_nM
rep.	72	24
d.f.	129	129
s.e.d.	0.1649	0.2857

Table	%24D_Concentration_nM	Genotype
rep.	Inoculation	Inoculation
d.f.	36	24
s.e.d.	129	129
	0.2333	0.2857

Table	%24D_Concentration_nM
rep.	Genotype
d.f.	Inoculation
s.e.d.	12
	129
	0.4040

**Supplementary Information 28: Analysis of the effects of PAA and *Rhizoctonia solani* AG2-1 inoculation on the number of lateral roots of *Arabidopsis thaliana* auxin mutant plants.**

## Analysis of variance

Variate: n\_child

Source of variation	d.f.	s.s.	m.s.	v.r.	F pr.
Plate_rep stratum	3	2.056	0.685	0.51	
Plate_rep.*Units* stratum					
PAA_concentration_uM	1	7.111	7.111	5.28	0.023
Genotype	2	19.056	9.528	7.08	0.001
Inoculation	1	0.000	0.000	0.00	1.000
PAA_concentration_uM.Genotype	2	14.389	7.194	5.35	0.006
PAA_concentration_uM.Inoculation	1	1.000	1.000	0.74	0.390
Genotype.Inoculation	2	0.500	0.250	0.19	0.831
PAA_concentration_uM.Genotype.Inoculation	2	1.167	0.583	0.43	0.649
Residual	129	173.611	1.346		
Total	143	218.889			

*Message: the following units have large residuals.*

Plate_rep 1 *units* 3	3.083	s.e. 1.098
Plate_rep 1 *units* 29	3.167	s.e. 1.098
Plate_rep 3 *units* 35	4.278	s.e. 1.098
Plate_rep 3 *units* 36	3.278	s.e. 1.098
Plate_rep 4 *units* 14	3.333	s.e. 1.098
Plate_rep 4 *units* 27	4.250	s.e. 1.098

## Tables of means

Variate: n\_child

Grand mean 0.722

PAA_concentration_uM	0	10			
	0.500	0.944			
Genotype	aux1	axr1	WT		
	1.000	0.208	0.958		
Inoculation	inoc	non-inoc			
	0.722	0.722			
PAA_concentration_uM	Genotype	aux1	axr1	WT	
	0	0.958	0.250	0.292	
	10	1.042	0.167	1.625	
PAA_concentration_uM	Inoculation	inoc	non-inoc		
	0	0.583	0.417		
	10	0.861	1.028		
Genotype	Inoculation	inoc	non-inoc		
	aux1	0.917	1.083		
	axr1	0.250	0.167		
	WT	1.000	0.917		

PAA_concentration_uM	Genotype	Inoculation	inoc	non-inoc
0	aux1		0.917	1.000
	axr1		0.500	0.000
	WT		0.333	0.250
10	aux1		0.917	1.167
	axr1		0.000	0.333
	WT		1.667	1.583

## Standard errors of differences of means

Table	PAA_concentration_uM	Genotype
rep.	72	48
d.f.	129	129
s.e.d.	0.1933	0.2368

Table	Inoculation	PAA_concentration_uM Genotype
rep.	72	24
d.f.	129	129
s.e.d.	0.1933	0.3349

Table	PAA_concentration_uM Inoculation	Genotype Inoculation
rep.	36	24
d.f.	129	129
s.e.d.	0.2734	0.3349

Table	PAA_concentration_uM Genotype Inoculation
rep.	12
d.f.	129
s.e.d.	0.4736

### Supplementary Information 29: Analysis of the effects of NAA and *Rhizoctonia solani* AG2-1 inoculation on the number of lateral roots of *Arabidopsis thaliana* auxin mutant plants.

## Analysis of variance

Variate: n\_child

Source of variation	d.f.	s.s.	m.s.	v.r.	F pr.
plate_rep stratum	3	3.354	1.118	0.46	
plate_rep.*Units* stratum					
NAA_concentration_nM	1	437.507	437.507	179.32	<.001
genotype	2	161.542	80.771	33.11	<.001
inoculation	1	1.563	1.563	0.64	0.425
NAA_concentration_nM.genotype	2	163.014	81.507	33.41	<.001
NAA_concentration_nM.inoculation	1	0.563	0.563	0.23	0.632
genotype.inoculation	2	0.792	0.396	0.16	0.850

NAA_concentration_nM.genotype.inoculation	2	0.875	0.437	0.18	0.836
Residual	129	314.729	2.440		
Total	143	1083.938			

*Message: the following units have large residuals.*

plate_rep 1 *units* 26	-4.19	s.e. 1.48
plate_rep 1 *units* 29	4.65	s.e. 1.48
plate_rep 1 *units* 35	-4.27	s.e. 1.48
plate_rep 2 *units* 26	5.53	s.e. 1.48
plate_rep 2 *units* 30	5.37	s.e. 1.48
plate_rep 3 *units* 25	4.95	s.e. 1.48
plate_rep 4 *units* 20	4.95	s.e. 1.48
plate_rep 4 *units* 30	-4.47	s.e. 1.48

## Tables of means

Variate: n\_child

Grand mean 1.81

NAA_concentration_nM	0	200			
	0.07	3.56			
genotype	aux1	axr1	WT		
	2.90	0.38	2.17		
inoculation	inoc	non-inoc			
	1.71	1.92			
NAA_concentration_nM	genotype	aux1	axr1	WT	
0		0.08	0.08	0.04	
200		5.71	0.67	4.29	
NAA_concentration_nM	inoculation	inoc	non-inoc		
0		0.03	0.11		
200		3.39	3.72		
genotype	inoculation	inoc	non-inoc		
aux1		2.75	3.04		
axr1		0.21	0.54		
WT		2.17	2.17		
NAA_concentration_nM	genotype	inoculation	inoc	non-inoc	
0	aux1		0.08	0.08	
	axr1		0.00	0.17	
	WT		0.00	0.08	
200	aux1		5.42	6.00	
	axr1		0.42	0.92	
	WT		4.33	4.25	

## Standard errors of differences of means

Table	NAA_concentration_nM	genotype
rep.	72	48
d.f.	129	129
s.e.d.	0.260	0.319

Table	inoculation	NAA_concentration_nM
		genotype
rep.	72	24
d.f.	129	129
s.e.d.	0.260	0.451

Table	NAA_concentration_nM	genotype
	inoculation	inoculation
rep.	36	24
d.f.	129	129
s.e.d.	0.368	0.451

Table	NAA_concentration_nM
	genotype
	inoculation
rep.	12
d.f.	129
s.e.d.	0.638

**Supplementary Information 30: Analysis of the effects of 2,4-D and *Rhizoctonia solani* AG2-1 inoculation on the angle of root growth as an absolute proportion of 180° of *Arabidopsis thaliana* auxin mutant plants.**

## Analysis of variance

Variate: abs\_prop\_direction

Source of variation	d.f.	s.s.	m.s.	v.r.	F pr.
Plate_rep stratum	3	0.33758	0.11253	4.53	
Plate_rep.*Units* stratum					
%24D_Concentration_nM	1	0.06059	0.06059	2.44	0.121
Genotype	2	2.02706	1.01353	40.84	<.001
Inoculation	1	0.00758	0.00758	0.31	0.582
%24D_Concentration_nM.Genotype	2	0.15091	0.07545	3.04	0.051
%24D_Concentration_nM.Inoculation	1	0.01619	0.01619	0.65	0.421
Genotype.Inoculation	2	0.00970	0.00485	0.20	0.823
%24D_Concentration_nM.Genotype.Inoculation	2	0.09797	0.04898	1.97	0.143
Residual	129	3.20126	0.02482		
Total	143	5.90883			

*Message: the following units have large residuals.*

Plate_rep 2 *units* 1	0.520	s.e. 0.149
Plate_rep 2 *units* 10	0.460	s.e. 0.149
Plate_rep 2 *units* 12	0.424	s.e. 0.149
Plate_rep 2 *units* 21	0.513	s.e. 0.149
Plate_rep 3 *units* 28	0.425	s.e. 0.149
Plate_rep 4 *units* 2	0.658	s.e. 0.149

## Tables of means

Variate: abs\_prop\_direction

Grand mean 0.164

%24D_Concentration_nM	0	100
	0.185	0.144

Genotype	aux1	axr1	WT
	0.330	0.104	0.059

Inoculation	inoc	non-inoc
	0.157	0.171

%24D_Concentration_nM	Genotype	aux1	axr1	WT
0		0.396	0.098	0.060
100		0.264	0.110	0.057

%24D_Concentration_nM	Inoculation	inoc	non-inoc
0		0.188	0.181
100		0.126	0.161

Genotype	Inoculation	inoc	non-inoc
aux1		0.334	0.326
axr1		0.092	0.116
WT		0.045	0.073

%24D_Concentration_nM	Genotype	Inoculation	inoc	non-inoc
0	aux1		0.448	0.344
	axr1		0.078	0.117
	WT		0.038	0.083
100	aux1		0.221	0.307
	axr1		0.105	0.115
	WT		0.052	0.063

## Standard errors of differences of means

Table	%24D_Concentration_nM	Genotype
rep.	72	48
d.f.	129	129
s.e.d.	0.0263	0.0322

Table	Inoculation	%24D_Concentration_nM
rep.	72	Genotype
d.f.	129	24
s.e.d.	0.0263	129
		0.0455

Table	%24D_Concentration_nM	Genotype
rep.	Inoculation	Inoculation
d.f.	36	24
s.e.d.	129	129
	0.0371	0.0455

Table	%24D_Concentration_nM
rep.	Genotype
d.f.	Inoculation
s.e.d.	12
	129
	0.0643

**Supplementary Information 31: Analysis of the effects of PAA and *Rhizoctonia solani* AG2-1 inoculation on the angle of root growth as an absolute proportion of 180° of *Arabidopsis thaliana* auxin mutant plants.**

## Analysis of variance

Variate: abs\_prop\_direction

Source of variation	d.f.	s.s.	m.s.	v.r.	F pr.
Plate_rep stratum	3	0.08906	0.02969	0.75	
Plate_rep.*Units* stratum					
PAA_concentration_uM	1	0.06334	0.06334	1.59	0.209
Genotype	2	3.13108	1.56554	39.40	<.001
Inoculation	1	0.00876	0.00876	0.22	0.639
PAA_concentration_uM.Genotype	2	0.23152	0.11576	2.91	0.058
PAA_concentration_uM.Inoculation	1	0.00086	0.00086	0.02	0.883
Genotype.Inoculation	2	0.00018	0.00009	0.00	0.998
PAA_concentration_uM.Genotype.Inoculation	2	0.03437	0.01718	0.43	0.650
Residual	129	5.12550	0.03973		
Total	143	8.68466			

*Message: the following units have large residuals.*

Plate_rep 2 *units* 10	0.528	s.e. 0.189
Plate_rep 3 *units* 1	0.551	s.e. 0.189
Plate_rep 4 *units* 21	0.664	s.e. 0.189

## Tables of means

Variate: abs\_prop\_direction

Grand mean 0.178

PAA_concentration_uM	0	10			
	0.199	0.157			
Genotype	aux1	axr1	WT		
	0.386	0.082	0.066		
Inoculation	inoc	non-inoc			
	0.186	0.170			
PAA_concentration_uM	Genotype	aux1	axr1	WT	
	0	0.463	0.067	0.067	
	10	0.310	0.097	0.065	
PAA_concentration_uM	Inoculation	inoc	non-inoc		
	0	0.209	0.189		
	10	0.162	0.152		



Genotype	Inoculation	inoc	non-inoc
aux1		0.393	0.379
axr1		0.089	0.075
WT		0.076	0.057

PAA_concentration_uM	Genotype	Inoculation	inoc	non-inoc
0	aux1		0.495	0.432
	axr1		0.067	0.067
	WT		0.067	0.068
10	aux1		0.292	0.327
	axr1		0.111	0.083
	WT		0.084	0.046

## Standard errors of differences of means

Table	PAA_concentration_uM	Genotype
rep.	72	48
d.f.	129	129
s.e.d.	0.0332	0.0407

Table	Inoculation	PAA_concentration_uM	Genotype
rep.	72		24
d.f.	129		129
s.e.d.	0.0332		0.0575

Table	PAA_concentration_uM	Inoculation	Genotype	Inoculation
rep.		36		24
d.f.		129		129
s.e.d.		0.0470		0.0575

Table	PAA_concentration_uM	Genotype	Inoculation
rep.		12	
d.f.		129	
s.e.d.		0.0814	

**Supplementary Information 32: Analysis of the effects of NAA and *Rhizoctonia solani* AG2-1 inoculation on the angle of root growth as an absolute proportion of 180° of *Arabidopsis thaliana* auxin mutant plants.**

## Analysis of variance

Variate: abs\_prop\_direction

Source of variation	d.f.	s.s.	m.s.	v.r.	F pr.
plate_rep stratum	3	0.03906	0.01302	0.72	
plate_rep.*Units* stratum					
NAA_concentration_nM	1	0.15439	0.15439	8.54	0.004
genotype	2	1.14922	0.57461	31.78	<.001
inoculation	1	0.01280	0.01280	0.71	0.402
NAA_concentration_nM.genotype	2	0.62686	0.31343	17.33	<.001

NAA_concentration_nM.inoculation					
	1	0.00003	0.00003	0.00	0.965
genotype.inoculation	2	0.00112	0.00056	0.03	0.970
NAA_concentration_nM.genotype.inoculation					
	2	0.00249	0.00125	0.07	0.933
Residual	129	2.33261	0.01808		
Total	143	4.31858			

*Message: the following units have large residuals.*

plate_rep 1 *units* 1	0.527	s.e. 0.127
plate_rep 1 *units* 3	0.529	s.e. 0.127
plate_rep 3 *units* 12	0.487	s.e. 0.127
plate_rep 3 *units* 21	0.361	s.e. 0.127
plate_rep 4 *units* 10	0.383	s.e. 0.127

## Tables of means

Variate: abs\_prop\_direction

Grand mean 0.143

NAA_concentration_nM		0	200		
		0.176	0.111		
genotype	aux1	axr1	WT		
	0.268	0.100	0.063		
inoculation	inoc	non-inoc			
	0.134	0.153			
NAA_concentration_nM	genotype	aux1	axr1	WT	
	0	0.394	0.079	0.056	
	200	0.142	0.120	0.070	
NAA_concentration_nM	inoculation	inoc	non-inoc		
	0	0.167	0.185		
	200	0.101	0.121		
genotype	inoculation	inoc	non-inoc		
aux1		0.255	0.281		
axr1		0.093	0.106		
WT		0.054	0.072		
NAA_concentration_nM	genotype	inoculation	inoc	non-inoc	
	0	aux1	0.382	0.405	
		axr1	0.068	0.090	
		WT	0.052	0.060	
	200	aux1	0.128	0.157	
		axr1	0.119	0.122	
		WT	0.056	0.083	

## Standard errors of differences of means

Table	NAA_concentration_nM	genotype
rep.	72	48
d.f.	129	129
s.e.d.	0.0224	0.0274

Table	inoculation	NAA_concentration_nM
rep.	72	genotype
d.f.	129	24
s.e.d.	0.0224	129
		0.0388

Table	NAA_concentration_nM	genotype
rep.	inoculation	inoculation
d.f.	36	24
s.e.d.	129	129
	0.0317	0.0388

Table	NAA_concentration_nM
rep.	genotype
d.f.	inoculation
s.e.d.	12
	129
	0.0549

**Supplementary Information 33: Nonlinear regression analysis using a critical exponential standard curve to measure the effect of exogenous PAA concentrations on *Rhizoctonia solani* AG2-1 growth in liquid media**

## Nonlinear regression analysis

Response variate: percentage\_of\_0mM  
 Explanatory: Concentration\_mM  
 Fitted Curve:  $A + (B + C * X) * (R^{**X})$   
 Constraints:  $R < 1$

## Summary of analysis

Source	d.f.	s.s.	m.s.	v.r.	F pr.
Regression	3	4.9626	1.65421	30.18	<.001
Residual	14	0.7675	0.05482		
Total	17	5.7301	0.33706		

Percentage variance accounted for 83.7  
 Standard error of observations is estimated to be 0.234.

*Message: the following units have large standardized residuals.*

Unit	Response	Residual
4	1.751	2.39
9	0.873	-2.21

## Estimates of parameters

Parameter	estimate	s.e.
R	0.1920	0.0833
B	1.053	0.175
C	3.85	1.63
A	0.019	0.113

## Accumulated analysis of variance

Change	d.f.	s.s.	m.s.	v.r.	F pr.
+ Concentration_mM	3	4.96263	1.65421	30.18	<.001
Residual	14	0.76746	0.05482		
Total	17	5.73009	0.33706		

**Supplementary Information 34: Analysis of variance for the concentrations of IAA identified by LC-MS/MS analysis from broth cultures of *Rhizoctonia solani* AG2-1.**

## Analysis of variance

Variate: Concentration

Source of variation	d.f.	(m.v.)	s.s.	m.s.	v.r.
	F pr.				
Rep stratum	5		326.2	65.2	0.27
Rep.*Units* stratum	6		15300.6	2550.1	10.57
Sample	<.001				
Residual	29	(1)	6996.3	241.3	
Total	40	(1)	22416.9		

*Message: the following units have large residuals.*

Rep 1 *units* 2	27.8	s.e. 12.9
Rep 2 *units* 4	50.2	s.e. 12.9
Rep 2 *units* 7	-27.3	s.e. 12.9

## Tables of means

Variate: Concentration

Grand mean 22.2

Sample	#1926	#1927	#1933	#1934
	39.1	13.6	14.5	24.0
Sample	#1942	#2076	Non-inoc control	
	10.8	58.0	-4.5	

## Standard errors of differences of means

Table	Sample
rep.	6
d.f.	29
s.e.d.	8.97

(Not adjusted for missing values)

## Tukey's 95% confidence intervals

### Sample

	Mean	
Non-inoc control	-4.51	a
#1942	10.84	ab
#1927	13.60	ab
#1933	14.46	ab
#1934	24.04	b
#1926	39.12	bc
#2076	58.03	c

**Supplementary Information 35: Analysis of variance for the concentrations of PAA identified by LC-MS/MS analysis from broth cultures of *Rhizoctonia solani* AG2-1.**

## Analysis of an unbalanced design using Genstat regression

Variate: Concentration

### Accumulated analysis of variance

Change	d.f. v.r.	s.s. F pr.	m.s.
+ Rep	5 1.44	70.536 0.252	14.107
+ Sample	6 3.31	194.688 0.019	32.448
Residual	21	206.148	9.817
Total	32	471.373	14.730

### Predictions from regression model

Response variate: Concentration

Sample	Prediction
#1926	0.228
#1927	0.734
#1933	0.497
#1934	0.547
#1942	0.493
#2076	5.069
Non-inoc control	-3.576

Minimum standard error of difference	1.898
Average standard error of difference	2.083
Maximum standard error of difference	2.394

### Fisher's least significant difference test

## Sample

*Warning 2, code UF 2, statement 248 in procedure MCOMPARISON*

Variances vary and decisions regarding group membership are inconsistent, so there may be gaps in the lines or letters linking means in identical groups.

	Mean	
Non-inoc control	-3.576	a
#1926	0.228	ab
#1942	0.493	b
#1933	0.497	b
#1934	0.547	b
#1927	0.734	abc
#2076	5.069	c

**Supplementary Information 36: Promising candidate genes identified through GEMs analysis. Additional information from TAIR (Huala *et al.*, 2001) is shown along with the highest log<sub>10</sub>P value for the GEMs associated with these genes.**

<i>A. thaliana</i> gene identifier	Gene names	GO Biological process	Additional description	Highest log <sub>10</sub> P value
AT1G09970	RECEPTOR-LIKE KINASE 7, RLK7	innate immune response, protein autophosphorylation, response to oxidative stress, seed germination	RLK7 belongs to a leucine-rich repeat class of receptor-like kinase (LRR-RLKs). It is involved in the control of germination speed and the tolerance to oxidant stress.	6.42
AT1G63740		signal transduction	Disease resistance protein (TIR-NBS-LRR class) family.	5.95
AT5G18650	MIEL1, MYB30-INTERACTING E3 LIGASE 1	negative regulation of defence response to bacterium, positive regulation of transcription factor catabolic process, protein ubiquitination, ubiquitin-dependent protein catabolic process	Encodes a RING-type E3 ubiquitin ligase that interacts with and ubiquitinates MYB30, leads to MYB30 proteasomal degradation and downregulation of its transcriptional activity. Since MYB30 is a positive regulator of <i>Arabidopsis</i> HR and defence responses, MIEL1 is involved in the negative regulation of these processes.	4.67
AT3G51570		signal transduction	Disease resistance protein (TIR-NBS-LRR class) family.	4.77

<i>A. thaliana</i> gene identifier	Gene names	GO Biological process	Additional description	Highest log <sub>10</sub> P value
AT3G51550	FER, FERONIA	circadian regulation of gene expression, defence response to fungus, negative regulation of abscisic acid-activated signalling pathway, negative regulation of cell growth, pollen tube reception, post-embryonic development, protein autophosphorylation, response to brassinosteroid, response to ethylene, root development, stomatal movement	Encodes a synergid-expressed, plasma-membrane localized receptor-like kinase that accumulates asymmetrically in the synergid membrane at the filiform apparatus and mediates male-female gametophyte interactions during pollen tube reception. Also involved in powdery mildew infection. Mutants show faster root elongation under dim light, the protein is required for intracellular accumulation of AHA2 under dim-light growth conditions. Positively regulates flowering by modulating the transcript accumulation and mRNA alternative splicing of certain flowering-related genes, including FLOWERING LOCUS C (FLC) and its homolog MADS AFFECTING FLOWERING (MAF). However, the RALF1 ligand negatively regulates flowering compared with FER.	6.02



<i>A. thaliana</i> gene identifier	Gene names	GO Biological process	Additional description	Highest log <sub>10</sub> P value
AT2G46070	MITOGEN-ACTIVATED PROTEIN KINASE 12, MPK12	cellular response to carbon dioxide, intracellular signal transduction, protein autophosphorylation, regulation of gene expression, regulation of stomatal closure, regulation of stomatal movement, response to auxin, response to indolebutyric acid, signal transduction	MPK12 interacts with the IBR5 protein phosphatase <i>in vitro</i> and <i>in vivo</i> , and it can be dephosphorylated and inactivated by IBR5. MPK12 appears to be a negative regulator of auxin signalling. MPK12 RNAi lines are hypersensitive to auxin in root elongation and transcriptional response assays, but they appear to have normal sensitivity to ABA. MPK12 is a nuclear protein and its kinase activity is increased following auxin treatment. MPK12 transcripts are widely expressed in seedlings, but MPK12 expression is stronger in guard cells than in other cell types in mature plants.	4.34
AT4G11690	ABA OVERLY SENSITIVE MUTANT, ABO8	mitochondrial mRNA modification, response to abscisic acid	Encodes ABO8, a pentatricopeptide repeat (PPR) protein responsible for the splicing of NAD4 intron 3 in mitochondrial complex I. Abo8 mutants accumulate more reactive oxygen species (ROS) in root tips than the wild type.	4.44

<i>A. thaliana</i> gene identifier	Gene names	GO Biological process	Additional description	Highest log <sub>10</sub> P value
AT5G43470	HRT, HYPERSENSITIVE RESPONSE TO TCV, RCY1, RECOGNITION OF PERONOSPORA PARASITICA 8, RESISTANT TO CMV(Y) 1, RPP8	cellular response to salicylic acid stimulus, defence response, defence response to virus, plant-type hypersensitive response, positive regulation of defence response to virus by host, response to absence of light, response to blue light, response to light stimulus, response to oomycetes, response to other organism, response to salicylic acid, response to wounding	Confers resistance to <i>Peronospora parasitica</i> . In <i>Arabidopsis</i> ecotype Dijon-17, HRT-mediated signalling is dependent on light for the induction of hypersensitive response and resistance to turnip crinkle virus.	4.32
AT1G15750	TOPLESS, TPL, WSIP1, WUS-INTERACTING PROTEIN 1	jasmonic acid mediated signalling pathway, negative regulation of transcription, DNA-templated, primary shoot apical meristem specification, regulation of transcription, DNA-templated, response to auxin, xylem and phloem pattern formation	Encodes a protein with several WD40 repeats at the C-terminus and predicted protein-protein interaction domains at the N-terminus. Together with the TOPLESS-RELATED PROTEINS (TPRs), it is thought to be involved in transcriptional repression of root-promoting genes in the top half of the embryo during the transition stage of embryogenesis. It can also interact with IAA12 through the EAR domain of IAA12 and the CTLH domain of TPL. The ability of IAA12 to repress transcription is diminished in a <i>tpl-1</i> mutant background.	4.34

<i>A. thaliana</i> gene identifier	Gene names	GO Biological process	Additional description	Highest log <sub>10</sub> P value
AT1G30570	HERCULES RECEPTOR KINASE 2, HERK2	protein autophosphorylation, response to brassinosteroid, unidimensional cell growth	Encodes HERCULES2 (HERK2), a receptor kinase regulated by Brassinosteroids and required for cell elongation during vegetative growth.	3.88
AT3G46290	HERCULES RECEPTOR KINASE 1, HERK1	brassinosteroid mediated signalling pathway, post-embryonic development, protein autophosphorylation, regulation of unidimensional cell growth, response to brassinosteroid, unidimensional cell growth	Encodes HERCULES1 (HERK1), a receptor kinase regulated by Brassinosteroids and required for cell elongation during vegetative growth.	4.17
AT3G23750	BAK1-ASSOCIATING RECEPTOR-LIKE KINASE 1, BARK1	protein phosphorylation	Leucine-rich repeat protein kinase family protein.	4.46
AT4G05320	POLYUBIQUITIN 10, UBI10, UBIQUITIN 10, UBQ10	aging, cellular protein modification process, modification-dependent protein catabolic process, protein ubiquitination, response to salicylic acid	One of five polyubiquitin genes in <i>A.</i> <i>thaliana</i> . These genes encode the highly conserved 76-amino acid protein ubiquitin that is covalently attached to substrate proteins targeting most for degradation. Polyubiquitin genes are characterized by the presence of tandem repeats of the 228 bp that encode a ubiquitin monomer. Induced by salicylic acid. Independent of NPR1 for their induction by salicylic acid.	4.22

<i>A. thaliana</i> gene identifier	Gene names	GO Biological process	Additional description	Highest log <sub>10</sub> P value
AT3G14420	GLYCOLATE OXIDASE 1, GOX1	defence response to bacterium, hydrogen peroxide biosynthetic process, oxidative photosynthetic carbon pathway	Encodes a glycolate oxidase that modulates reactive oxygen species- mediated signal transduction during nonhost resistance.	3.88
AT2G32800	AP4.3A, L-TYPE LECTIN RECEPTOR KINASE S.2, LECRK-S.2	cellular response to jasmonic acid stimulus, cellular response to salicylic acid stimulus, defence response, defence response to bacterium, defence response to oomycetes, protein phosphorylation, response to bacterium, response to wounding	Protein kinase family protein.	3.24
AT3G02880	KIN7, KINASE 7	protein phosphorylation, response to abscisic acid	Leucine-rich repeat protein kinase family protein.	3.14
AT5G53160	PYL8, PYR1-LIKE 8, RCAR3, REGULATORY COMPONENTS OF ABA RECEPTOR 3	abscisic acid-activated signalling pathway, positive regulation of abscisic acid-activated signalling pathway, regulation of protein serine/threonine phosphatase activity, response to abscisic acid	Encodes RCAR3, a regulatory component of ABA receptor. Interacts with protein phosphatase 2Cs ABI1 and ABI2. Stimulates ABA signalling.	3.41
AT5G65210	TGA1, TGACG SEQUENCE- SPECIFIC BINDING PROTEIN 1	defence response to bacterium, regulation of transcription, DNA- templated, transcription, DNA- templated	Encodes TGA1, a redox-controlled regulator of systemic acquired resistance. TGA1 targets the activation sequence-1 (as-1) element of the promoter region of	2.83

<i>A. thaliana</i> gene identifier	Gene names	GO Biological process	Additional description	Highest log <sub>10</sub> P value
			defense proteins. TGA1 are S-nitrosylated.	
AT5G19010	MITOGEN-ACTIVATED PROTEIN KINASE 16, MPK16	intracellular signal transduction, regulation of gene expression, signal transduction	Member of MAP Kinase.	2.81
AT5G66900	N REQUIREMENT GENE 1.1, NRG1.1		RPW8 -CNL gene is required for signal transduction of TNLs; functionally redundant to NRG1.2. Exhibits autoimmunity.	2.99
AT4G11890	ABA- AND OSMOTIC- STRESS-INDUCIBLE RECEPTOR-LIKE CYTOSOLIC KINASE1, ARCK1, CRK45, CYSTEINE- RICH RECEPTOR-LIKE PROTEIN KINASE 45	positive regulation of defence response, protein phosphorylation, regulation of abscisic acid-activated signalling pathway, response to abscisic acid, response to cold, response to oomycetes, response to salt stress, response to water deprivation	Encodes a receptor-like cytosolic kinase ARCK1. Negatively controls abscisic acid and osmotic stress signal transduction.	3.73
AT1G44170	ALDEHYDE DEHYDROGENASE 3H1, ALDEHYDE DEHYDROGENASE 4, ALDH3H1, ALDH4	cellular aldehyde metabolic process, response to abscisic acid, response to desiccation, response to salt stress	Encodes an aldehyde dehydrogenase induced by ABA and dehydration that can oxidize saturated aliphatic aldehydes. It is also able to oxidize beta-unsaturated aldehydes, but not aromatic aldehydes.	2.79

<i>A. thaliana</i> gene identifier	Gene names	GO Biological process	Additional description	Highest log <sub>10</sub> P value
			Activity of ALDH3H1 is NAD +- dependent.	
AT2G27050	EIL1, ETHYLENE- INSENSITIVE3-LIKE 1	defence response to bacterium, ethylene-activated signalling pathway, response to ethylene		4.10
AT3G20770	EIN3, ETHYLENE- INSENSITIVE3	defence response to bacterium, ethylene-activated signalling pathway, regulation of L-ascorbic acid biosynthetic process, regulation of transcription, DNA-templated, response to ethylene, response to hypoxia, sugar mediated signalling pathway	Encodes a nuclear transcription factor that initiates downstream transcriptional cascades for ethylene responses. EIN3 interacts with MYC2, MYC3 and MYC4 to inhibit jasmonate-induced expression of wound-responsive genes and herbivory- inducible genes, and plant defence against generalist herbivores.	3.55
AT3G23030	IAA2, INDOLE-3-ACETIC ACID INDUCIBLE 2	regulation of transcription, DNA- templated, response to auxin	Auxin inducible gene expressed in the nucleus.	3.24
AT5G46330	FLAGELLIN-SENSITIVE 2, FLS2, MPL12.8	defence response by callose deposition in cell wall, defence response to bacterium, detection of bacterium, protein phosphorylation, receptor-mediated endocytosis, regulation of anion channel activity	Encodes a leucine-rich repeat serine/threonine protein kinase that is expressed ubiquitously. FLS2 is involved in MAP kinase signalling relay involved in innate immunity. Essential in the perception of flagellin, a potent elicitor of the defence response. FLS2 is directed	2.81

<i>A. thaliana</i> gene identifier	Gene names	GO Biological process	Additional description	Highest log <sub>10</sub> P value
			for degradation by the bacterial ubiquitin ligase AvrPtoB.	
AT2G17520	INOSITOL REQUIRING 1-2, IRE1-2, IRE1A	IRE1-mediated unfolded protein response, RNA splicing, defence response to bacterium, incompatible interaction, endoplasmic reticulum unfolded protein response, intrinsic apoptotic signalling pathway in response to endoplasmic reticulum stress, protein autophosphorylation, response to salicylic acid	Encodes an endoribonuclease/protein kinase IRE1-like protein that is predicted to form a type I transmembrane protein structure and contain kinase/endoribonuclease domains at their C-terminal halves. The transcript levels for several ER-stress responsive genes, including six protein disulphide isomerases (PDIs), BiP2, and AtbZIP60 are not affected in ire1-2 null mutants.	4.24
AT3G06550	REDUCED WALL ACETYLATION 2, RWA2	carbohydrate metabolic process, defence response to fungus, plant-type secondary cell wall biogenesis, polysaccharide metabolic process, response to abscisic acid, xylan acetylation, xylan biosynthetic process, xylan metabolic process, xyloglucan metabolic process	Encodes a homolog of the protein Cas1p known to be involved in polysaccharide O-acetylation in <i>Cryptococcus neoformans</i> . Mutants show reduced cell wall polysaccharide acetylation and increased resistance to <i>Botrytis cinerea</i> . The protein is expressed in the Golgi and is involved in the acetylation of xylan during secondary wall biosynthesis.	3.98

<i>A. thaliana</i> gene identifier	Gene names	GO Biological process	Additional description	Highest log <sub>10</sub> P value
AT1G07640	OBP2, UAS-TAGGED ROOT PATTERNING3, URP3	regionalization, regulation of glucosinolate biosynthetic process, regulation of root development, regulation of transcription, DNA-templated, response to insect, response to jasmonic acid, response to wounding, root radial pattern formation	A member of the DOF transcription factors. Prominently expressed in the phloem of leaves and other organs. Expression is induced by wounding, MeJA and insect feeding. Upregulates glucosinolate biosynthesis. PEAR protein involved in the formation of a short-range concentration gradient that peaks at protophloem sieve elements and activates gene expression that promotes radial growth. Locally promotes transcription of inhibitory HD-ZIP III genes, and thereby establishes a negative-feedback loop that forms a robust boundary that demarks the zone of cell division.	3.70
AT3G55560	AGF2, AHL15, AT-HOOK MOTIF NUCLEAR-LOCALIZED PROTEIN 15, AT-HOOK PROTEIN OF GA FEEDBACK 2	negative regulation of innate immune response	AT-hook protein of GA feedback 2.	3.43



<i>A. thaliana</i> gene identifier	Gene names	GO Biological process	Additional description	Highest log <sub>10</sub> P value
AT1G02860	BAH1, BENZOIC ACID HYPERSENSITIVE 1, NITROGEN LIMITATION ADAPTATION, NLA, SYG1	defence response to bacterium, plant-type hypersensitive response, protein ubiquitination, regulation of salicylic acid metabolic process, response to benzoic acid, response to nitrate, response to salicylic acid, salicylic acid biosynthetic process, systemic acquired resistance	Encodes a ubiquitin E3 ligase with RING and SPX domains that is involved in mediating immune responses and mediates degradation of PHT1s at plasma membranes. Targeted by MIR827. Ubiquitinates PHT1;3, PHT1;2, PHT1;1/AtPT1 and PHT1;4/AtPT2.	3.51
AT1G80460	GLI1, NHO1, NONHOST RESISTANCE TO P. S. PHASEOLICOLA 1	defence response to bacterium, glycerol catabolic process, glycerol metabolic process, glycerol-3- phosphate biosynthetic process, glycerol-3-phosphate metabolic process, phosphorylation, response to bacterium, response to karrikin, response to microbial phytotoxin, response to molecule of bacterial origin, triglyceride metabolic process	Encodes a protein similar to glycerol kinase, which converts glycerol to glycerol 3-phosphate and performs a rate-limiting step in glycerol metabolism. This gene is required for both general and specific resistance against bacteria and fungi. <i>Arabidopsis thaliana</i> glycerol kinase (GLR1) mRNA. Involved in flagellin-induced non-host resistance to <i>Pseudomonas</i> . Coronatine partially suppresses flagellin-induced expression of NHO1.	3.31
AT1G05010	ACO4, EAT1, EFE, ETHYLENE FORMING ENZYME, ETHYLENE- FORMING ENZYME	cellular response to fatty acid, ethylene biosynthetic process, oxidation-reduction process, response to fungus	Encodes 1-aminocyclopropane-1- carboxylate oxidase.	3.49

<i>A. thaliana</i> gene identifier	Gene names	GO Biological process	Additional description	Highest log <sub>10</sub> P value
AT3G14415	GLYCOLATE OXIDASE 2, GOX2	defence response to bacterium, hydrogen peroxide biosynthetic process, oxidative photosynthetic carbon pathway	Encodes a glycolate oxidase that modulates reactive oxygen species- mediated signal transduction during nonhost resistance.	3.18
AT1G79380	RGLG4, RING DOMAIN LIGASE 4	defence response to bacterium, jasmonic acid mediated signalling pathway, response to wounding	Encodes a ubiquitin ligase that is an essential upstream modulator of JA signalling in response to various stimuli.	2.92
AT5G60360	AALP, ALEURAIN-LIKE PROTEASE, ALP, SAG2, SENESCENCE ASSOCIATED GENE2	aging, proteolysis, proteolysis involved in cellular protein catabolic process, response to ethylene	Encodes a senescence-associated thiol protease.	2.76

**Supplementary Information 37: Pr (>F) and log10P values for the genes selected from GWAS analysis. Pr (>F) values are given for both the hypocotyl and root disease indices (DIH%, DIR%) and log10P values. These are given for all GEMs across the *Brassica napus* genomes and differentiated by the chromosome on which they were found. GEMs with a Pr (>F) value greater than 0.05 are not shown.**

<i>A. thaliana</i> gene identifier	<i>B. napus</i> loci	Pr (>F)	Log10P
AT1G22530	A09_031604381_031608260	DIH% A09: <.001	DIH% A09: 5.595
	C05_012131150_012133789	DIH% C05: <.001	DIH% C05: 3.764
		DIR% A09: <.001	DIR% A09: 5.007
		DIR% C05: 0.001	DIR% C05: 2.893
AT1G29720	A02_025900692_025904771.001	DIH% A02: 0.003	DIH% A02: 2.496
	A05_015856274_015853926	DIH% A05: <.001	DIH% A05: 3.486
	A07_009613857_009609858	DIH% A07: 0.001	DIH% A07: 2.929
	A08_017897547_017916374	DIH% A08: 0.036	DIH% A08: 1.441
	C03_052350395_052356011	DIH% C03: 0.013	DIH% C03: 1.886
	C05_027432309_027437206	DIH% C05: 0.006	DIH% C05: 2.253
	C06_016177421_016182484	DIH% C06: 0.043	DIH% C06: 1.366
		DIR% A02: 0.006	DIR% A02: 2.247
		DIR% A05: 0.002	DIR% A05: 2.788
		DIR% A07: 0.002	DIR% A07: 2.619
		DIR% A08: 0.010	DIR% A08: 2.000
		DIR% C03: 0.023	DIR% C03: 1.638
	DIR% C05: 0.012	DIR% C05: 1.904	

AT1G31770	A09_025773795_025770164	DIH% A09: 0.034 DIR% A09:0.030	DIH% A09: 1.473 DIR% A09: 1.519
AT1G63740	A04_017309981_017306816	DIH% A04: <.001 DIR% A04: <.001	DIH% A04: 4.798 DIR% A04: 5.952
AT1G80410	A07_028405317_028398856 C06_039686055_039692634 A02_016425680_016417367 C02_027236906_027243307	DIH% A07: <.001 DIH% C06: <.001 DIR% A02: 0.022 DIR% A07: <.001 DIR% C02: 0.034 DIR% C06: <.001	DIH% A07:4.068 DIH% C06: 6.155 DIR% A02: 1.656 DIR% A07: 3.643 DIR% C02:1.465 DIR% C06: 4.817
AT1G80450	A07_028391964_028391461 C06_039673647_039674150	DIH% A07: <.001 DIH% C06: <.001 DIR% A07: 0.005 DIR% C06: <.001	DIH% A07: 3.876 DIH% C06: 5.389 DIR% A07: 2.267 DIR% C06: 5.864
AT2G01570	A09_015678837_015680576 C07_029836437_029838176	DIH% A09: 0.023 DIH% C07: <.001 DIR% A09: 0.023 DIR% C07: <.001	DIH% A09: 1.639 DIH% C07: 4.465 DIR% A09: 1.634 DIR% C07: 4.347
AT3G21360	A03_004272015_004273142.001 A04_002009590_002009297.001 A09_004397130_004396208 C08_022227969_022232922.003	DIH% A03: <.001 DIH% A04: <.001 DIH% A09: 0.001 DIH% C08: <.001 DIR% A03: <.001	DIH% A03: 3.661 DIH% A04: 4.553 DIH% A09: 2.840 DIH% C08: 4.401 DIR% A03: 4.065

		DIR% A04: <.001	DIR% A04: 4.703
		DIR% A09: <.001	DIR% A09: 3.454
		DIR% C08: <.001	DIR% C08: 4.865
AT4G14580	A01_012996122_012997710	DIH% A01: <.001	DIH% A01: 4.781
		DIR% A01: <.001	DIR% A01:4.863
AT4G18010	A01_005037291_005040095	DIH% A01: <.001	DIH% A01: 7.615
	A03_025135870_025138904	DIH% A03: 0.030	DIH% A03: 1.523
	C01_006522441_006525299	DIH% C01: <.001	DIH% C01: 3.121
	C07_040808880_040812141	DIH% C07: 0.048	DIH% C07:1.315
		DIR% A01: <.001	DIR% A01: 5.787
		DIR% C01: 0.006	DIR% C01: 2.191
AT5G57940	A02_006105987_006108902	DIH% A02: <.001	DIH% A02: 5.172
	C02_008713570_008716224	DIH% C02: 0.011	DIH% C02: 1.961
		DIR% A02: <.001	DIR% A02: 5.939
		DIR% C02: 0.016	DIR% C02: 1.809

---

## Professional Internships for PhD Student (PIPS)

### reflection

#### Note to examiners

This statement is included as an appendix to the thesis in order that the thesis accurately captures the PhD training experienced by the candidate as a BBSRC Doctoral Training Partnership student.

The Professional Internship for PhD Students is a compulsory 3-month placement which must be undertaken by DTP students. It is usually centered on a specific project and must not be related to the PhD project. This reflective statement is designed to capture the skills development which has taken place during the student's placement and the impact on their career plans it has had.

#### PIPS Reflective Statement

I completed my Professional Internship for Postgraduate Students (PIPS) at the Agriculture and Horticulture Development Board (AHDB) from June to August 2021. Due to COVID-19, I was predominantly based working from home, but I did have the opportunity to attend a couple of in-person events.

During my time at the AHDB, I worked on two projects. The first was to produce horizon scans and prioritisation spreadsheets for two diseases of Oilseed Rape (OSR): Light Leaf Spot (LLS) and Phoma Leaf Spot

(PLS). This involved writing a report on the biology and current management of both diseases and exploring future opportunities and challenges. The prioritisation spreadsheets will be used to inform future research calls. The second project was to create and optimise webpages for the Encyclopaedia of pests and natural enemies in field crops, and the Encyclopaedia of arable weeds. These documents both exist as pdfs and in print, but the information was not previously displayed as webpages, only as a download of the original document. The creation of these pages and their search-engine optimisation has made it easier for users to find the information they are searching for, enabling the information to reach a greater audience in a more user-friendly manner.

As well as working on these projects, I also had the opportunity to visit the Cereals Event, where I was able to network with a wide variety of research and industry contacts and gain a greater understanding of the bigger picture for arable farming. I also attended two Monitor Farm events, which gave me the opportunity to meet farmers and hear first-hand about the problems they are facing.

Working on the horizon scans has needed me to think about future research and required creative thinking about the opportunities arising from research. I have learnt a lot about the two diseases in a short time and have reflected on the current management strategies and previous research. I have developed my abilities to critically analyse research reports and synthesise ideas about future work. I gave a virtual

presentation about the horizon scans to the Crop Health and IPM group towards the end of my placement. Working on the Knowledge Library content has given me the opportunity to develop my communication skills and understand how best to communicate via the web. It has also given me the chance to learn about varied arable pests and weeds. As the placement has been mostly home-based, I have continued to develop as an independent worker, and had the opportunity to collaborate with new colleagues virtually.

Working at the AHDB has given me the chance to meet crop protection scientists working outside of academia and meet PhD holders who have followed a wide variety of career paths. Attending the Cereals Event also gave me the chance to meet a lot of people who work in all areas of agriculture and has given me a much better understanding of the kinds of roles available to me after my PhD.

Overall, I have really enjoyed my time at the AHDB, and I'm grateful to all those who helped arrange the placement and supported me throughout.



## COVID Impact Statement

The COVID-19 pandemic had a significant impact on my PhD research. After the lockdown began in March 2020, I was first able to return to the laboratory in July 2020, although this was only for a few days to complete a specific experiment which I started before the pandemic. I was unable to re-start growing plants until October 2020 and did not return to the laboratory on a regular basis until November 2020. I was unable to use my office computer on campus until the middle of November 2020, and this was restricted to one quarter of the time due to the room being shared between three other PhD students.

After the return to working on campus, work remained much slower, more difficult and more stressful than before COVID. Bottlenecks in laboratory spaces formed as we could not use laminar flow cabinets. Equipment breakdowns, including the benchtop autoclave and pH meter, were more frequent and took a long time to be repaired due to pandemic related backlogs and slow deliveries. Reduced laboratory staff numbers also limited the supervision available when learning new techniques and troubleshooting unanticipated issues during experiments.

Living alone in a newly purchased property that I was not able to fully furnish also took a considerable personal toll throughout the pandemic that impacted my ability to work productively from home. I was unable to take my desktop computer home from campus, instead having to

work from an old, low-spec personal device that lacked the computational power to cope with Microsoft Teams calls, let alone my desk-based research. These issues exacerbated the isolation I felt during this period, further compromising my concentration and productivity levels.